ABSTRACT

Title of Document: TUBULAR PERFUSION SYSTEM BIOREACTOR FOR THE DYNAMIC CULTURE OF HUMAN MESENCHYMAL STEM CELLS

Andrew Bryan Yeatts, Doctor of Philosophy, 2012

Directed By: Associate Professor John P. Fisher, Fischell Department of Bioengineering

In vitro culture techniques must be improved in order to increase the feasibility of cell based tissue engineering strategies. Limitations of current techniques are largely a result of the slow diffusion of molecules such as oxygen into the interior of three dimensional scaffolds in static culture. In order to enhance nutrient transport we have developed a novel bioreactor, the tubular perfusion system (TPS), to culture human mesenchymal stem cells (hMSCs) in three dimensional scaffolds. In our design, hMSCs are cultured on scaffolds tightly packed in a tubular growth chamber. Media is perfused by a peristaltic pump through the growth chamber and around the tightly packed scaffolds. In the first part of the work hMSCs are encapsulated in alginate scaffolds and results demonstrate bioreactor culture enhances late osteoblastic differentiation of hMSCs. An investigation into shear stress in the system revealed that osteogenic markers increase with increasing shear stress and that the differentiation of hMSCs is dependent on cell radial position within scaffolds. In order to enhance the ability to implant these constructs *in vivo*, a method to create an

aggregated cell containing construct *in vitro* in a bioreactor system was developed. In this part of the work hMSCs are cultured in individual alginate beads in the TPS bioreactor and the beads are aggregated to form one large construct. Following this the TPS bioreactor was investigated to culture synthetic poly-L-lactic acid scaffolds which were fabricated using supercritical carbon dioxide gel drying. In addition to investigating the effects of perfusion on hMSC growth in these scaffolds, the effect of microporosity was investigated. In the final part of the work, a study was completed to determine how TPS culture influenced *in vivo* bone regeneration. Here alginate beads as well as synthetic PLGA/PCL constructs were used as scaffolds. Results revealed the efficacy of using the tubular perfusion system for bone tissue engineering and demonstrated increased bone formation as a result of hMSC implantation in both alginate and PLGA/PCL scaffolds. These studies highlighted the need for bioreactor culture *in vitro* as well as scaffolds to support *in vivo* tissue interaction.

TUBULAR PERFUSION SYSTEM BIOREACTOR FOR THE DYNAMIC CULTURE OF HUMAN MESENCHYMAL STEM CELLS

By

Andrew Bryan Yeatts

Dissertation submitted to the Faculty of the Graduate School of the
University of Maryland, College Park, in partial fulfillment
of the requirements for the degree of
Doctor of Philosophy
2012

Advisory Committee:
Associate Professor John P. Fisher, Chair
Associate Professor John Caccamese
Associate Professor Adam Hsieh
Professor Lyle Isaacs
Professor Gregory Payne

Dedication

This work is dedicated to Heather whose love and support made it possible.

Acknowledgements

I would like to thank my advisor Dr. John Fisher for his instruction and guidance throughout the completion of this work. Without his advice, direction, and ever encouraging attitude this would not have been possible. I would next like to thank Dr. John Jansen for hosting me in his lab in the Netherlands and for his input with the *in vivo* study. I would also like to thank my other collaborators on that project, Dr. Sanne Both, Dr. Fang Yang, Wanxun Yang, and Hamdan Alghamdi. I would next like to thank my undergraduate researchers who contributed significantly to this project specifically to Daniel Choquette for his cell signaling research, Carly Gordon for her work on the aggregated constructs, Fayola Fears for her histology work, and finally to Elyse Geibel who worked with me throughout the completion of this thesis and contributed significantly to the hMSC radial position work. I would also like to thank Paola Pisanti who traveled from Italy to work with me on the PLLA scaffold research. I am also grateful to my committee members for their input at both my proposal and throughout completion of my project. I owe a debt of gratitude to past members of the Tissue Engineering and Biomaterials Laboratory for teaching me the techniques for this project and for their friendship and support. I would also like to thank my current lab members for their advice, encouragement, and friendship. I would finally like to thank all my family and friends for supporting me throughout this project, especially to my parents for their love and support of my education and to my grandparents for always having faith in me.

Table of Contents

List of Tables

List of Figures

Chapter 1: Introduction

Cell based tissue engineering represents a promising alternative treatment for bone injuries that do not heal by endogenous repair mechanisms. While other treatments have significant drawbacks, tissue engineering could provide a mechanism to repair bone injuries using an autologous stem cell population. In this strategy mesenchymal stem cells (MSCs), a cell population present in the bone marrow as well as other locations in the body are removed and cultured *in vitro*. These cells can be differentiated into several cell types, including osteoblasts and chondrocytes. *In vitro* these cells are often cultured on a three dimensional scaffold which then can be implanted back into the defect site to support the cell population. However *in vitro* culture techniques must be improved to increase the feasibility of this strategy. When three dimensional cell containing scaffolds are cultured in static culture, a nutrient gradient often develops in which cells consume nutrients faster than they are replaced via diffusion. Bioreactor culture can be used to improve these *in vitro* culture techniques. These bioreactor systems culture scaffolds dynamically by flowing media through culture chambers. This not only increases nutrient transport but also exposes cells to fluid shear stress, an important stimulus for osteoblastic differentiation. Commonly used bioreactor systems include spinner flasks, rotating wall bioreactors, and perfusion systems. While spinner flask and rotating wall bioreactors primarily focus on media mixing, perfusion systems force media through porous scaffolds to enhance culture. However, current perfusion systems are often difficult to build and use as the pressure required to force media through the pores of scaffolds often leads to leaks.

To this end we utilize a new bioreactor, the tubular perfusion system (TPS) for the culture of human mesenchymal stem cells. The TPS bioreactor features a modular design in which cell containing scaffolds are tightly packed in a tubular growth chamber. Media is then pumped through this growth chamber using a pump. Three different scaffolds types are evaluated through the course of this work. First an alginate scaffold is evaluated. Alginate is a natural material which can be crosslinked into beads following exposure to a divalent cation such as calcium. This encapsulates the cells within the beads although the cells can be easily removed by using a calcium chelating agent to dissolve the beads. Following this analysis of alginate scaffolds, a synthetic poly-L-lactic acid (PLLA) scaffold is used in the bioreactor. These scaffolds are fabricated using a modified supercritical carbon dioxide (SC-CO_2) gel drying process and feature a microporous design. In the final chapter of research *in vivo* bone growth following culture of hMSCs in the TPS bioreactor is investigated. In this chapter both an alginate scaffold and an electronspun poly(lactic-co-glycolic acid) (PLGA)/ polycaprolactone (PCL) scaffold are used. In this manner comparisons can be drawn between the two differing scaffold types.

Through the course of this research a new bioreactor system is developed for bone tissue engineering. This bioreactor system is used to create modular tissue engineering constructs from smaller building blocks. In addition alginate, PLLA, and PLGA/PCL scaffolds are cultured in the system to demonstrate its utility for both *in vitro* culture and *in vivo* bone regeneration.

Chapter 2: Objectives

The overall goal of this work is to develop and evaluate a new bioreactor system for bone tissue engineering. To this end this work has five primary objectives:

1. The first objective is to effectively develop the tubular perfusion system, to demonstrate its ability to support the growth and differentiation of hMSCs, and to evaluate the effects of flow rate on hMSC late osteoblastic differentiation and matrix production.
2. The second objective is to evaluate the effect of shear stress on hMSC osteoblastic differentiation in the TPS bioreactor and to evaluate the effect of dynamic culture on the proliferation and osteoblastic differentiation of hMSCs as a function of radial distance in the scaffold.
3. The third objective is to develop an aggregated construct in the TPS bioreactor, to characterize its mechanical properties, to encapsulate hMSCs in the construct, and to determine the viability of these cells throughout the creation of this construct.
4. The fourth objective is to demonstrate cell viability on microporous PLLA scaffolds fabricated using a modified supercritical fluid based technique and cultured in the TPS bioreactor and to evaluate hMSC response to dynamic culture and pore size.
5. The fifth objective is to evaluate the effect statically and TPS cultured hMSCs cultured in alginate and PLGA/PCL scaffolds have on bone regeneration in a rat femoral condyle defect and to compare bone in growth and regeneration between the two scaffold types.

Chapter 3: Bone Tissue Engineering Bioreactors: Dynamic Culture and the Influence of Shear Stress[1]

3.1 Introduction

Every year over six million bone injuries occur in the United States and approximately one million bone grafting procedures are performed [1]. The source of bone for these grafts is either from the patient's own body in the case of an autograft or from a cadaver in the case of an allograft. Unfortunately both of these methods have significant disadvantages. The incidence of medical complications arising after surgery involving an autograft from the iliac crest are nearly 30% [2]. Allografts are subject to an immune response and may transmit disease [2, 3]. Since these traditional means of treating bone injuries are associated with limitations, a tissue engineering approach to replace damaged bone represents a promising alternative. A tissue engineering approach involves seeding and growing a cell source on a scaffold and implanting the scaffold and cells into the injury site [4]. Prior to implantation into the body the cell containing constructs are often cultured *in vitro* in order to increase cell proliferation on the scaffold and to allow for differentiation of the stem cells into osteoblasts. However, *in vitro* culture techniques of 3D tissue engineering scaffolds have limitations that must be overcome in order to increase the feasibility of cell based tissue engineering strategies. Bioreactor systems are used to alleviate this nutrient transfer limitation by continuously mixing media and by convectively transporting nutrients to cells.

---

[1] As published in Yeatts, A.B. and J.P. Fisher, *Bone tissue engineering bioreactors: dynamic culture and the influence of shear stress.* Bone, 2011. **48**(2): p. 171-81.

In the overall cell based bone tissue engineering strategy of expanding a stem cell source *in vitro*, culturing and differentiating this cell source on a three dimensional scaffold, and implanting this scaffold *in vivo*, bioreactors can be used to enhance *in vitro* culture steps. Bioreactors utilize materials and cells that have already been proven effective for bone tissue engineering including polymer scaffolds that are biodegradable and mesenchymal stem cells (MSCs), a population of cells that exists in the bone marrow capable of differentiating into osteoblasts, chondrocytes, and adipocytes [5, 6]. This population represents only a small percentage of cells found in the bone marrow, thus expanding MSCs to clinically relevant numbers represents a significant hurdle to the implementation of a tissue engineering strategy utilizing these cells. In addition to a readily available cell source, the use of biodegradable scaffolds is also of importance as ideally scaffolds degrade *in vivo* and are replaced by new bone, healing the defect without a permanent scaffold presence. Since bones are load bearing, this degradation-regeneration balance is exceptionally important as the scaffold cell construct must provide continuous structural support. Bioreactors have been shown to be used to improve cell seeding efficiency [7-9], cell proliferation [10-13], and mesenchymal stem cell osteoblastic differentiation [14-20]. In addition to enhancing differentiation and proliferation perhaps the most notable contribution of bioreactor systems to a bone tissue engineering strategy is the possibility of automation. A clinically relevant strategy must greatly minimize the risk of contamination from bacteria and other cells, reduce labor intensity, and reduce costs associated with *in vitro* cell culture. Bioreactor systems have the potential to minimize all of these aspects through automated cell culture. A cell source could be added to a bioreactor, seeded using the bioreactor, and cultured continuously in the closed system.

Nutrient and oxygen concentrations could be monitored by the system and media changes could be automated. By reducing the potential for contamination and the labor intensity bioreactors could eventually greatly improve the feasibility of bone tissue engineering strategies. Continued research both on developing new innovative bioreactor systems and using established systems to determine relationships between system parameters and cell proliferation and differentiation should be completed to bring this to fruition.

In addition to the possibility of automation, bioreactors can improve *in vitro* cell culture. *In vitro* cell growth is especially hindered in three-dimensional scaffold culture of these cells. In these scaffolds nutrient gradients develop in static culture where the cells at the surface are consuming oxygen, glucose and other nutrients faster than their replacement by diffusion. This creates a gradient where cells nearer to the surface of the scaffold receive adequate nutrients, but the concentration of these nutrients decrease toward the center of the scaffold. Cell death then occurs at the center of the scaffold as nutrient and oxygen concentrations drop below the minimum necessary to sustain cell growth [21]. In the case of a bone tissue engineering construct in which cells are producing matrix, this gradient is magnified as the matrix produced by cells on the exterior portion of the scaffold further reduces nutrient transfer. In order to mitigate this hurdle bioreactor systems have been developed to optimize *in vitro* culture conditions. A bioreactor is a culture system designed to support or expand a population of cells through dynamic culture and a controlled environment. This definition provides for a wide array of designs that would qualify as bioreactors, but this review focuses on three classes of bioreactor systems that have been widely utilized in bone tissue engineering: spinner flasks [22-24], rotating wall [22-26], and perfusion systems [15, 18, 27-31]. Each of

these bioreactor types has been demonstrated to be an effective means to culture cells for bone tissue engineering purposes. Spinner flask and rotating wall bioreactor systems are effective at creating a homogenous media solution on the exterior of the scaffold, but do not effectively perfuse media into the scaffold. Perfusion systems have been demonstrated to effectively perfuse media throughout the scaffold and have been shown to upregulate osteoblastic markers and increase calcium deposition. Emphasis is placed on perfusion systems as these systems are more complex than spinner flasks and rotating wall bioreactors and feature a variety of designs. Bioreactor systems and perfusion systems in particular enhance nutrient transport and expose cells to fluid shear stresses.

An important aspect of bioreactor systems is their ability to create an *in vitro* environment that is more like the *in vivo* environment of bone [32]. Although bioreactor systems cannot replicate this environment, mechanical stresses and improved nutrient transport aid in improving *in vitro* cell culture. For example limited transport of nutrients in static culture is in contrast to the *in vivo* conditions of bone as it is a vascular tissue. Because of this *in vitro* nutrient transfer should be improved to optimize culture of cells in three-dimensional scaffolds. Bioreactor systems overcome these barriers via dynamic culture which convectively transports nutrients and exposes cells to mechanical stress. Mechanical stimulation through fluid shear stresses has been shown to be influential on bone differentiation and mineralization [20, 27, 32]. *In vivo* bone constantly remodels in response to mechanical stresses. It is hypothesized that *in vivo* these stresses are mainly transmitted to bone cells via fluid shear stresses [33]. As load is applied to bone interstitial fluid flows through pores in the bone and the shear stress is sensed by terminally differentiated osteoblasts known as osteocytes. The matrix network around

these osteocytes may allow for communication with osteoblasts and osteoprogenitor cells. It is estimated that in response to loading bone cells experience *in vivo* shears from 8 to 30 dynes/cm^2 [34, 35]. Osteoblasts and MSCs have also been shown to directly respond to shear stress [14, 20, 31, 36-40]. Based on the natural environment of bone, an optimal *in vitro* culture system should provide for adequate nutrition and oxygen to cells throughout the scaffold. Furthermore just as cells respond *in vivo* to fluid shear stress, *in vitro* shear stresses also affect bone cells. This review seeks to highlight experiments that demonstrate the effects of both of these as well as provide some comparison between various perfusion systems in terms of shear stresses.

3.2 Spinner Flasks and Rotating Wall Bioreactors

A simple bioreactor system to achieve thorough media mixing is the spinner flask (see Table 3.1 for a summary of spinner flask and rotating wall bioreactor studies). Spinner flasks are composed of a glass media reservoir with side arms that can be opened to remove scaffolds and media and often have porous covers to allow for gas exchange (Figure 3.1).

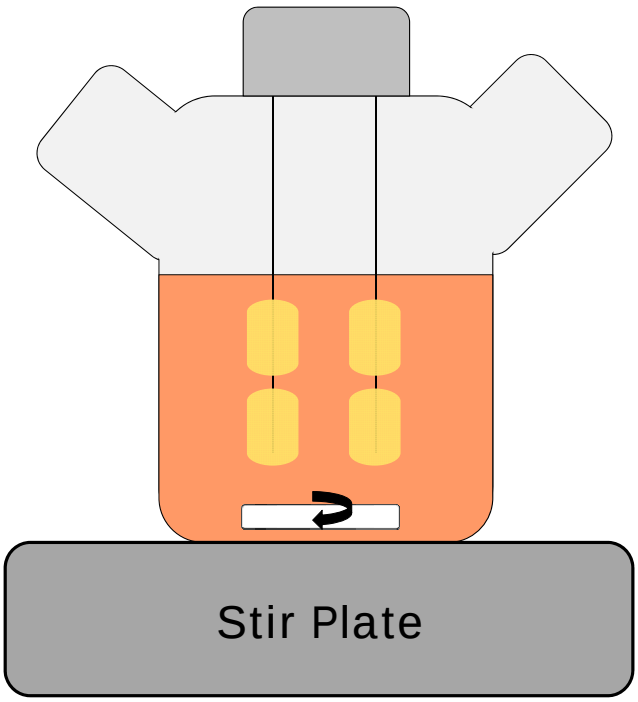

Figure 3.1: Schematic of spinner flask bioreactor. Scaffolds are suspended in culture while media is circulated using a stir bar

The flask has a stir bar or other stirring mechanism that stirs the media in the flask. Scaffolds are typically suspended from the top of the flask using needles or thread [23, 41, 42]. Spinner flasks are often used in the culture of cells for bone tissue engineering as they have been shown to increase expression of early osteoblastic marker alkaline phosphatase (ALP), late osteoblastic marker osteocalcin (OC), and calcium deposition as compared to static culture and rotating wall bioreactors [42]. This effect is thought to result from the convective transport of nutrients to the surface of the scaffold in spinner flask culture in contrast to the purely diffusional transport in static culture. This will then increase concentrations of oxygen throughout the scaffold. In static culture a nutrient concentration gradient can form where cells in the center of the scaffold receive an insufficient supply of nutrients. A nutrient gradient may still exist in spinner flask culture as matrix deposition of rat marrow stromal cells induced into an osteoblastic lineage has

been shown to be concentrated on the exterior portions of the scaffold in both spinner flask and static culture [42]. This result was also observed when human mesenchymal stem cells (hMSCs) were cultured for five weeks on collagen scaffolds in spinner flasks and bone formed only in the outer 0.5-1.0 mm of 11 mm diameter scaffolds [22]. The authors of this review speculate that in larger scaffolds such as these, spinner flask culture does not adequately enhance mass transport and a sharp nutrient gradient results leading to cell death in the center of the scaffold, resulting in confinement of matrix to exterior portions of the scaffold. These scaffolds had interconnected pores and were only 1.5 mm thick, but the penetration depth of transport in spinner flasks appeared to be limited to 1.0 mm or less. Despite these results, spinner flasks may also expose cells at the surface of constructs to shear stress which could also aid in enhancing osteogenic differentiation [24].

hMSCs cultured in spinner flasks for 84 days showed similar trends in osteogenic behavior, but both proliferation and differentiation appeared to be accelerated in spinner flask culture [43]. For clinical relevance *in vitro* culture times should be reduced far below 84 days to decrease costs and the time the patient must wait for an implant. The differences in proliferation and differentiation observed between spinner flask and static culture could be caused by increased nutrient transfer or exposure to shear stresses. Along these lines culture conditions of spinner flask systems have been shown to affect stem cell differentiation and proliferation [44]. Not only was the expression of ALP higher in spinner flask culture but also the expression was influenced by the rate of stirring. This could indicate that the increased shear resulting from higher stirring rates affects the osteoblastic differentiation of the rat bone marrow stromal cells (BMSCs) used

in the study. This increased ALP expression in response to shear may explain the results of another study which compares perfusion culture to spinner flask culture [45]. Rat BMSCs seeded on poly (glycolic acid) (PGA) scaffolds exhibited higher ALP expression levels in spinner flask culture as compared to static culture, but this expression was significantly higher in a perfusion system. In addition to stirring speed, material properties such as pore size have been shown to affect mesenchymal stem cell in growth and differentiation [11]. Immortalized hMSCs exhibited a faster rate of differentiation as shown by ALP expression in 200 μm hydroxyapatite (HA) scaffolds as compared to 500 μm pore size scaffolds. Cell proliferation was slightly higher in the 500 μm pore size group, though limited proliferation was observed throughout the study. As pore size has also been shown to affect stem cell differentiation in static culture, it is not surprising that this effect is also observed in spinner flask culture; however dynamic culture adds additional variables which may affect osteogenic differentiation beyond what is seen in static culture. Despite being a simple system several studies have shown spinner flasks to support mesenchymal stem cell expansion and osteoblastic differentiation. However, matrix production is still observed to be restricted to the exterior of the surface. MSC culture may benefit more from systems that provide direct perfusion of nutrients and expose the cells to greater shear stresses.

Another system used in bone tissue engineering to enhance media mixing is the rotating wall bioreactor. The design features two concentric cylinders, an inner cylinder that is stationary and provides for gas exchange and an outer cylinder that rotates (Figure 3.2).

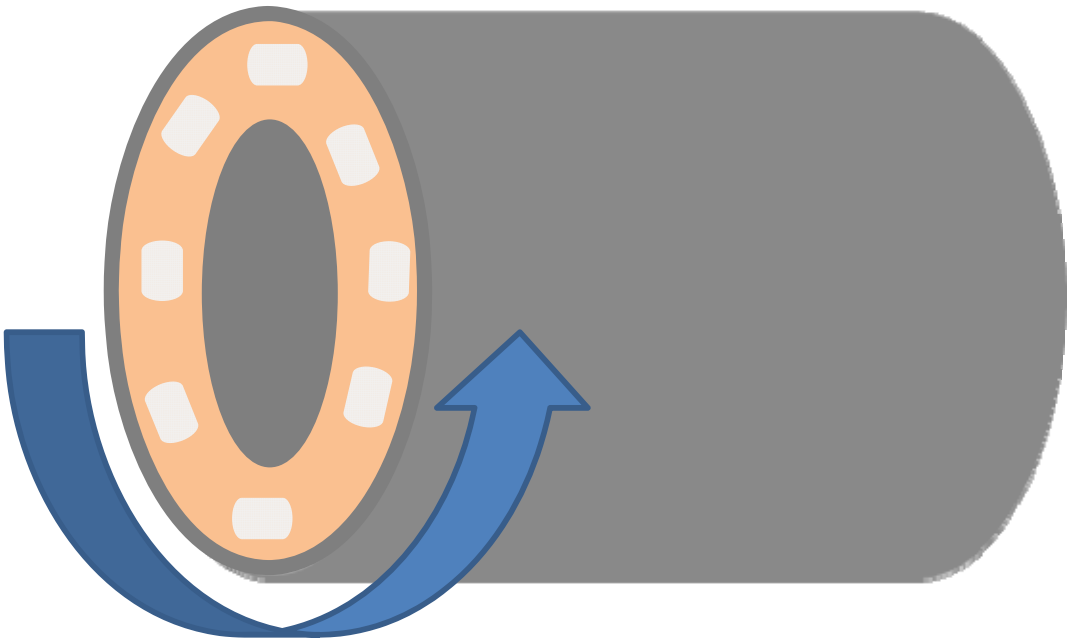

Figure 3.2: Schematic of rotating wall bioreactor. Outside wall of bioreactor rotates to circulate media

The space between the two cylinders is completely filled with culture media and cell containing scaffolds are placed freely moving in this space. The free movement of the scaffolds leads to a microgravity environment whereas the flow of the fluid caused by the centrifugal forces of the cylinder balance with the force of gravity [41, 42]. Using rat osteoblast cells rotating wall bioreactor culture was shown to cause an upregulation in ALP, OC and osteopontin (OPN), but no increase in cell proliferation [25]. Other studies have showed rotating wall bioreactors to be relatively ineffective for the culture of osteoblastic cells. Using rat BMSCs seeded onto poly (lactic-co-glycolic) acid (PLGA) foam scaffolds ALP and OC activity were shown to be higher in a spinner flask and a perfusion system as compared to the rotating wall bioreactor, which was not shown to be significantly different from a static control [46]. It is speculated that this rather disappointing result could be attributed to the scaffolds moving haphazardly in the system and colliding with the wall of the bioreactor. This effect was mitigated in a rotating wall

bioreactor system utilizing poly (lactic-co-glycolic acid) scaffolds that are less dense than water. These scaffolds avoid collisions with the bioreactor wall and thus expressed higher amounts of ALP and calcium than scaffolds cultured in static culture [47-49]. A slight variation of the rotating wall bioreactor is used in the Rotational Oxygen-Permeable Bioreactor System (ROBS) where constructs are cultured in a 50 mL polypropylene centrifuge tube modified with a silicone elastomer to provide for gas exchange [50]. The tubes containing the constructs are then placed on a roller device and housed in an incubator. This system provides both for gas exchange and rotational shear forces and was successfully used to culture BMSCs on polycaprolactone scaffolds [12, 51]. Mineralization and type one collagen was observed in scaffolds cultured in this system after four weeks. Using another slight variation of the traditional rotating wall bioreactor in which scaffolds are fixed to the vessel wall rather than allowed to move freely, rat osteoblasts were shown to proliferate at a greater rate and produce more extracellular matrix (ECM) proteins and mineralization as shown by alizarin red and Von Kossa staining compared to both spinner flasks and static culture [52]. Other studies comparing rotating wall bioreactors to static and spinner flask culture have been completed and have found less encouraging results for rotating wall bioreactors. Osteocalcin and ALP expression of rat marrow stromal cells has been shown to be lower in rotating wall bioreactor culture than spinner flask and static culture [42]. Similar results were also observed in a rotating wall bioreactor using hMSCs [24]. This low expression of osteoblastic markers in rotating wall bioreactors could be caused by collisions of scaffolds in the bioreactor or the low shear stresses on cells in the bioreactor. Rotating wall bioreactors are another relatively simple bioreactor system that have shown

effectiveness in some instances; however perfusion systems have been shown to have greater positive effects on osteoblastic differentiation.

Table 3.1: Studies utilizing rotating wall bioreactors and spinner flasks for bone tissue engineering

Scaffold Material	*Effects on osteoblastic differentiation*	*Reference*
Coralline HA	Spinner flask improves cell distribution, proliferation and osteoblastic differentiation of hMSCs	[11]
	Cells in 200 μm pore size scaffolds differentiated faster than 500 μm scaffolds	[11]
PLGA	Spinner flask cultured hMSCs have higher DNA content and 10 fold increase in calcium deposition after 21 days	[23]
	Rat MSC calcium production 30 fold higher in spinner flask than rotating wall bioreactor	[42]
	Rat MSC derived osteoblasts mineralized throughout scaffold after rotating wall culture	[50]
Silk	84 days of culture of hMSCs in 15 mm x 5 mm scaffolds showed greater calcium deposition in spinner flask	[43]
PLG	Higher expression of ALP, osteopontin and calcium deposition in rat osteoblasts cultured in spinner flask compared to rotating wall	[25]
	Developed a microcarrier system to culture osteoblasts in rotating wall system	[47-49]
Bio-derived bone	Rat osteoblasts proliferate slower and produce less bony nodules in spinner flasks as compared to rotating wall	[52]
Gelatin/ hyaluronic acid	Histology shows stronger staining of type I collagen, ALP, and osteocalcin in hMSCs after 21 days of culture in spinner flask compared to static and rotating wall	[24]
PCL	Rat MSCs cultured for 4 weeks in rotating wall bioreactor and implanted in rats for 4 weeks. ECM, mineralization, and type I collagen detected throughout the scaffold	[12]
	Rat MSCs showed mineralization and type 1 collagen after 4 weeks of culture in rotating wall bioreactor	[51]
Collagen	hMSCs express increase amounts of ALP and deposit	[22]

	increased amounts of calcium in spinner flask compared to perfusion and static	
PLGA	Higher ALP activity and cell uniformity in flow perfusion system compared to spinner flask and rotating wall, similar osteocalcin expression and cell numbers in all three systems	[46]
PGA and Collagen	Increased OC, ALP, and cell proliferation in spinner flask compared to static, decreased compared to perfusion	[45]
Polyethylene Terephthalate	RPM of stirrer increases osteogenic differentiation and proliferation from 10 rpm to 100 rpm in rat BMSCs	[44]

3.3 Perfusion Bioreactors

Spinner flasks and rotating wall bioreactors do not effectively perfuse media into a scaffold. Bioreactors that use a pump system to perfuse media directly through a scaffold are known as perfusion bioreactors (please see table 3.2 for a summary of perfusion bioreactor studies). Many different perfusion bioreactor systems have been developed but most systems consist of a similar basic design consisting of a media reservoir, a pump, a tubing circuit, and a perfusion cartridge (Figure 3.3) [32].

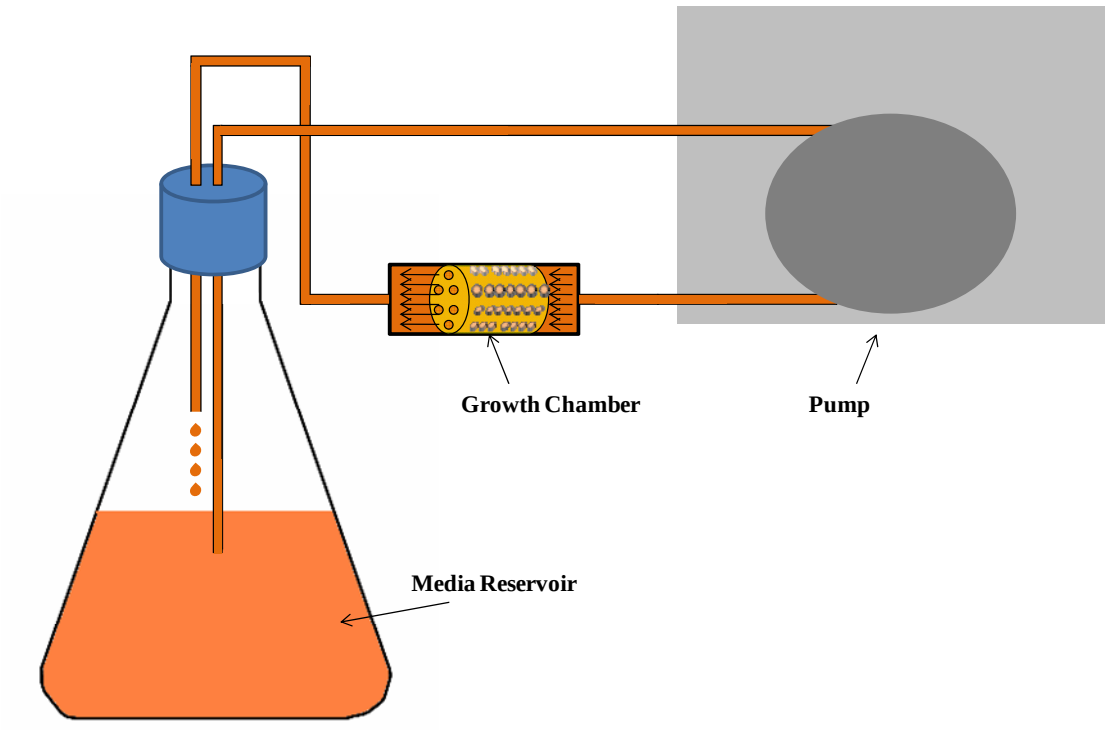

Figure 3.3: Schematic of perfusion bioreactor. Media is directly perfused through porous scaffold sealed into a growth chamber

The perfusion cartridge houses the scaffold which is sealed so that media cannot flow around it, thus perfusing media directly through the pores of the scaffold. This direct perfusion makes these systems difficult to develop as the perfusion cartridge must be custom made to tightly fit a scaffold and the scaffold must have highly interconnected pores. Despite these difficulties many perfusion bioreactor systems have been developed and tested for bone tissue engineering purposes [10, 13, 18, 27, 28, 30, 53-56].

Perhaps most prevalent in the literature is the flow perfusion culture bioreactor utilizing two media reservoirs to allow for complete media changes and a cassette that contains a scaffold press fit between two O-rings [20, 27]. This bioreactor design has been used with an array of scaffold materials including titanium, starch based scaffolds and calcium phosphate ceramics [14, 20, 28, 29, 57-59]. In a study utilizing this perfusion bioreactor

and rat marrow stromal cells a continuous flow rate of 0.3-3.0 mL/min was shown to increase both the calcium matrix deposition and the rate of late osteoblastic differentiation [20]. This study utilizes a titanium fiber mesh scaffold and though little changes were seen in early osteoblastic marker ALP the effect on late osteoblastic differentiation was very pronounced. Osteopontin was measured as a marker of late osteoblastic differentiation. Based on peaks in osteopontin expression it was concluded that fluid flow increased the rate at which the cells were differentiating. Most notable was a dramatic increase in calcium deposition in response to flow. As calcium is deposited only in late stages of osteoblastic differentiation, this result showed that the bioreactor culture was greatly enhancing differentiation of stem cells into mature osteoblasts and matrix deposition. Shear stresses in this study were reported not to exceed 1 dyne/cm^2, but exposure to these shears was attributed as the cause for the acceleration of late osteoblastic differentiation. The use of titanium fiber meshes was likely dictated by the need for highly porous scaffolds so that media can be perfused through the scaffold.

To increase the clinical relevance a biodegradable starch based scaffold was then used in this perfusion system [28, 60]. Biodegradable scaffolds ideally degrade as new bone is being generated, so that the bone defect can heal leaving no scaffold. Non-biodegradable scaffolds like titanium would remain even after the defect has healed. These scaffolds were shown to support osteoblastic differentiation and calcium production was shown to increase with flow. In addition, scaffolds with porosities of 75% had greater calcium deposition than those of 50% porosity. This demonstrated the combined effects of scaffold design parameters and flow perfusion. Studies evaluating the combined effects

of these parameters are necessary to fully optimize a system as scaffold parameters have also been shown to influence osteogenic signal expression [61, 62]. The increased extracellular matrix production observed in this study may have an effect on osteoblastic differentiation itself as demonstrated in another perfusion bioreactor study [14]. Rat marrow stromal cells were cultured for 12 days in flow perfusion cultures on titanium scaffolds and the cells removed leaving the extracellular matrix deposits. The marrow stromal cells were then cultured in the perfusion system on the scaffolds with ECM and compared to normal titanium scaffolds. The constructs with ECM showed a 40 fold increase in calcium deposition when compared to normal titanium scaffolds even when cultured without dexamethasone, a glucocorticoid steroid widely used to induce osteogenic differentiation. This result reveals a synergistic effect between the extracellular matrix and fluid shear stress, revealing that both have a strong positive effect on matrix production. Findings of fluid shear having similar effects of dexamethasone were also reported in another study using this bioreactor system [29]. Samples cultured for 16 days showed significant increases of calcium deposition under flow perfusion without dexamethasone as compared to static cultured samples with dexamethasone. Adding dexamethasone to the flow culture further increased calcium production. Osteopontin levels in bioreactor groups cultured with dexamethasone were increased to levels greater than static culture with dexamethasone and bioreactor culture without dexamethasone indicating that flow has a synergistic induction effect.

The role of growth factors in bioreactor culture also should be investigated to fully elucidate the effect of perfusion systems on osteoblastic differentiation. Dynamic culture could both enhance the production of growth factors through cell stimulation, but also

potentially reduce the local concentration of soluble factors through increased mass transport. One such study utilized polycaprolactone scaffolds and analyzed the localization of several endogenously expressed growth factors including transforming growth factor beta 1 (TGF-β1), fibroblast growth factor-2 (FGF-2), vascular endothelial growth factor (VEGF), and bone morphogenetic protein-2 (BMP-2) [63]. Using immunohistochemistry, positively stained areas increase with increasing flow rate indicating flow enhanced expression of these growth factors. *In vitro* enhancement of these growth factors could enhance *in vivo* bone growth. For example VEGF, an angiogenic growth factor, has been used to enhance endothelial cell proliferation and encourage vessel sprouting aiding in the vascularization of an implanted construct [64, 65]. BMP-2 has been widely investigated for its role in enhancing *in vivo* bone growth and *in vitro* osteoblastic signaling [66-69]. *In vivo* studies should be performed to establish that the increased *in vitro* production of these growth factors translates to enhanced *in vivo* bone formation.

Shear stress has been shown to play a substantial role in the increased matrix production observed in perfusion culture, but it is also possible that the increased media flow could also cause this result. The contribution of nutrient availability and shear stress have been examined independently in studies which use a thickening agent to increase media viscosity and are discussed later in this review. In 9 mm diameter and 5 mm in height scaffolds seeded with a preosteoblast line, central oxygen concentration dropped to 0% in 5 days of culture [21]. Cell death was subsequently observed in these areas of the scaffold. When the demineralized bone matrix scaffolds were placed in a perfusion cartridge central oxygen concentration was raised to 4%. Though this oxygen

concentration is still lower than the bulk media (~20%) it was high enough to prevent cell death. Even in relatively small scaffold (cells in these scaffolds were no more than 2.5 mm from the scaffold surface) concentration gradients occur in static culture, underscoring the importance of systems that enhance nutrient transport to cells.

The ultimate goal of these perfusion systems is to develop a method to grow cells *in vitro* that can be implanted to repair bone injury sites. Using a perfusion design made of a custom machined piece of polycarbonate with space for up to six scaffolds, hMSCs were shown respond to shear, increasing amounts of deposited protein [10]. This same culture system was shown to be effective for the osteoblastic differentiation of human adipose derived stem cells (hASCs) [70]. hASCs have been used as an accessible cells source for osteoblasts as an alternative to bone marrow derived MSCs [71-74]. The distribution of cells and bone matrix in the scaffolds was shown to increase in the bioreactor system compared to static culture. Increasing the clinical relevance of the work, the same bioreactor system was used to culture a demineralized bone scaffold machined to a defect shape based on CT scans. When hMSCs were cultured on the construct, cell number and bone volume were both significantly greater in the bioreactor as compared to a static control [15]. This study revealed a strategy of how bioreactors could be used to aid in the regeneration of bone tissue, but limited *in vivo* studies have been completed to assist in bringing such a strategy to the clinic.

In one such *in vivo* study calcium phosphate ceramics seeded with goat bone marrow stromal cells were cultured in a perfusion bioreactor and implanted subcutaneously in mice [30]. The scaffold system could be used to produce as much as 10 cm^3 of bone like engineered tissue, but the sample size of the study was small and statistical difference

was not observed between bioreactor and static culture. The perfusion system used consisted of a growth chamber, pump, oxygenator, and media reservoir. Oxygen probes were added before and after the growth chamber and measurements from these probes were used to predict cell doubling time based on oxygen consumption [75]. Human stem cells were then cultured in the bioreactor system with the goal of demonstrating bone tissue growth and though bone growth was observed after implantation in nude mice, no significant differences in bone formation or osteogenic signaling was observed between dynamically and statically cultured constructs [16]. While this result demonstrates the efficacy of using bioreactor systems, these systems must be demonstrated to enhance bone formation if bioreactor systems are to be utilized in a tissue engineering strategy. In addition to illustrate clinical relevance this result should be demonstrated in a bone defect model. In a different study again using a skin fold model human BMSCs were seeded on hydroxyapatite scaffolds and grown in a bioreactor also used for cell seeding [9, 76]. Increased bone formation was observed when the constructs were implanted in an ectopic mouse model as compared to static controls. Quantitative scoring of hematoxylin and eosin staining was used to gain these results, but nonetheless demonstrate the efficacy of using bioreactor systems; however more studies are necessary to confirm this result. Small sample sizes and large errors could make it difficult to observe significance in *in vivo* models, but careful experimentation must be completed to conclude whether or not bioreactor systems can improve *in vivo* bone growth. Another advantage of *in vivo* models is a further demonstration of clinical relevance. In one study osteoconductive grafts were created using a different seeding method that could increase clinical relevance [77]. Rather than isolate BMSCs from bone marrow by growing the cells in monolayer,

whole bone marrow was isolated, bone marrow stromal cells were enriched using a density gradient, and these cells were seeded directly into the bioreactor system, rather than first being expanded in 2D. Bone tissue formation was observed in a mouse ectopic model using these constructs. Potentially increasing the clinical relevance of bioreactor work, this result is interesting as adding BMSCs directly to scaffolds without prior expansion would shorten the time and difficulty required in implementing a tissue engineering strategy. These *in vivo* experiments were completed in a skinfold model, but *in vivo* studies using a bone defect model have also been completed.

Using the flow perfusion culture bioreactor rat BMSCs were cultured dynamically on titanium scaffolds and implanted in a rat cranial defect model [78]. After 30 days bone growth was observed in all cell groups, but there were not significant differences between the treatment groups of perfusion versus static and varying *in vitro* culture times. The authors speculate this again could potentially be attributed to the difficultly of observing statistical significance in *in vivo* models. This study demonstrates the principle of a bone tissue engineering strategy using a perfusion bioreactor. Further *in vivo* studies utilizing perfusion bioreactors are required to prove the effectiveness of these systems especially those that use a bone defect model rather than simply implanting the construct subcutaneously. The lack of *in vivo* studies could potentially be explained from the difficulty of developing and testing a perfusion system. Because of the need for custom made parts and the difficulty of perfusing media directly through a scaffold development and maintenance of these systems can be time consuming. These shortcomings need to be overcome and an increased amount of *in vivo* studies need to be completed to demonstrate the clinical relevance of perfusion bioreactor systems. The clinical

relevance of perfusion bioreactor systems will be defined by their ability to be used with other strategies for bone tissue engineering including biodegradable scaffolds, scaffolds and growth factors that enhance osteoinduction and osteoconduction, and readily available stem cell populations. Much of this work has begun to be completed, however additional studies focusing on scaffold parameters such as pore size and stiffness and exogenous growth factor delivery should be completed in conjunction with bioreactor studies to observe how bioreactors influence cell response to these factors. The ultimate advantage of bioreactor systems over conventional techniques is the ability of bioreactor systems to produce reproducible culture conditions that enhance stem cell proliferation and differentiation and can be made to minimize handling of scaffold and human labor. By automating the process of 3D cell culture a bone tissue engineering strategy can be developed that can be feasibly implemented in the clinic on a large scale.

Table 3.2: Studies utilizing perfusion bioreactors for bone tissue engineering grouped by bioreactor design

Bioreactor Design	*Principle Findings*	*Reference*
Flow perfusion culture bioreactor	Fluid flow increases matrix deposition and accelerates osteoblastic differentiation of rat BMSCs	[20]
	Presence of extracellular matrix on titanium scaffolds enhances osteoblastic differentiation with shear stress	[14]
	Osteoblastic differentiation of rat BMSCs grown on calcium phosphate ceramics enhanced	[58]
	Flow enhances calcium deposition, porosity of starch scaffolds affects ALP expression and proliferation of rat BMSCs	[28, 57]
	Rat BMSCs can differentiate into osteoblasts under flow perfusion without osteogenic supplements	[29]
	Flow enhances calcium production of rat BMSCs cultured on PLLA nonwoven meshes and improves cell homogeneity	[18]
	Flow perfusion enhances production and localization of osteoblastic growth factors TGF-β1, VEGF, BMP-2, and FGF-2	[63]
	Rat BMSC seeding improved using bioreactor system set to oscillatory flow	[7, 8]
	Increasing shear stress while keeping flow rate constant increases mineralized matrix production in rat BMSCs	[17]
	hMSCs increase expression of BMP-2, BSP-2, RUNX2, OPN, and ALP in response to fluid flow	[59]
	Rat BMSC/titanium constructs cultured in bioreactor implanted in cranial defect model	[78]
Radial channel perfusion system	Improved cell number, distribution and amounts of bone proteins with increased flow velocity of hMSCs cultured on bone plugs	[10]
	Improved cell distribution and bone matrix of hASCs in perfusion system	[70]

Complex geometry perfusion system	hMSCs cultured on decellularized bone scaffold manufactured to anatomical shape in bioreactor	[15]
Central tunnel perfused scaffold	Sheep MSCs seeded on β-tricalcium phosphate increase glucose consumption and proliferate throughout the scaffold under perfusion	[79]
	Shear stress shown to accelerate osteoblastic differentiation of human BMSCs while mass transport shown to increase differentiation among lower ranges	[80]
Direct perfusion bioreactor	Homogenous cell growth of goat BMSCs, ability to measure oxygen consumption	[75]
	Dynamically cultured goat BMSCs grown on calcium phosphate ceramic produced bone when implanted into mice	[30]
	Human BMSCs formed *in vivo* bone in mice after dynamic culture. Limited differences in osteogenic markers between dynamic and static	[16]
Tissue Culture Under Perfusion	Human BMSCs cultured in bioreactor form bone when implanted into mice	[77]
U-tube cell seeding perfusion bioreactor system	Bioreactor used for cell seeding, enhanced number of viable seeded cells and cell uniformity	[9]
	Human BMSCs seeded directly on 3D scaffolds and cultured in bioreactor, produced bone tissue when implanted into mice	[76]
Stainless steel perfusion block	Osteoblasts seeded on trabecular bone scaffolds showed higher proliferation as lower flow rates while Runx2, osteocalcin and ALP increased with flow rate	[53]
Axial perfusion bioreactor system	Rate of mineralized matrix production of rat BMSCs increased, measured by micro-CT imaging	[81]
Gradient container	hMSCs remain viable for 14 days of *in vitro* culture and 12 weeks of *in vivo* culture	[82]
	Perfusion system increased central oxygen concentration and prevented cell death	[21]
Perfusion bioreactor system	Flow enhances proliferation and differentiation of hTERT-hMSCs	[13]
	After 40 days higher cell densities of hMSCs in	[83]

bioreactor	
Higher metabolic rates and more even distribution of hMSCs in perfusion culture, mathematical modeling completed	[84]
Shear stress upregulated osteoblastic differentiation of hMSCs	[31]
Dynamic culture affected ability of hMSCs to form organized matrix and altered nuclear morphology, but increased expression of OPN	[85]
BMP-2 expression of rat MSCs impregnated with plasmid DNA encoding for BMP-2 enhanced with perfusion culture	[55]
In vivo ectopic bone formation enhanced after rat MSCs impregnated with BMP-2 cultured under perfusion	[56]
Significant increase in ALP and OC expression at sites of implanted collagen-PGA scaffolds seeded with rat MSCs cultured in perfusion system versus static in ectopic rat model	[54]
Bone marrow derived osteoblasts exhibit higher ALP and OC expression in perfusion container than static culture. Enhancement of *in vivo* bone formation was also observed in mouse skinfold	[86]
ALP expression increases in rat osteoblastic cells cultured in perfusion container	[87]

3.4 Effect of Shear Stress and Mass Transfer on Proliferation and Osteoblastic Differentiation

Studies focused on the effects of fluid shear on osteoblastic differentiation have shown that shear stress affects osteogenic signal expression of mesenchymal stem cells [36, 38-40, 88, 89]. Studies reported in this section utilize laminar flow regimes. In addition to the velocity of flow which affects the magnitude of shear, studies utilize flow patterns

including oscillatory and continuous flow. Nearly all long term three dimensional bioreactor studies utilize a continuous flow rate, while many short two dimensional studies analyze continuous, pulsatile, and oscillatory flow. Because most long term three dimensional bioreactor studies use continuous flow regimes, this section focuses on 2D and 3D flow systems that utilize continuous flow. In one such study utilizing a flow that occurred for 5, 30, or 120 minutes every other day for 20 days shear stresses of 1.6 dynes/cm^2 were used and osteopontin and bone sialoprotein (BSP) expression were shown to increase in response to shear [39]. Significant changes in osteogenic signal expression have also been observed after shorter exposure to shear stresses in this range [40]. When rat BMSCs were exposed in 2D to shear stresses of 2.6 dynes/cm^2 significant changes in osteogenic signaling pathways were observed. Shear stress was administered for periods of 30 minutes to 24 hours and flow regimes were either continuous or intermittent. After 30 minutes flow was shown to significantly enhance the phosphorylation of mitogen activated protein kinases (MAPK), p38 and extracellular signal-related kinase (ERK). To test if the effect of shear stress on MAPK signaling processes also influenced additional osteogenic signal expression, collagen 1α1, osteopontin, cyclooxygenase-2 (COX-2), and VEGF were analyzed. No changes after four hours of flow were observed in osteopontin or collagen 1α1, but COX-2 and VEGF were significantly upregulated. However when cells were exposed to shear for 24 hours and then cultured in static conditions for 14 additional days, significant upregulation of osteopontin, collagen 1α1, bone sialoprotein, and osteocalcin were observed, indicating this early impact on osteoblastic signal expression affected late osteoblastic differentiation [40]. This effect on early osteoblastic differentiation was observed at a

high shear stress when human osteoblast ALP protein levels were shown to double after just 30 minutes of exposure to 20 dynes/cm^2 shear stresses [38].

Long term exposure to shear stresses an order of magnitude lower has been shown to generate similar results [88]. Human bone marrow stromal cells were exposed to shear stresses of 0.012 dynes/cm^2 for ten days using a two dimensional parallel plate. Following exposure to the shear stress, the cells were shown to proliferate at a slower rate as compared to static culture; however immunohistochemical staining for type one collagen and Von Kossa staining showed more intense staining for fluid flow groups. This indicates that cells exposed to shear are producing more calcium and collagen, components of bone extracellular matrix. Signal expression data showed mixed results after exposure to shear with upregulation of collagen type 1 and osterix, but downregulation of ALP and OC. BSP and OPN were also analyzed and these genes were either upregulated or downregulated by shear depending on substrate type [88]. These studies on short or long term shear rate in 2D cultures indicate that osteogenic signal expression is greatly affected by fluid shear stresses with magnitudes as little as 0.01 dynes/cm^2 and as high as 20 dynes/cm^2. These 2D studies allow for greater control of experimental variables and can give beneficial information on how MSCs and osteoblasts are responding to shear.

Bioreactor studies using three-dimensional scaffolds also provide information about shear, but additional variables in the systems can make it difficult to calculate exact shear stresses cells are exposed to. Complex modeling is required to accurately compute flow rate induced shears from fluid flowing through the pores of three-dimensional scaffolds and these shears are influenced by factors that are difficult to measure including cell

growth and extracellular matrix deposition. These two factors can effectively alter the path that fluid flows, thus altering local velocities and shear rates. Bioreactor systems also enhance mass transport which could also be influencing osteogenic signal expression, as well as influencing local concentrations of soluble factors influencing osteoblastic differentiation. Long term perfusion bioreactor studies have reported shear stresses from 0.05 to 1.0 dynes/cm^2 (table 3.3). Increased calcium matrix production is often observed in these studies and this outcome is often attributed to shear stress. Based on short term and 2D studies this is a valid conclusion, and it is further verified by studies that isolate the effects of shear stress by holding mass transport constant and increasing shear through the use of thickening agents such as dextran. The addition of dextran to culture media increases the viscosity and dextran itself does not affect osteoblastic differentiation [90]. Two studies are reported that evaluate the direct effect of shear stress on osteoblastic differentiation in three dimensional perfusion systems.

One of these studies performed in a bioreactor system previously discussed and utilizing titanium fiber mesh scaffold used dextran to increase fluid viscosity 2 and 3 fold [17]. As viscosity increased, calcium deposition also increased, with a 7 fold increase as a result of the 3 fold viscosity increase. Though the shear stresses in the system were still relatively low, the extended culture time (16 days) with fluid flow induces the changes in osteoblastic differentiation. Shear is an important variable to isolate in bioreactor systems as most studies that increase shear also increase flow rate, enhancing mass transport. Isolating the effect of shear from mass transport enables researchers to greater understand the results of their experiments. The effect of this increased mass transport from perfusion systems was studied in detail in a recent work. This study uses a

perfusion system in which a porous β-tricalcium phosphate scaffold (TCP) is placed in a media reservoir and a tube sealed into an opening in the middle of it. Media is then pumped from the reservoir by a pump into the opening and the media is forced through the pores perfusing the scaffold [79]. Flow rate was first held constant while the shear stress increased through addition of dextran to the media. In other experimental groups the shear stress was held constant while the flow rate was increased, permitting the effects of both shear stress and mass transport to be analyzed separately. Results revealed that increasing mass transport increases osteogenic markers ALP and OPN over lower values (0-6 mL/min), but begins to have an inhibitory effect at 9 mL/min [80]. This likely occurs as a certain flow rate is required to sufficiently supply nutrients to the cells, but once that flow rate is reached, high mass transport rates interfere with cell-cell signaling mechanisms. This result indicates that there is an optimal mass transport rate that exists. As in previous studies, increased shear stress (approximately 0.11 dynes/cm^2 to 0.15 dynes/cm^2) induced a higher amount of OPN and OC activity at 28 days. It is also likely that a maximum shear stress exists above which either no further enhancement of cell signaling is observed or that shear begins to be inhibitory. This study however did not reach that level. The result that shear stress can accelerate osteoblastic differentiation is confirmed by this study, but it also reveals that this effect occurs in tandem with increased mass transport.

Mathematical modeling can be an important tool to determine what shear stresses a bioreactor system exposes cells to and how the system affects mass transport. These analyses can be difficult to complete as flow through random porous architecture scaffolds can be difficult to model and this architecture changes with cell growth. A

possible way to account for cell growth would be to combine mathematical modeling with an advanced imaging technique that could map cell growth and matrix production [81]. A mathematical model that does not account for cell proliferation was completed on a system shown to increase stem cell osteoblastic differentiation and growth [31, 83-85]. According to the simulation, cells in the scaffold experienced shear stresses from 0.0001 to 0.001 dynes/cm^2. These shears are low compared to others reported in the literature and were shown to only penetrate 70 μm into a 1.2 mm diameter scaffold. Analysis of oxygen content revealed that oxygen levels were sufficient for cell growth, so any differences in cell behavior observed could be attributed to the shear stresses in the system. Mathematical models of bioreactor systems such as this one should be completed on bioreactor systems to add insight into the mechanisms behind cell behavior in the systems. Shear has been shown to influence osteoblastic differentiation, but it is unknown exactly what magnitude of shear stress cells are exposed to in many bioreactor systems. Modeling should be used as a tool to determine these values and yield information to explain the phenomena behind increased stem cell growth and osteoblastic differentiation. Detailed math models, experiments isolating shear stress and mass transport and monitoring of oxygen and nutrient concentrations are all tools to determine what effect bioreactor shear stress and mass transport have on stem cells. Short term experiments exposing osteoblasts or stem cells to shear stress in monolayer have provided insight on the cell signaling pathways affected by shear stress, but analysis in perfusion systems must also be completed to determine the effect of long term shear stress. Determining this effect will allow for a greater understanding of perfusion

systems and lead to more effective optimization of these systems and potentially a more effective introduction of these systems into clinical bone tissue engineering.

Table 3.3: Comparison of shear stresses reported in bioreactor studies

Reported Shear Stress (dynes/cm^2)	*Effects on osteoblastic differentiation*	*Reference*
Not exceeding 1.0	Significant acceleration of late osteoblastic differentiation (calcium deposition and osteopontin) in rat MSCs throughout 16 days of culture	[20]
0.2-0.3	Significant increase in calcium deposition in 0.3 dynes/cm^2 compared to 0.2 dynes/cm^2 (porosity changes from 75% to 50%) over 15 days in rat MSCs	[57]
0.05	Greater calcium deposition after 16 days of culture of rat MSCs	[18]
0.1-0.3	Increasing shear stress by increasing viscosity 2x and 3x increased calcium deposition of rat MSCs 4 and 7 fold after 16 days	[17]
0.1	Using hASCs perfusion culture increased expression of collagen, bone sialoprotein and osteopontin compared to static	[70]
0.007-0.1	Increasing perfusion rate increased cell number distribution and protein production of hMSCs over 5 weeks	[10]
<0.05	Lower calcium content as compared to spinner flask using hMSCs	[22]
1.6	BMSCs cultured for twenty days exposed to flow every other day for 5, 30, or 120 minutes showed greatest expression of late osteoblastic markers after 30 min	[39]
0.05-0.15	Holding flow rate constant while raising shear from 0.05 to 0.15 dynes/cm^2 increased mineralization and accelerated osteoblastic differentiation of human BMSCs	[80]

3.5 Bioreactors for Cell Seeding

This review has mainly focused on bioreactor systems for the long term culture of bone tissue engineering constructs; however the use of bioreactors for cell seeding represents another important use of these systems. Cells seeded on tissue engineering constructs are often loaded by directly adding a cell suspension to the scaffold. Though this method is simple and thus widely used, it can result in low seeding efficiencies and non homogenous seeding distributions [7, 9, 91]. Seeding efficiency can be improved by placing porous scaffolds in a mixing cell solution. Spinner flask systems have been used for this purpose however perfusion bioreactor seeding systems have shown to further improve seeding efficiency [7-9, 19, 83, 91-94]. Bone marrow stromal cell and chondrocyte loading efficiency have been shown to be 20% higher using a perfusion system as compared to static and spinner flask loading and significantly more uniformly distributed [9]. Using another bioreactor system that has been discussed in this review, the flow perfusion culture bioreactor, oscillatory flow was used to seed preosteoblastic cells on polystyrene matrices and foams as well as PLLA scaffolds [7]. Dynamic seeding yielded higher seeding efficiencies under most culture conditions. Even more relevant to bioreactor bone tissue engineering, perfusion seeding yielded higher cell attachment after exposure to shear when compared to statically loaded cells exposed to shear. This has important ramifications for bioreactor systems as most perfusion systems are statically seeded and then loaded into a bioreactor. Perfusion seeding may increase seeding efficiency and reduce risk of contamination by decreasing the amount of time the scaffolds are handled outside the bioreactor system. Further studies indicate that flow rate used in dynamic seeding of PLLA scaffolds influences scaffold cellularity with lower

flow rates yielded higher cellularity [8]. The exact nature of this relationship will likely vary with bioreactor type, scaffold material and porosity, and cell loading concentration, thus it should be customized for each seeding perfusion bioreactor. The use of perfusion bioreactors for cell seeding represents another aspect of bone tissue engineering that bioreactor systems can improve upon. Continued experimentation in this area could lead to a bone tissue engineering strategy in which cells are loaded onto scaffolds in bioreactor systems and cultured long term in the same system, maximizing efficiency and minimizing contamination risk.

3.6 Commercial Bioreactor Systems

Despite the hurdles to developing a bioreactor system for bone tissue engineering some bioreactor systems are currently on the market or in the process of commercial development. Several of these systems are summarized in Table 3.4. Some of the products listed in Table 3.4 are not specifically designed for bone tissue engineering; however these systems could potentially be used for a bone application. Others have been used for bone tissue engineering and have been reported in the literature including the gradient container, and perfusion containers [82, 86, 87, 95-98]. Following culture of BMSCs seeded on β-TCP scaffolds in the Minucell and Minutissue perfusion container system higher expression of ALP was observed throughout a four week study as compared to a static control [87]. Osteocalcin was also shown to increase in this system as well as *in vivo* subcutaneous bone growth [86]. Results from studies utilizing rotating wall bioreactors marketed by Synthecon have also been published in the literature [25, 99, 100]. Human BMSCs seeded on porous silk scaffolds were shown to produce homogenous bone like constructs after five weeks of culture in the Synthecon rotating

wall bioreactor [100]. Studies like these completed using commercially available systems are highly valuable as these studies have increased clinical relevance as commercial systems can be purchased by multiple labs and have already begun to be mass produced. Development, testing, and experimentation on commercial systems should be continued as currently these systems are not FDA approved for clinical use. Companies motivated by commercial use will have incentive to seek regulatory approval on bioreactor systems. Thus bioreactor systems can be developed beyond what is done in academic labs.

Table 3.4: List of companies with commercial bioreactor systems

Company	*Product Description*	*Website*
Aastrom	Developing bioreactor system for stem cell expansion	www.aastrom.com
Histogenics	Developing NeoCart® autologous engineered neocartilage which utilizes bioreactor system	www.histogenics.com
New Brunswick	Bioreactor systems for scale up of mammalian cells	www.nbsc.com
Minucell and Minutissue	Various bioreactor systems for 3D tissue culture including gradient container, container tissue factory, and perfusion culture container	www.minucells.de
Synthecon	Produce many batch systems including the NASA developed Rotating Cell Culture System and a Perfused Culture System	www.synthecon.com
Pluristem Therapeutics	Patented PluriX™ 3D Bioreactor for expansion of marrow stromal cells	www.pluristem.com
FiberCell™ Systems Inc.	Manufacture Hollow Fiber bioreactors that can be used for endothelial cell and other mammalian cell culture	www.fibercellsystems.com
Biovest International	AutovaxID™ automated cell culture system for use in mammalian cell culture	www.biovest.com
Wyle Labs and Celdyne	Hydrodynamic focusing bioreactor developed by NASA for cell expansion and culture	www.wyle.com

3.7 Conclusions and Future Directions

A significant volume of work has been reported to support the use of bioreactor systems for bone tissue engineering. Spinner flasks and rotating wall bioreactors can be readily implemented for culture of three dimensional constructs and these systems have shown some promising results, but the inability of these systems to greatly enhance nutrient

transfer throughout a scaffold limits the degree of improvement over static culture. However, use of these systems should be continued at least into the near future as implementation of these systems is more readily achieved than more complicated perfusion systems. Experiments utilizing perfusion systems have shown very promising results including induction of osteoblastic differentiation without dexamethasone [14, 29] and growth of cells on a scaffold custom designed for a bone defect [15]. Despite these successes more progress needs to be made in order for perfusion bioreactor systems to be used in a clinical setting. Researchers should focus on the clinical strategy for implementing their bioreactor system including improving ease of use, minimizing failure rates, and optimizing cell proliferation and differentiation (Figure 3.4).

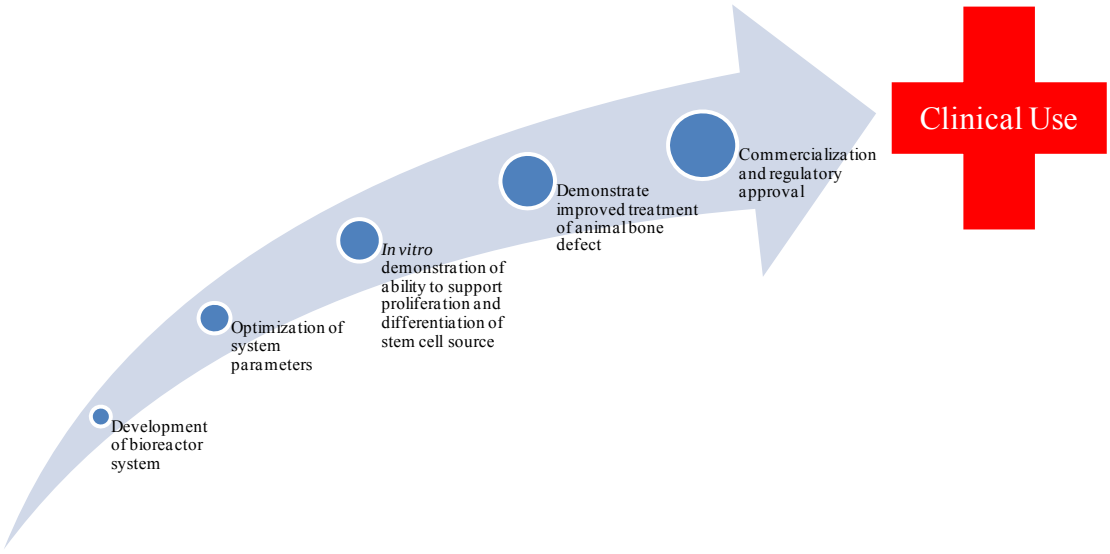

Figure 3.4: Clinical roadmap for bone tissue engineering bioreactors

This focus should include the entire strategy including cell type (readily available cells sources such as MSCs should be focused on), biomaterial (non-toxic biodegradable scaffolds), and bioreactor components (FDA approved). Attention to these items will allow for more rapid transference of bioreactor systems to a clinical setting. Furthermore

research should be conducted in a linear manner with experiments focusing on demonstrating effectiveness in a clinical setting. Despite the plethora of work completed on perfusion bioreactor systems, minimal work has been reported utilizing perfusion bioreactor cultured bone tissue engineering constructs in an animal defect model. Given the promise and amount of research conducted on many bioreactor systems a defect experiment must be the next step to utilize perfusion bioreactors in a clinical setting. Once these studies are completed researchers should focus on commercializing their bioreactor system and overcoming regulatory hurdles to begin clinical use. The potential associated with these systems is great, but significant additional progress must be made. Ideally a bioreactor based bone tissue engineering strategy would start with the extraction of a stem cell population from a patient. This population would then be expanded in a bioreactor system then uniformly seeded on a biodegradable, biocompatible three dimensional scaffolds in the bioreactor system. The construct would be cultured within an environment that would cause the stem cells to rapidly proliferate and undergo osteoblastic differentiation with the bioreactor system monitoring oxygen content and automatically changing media when necessary. After a short but sufficient culture time this construct would be removed and directly implanted in the patient where it would foster osteoinduction and osteoconduction for rapid repair of the defect site. The scaffold would biodegrade leaving only regenerated bone tissue where there was once an injury. With an increased amount of relevant animal studies and development of a clear strategy bioreactor systems could play a key role in a tissue engineering treatment for bone defects and bring this strategy to clinical reality.

Chapter 4: Bioreactors to Influence Stem Cell Fate: Augmentation of Mesenchymal Stem Cell Signaling Pathways via Dynamic Culture Systems

4.1 Introduction

Mesenchymal stem cells (MSCs), a multipotent stem cell population present in bone marrow as well as other tissue including adipose, and can be readily differentiated *in vitro* into osteoblasts, chondrocytes, and adipocytes as well as tenocytes and myoblasts [5, 6, 101]. Therefore these cells are a promising therapeutic cell source for regenerative medicine therapies to replace and repair these tissues. Therapies involving MSCs include direct transplantation of an MSC population, growth factor loaded scaffolds for MSC recruitment, and implantation of scaffolds containing an *in vitro* cultured MSC population [102-105]. Successful *in vitro* culture of MSCs requires an understanding of the signaling pathways that cue both the proliferation and guided differentiation of these cells. During differentiation chemical, biological, and mechanical cues induce these cells to follow a specific pathway dictating if the cell remains multipotent or differentiates into a specific cell type. These cues signal the release and uptake of cytokines, hormones, and growth factors which induce dynamic signaling pathways and mediate cell fate. Key signaling cascades include mitogen activated protein kinase (MAPK), Wnt, and transforming growth factor beta (TGF-β) are mediated by growth factors including bone morphogenic protein 2 (BMP-2), transforming growth factor β2 (TGF-β2), and fibroblast growth factor (FGF). Release of these growth factors is modulated by the environment of the cell including surrounding cell types, physical culture parameters, factors present in

the media, and mechanical stimuli [62, 69, 106-109]. Thus the cell environment must be regulated during *in vitro* stem cell culture. Bioreactor systems represent an important tool to regulate this environment. Bioreactors provide controlled mechanical stimuli to the cell as well as regulating the cell culture medium. In that way they provide a level of control of cell culture parameters perhaps not possible in static culture.

Bioreactors, extensively used in the culture of MSCs, include simple systems such as spinner flask and rotating wall bioreactors and more complicated systems including perfusion and dynamic loading bioreactors [10, 15, 17, 18, 20, 28-30, 48, 58, 110-113]. While spinner flasks and rotating wall bioreactors fail to provide full control of culture parameters, perfusion and dynamic loading systems have been demonstrated to be very effective in MSC culture. These systems have been shown to enhance both MSC chondrogenesis and osteogenesis as well as increase proliferation of these cells. By perfusing media through a porous scaffold bioreactors can provide homogenous nutrient and oxygen concentrations to cells. This ability makes these systems a key part of an *in vitro* culture strategy as statically cultured constructs often suffer from lack of nutrient deprivation and hypoxia leading to cell death. This review will focus on another advantage of these systems: the potential to mediate cell signaling pathways to direct MSC proliferation and differentiation. *In vitro* these signaling pathways can be potentially triggered by environmental cues including mechanical stress and oxygen content which can be controlled using bioreactor systems. Thus this review will attempt to answer the following questions: What aspects of dynamic culture affect MSC differentiation pathways? How can bioreactors be used to augment these pathways?

4.2 Bioreactor Systems for MSC Culture

Many different bioreactors systems exist for the culture of mesenchymal stem cells including spinner flask [11, 22-24, 42, 43, 46], rotating wall [24, 42, 47, 52, 114], and perfusion [10, 15, 16, 18, 27, 29, 80, 112, 113, 115] bioreactor systems (Figure 4.1). Recent reviews have described the role of shear stress for bone tissue engineering [110, 111] as well as detailing these systems [116-118]. All of these systems feature culture of MSCs in a three dimensional environment.

Spinner flask culture consists of MSC containing scaffolds either suspended or free floating in a flask of culture media (Figure 4.1A). The media is then circulated throughout the flask using a stir bar. Rotating wall bioreactors feature scaffolds placed between two concentric cylinders in culture media (Figure 4.1B). While the inner cylinder remains stationary the outer cylinder rotates, moving the media in a circulatory manner. These systems have been shown to increase MSC proliferation and osteoblastic differentiation [11, 22]; however these systems lack the ability to regulate oxygen and shear stress throughout a scaffold. This is because these systems focus primarily on media mixing while exhibiting a small amount of shear stress to the outer regions of scaffolds. Media mixing ensures a homogenous oxygen gradient in the bulk media, but non-homogenous concentrations can result throughout the scaffold. Perfusion bioreactor systems have the ability to yield a more tight control over scaffold exposure to oxygen and shear stress. The basic perfusion bioreactor design features media pumped from a media reservoir through a tubing circuit via a pump (Figure 4.1C). Within the tubing circuit there is a growth chamber containing the scaffolds. In many perfusion bioreactor designs a porous scaffold is used and is press fit into the growth chamber [15, 20, 27].

Media is then directly perfused through pores in the scaffold. An alternative type of perfusion bioreactor uses a modular design in which scaffolds are packed into a growth chamber [112, 113, 119-121]. In these designs a collection of smaller scaffolds is cultured in a growth chamber and then can be implanted as one larger construct.

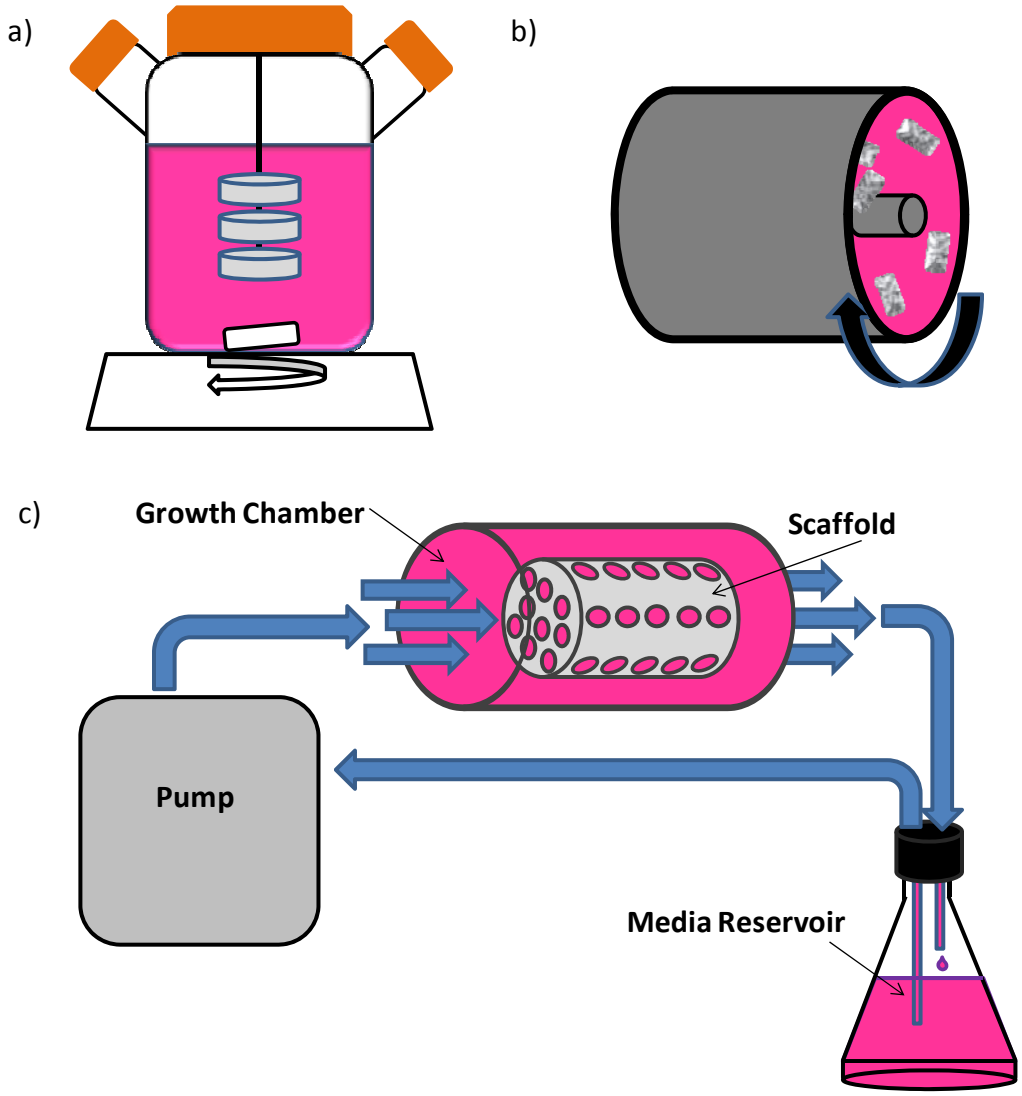

Figure 4.1: Schematic of three commonly used tissue engineering bioreactor systems. The spinner flask (a) and the rotating wall bioreactor (b) focus on mixing media around scaffolds while provided some mechanical stimulation. The perfusion bioreactor (c) provides more direct stimulation to cells by perfusing media directly through a cell containing scaffold.

Perfusion bioreactor systems have been very effective for the culture of MSCs, being demonstrated to increase proliferation [13, 21, 112] , osteogenesis [15, 18, 20], and chondrogenesis [122]. These observed results are attributed to the ability of the systems to increase nutrient transport including oxygen and expose the cells to mechanical stimulus. When the effect of these two stimuli were independently evaluated shear stress and mass transport were each shown to have an effect on human mesenchymal stem cell (hMSC) growth and osteoblastic differentiation [80]. In this study shear and mass transport could be decoupled by changing media viscosity. In this way it was shown that increasing shear from 0.05 to 0.15 dynes/cm^2 caused hMSCs to express higher levels of late osteoblastic markers osteopontin (OPN) and osteocalcin (OC) at 28 days. Higher flow rates (while keeping shear constant) also led to higher levels at low levels, but became inhibitory at 9 mL/min. This demonstrates that MSCs cultured in perfusion systems respond to flow rates in two ways, through both changes in nutrient transport and shear stresses. Because of the multitude of factors influencing differentiation in bioreactor systems the exact parameters influencing MSC differentiation may be difficult to discern. However, such studies decoupling these parameters can lead to a greater understanding of MSC culture in bioreactor systems.

4.3 Bioreactors to Mediate Shear Stress

Another powerful mechanism by which bioreactor culture can augment stem cell signaling and fate is through exposure to mechanical stresses [103]. Shear has a dramatic effect on MSC differentiation and bioreactors have the capability to regulate shear in three dimensional constructs [110, 111]. A notable demonstration of this is the ability of bioreactor systems to direct osteoblastic differentiation of MSCs without any chemical

osteogenic supplements [14, 29]. Typical osteogenic induction media consists of chemical supplements including the glucocorticoid steroid dexamethasone. However based on alkaline phosphatase (ALP) and osteopontin levels dynamic culture can be a strong inducer of MSC osteoblastic differentiation than dexamethasone [29]. As a possible mechanism human MSCs exposed to 12 dynes/cm^2 of shear stress show an upregulation of ALP expression dependent on p38 and extracellular signal-related kinase (ERK) activation [36]. These two signaling mechanisms of the mitogen activated protein kinase (MAPK) pathway described in detail later in the review may provide a mechanism for shear stress regulation of MSC osteoblastic differentiation. In addition to the presence and magnitude of shear, the particular shear regime may also influence stem cell fate [39, 40]. When rat bone marrow stromal cells (BMSCs), containing a heterogenous population of MSCs, were differentiated into immature osteoblasts and exposed to a continuous shear stress of 2.3 dynes/cm^2 the cells underwent a rapid phosporalization of ERK and p38. When this shear was delivered intermittently the phosporalization was delayed. Synthesis of prostaglandin E_2 (PGE_2) however was increased with intermittent flow, hypothesized to be a result of signaling molecules being permitted to accumulate during breaks in the flow regime. Following just 24 hrs of stimulation, cells expressed higher levels of osteoblastic differentiation markers 13 days later; however the flow regime did not affect these markers. Thus shear may have a powerful effect on MSC differentiation after just a short regime, and the nature of the shear regime could have an outcome on the differentiation pathways, especially if this regime in enacted over a long period of time. Shear stress also upregulated cyclooxygenase-2 (COX-2) expression [40]. COX-2 regulates PGE_2 production. This in turn can then regulate the BMP

signaling pathway through binding to cell surface receptor prostaglandin E receptor 4 (EP4) [123]. Thus osteoblastic differentiation can be upregulated by fluid shear stress through regulation of the BMP signaling pathway.

MSC chondrogenic differentiation is also highly influenced by exposure to shear stresses [115, 124-126]. Similar to osteoblastic differentiation chondrogenic differentiation is also regulated by MAPK activation [127, 128]. While both dynamic loading and shear upregulate chondrogenic markers, blocking ERK1/2 and p38 activation diminished the effects on most of these markers. Shear induced chondrogenic differentiation is also regulated through COX-2 to regulate PGE2 production via c-Jun N-terminal protein kinase (JNK2) and c-jun [129]. JNK as well as ERK MAPK signaling cascades have been shown to influence Runx2 activation in chondrocytes exposed to dynamic loading [130]. Dynamic culture systems present the opportunity to leverage these effects on chondrogenic differentiation pathways to optimize production of MSC derived chondrocytes. Under fluid flow of 1 dyne/cm^2 chondrocyte production of type II collagen greatly increased and the tensile strength of the cartilage constructs was improved [131]. Mechanical loading of MSCs during chondrogenesis increased amount of collagen markers [132]. It is important to point out that optimal leverage of these pathways in bioreactor culture will not be a trivial matter as many different factors influence these pathways. Oxygen content in combination with shear [133], variation of shear throughout constructs, influence of supplements and growth factors in the media [132], and cell-substrate interactions [134] all will modify cell response. Thus tissue engineers must carefully consider differentiation pathways along with shear and oxygen regimes to tightly control stem cell fate. Bioreactors must then be designed to

accommodate osteoinductive and osteoconductive scaffolds, to utilize growth factors and supplements, and to deliver shear and oxygen in a controlled manner for the direction of MSC differentiation.

4.3.1 Shear Stress Mediated Signaling

In order to fully leverage the role of shear stress in dynamic culture systems, the signaling mechanisms that depend on these stresses must be understood. While the role of mechanical forces in hMSC tissue engineering and regenerative medicine has been well observed, the signaling pathways involved in converting mechanical stress to biochemical signals in dynamic cultures systems is studied far less frequently.

4.3.1.1 Shear Stress Mediated MAPK Signaling

A primary signaling pathway influenced by shear stress is mitogen activated protein kinases (MAPKs) which are highly involved in the differentiation of MSCs and include the ERK 1/2, JNK, and p38 pathways (Figure 4.2). The mechanisms of MAPK signaling have been extensively reviewed elsewhere [135-141]. Briefly the general mechanism consists of three kinase molecules that bridge the cellular signal from the cell surface deep into the cytoplasm and nucleus. Signaling from the cell surface, usually in the form of growth factors including the TGF- β/BMP family, bind to a receptor tyrosine kinase (RTK). The binding causes a conformational change that allows the receptor to self-phosphorylate. Adaptor proteins bind to these phosphorylated tyrosines and in turn activate a GTPase such as Ras [142]. This GTPase phosphorylates the first member of the MAPK pathway, a MAPK Kinase Kinase (MAPKKK). This MAPKKK in turn

phosphorylates a MAPKK who then phosphorylates the MAP kinase itself be it ERK 1/2, p38, or JNK. This MAPK then phosphorylates its downstream targets.

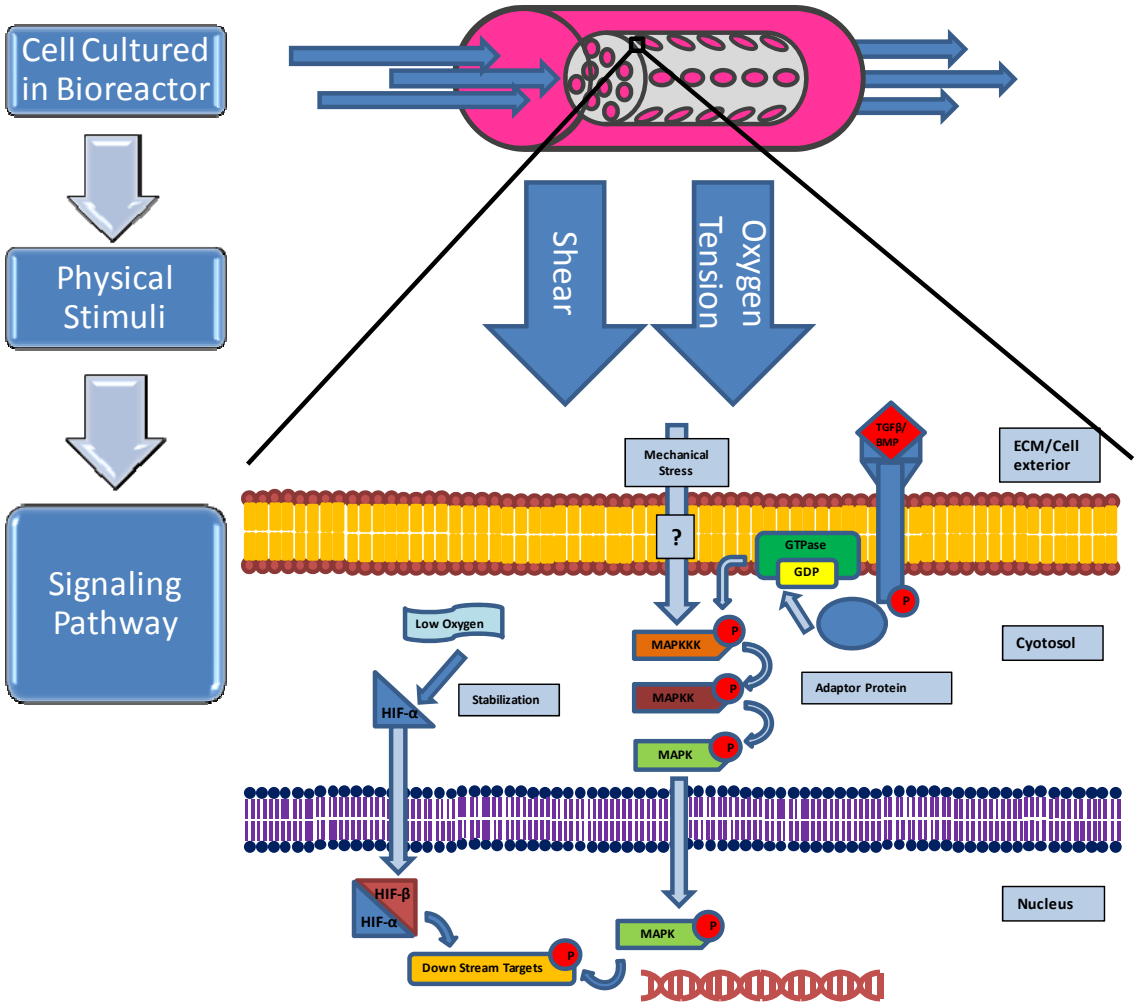

Figure 4.2: Demonstration of signaling influenced by culture conditions in a perfusion system. Shear stress and controlled oxygen tension provide stimulus to cells growing on three dimensional scaffolds. This in turn influences HIF (left) and MAPK (right) signaling pathways.

The ERK, JNK, and p38 pathways are all activated in osteogenic differentiation of MSCs [143, 144] and can be impacted via shear stress. Signaling via these three pathways is also activated during TGF-β induced chondrogenesis, and inhibition of any of the pathways resulted in partial or complete inhibition of chondrogenesis [145-147]. Another

aspect crucial to augmenting MAPK signaling pathways is the specific time of activation along the MSC differentiation progression.

While ERK 1/2 remains relatively active during a substantial portion of the differentiation process, the JNK and p38 pathways are more specific [148]. The JNK pathway is activated much later in hMSC differentiation and is associated with matrix deposition [148]. A recent study demonstrated that the JNK pathway inhibits early and late osteogenic differentiation [149]. In osteoblasts, the BMP/TGF-β activation of the p38 and ERK 1/2 pathways occurs within the first few hours, whereas the JNK pathway was activated later [150]. The p38 pathway was shown to up-regulate osteogenic genes such as ALP and Osterix (Osx) but down-regulate OC, a late osteoblastic marker, indicating it is inhibitory to late osteoblast maturation [142, 151, 152]. Future studies should focus on better understanding the different activation timings of different signal pathways involved in MSC differentiation. In this way shear could potentially be delivered in a temporal manner to best stimulate this signaling pathway for osteoblastic differentiation.

4.3.1.2 Mechanotransduction in Mesenchymal Stem Cells

In vivo bone and cartilage are constantly exposed to mechanical forces and the transmission of these signals is known as mechanotransduction [153-156]. Channel proteins including calcium ion channels, G-Proteins imbedded in cell membrane, and integrins all have a significant role in mechanotransduction [157]. Mechanistically, mechanical shear created by fluid flow has been shown to promote osteogenesis via the ERK 1/2 pathway through up-regulation of Runx2. Fluid flow up-regulated expression

of β1 integrins via a signaling pathway involving activating nuclear factor kappa B (NF-KB) indicating a possible pathway for fluid-induced mechanotransduction [158]. In another study fluid shear was shown to upregulate MAP3k8, a MAPKKK as well as growth factor interleukin 1-beta. This indicates that not only are mechanical stresses involved in pathway activation, but also in the upregulation of the proteins these pathways depend on [159]. Oscillatory fluid flow was also show to cause an influx of calcium that corresponded to enhanced differentiation and proliferation of MSCs as well as promote osteogenic genes in osteoblasts themselves. This indicates that calcium signaling, which could be mediated by a mechanosensitive protein channel, also plays a role in MSC differentiation and function [160-162]. A role for focal adhesions in MSC differentiation has also been demonstrated. When focal adhesion kinase function was inhibited, both Runx2 and osterix function was significantly impaired and the hMSCs were prevented from undergoing osteogenesis [163]. Focal adhesions are important "signaling hubs" for mechanotransduction, and this role in osteogenesis suggests that they may serve a similar function in MSCs. As MSCs are more and more frequently cultured in dynamic culture systems the specific mechanisms of *in vitro* mechanotransduction must be understood to better more effectively culture and differentiate these cells.

4.3.1.3 Wnt Signaling as a Regulator of Stem Cell Fate

Wnt signaling has been identified as a key signaling pathway to determine MSC differentiation or proliferation (Figure 4.3) [164-166].

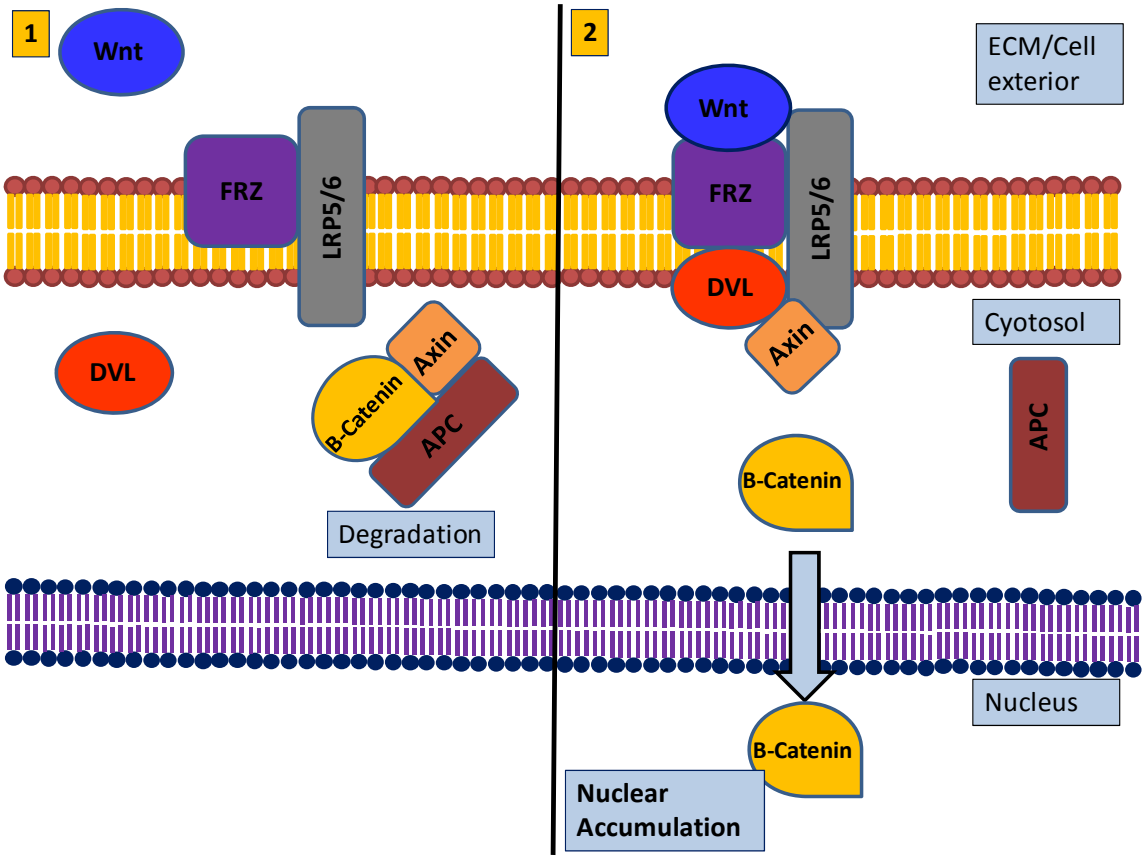

Figure 4.3: Overview of canonical Wnt signaling pathway. Wnt proteins bind to a receptor of the frizzled family which in turn causes the recruitment of Disheveled forming a receptor complex. LRP is a protein believed to stabilize the complex. This receptor complex causes the disassembly and inactivation of a protein complex, which degrades β-Catenin, by binding to Axin, a protein crucial to the degradation complex. This causes a buildup of β-catenin and accumulation in the nucleus where the molecule impacts gene transcription.

Wnt signaling is carried out through a diverse number of pathways and molecules; however there are two general classifications that Wnt signaling is divided into. If the pathway creates its effect through the accumulation of β-Catenin in the cell, and thus the nucleus, the signaling is referred to as canonical signaling. If the Wnt signal protein uses a different pathway it is categorized as non-canonical. Wnt signaling begins with the binding of a Wnt protein to cell-surface receptors which are a part of the Frizzled (FRZ) family of proteins. The major role canonical Wnt signaling has is to maintain cell

potency, especially regarding stem cells. Differentiation of any kind is inhibited in a rate dependent manner with increased levels of canonical Wnt signaling, which promotes cellular proliferation as well as reduces cellular apoptosis [165-167]. MSCs in the process of differentiating are more resistant to the inhibitory effects of canonical signaling because signal pathways and transcription factors related to osteo/chondrogenic differentiation downregulate and inhibit canonical signaling. Sox9 inhibits activation of B-catenin promoters and promotes the molecule's degradation [168]. Runx2 has a similar effect [169]. JNK, p38, and ERK1/2 signaling induced by TGF-B down regulates canonical Wnt signaling as seen by an increase in B-catenin after MAPK inhibition.

Unlike canonical Wnt signaling, non-canonical Wnt signaling does not use β-catenin as its method of affecting gene transcription and has been shown to directly promote both osteogenesis and chondrogenesis [166]. Mechanistically, this difference is likely due to the differences in signal cascades used. For example several non-canonical Wnts have been shown to activate the JNK and p38 pathways as well as activate Rho; all of which are important in TFG-β/BMP signaling. Non-canonical Wnt signaling diverges from the canonical pathway at Disheveled where in this case it activates the JNK pathway instead of events leading to the accumulation of β-catenin [137]. Non-canonical Wnt 4a promotes osteogenesis through the activation of the p38 pathway [170]. Non-canonical Wnt signaling has been shown to be upregulated by fluid shear in osteoblasts [171], however little work has done to study Wnt signaling in MSCs grown in bioreactor systems. Investigation of this key pathway could lead to another avenue to direct MSCs to proliferate or differentiate in bioreactor systems.

4.3.1.4 Downstream Targets Influenced by Dynamic Culture

While stimuli in dynamic culture affect different steps along signaling pathways, downstream targets are typically analyzed by tissue engineers as a metric to determine study outcomes. Understanding of these downstream targets and how they relate to signaling pathways is key to understanding the mechanisms influencing dynamic culture mediated signaling pathways. The activity and upregulation of several key transcription factors including Runx2 and Osx for osteoblasts and Sox9 for chondrocytes are vital to MSC commitment down a specific lineage. Runt-related transcription factor 2 (Runx2), also known as cbfa1, is the "master control" for osteogenesis as it up-regulates extracellular matrix (ECM) proteins as well as other downstream transcription factors such as osterix. In the nucleus, the SMAD complex associates with Runx2 to form a new transcription complex that is essential for both BMP and TGF-B induced osteogenesis (Figure 4.4) [172].

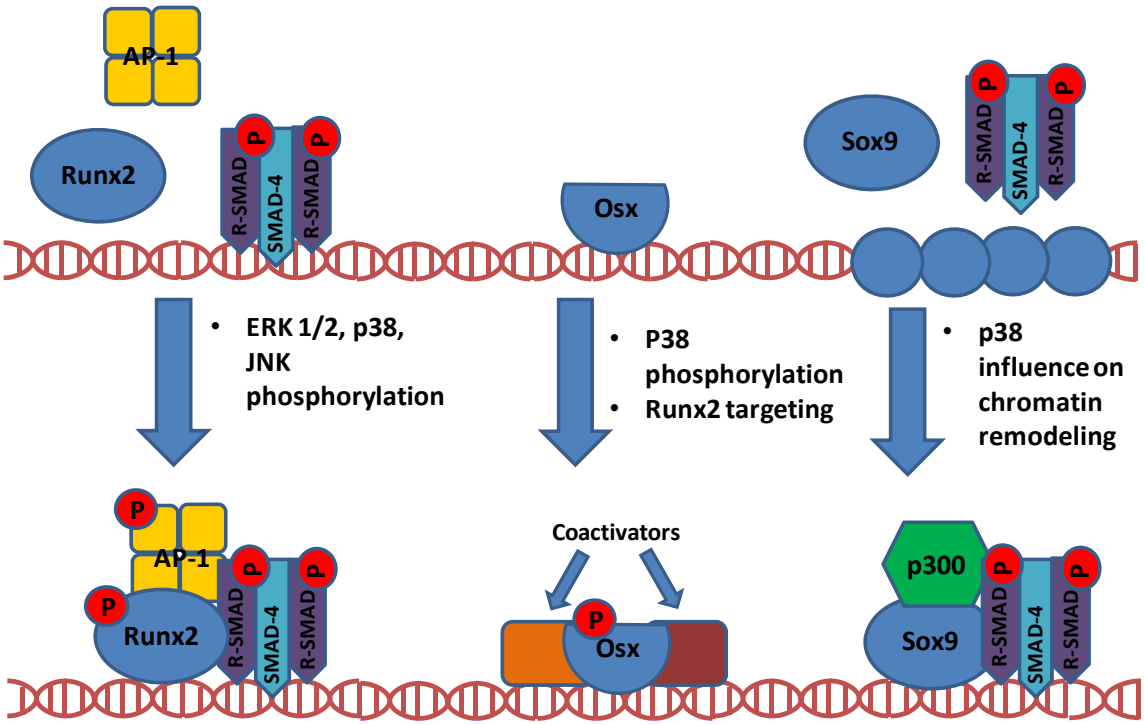

Figure 4.4: A simplified diagram of signal pathway convergence at downstream nuclear targets. It is important to note that these figures depict only the specific interactions explained in this paper and that there are numerous other proteins involved in these complex as well as multiple combinations of these complexes.

The major downstream targets of another pathway mediated by mechanical forces, the JNK pathway, are AP-1 proteins, namely C-jun [135, 137]. The SMAD and JNK signaling pathways converge at AP1-binding promoter sites where C-jun and C-fos associate with SMAD proteins to mediate TGF- β and BMP induced gene transcription [142, 173]. AP-1 proteins C-fos and C-jun have also been shown to be capable of directly interacting with Runx2 to regulate gene transcription as well [174]. Downstream of Runx2 is Osx a transcription factor that becomes active later in the osteogenic differentiation pathway [175]. It was demonstrated that inhibition of the ERK 1/2 pathway did not inhibit Runx2 expression but did inhibit Osx expression, however this could simply be that this MAPK pathway phosphorylates Runx2 promoting it and thus its

downstream targets, including Osx [151]. Inhibition of the p38 MAPK pathway was shown not to inhibit mineralization but it did significantly downregulate Osx [151]. Osx was the only transcription factor related to osteogenic differentiation that was downregulated in response to p38 inhibition [176]. Osterix is a substrate of p38, and that phosphorylation of the transcription factor improves its ability to recruit co-activators [177].

In cartilage development SRY-type high mobility group box 9, or Sox9, is the major transcription factor for the chondrogenic lineage, upregulating lineage specific genes such as aggrecan and collagen II [162, 178, 179]. SMAD complexes facilitate Sox9-dependent transcription in a similar manner to Runx2, by associating with the transcription factor and a cofactor, in this case CBP/p300, in order to regulate gene expression [180]. The p38 pathway has been shown to promote Sox9-dependent transcription by facilitating the formation of the SMAD/Sox9/p300 complex via one of its downstream substrates, MSK1 who plays a role in remodeling chromatin [181]. This indicates that the p38 pathway facilitates complex formation by affecting the exposure of DNA binding sites rather than direct interaction with the complex itself. While examination of these downstream targets such as Sox9, Runx2, Osx as well as markers and growth factors including BMP-2, TGF-β, ALP, OPN and OCN, are typically assayed, upstream signaling mechanisms must also be understood to determine how dynamic culture is affecting MSC differentiation.

4.4 Bioreactors to Mediate Oxygen Content

Though shear is often the focus of dynamic culture studies, oxygen is also a powerful mediator of mesenchymal stem cell fate [182-188]. In their undifferentied state in the bone marrow mesenchymal stem cells are maintained in an environment of approximately 7% oxygen tension [189]. Chondrocytes reside in an avascular environments with oxygen tensions from 1-3% [190]. The oxygen tension of the native environment of bone is higher at approximately 12%, but can drop significantly during fracture [191, 192]. However mesenchymal stem cells are cultured in an *in vitro* environment of 20% oxygen tension with any lower oxygen tension typically referred to as hypoxia. When MSCs are cultured in three dimensional scaffolds the oxygen tension becomes much more complex. An oxygen gradient can form as cells on the outer layers of the scaffold consume oxygen, leaving cells in the inner regions of the scaffold with an anoxic or hypoxic environment. In three dimensional culture oxygen content can begin to significantly drop after just hundreds of microns. In scaffolds with a minimum diameter of just 5 mm, central oxygen concentrations dropped to 0% after just 5 days of culture [21]. This drop in oxygen content led to massive cell death of the pre-osteoblast cell line being cultured. Bioreactor culture was then used to mitigate these transport insufficiencies and cell viability improved. This highlights a critical need of bioreactor systems to regulate oxygen content. However the role of oxygen is greater than a required nutrient; it can act as signaling molecule to affect stem cell fate.

Despite strong evidence that oxygen tension can regulate stem cell proliferation and differentiation, regulation of oxygen content throughout three dimensional of a scaffold is difficult. Bioreactor culture can be used to create a regulated oxygen environment for the

maintenance or differentiation of mesenchymal stem cells. In a modular bioreactor system equipped with a probe to measure oxygen, a 20% oxygen content was used for the adipogenic differentiation of hMSCs, while a 5% oxygen content was used for chondrogenic differentiation [121]. Compared to the opposite oxygen concentrations, this oxygen regime proved to increase the expression of both chondrogenic and adipogenic markers. Bioreactors such as this could be used as a powerful tool to control stem cell fate. Even within bioreactor cultured constructs oxygen content can vary throughout scaffolds, thus careful monitoring throughout the scaffold may be necessary. As an alternative to continuous oxygen monitoring mathematical models can be developed to predict oxygen content throughout scaffolds [84]. Mathematical models for oxygen distribution throughout scaffolds could then be combined with oxygen monitoring to offer tight control in bioreactor systems. One bioreactor using an oxygen monitoring system has been able to culture hMSCs to produce a large construct with bone forming potential [16]. Though this bioreactor did not actively control oxygen in addition to actively monitoring it the technology exists to create a bioreactor to actively monitor and control oxygen content [16, 84, 193, 194].

4.4.1 Signaling Mediated by Oxygen Concentration

Examples of the influence of oxygen content on mesenchymal stem cell fate are quite prevalent. When rat MSCs were cultured in 5% oxygen compared to the standard 20% oxygen the cells proliferated more rapidly. In addition the 5% oxygen cultures exhibited an increase in common osteoblastic markers including alkaline phosphatase (ALP), and calcium content. When implanted *in vivo* these cells cultured in low oxygen content led to a greater amount of *in vivo* bone formation [195]. In a study culturing human

mesenchymal stem cells under 2% oxygen proliferation was greatly increased [196]. In addition to proliferation increases an increase of mRNA Oct-4, a stemness gene, expression was noted with hypoxia. This increase was concurrent with an increase in hypoxia inducible factor 2α (HIF-2α) indicating a possible mechanism by which oxygen regulates stem cell fate. Though these results were obtained in two-dimensional culture, similar results were acquired when the hMSCs were exposed to 2% oxygen in three dimensional culture [197]. In a recent study culture in 1% oxygen was shown to increase expression of stemness genes Oct4, Nanog, Sall4 and Klf4 of hMSCs compared to 20% [198]. Interestingly the osteogenic potential was increased when cultured under 1% oxygen conditions in induction media, but chondrogenic and adipogenic capacity were reduced. In another study utilizing hMSCs 3% oxygen increased the proliferative lifespan of hMSCs, but was shown to reduce their differentiation potential [199].

In addition to osteoblastic differentiation oxygen concentration mediates MSC chondrogenic differentiation. Cells expanded in 2% oxygen compared to 20% have been shown to have greater chondrogenic potential than osteoblastic [200]. Similar results are ascertained when comparing 3% oxygen tension to 20% tension cultured MSCs [201]. As a possible mechanism for increased chondrogenesis of MSCs HIF-1α was evaluated [202]. After rat MSCs were cultured under 2% oxygen and induced to undergo chondrogenesis, differentiation was enhanced in the 2% cultured cells. However, when HIF-1α was knockdowned using siRNA no upregulation of chondrogenesis was observed. The shift to chondrogenesis over osteogenesis was thought to occur via p38 mitogen activated protein kinase [203]. In bioreactor culture mechanical forces via dynamic shear or mechanical loading also play and important role [133]. However when

compared directly to each other oxygen content played a greater role than dynamic compression as MSCs cultured at 5% oxygen in agarose gels showed a greater tendency toward chondrogenesis than cells cultured under dynamic compression in 20% oxygen tension [133]. These findings are important in dynamic culture where both mechanical forces and oxygen regulation could be regulated concurrently.

Even beyond the ability for oxygen content to control stem cell proliferation oxygen content may have a role in cell organization within a construct and cell subpopulations. *In vivo* chondrocytes are organized into three zonal subpopulations the superficial, middle and deep [204]. Chondrocyte subpopulations in these zones have distinct phenotypes and can respond differently to substrate properties and growth factors [164, 205]. Zonal phenotype can also be retained by oxygen content [206]. Though this study was completed on adult chondrocytes it is possible oxygen may play a role in MSC chondrogenic differentiation into zonal subpopulations and proper oxygen maintenance could yield a greater deal of phenotype control leading to a more functional cartilage construct.

It is important to point out that aside from mediating signaling mechanisms bioreactor maintenance of oxygen in 3D scaffolds is necessary to sustain stem cell phenotype. In a recent study using human mesenchymal stem cells exposure to oxygen tensions less than 1% for just 48 hrs led to a long term downregulation of osteoblastic markers including Runx2, osteocalcin, and type 1 collagen [191]. Thus even temporary lack of oxygen can cause permanent loss of bone forming potential. If this lack of oxygen is combined with a lack of nutrients, massive cell death will occur [207]. Thus proper maintenance of

oxygen concentrations is crucial to maintain stem cell viability and phenotype. Further maintenance above minimum levels may lead to an increased control of stem cell fate.

4.4.1.1 Oxygen Regulation of Stem Cells via HIF

Hypoxia-inducible factor (HIF) is the major transcription factor for a cellular response to hypoxia. Like other cell types, hypoxia causes the activation of HIF in MSCs [202]. HIF is made of two subunits: β and α. While HIF-β exists in stable amounts in both the nucleus and cytosol, HIF-α, which resides in the cytosol normally, is degraded under normoxia. HIF-α is allowed to stabilize in hypoxic conditions and translocate into the nucleus where it can bind to HIF-β. Once dimerized, HIF recruits coactivator proteins and facilitates the transcription of a wide variety of genes (Figure 5.2) [208].

A recent study has yielded a possible mechanism for the reduction in osteoblastic differentiation potential observed in cells exposed to hypoxia. When hMSCs were cultured under 1% hypoxia under osteogenic induction conditions, osteoblastic differentiation of human MSCs was downregulated compared to cells cultured at 20% oxygen [209]. Hypoxia was shown to decrease expression of Runx2, which then led to downstream reduction of osteoblastic genes including osteocalcin, osteopontin, collagen Type I alpha 1, bone sialoprotein (BSP), and alkaline phosphatase. This downregulation was shown to be mediated by HIF-1α via TWIST, a downstream target. TWIST was discovered to bind to the Runx2 P2 promoter, suppressing transcription of Runx2. This in turn inhibits expression of Runx2 downstream targets. The same group further investigated HIF-TWIST and found that though osteoblastic differentiation was downregulated during hypoxia, MSC proliferation and phenotype maintenance were

increased [210]. When cultured under 1% oxygen tension hMSCs exhibited a more efficient expansion profile. The differentiation potential of these cells was maintained even at late passages, while cells cultured in 20% oxygen exhibited a decreased differentiation potential. In addition hMSCs grown under hypoxia had both an increased differentiation potential and bone repair capacity when implanted into an *in vivo* mouse model. This increased differential potential was shown to be regulated through p21 by transcription factor E2A. P21 activation leads to cellular senescence and was shown to be downregulated by HIF-1α via TWIST in response to a hypoxic environment. These two studies provide evidence for a mechanism by which oxygen content regulates stem cell fate. While a low oxygen environment inhibits osteoblastic differentiation, it increases proliferation and stem cell phenotype maintenance. In addition to osteoblastic differentiation cells under hypoxia were shown to better differentiate into adipocytes as well after culture in 5% oxygen compared to 20% oxygen [211]. This was due to a variety of genetic changes that maintained an undifferentiated state.

Though HIF can inhibit osteogenesis it can have a stimulatory effect on chondrogenesis. Sox9 is a target of HIF regulation and chondrogenesis was shown to be significantly enhanced when MSCs were exposed to hypoxic condition [202, 212]. Hypoxia (2% oxygen) triggered the activation of the p38 pathway and inhibition of it inhibited HIF-α stabilization [202]. Activation of the JNK pathway has also been shown to be required for HIF-dependent signaling and transcription, indicating a role for MAPKs in the response of MSCs to oxygen tension [213]. When HIF- α function was silenced by siRNA, the increased upregulation of chondrogenic genes such as proteoglycan and collagen II due to hypoxia was absent [202].

HIF offers a mechanism by which oxygen can mediate stem cell fate. In bioreactors with the ability to regulate oxygen content, regimes could be developed to foster proliferation followed by osteogenic or chondrogenic differentiation. In this manner bioreactor systems could be made even more effective for the culture of three dimensional MSC containing constructs.

4.5 Conclusion and Future Directions

Dynamic culture of MSCs has expanded greatly in the last ten years and bioreactor culture is now widely used. In addition bioreactor design has advanced considerably including bioreactors to measure oxygen content [16], culture anatomically shaped grafts [15], and develop prevascular networks [121, 214]. Bioreactor culture creates a more efficient means to culture MSCs and provides for the differentiation to chondrocytes and osteoblasts in an environment more similar to native tissue. The signaling cascades covered in this review provide a mechanism for this differentiation. However, despite the volume of work on stem cell signaling mechanisms there still is research to be done on how these pathways are affected in dynamic culture systems. This knowledge could be improved by a greater emphasis on experiments designed to characterize these pathways in clinically relevant situations. Much of the work regarding signaling pathways has been completed with cell lines and two-dimensional culture, while emphasis in the tissue engineering community is placed on primary cells grown in clinically relevant situations including bioreactors and biocompatible three dimensional scaffolds. However many tissue engineering experiments are designed to be outcome oriented and do not evaluate mechanisms and pathways in great detail. Since cell-substrate interactions and dynamic culture can have a profound effect on signaling mechanisms, evaluating these

mechanisms in situations relevant to tissue engineering is paramount to understanding ways to leverage these mechanisms to create *in vitro* engineered tissue. Thus greater communication and collaboration between labs with expertise evaluating MSC signaling and those developing new bioreactor culture systems should be undertaken to design the proper experiments to evaluate how bioreactor culture is augmenting these signaling pathways. In this manner a relationship between oxygen content, shear, and stem cell differentiation could be developed. Following this development, advanced bioreactor systems with the ability to temporally regulate oxygen content and mechanical stimuli could be used to augment these signaling pathways and optimize creation of *in vitro* engineered tissue.

Chapter 5: Tubular Perfusion System for the Long Term Dynamic Culture of Human Mesenchymal Stem Cells[2]

5.1 Introduction

In vitro culture techniques of three dimensional scaffolds have limitations that must be overcome in order to increase the feasibility of cell based tissue engineering strategies. The central limitation in static culture is insufficient transport of oxygen and other nutrients to regions more than a few hundred microns from the scaffold surface, which leads to non-homogenous cell distribution and extracellular matrix production [21, 25, 28, 215, 216]. Bioreactor systems overcome these barriers by increasing nutrient transfer to cells via dynamic culture. Furthermore, mechanical stimulation through fluid shear stresses has been shown to be influential on bone differentiation and mineralization [20, 27, 32]. Previous studies have demonstrated bioreactor systems to be an effective means to culture cells for bone tissue engineering purposes [10, 17, 18, 20, 22, 27, 29, 30, 42, 111, 217]. Several different types of bioreactor systems have been investigated, including spinner flasks [22-24], rotating wall bioreactors [24, 25], and perfusion systems [10, 14, 20-22, 29, 30, 60, 217]. Spinner flask and rotating wall bioreactor systems are effective at creating a homogenous media solution on the exterior of the scaffold, but do not effectively perfuse media into the scaffold. Perfusions systems have been demonstrated to effectively perfuse media throughout the scaffold and have been shown to upregulate osteoblastic markers and increase calcium deposition. In a study utilizing a

[2]As published in Yeatts, A.B. and J.P. Fisher, *Tubular perfusion system for the long-term dynamic culture of human mesenchymal stem cells.* Tissue Eng Part C Methods, 2011. **17**(3): p. 337-48.

perfusion bioreactor flow rate was shown to increase both the calcium matrix deposition and the rate of late osteoblastic differentiation as shown by osteopontin expression [20]. In a subsequent study dextran was used to increase fluid viscosity, thus increasing fluid shear while keeping flow rate constant. Results of this study revealed calcium deposition increased with shear indicating the stimulatory effects of the bioreactor culture were largely due to fluid shear stresses [17]. In a different study the effects of both mass transport and shear stress on human bone marrow stromal cells were evaluating using a similar means to modify the viscosity. This study revealed that cell growth and differentiation in the bioreactor system were enhanced by both mass transport and shear stresses [80].

Perfusion systems typically enhance the flow of media to the center of the scaffold, but require custom made parts and specific scaffold design in order to successfully perfuse media into the scaffold, which can make them difficult to fabricate and use. To this end we have developed a new tissue engineering bioreactor, the tubular perfusion system (TPS) that creates a more effective environment for cell culture. In the TPS design, human mesenchymal stem cells (hMSCs) are encapsulated in alginate beads which are tightly packed in a tubular growth chamber. Though it is more frequently used for cartilage tissue engineering [106, 108, 109, 218], alginate is used as a scaffold because of its ability to be dissolved with a calcium chelating agent and the ease of which it can be formed into spherical scaffolds [219]. Alginate has previously been shown to support proliferation and osteoblastic differentiation of marrow stromal cells [220]. In addition alginate has been used for bone tissue engineering purposes including supporting 2D osteoblastic differentiation of marrow stromal cells, delivery of BMP-2 transfected bone

marrow stromal cells, the delivery of antibiotics and MSCs to bone injury sites, and mineralization of hMSCs in RGD modified microspheres [221-224]. Mesenchymal stem cells are used as a promising cell source for bone tissue engineering [225]. The packed scaffold design in the growth chamber is based on the packed or fixed bed bioreactor commonly used for the bulk production of recombinant proteins by mammalian cells [226, 227]. The tubular growth chamber design is more commonly used for the tissue engineering of vascular grafts, where vascular tissue growth is directed around the outside of a scaffold or the walls of a growth chamber [228-231]. This system differs from other perfusion systems where media is pumped directly through a porous scaffold sealed in a growth chamber. The system also differs in design from bioreactors used in vascular grafts as cell growth occurs inside the scaffolds rather than the outside of a scaffold or along the growth chamber wall. To our knowledge this tubular packed scaffold design has not been previously used for bone tissue engineering purposes. In the TPS bioreactor media is perfused through the growth chamber, exposing the cells to shear stress. This could potentially yield to a greater perfusion of nutrients into the scaffold than dynamic culture systems that focus on media mixing, while avoiding the technical difficulties such has high pressure, scaffold interconnectivity requirements, and leaking that can be associated with other perfusion systems. This system also provides for a potential clinical application as following extended culture the alginate can be dissolved leaving only cells and their extracellular matrix. The goal of this study is to (1) effectively develop this bioreactor system, (2) demonstrate its ability to support the growth and differentiation of hMSCs and (3) evaluate the effects of flow rate on late osteoblastic differentiation and matrix production.

5.2 Materials and Methods

5.2.1 Human Mesenchymal Stem Cell Culture

Human mesenchymal stem cells ($p \leq 5$) from a single donor were purchased from Lonza (Walkersville, MD). As this is an initial study, single donor cells were used to minimize variability associated with a primary cell population. Cells were cultured prior to the study in control media consisting of DMEM (Gibco, Carlsbad, CA) supplemented with 10% fetal bovine serum (Gibco), 1.0 % v/v penicillin/ streptomycin (Gibco), 0.1 mM non essential amino acids (Gibco), and 4 mM L-glutamine (Gibco) using protocols set forth by the manufacture and previously described [69, 232]. Cells were cultured on tissue culture polystyrene flasks with media changes every three days according to the manufacture's specifications. Cells were stored in a cell culture incubator at 37º C and 5% CO_2 and passaged every 6-7 days using trypsin/EDTA (Lonza). Osteogenic media was formulated as described in the literature by supplementing control media with 100 nM dexamethasone (Sigma, St. Louis, MO), 10mM β-glycerophosphate, and 173 μM ascorbic acid (Sigma) [69, 232, 233].

5.2.2 hMSC Encapsulation in Alginate

Alginate solutions of 2.0% w/v were prepared as previously described by adding alginic acid sodium salt from brown algae (Sigma), into 0.15M NaCl (Sigma), and 0.025M HEPES (Sigma) in deionized water [106, 108, 109]. The alginate solution was then sterilized via autoclave. hMSCs were removed from tissue culture flasks using trypsin/EDTA and pelleted via centrifugation at 500 xg for five minutes. The cell pellet was resuspended in the alginate solution at a density of 1.25-2.5 x 10^6 cells/mL. The

alginate cell solution was added drop wise through an 18 gauge needle into a stirred solution of 0.1 M calcium chloride (Sigma) which immediately crosslinked the alginate to form beads. Beads were allowed to stabilize for 15 minutes and cultured in six well plates in control media for 24 hours. On study day 0 bioreactor groups were loaded into the bioreactor while control groups were placed in new osteogenic or control media. Control group cells were cultured in five milliliters of media at five beads per well for the duration of the study with media changes every three days for all groups.

5.2.3 Bioreactor Design

The bioreactor system consists of a tubular growth chamber and media reservoir connected via a tubing circuit (Figures 5.1 and 5.2). Media flow was driven by an L/S Multichannel Pump System (Cole Parmer, Vernon Hills, IL) at 3 mL/min for short term studies and at either 3 mL/min or 10 mL/min for the long term study. The entire tubing circuit is partially assembled outside the hood and sterilized via autoclave. The circuit consists of platinum cured silicone tubing (Cole Parmer) for all areas except the area that passes through the pump which is composed of Pharmed BPT tubing (Cole Parmer) chosen for its high mechanical durability. Tubing is connected using silver ion lined microbial resistant tubing connectors (Cole Parmer) to reduce the risk of bacterial contamination. The growth chamber consists of a length of platinum cured silicone tubing (Cole Parmer) with an inner diameter of 6.4 mm, an outer diameter of 11.2 mm and a wall thickness of 2.4 mm. The platinum cured silicone tubing was chosen for its low chemical leachability, minimal protein binding, and high gas permeability to allow for the easy exchange of carbon dioxide and oxygen. The growth chamber was 13 cm in length and was packed with thirty cell seeded alginate beads using a sterile spatula.

Growth chamber tubing connectors were modified by adding 60 mesh stainless steel screens (Fisher Scientific, Pittsburgh PA) to restrict bead movement. Following loading the autoclaved tubing was fully assembled inside a cell culture hood and then placed in a cell culture incubator at 37º C and 5% CO_2. Fifty mL of osteogenic media was loaded into separate 125 mL Erlenmeyer flasks for each growth chamber topped with rubber stoppers. Media is withdrawn and replaced from the reservoir through two tubes that penetrate the stopper and changed every three days by moving the bioreactor into a sterile culture hood, removing the media in the reservoir, and replacing it with fresh media. This provides for a change of 85% of the media. Beads are removed from the bioreactor by moving the entire bioreactor system into the hood, disconnecting one tubing circuit and flushing beads out of the growth chamber with phosphate buffered saline (PBS).

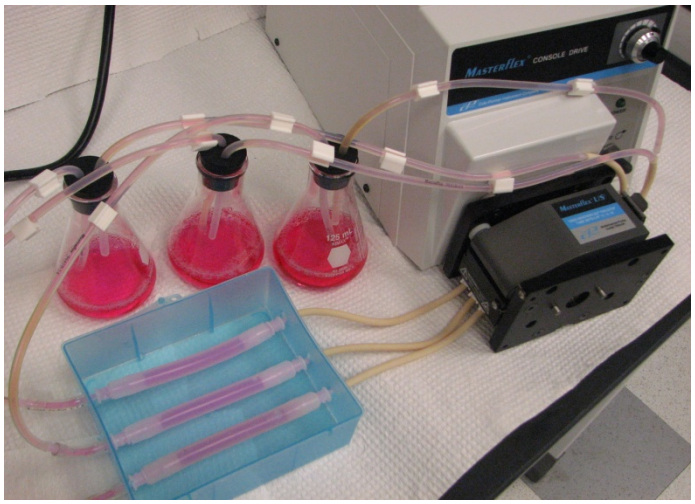

Figure 5.1: Image of the entire bioreactor system. Note entire system is stored in cell culture incubator.

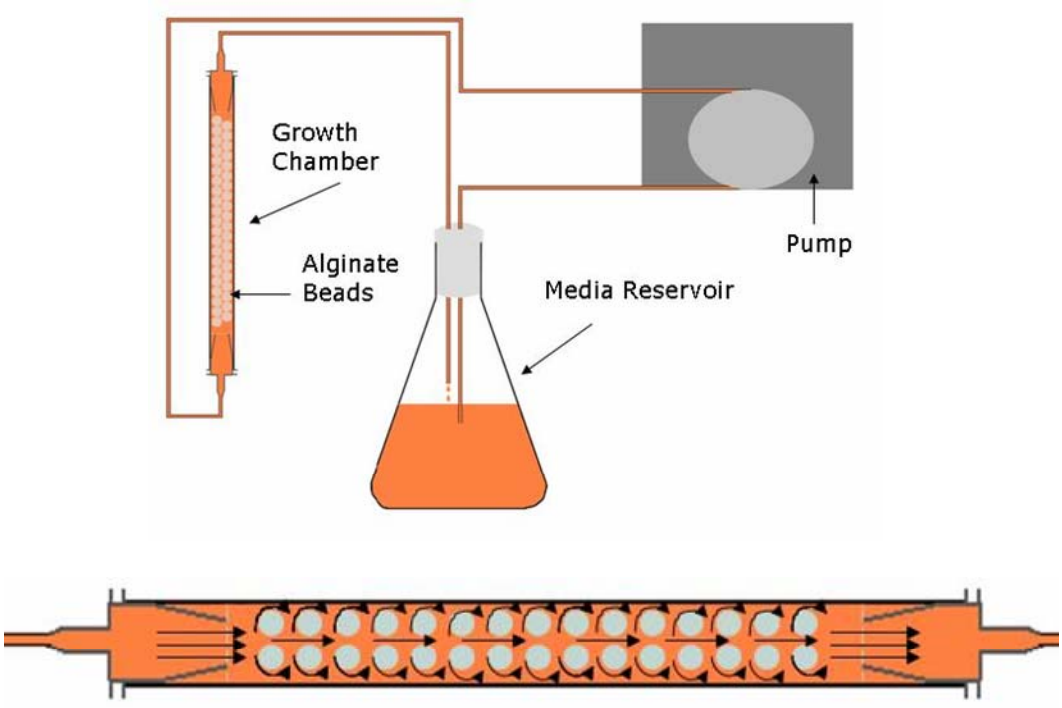

Figure 5.2: Schematic of the bioreactor system (top). Media is stored in the reservoir and perfused in and around the alginate beads (bottom) by the peristaltic pump.

5.2.4 Experimental Setup

On study day 0 bioreactor groups were loaded into the bioreactor while control groups were placed in osteogenic or control media. Control group cells were cultured in 5 mL of media at 5 beads per well for the duration of the study with media changes every three days for all groups. For all groups 5 beads were used for each replicate and 3 replicates were taken for each sample. In the TPS bioreactor different experimental groups and timepoints were cultured in different growth chambers while replicates were cultured in the same growth chamber. Short term proliferation and differentiation studies were conducted for eight days with time points on days 1, 4, and 8. Cell count data was not taken on day 1 but instead was taken on day 12 to provide more extended cell proliferation data. For all short term studies a group consisting of hMSCs cultured in the

TPS bioreactor at a 3 mL/min flow rate was compared to hMSCs cultured in alginate in static conditions in osteogenic and control media. For long term studies time points were taken at days 14 and 28 to evaluate late osteoblastic differentiation. Experimental groups consisted of hMSCs cultured in the bioreactor at both 3 mL/min and 10 mL/min flow rates. These groups were compared to a static osteogenic control as the goal of this study was to evaluate the effect of flow rate on late osteoblastic differentiation.

5.2.5 Mathematical Model of the Tubular Perfusion System

In order to determine flow velocities and calculate shear stresses a two-dimensional steady state Navier-Stokes model of the tubular perfusion system was developed using COMSOL Multiphysics Version 3.5 (COMSOL, Burlington MA). Initial flow into the growth chamber was modeled assuming fully developed flow. Walls of alginate beads were modeled as no slip and media was assumed to have a dynamic viscosity of 0.78 centipoise and a density of 0.993 grams/cm^3 [234]. Boundary shear stresses were calculated using the formula $\tau = \mu(\partial v/\partial y)$ where μ is the dynamic viscosity of the media, v is the velocity of fluid at the bead surface and y is the height of the boundary layer. The Sherwood number was calculated according to the standard equation for forced convection around a solid sphere with a diffusion coefficient of 2.56 x 10^{-9} m^2/sec [235-237]. Diffusion of oxygen through alginate scaffolds was calculated using a COMSOL model with an oxygen diffusion coefficient in media and alginate of 2.56 x 10^{-9} and 2.08 x 10^{-9} m^2/sec respectively [237]. hMSC cell respiration was modeled using Michaelis-Menten kinetics with an oxygen consumption rate of 0.012 μmol/10^6 cells/hr, and a saturation constant of 0.011 mol/m^3 [84]. For static culture media oxygen concentration was fixed at 0.21 mM at the media air interface and oxygen transport was

modeled through the well and the bead [238]. The ratio of air interface to bead surface area in the static model was modeled to reflect the ratio that exists in *in vitro* culture. Based on the Sherwood number indicating convective transport dominates diffusive transport the bioreactor beads were modeled as having a homogenous saturated oxygen concentration at the exterior. Boundary conditions in static culture model consisted of insulation at the three walls of the well plate and a fixed concentration of 0.21 mM at the media air interface. A continuity boundary was used for the alginate beads. All figures are shown at steady state.

5.2.6 hMSC Isolation from Beads

At each time point hMSCs were isolated from the beads by incubating the beads for 25 minutes at 37º C in 4 mL 0.025-0.1M ethyldiaminetetraacetic acid (EDTA) (Sigma) [109]. The cell solution was placed in a 15 mL falcon tube and centrifuged at 8000 xg for 8 minutes to form a cell pellet. The pellet was then resuspended in PBS.

5.2.7 DNA Quantification

DNA was extracted at each time point using the following procedure previously described in the literature [239]. Isolated cell pellets were resuspended in 200 uL of PBS isolated using a DNeasy Tissue Kit (Qiagen, Valencia CA) following standard protocols to produce 400 uL of eluate. Double stranded DNA was then quantified by mixing 100 uL of DNA eluate with 100 uL of diluted Quant-iT PicoGreen dsDNA reagent (Molecular Probes, Carlsbad, CA), incubating for five minutes in the dark and measuring fluorescence using an M5 SpectraMax plate reader (Molecular Devices, Sunnyvale, CA) with excitation/emission of 480/520 nm. All samples were preformed in triplicate (n=3).

5.2.8 Cell Counts

hMSCs were isolated from beads. Cell samples were removed, mixed with trypan blue (Sigma), and counted on a standard hemocytometer. Four counts were made for each sample (n=4).

5.2.9 Live Dead Assay

Cell viability was assessed using a live dead assay following standard protocols as described previously [239]. Beads were first soaked in PBS for 60 minutes to remove FBS and media. Dead controls were soaked in 70% methanol (Sigma) instead of PBS. Beads were then placed in 48 well plates and incubated in 2 μm ethidium homodimer and 4 μm calcein AM (Molecular Probes) for thirty minutes. Fluorescent images were then taken of the entire bead using a fluorescent microscope (Axiovert 40 CFL with filter set 23, Zeiss, Thornwood, NY) equipped with a digital camera (Diagnostic Instruments 11.2 Color Mosaic, Sterling Heights, MI). Live dead images of cross sections were not taken.

5.2.10 Quantitative Reverse Transcriptase Polymerase Chain Reaction (qRT-PCR)

RNA was extracted using an RNeasy mini plus kit (Qiagen) following standard protocols. The isolated RNA was then reverse transcribed to cDNA using a High Capacity cDNA Archive Kit (Applied Biosystems, Foster City, CA). The expression of bone morphogenetic protein-2 (BMP-2, Taqman Assay ID: Hs00154192_m1), osteocalcin (OCN, Hs01587813_g1), osteopontin (OPN, Hs00960641_m1) and alkaline phosphatase (ALP, Hs00758162_m1) was analyzed with glyceraldehyde-3-phosphate dehydrogenase (GAPDH, Hs00960641_m1) as an endogenous control gene for all samples. The

sequences are propietary. Gene expression assays (Applied Biosystems) were combined with the cDNA to be analyzed and Taqman PCR master mix (Applied Biosystems). The reaction was performed on a 7900HT real time PCR System (Applied Biosystems) using thermal conditions of 2 minutes at 50°C, 10 minutes at 95°C, and 40 cycles of 15 seconds at 95°C and 1 minute at 60°C. The relative gene expression level of each target gene was then normalized to the mean of the GAPDH in each group. For ALP the day 1 control media groups was used as a calibrator and for OPN, OCN, and BMP-2 the day 14 osteogenic media group was used as a calibrator. Fold change was calculated using the ΔΔCT relative comparative method as described previously [218, 240]. Samples were completed in triplicate and standard deviations are reported (n=3).

5.2.11 Histological Analysis

Alginate beads were collected and fixed in 4% paraformaldehyde (Sigma) and 0.1 M sodium cacodylate (Sigma) buffer containing 10mM $CaCl_2$ at pH 7.4 at 4° C for 4 hours. Following fixation, the beads were placed in cassettes and washed with 0.1M sodium cacodylate buffer and 10mM $CaCl_2$ at pH 7.4 at room temperature for 24 hours. The beads were then dehydrated for histological processing by ethanol washes followed by two Citrisolv (Fisher Scientific) washes. The samples were then embedded in paraffin (Fisher Scientific) and sectioned to 5 μm thickness sections and placed on glass slides. Sections were oven dried at 64° C for 2 hours, deparaffinized in Citrisolv and rehydrated in ethanol. Von Kossa staining was preformed to visualize mineralization using a Nuclear Fast Red (Poly Scientific, Bay Shore, NY) counterstain using standard protocols.

5.2.12 Statistical Analysis

All samples were completed in triplicate (n=3). Data was analyzed using single factor ANOVA followed by Tukey's Multiple Comparison Test assuming normal data distribution with a confidence of 95% ($p < 0.05$). Mean values of triplicates and standard deviation error bars are reported on each figure as well as relevant statistical relationships.

5.3 Results

5.3.1 Functionality of Bioreactor System

Throughout all experimental trials the bioreactor system was shown to be free of leaks and contamination. The current system can accommodate up to 4 independent tubing circuits and growth chambers. This allows for easy analysis of cells as 1 chamber can be removed without affecting the remaining chambers. Tubing connections were completed using silver ion coated polyvinylidene fluoride fittings which provide a secure yet highly customizable means to connect components of the system. The bioreactor system was quickly setup and scaffolds were easily removed for analysis. A two dimensional model of the growth chamber was completed and revealed the average shear stress at the bead surface to be 0.98 ± 0.08 dynes/cm^2 with a 3 mL/min flow rate and 2.98 ± 0.22 dynes/cm^2 with a 10 mL/min flow rate (Figure 5.3a). In order to determine the effect of bioreactor culture on nutrient mass transfer the Sherwood number was calculated to be 22.71 and 13.34 with 10 mL/min and 3 mL/min flow rates respectively, representing the ratio of convective to diffusive mass transfer. Diffusion models indicate that oxygen concentrations in the TPS bioreactor do not fall below 0.15 mM while static cultured

constructs fall to 0.03 mM (Figure 5.3b). Oxygen concentrations in static cultured beads fall to the minimum at the farthest distance from the media air interface while the homogeneity of the surrounding media causes the bioreactor minimum concentration to occur at the center of the construct.

(a)

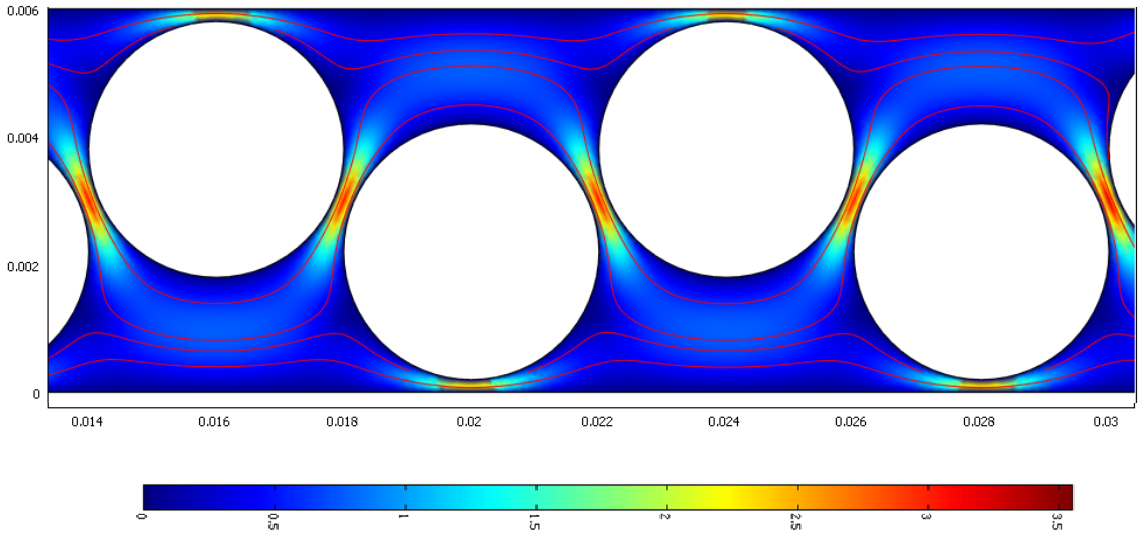

(b)

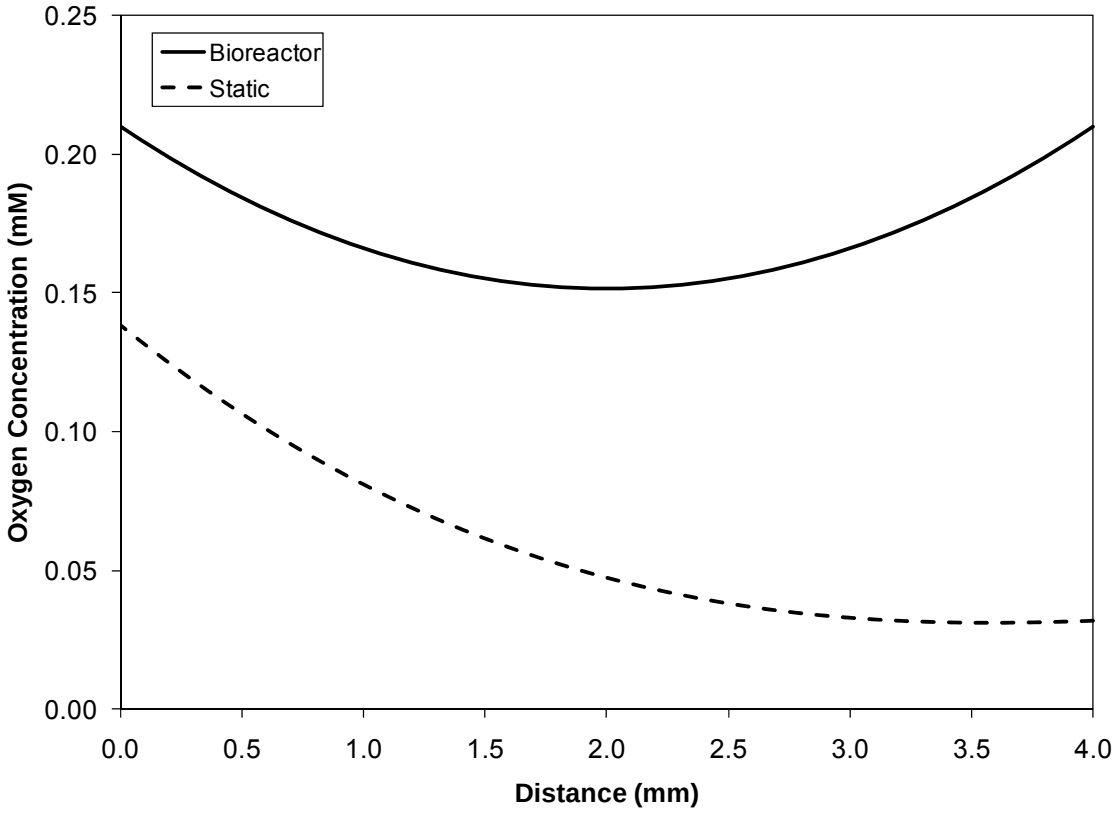

(c)

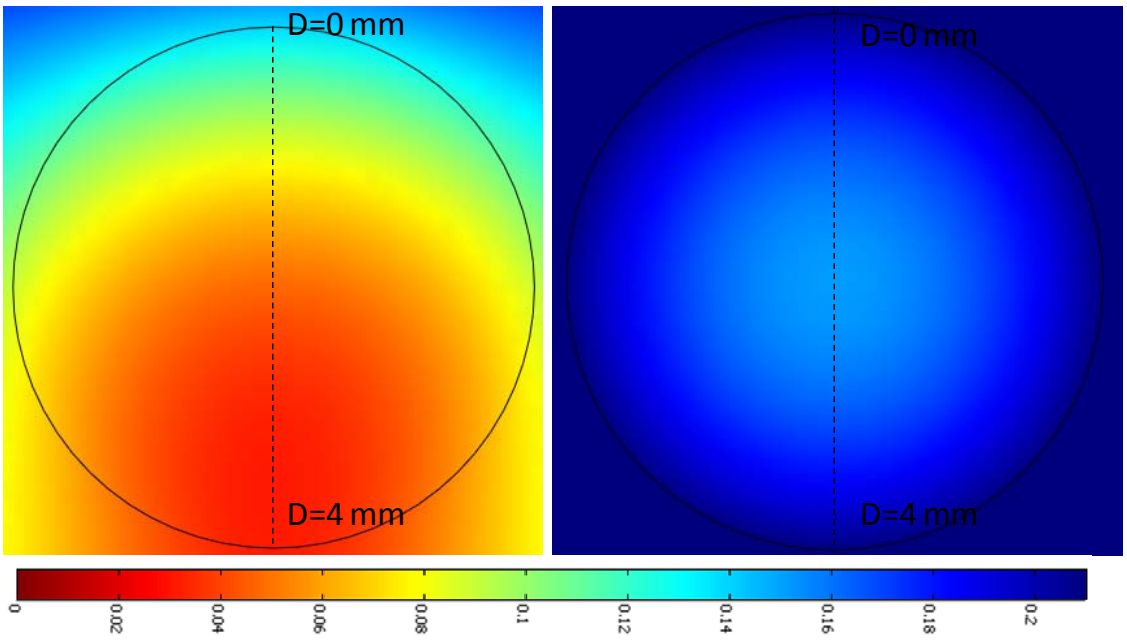

Figure 5.3: (a) Steady state COMSOL model of tubular perfusion system. Beads are shown as white circles. Streamlines and color map represent velocity in cm/sec. Dimensions of growth chamber and beads are in meters. Model represents middle section of tubular perfusion system growth chamber at a 3 mL/min flow rate. (b) Steady state oxygen concentrations throughout alginate scaffold in static (--) and bioreactor (—) plotted along bead diameter. Concentrations of oxygen are plotted along the center of the scaffold from the inferior (D=0 mm) to the superior end (D=4 mm). (c) Overall image of bead diffusion model. Dashed line represents cross section graphed in (b). Color map represents oxygen concentration in mM.

5.3.2 Short Term Culture

To demonstrate the effectiveness of the bioreactor system for short term culture alginate beads containing an encapsulated population of hMSCs were cultured for 8 days with live dead images taken of the entire bead on day 8 (Figure 5.4) and nearly all cells appeared viable.

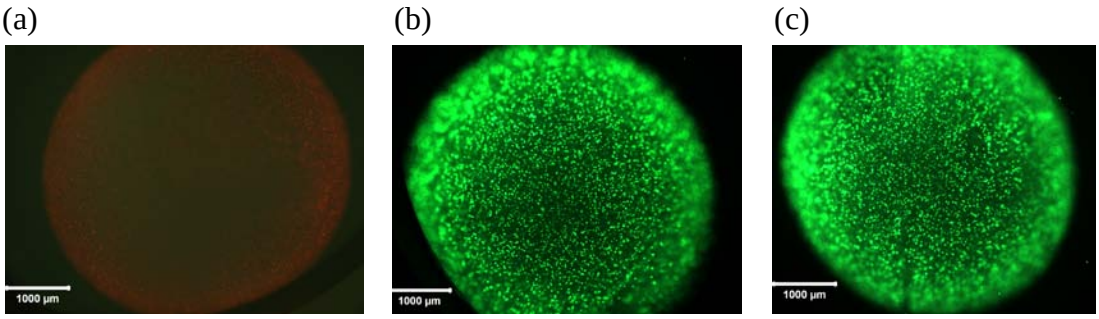

Figure 5.4: Live dead images of beads taken from day 8 of dead control (a) osteogenic control (b) and 3 mL/min flow bioreactor (c).

Cell count data showed a significant increase in cell growth in the bioreactor as compared to day 4 controls ($p < 0.05$), (Figure 5.5). Average day 4 cell number in the bioreactor beads was 67,300 ± 8,400 cells/bead while the osteogenic control only had 20,400 ± 6,100 cells/bead. Significant increase in cell growth was also observed on days 8 and 12 as compared to the osteogenic control ($p < 0.05$).

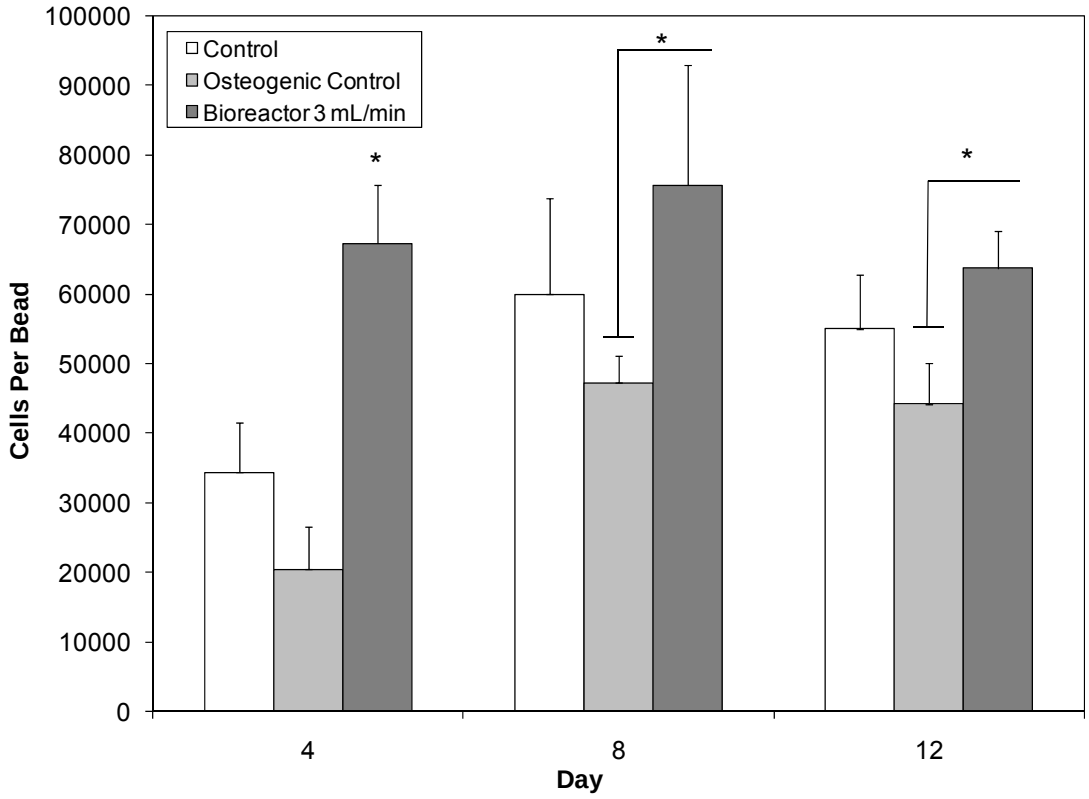

Figure 5.5: Cell count data taken on days 4, 8 and 12 in static controls (osteogenic and control media) and 3 mL/min flow in bioreactor. Cell counts indicate an elevated level of cells on day 4, 8, and 12 in the bioreactor over control groups. Cells not cultured in the bioreactor show minimal proliferation over the study period. The symbol (*) indicates statistical significance within a timepoint ($p < 0.05$).

DNA quantification indicated cell proliferation in the bioreactor throughout the study (Figure 5.6). By day 8 the bioreactor group had increased 3.41 ± 0.58 fold from its day 1 population numbers, greater than that observed in the controls. This data demonstrates the effectiveness of the TPS bioreactor at supporting cell growth.

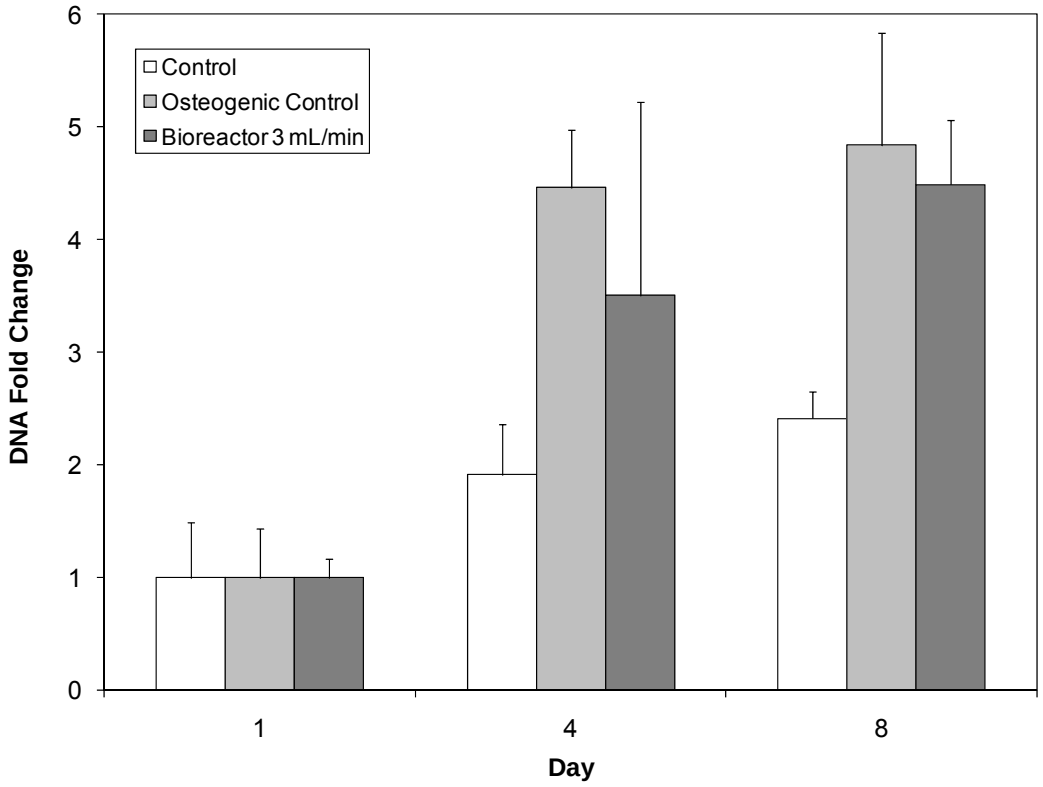

Figure 5.6: Fold change of DNA content of cells in static control, static osteogenic control, and bioreactor (3 mL/min) based on DNA quantification from pico green. Fold changes are based on day one DNA amounts. DNA amount indicates cell proliferation in the bioreactor throughout study.

Quantitative RT-PCR analysis was used to observe the gene expression of early osteogenic marker ALP on days 1, 4, and 8 (Figure 5.7). Results indicate a significant increase of ALP mRNA expression as compared to static control media bead on all days for both the static osteogenic control and the bioreactor flow group (3 mL/min), indicating the hMSCs are undergoing osteogenic differentiation in both groups ($p < 0.05$). On day 1 the static osteogenic group underwent a 5.6 ± 0.7 fold change in ALP expression as compared to the static control, while the bioreactor group underwent a 3.0 ± 0.4 fold change. By day 4 the bioreactor group showed a significantly higher 5.3 ± 0.5 fold day 4 expression increase than the 4.0 ± 0.6 fold increase of the static group ($p <$

0.05). On day 8, the osteogenic group had a slightly elevated expression over the bioreactor group, a 7.6 ± 0.7 fold change compared to 6.7 ± 0.7 fold change. Results indicate both bioreactor and static osteogenic groups are undergoing osteoblastic differentiation.

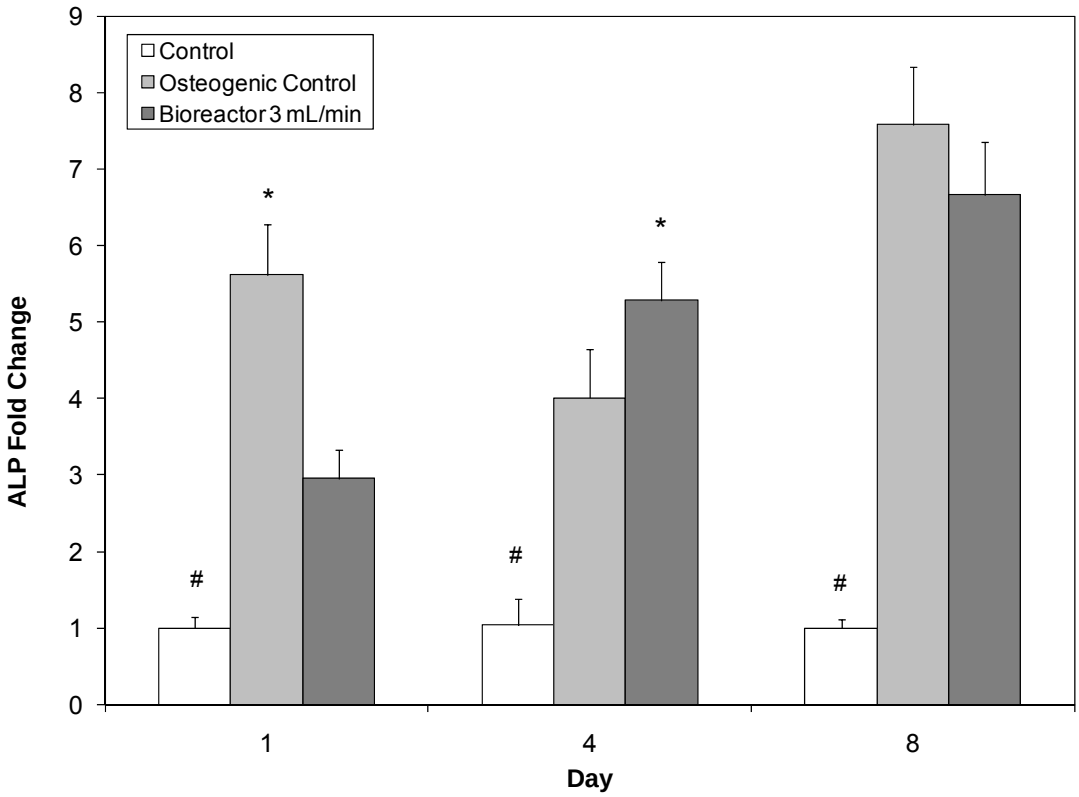

Figure 5.7: Quantitative RT-PCR analysis after 1, 4, and 8 days for ALP, an early osteogenic marker. Static osteogenic control and bioreactor are normalized to static control media samples. Results demonstrate higher day 1 expression of the osteogenic control as compared to the bioreactor on day 1, but greater expression on day 4 in the bioreactor group. Results indicate that the bioreactor system supports osteogenic differentiation of hMSCs. The symbols (*, #) indicates statistical significance within a timepoint ($p < 0.05$).

5.2.3 Long Term Culture

In order to determine the long term effects of the bioreactor system, cells were cultured in alginate beads in the TPS bioreactor for 28 days. Two different flow rates were used, 3

mL/min and 10 mL/min to evaluate the effect flow rate has on late osteoblastic differentiation. RT-PCR analysis of BMP-2, osteopontin, and osteocalcin was completed on days 14 and 28 (Figure 5.8). Results demonstrate a significantly increased expression of osteocalcin for both bioreactor groups as compared to static osteogenic control on day 28 ($p < 0.05$), (Figure 5.8a). Similar expression of osteocalcin was observed on day 14 for both static culture and the 3 mL/min flow rate group, but the 10 mL/min group showed a 6.2 ± 0.7 fold increase over the static group. On day 28 osteocalcin expression levels increased 78.1 ± 3.1 fold as compared to the day 14 control, while the 3 mL/min group increased 34.1 ± 1.7 fold. The static group increased 3.3 ± 0.3 fold from day 14 to day 28. This data indicates that flow rate has a significant effect on late term osteoblastic differentiation with higher flow rates having a greater effect than lower flow rates. Osteopontin gene expression data showed significant differences between all groups for both time points ($p < 0.05$). On Day 14 the 10 mL/min group had a 8.5 ± 0.3 fold expression change compared to the day 14 static control and the 3 mL/min group had a 2.5 ± 0.6 fold increase. On day 28 significant increases of 132.4 ± 31.8 and 41.2 ± 10.5 fold for the 10 mL/min and 3 mL/min groups respectively on day 28 were observed. BMP-2 expression was also evaluated on both time points and shown to be elevated in all bioreactor groups as compared to the osteogenic control. BMP-2 expression also increased with increasing flow rate as the 10 mL/min flow rate had higher BMP-2 expression levels for all time points. On day 28 BMP-2 shows approximately a 2 fold increase in the 10 mL/min group as compared to 3 mL/min, similar to the fold increase of osteopontin and osteocalcin between those groups on day 28.

(a)

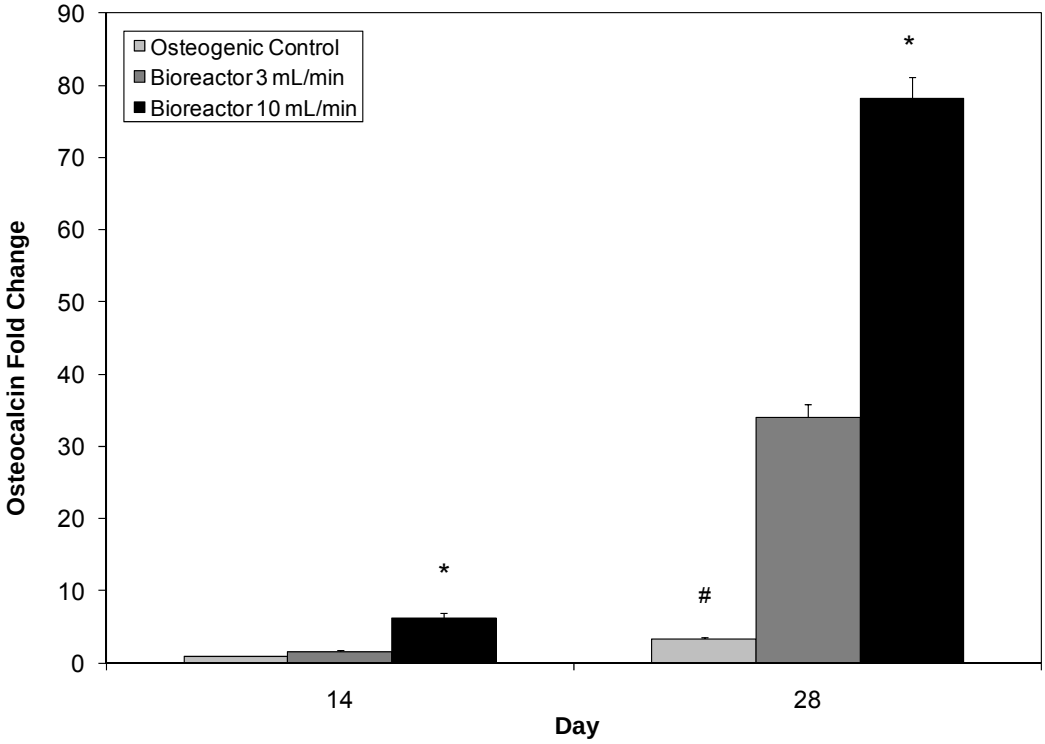

(b)

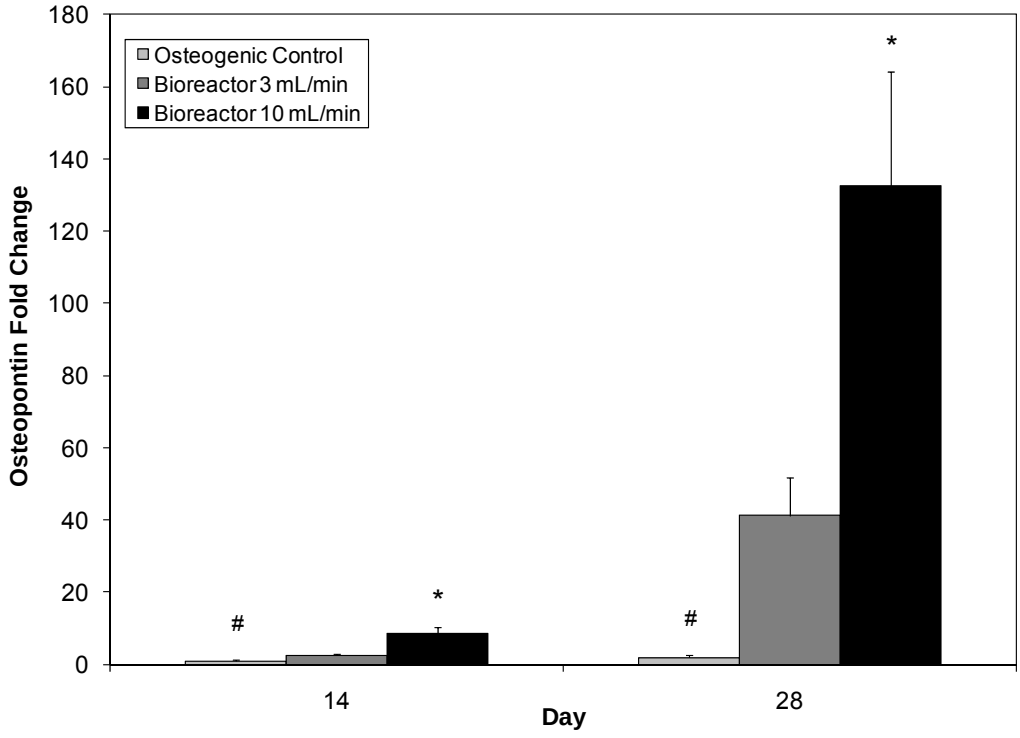

(c)

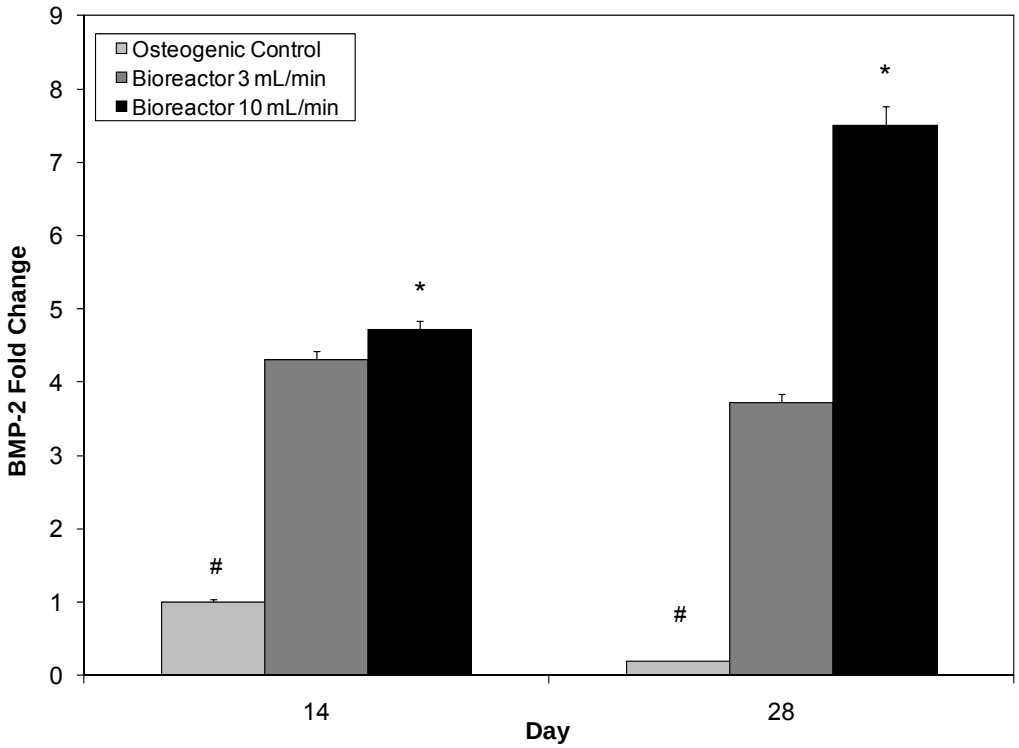

Figure 5.8: Quantitative RT-PCR analysis after 14 and 28 days for (a) osteocalcin expression, (b) osteopontin expression and (c) BMP-2 expression. Data is normalized to day 14 static control. All groups were cultured using osteogenic media. Osteocalcin expression is significantly higher in 10 mL/min group than all other groups on day 14. On day 28 the 10 mL/min group has higher osteocalcin expression than the 3 mL/min group and both groups show a significant increase over the static control (a). Osteopontin expression is significantly higher in the bioreactor groups on day 14 and day 28 as compared to the static control with the 10 mL/min group having the highest levels at both time points (b). BMP-2 expression levels differ between all groups on both day 14 and day 28 with the 10 mL/min group consistently having the highest expression level and the static control having the lowest (c). The symbols (*, #) indicates statistical significance within a timepoint ($p < 0.05$).

To visualize any macroscopic effects of bioreactor culture images of the cell containing scaffolds were taken prior to analysis on day 28 (Figure 5.9). White deposits can be seen on the surface of scaffolds removed from 3 mL/min bioreactor group (3.9c). In the 10 ml/min flow group the cells scaffold construct largely dissolved prior to the final timepoint, indicating that the flow may be too high to sustain tissue formation. In the

osteogenic control group minimal white deposits are observed and the scaffold appears less rigid, as the alginate dissolves over time (Figure 5.9b). Alginate beads were then dissolved for 30 minutes in 0.025 M EDTA and imaged. Photographs reveal that the alginate is completely dissolved in the control leaving only small amounts of visible material (Figure 5.9d). In the osteogenic control small fragments remain approximately 2 mm in diameter (Figure 5.9e). In the 3 mL/min bioreactor group, larger more intact structures are observed with diameters of approximately 4 mm (Figure 5.9f).

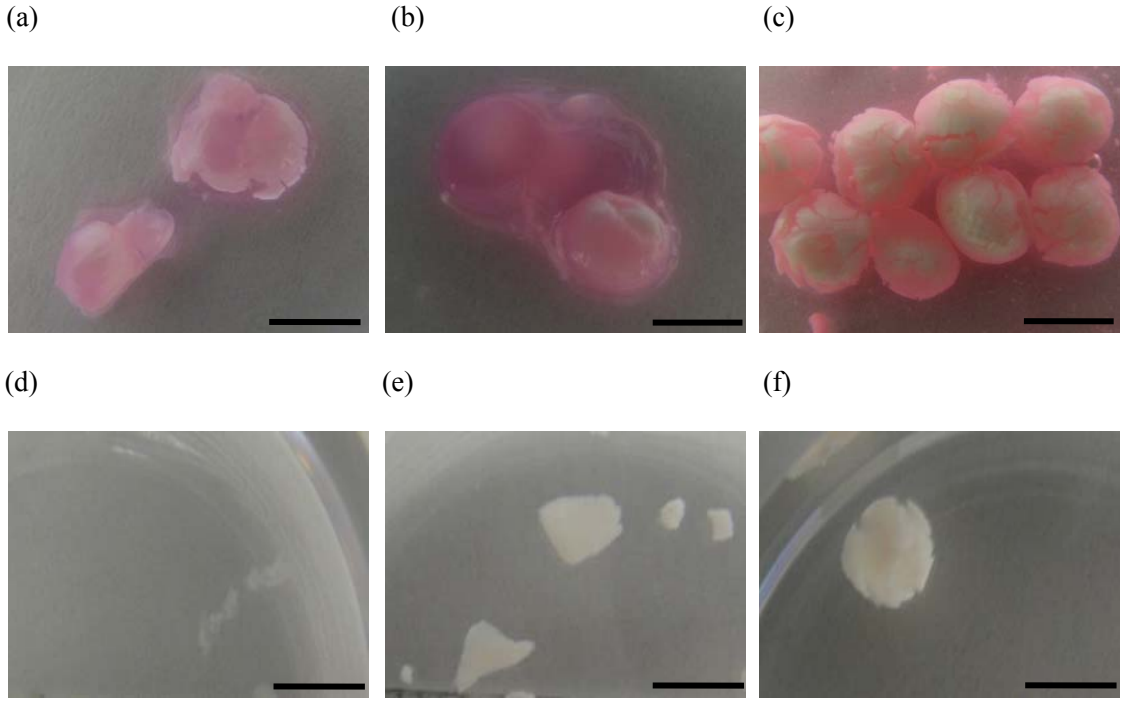

Figure 5.9: Images of scaffolds cultured for 28 days in static control media (a), static osteogenic media (b) and the bioreactor after 28 days of culture at 3 mL/min (c). Note in the bioreactor group white deposits can be seen on the surface of the scaffold and the scaffold has maintained its shape. Static groups do not have white deposits and scaffold appears much less rigid. Beads did not remain intact in the 10 mL/min group and were not photographed. Beads were then dissolved for 30 minutes in 0.025M EDTA. Images of scaffolds cultured in static control media (d) static osteogenic media (e) and bioreactor culture (3 mL/min) (f) after 28 days and 30 minutes in 0.025M EDTA. Alginate scaffold can no longer be observed in control media sample. In osteogenic control group small macroscopic formations remain. In bioreactor group larger more intact cell scaffold constructs are observed approximately 4 mm in diameter. Scale bars represent 5 mm.

Von Kossa staining was completed to visualize calcium deposition in the scaffolds. Images of alginate beads on day 14 demonstrate calcium deposition is restricted to the outside portion of the bead on day 14 (Figure 5.10a-c). Calcium deposits appear to be in greater concentration in the 10 mL/min bioreactor group as compared to osteogenic static group. Day 28 images reveal mineralization is considerably higher in the 3 mL/min bioreactor group as compared to the static osteogenic group and static control group. Cells can be seen completely surrounded by a calcium matrix. The osteogenic control also has formed a mineralized matrix, but it appears to much less dense than the bioreactor group.

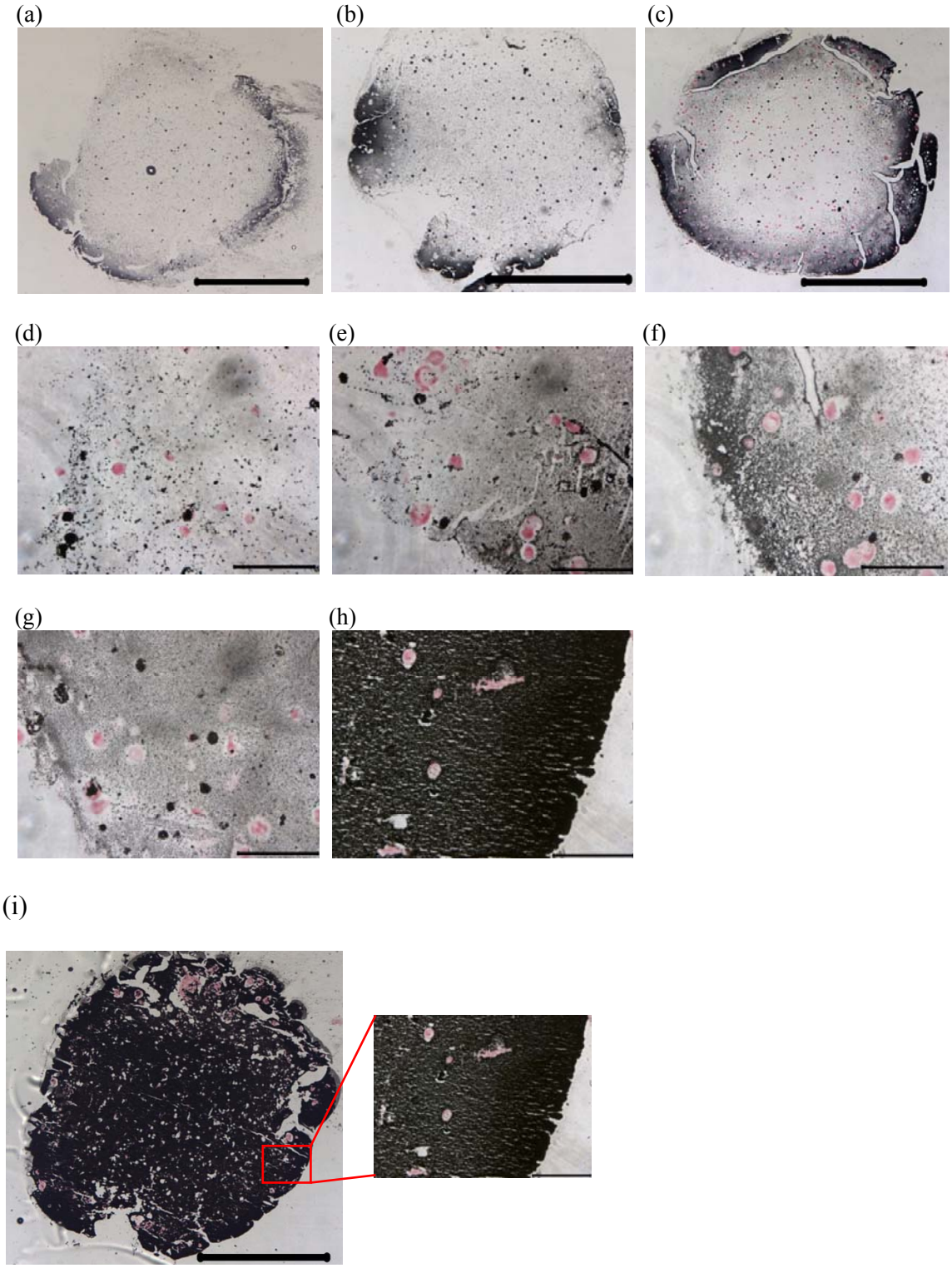

Figure 5.10: Von Kossa staining of alginate beads after 14 days of culture in static osteogenic culture (a,d), 3 mL/min bioreactor culture (b,e) and 10 mL/min bioreactor culture (c,f) at 2.5x objective (a,b,c) and 40x objective (d,e,f). Calcium deposits (black) appear to be confined to the perimeter of the bead in all groups, but darker in the

bioreactor groups, with the greatest amount of deposition observed in the 10 mL/min bioreactor group. Following 28 days of culture Von Kossa staining reveals 3 mL/min bioreactor culture (h) shows darker staining indicating increased calcium deposits compared to the static osteogenic control (g). Beads did not remain intact in the 10 mL/min group and Von Kossa staining was not completed on day 28. Scale bars represent 1000 μm (a,b,c) and 100 μm (d-h). Red box denotes size and approximate location of all 40x objective images in relation to the entire bead (i). Image is of 3 mL bioreactor groups after 28 days at 2.5x objective (left) and 40x objective (right). Scale bars represent 1000 μm and 100 μm respectively.

5.4 Discussion

Our first objective of this study was to effectively develop this bioreactor system. Following completion of this study a tissue engineering bioreactor system was successfully designed and fabricated to create a facile method for the dynamic culture of human mesenchymal stem cells in three dimensional scaffolds. The TPS bioreactor has several key advantages over existing bioreactor systems. Many perfusion bioreactor systems are composed of customized components that require custom manufacture [10, 27, 30, 53, 81]. The TPS bioreactor is composed entirely of off the shelf components making the system easy to manufacture and modify. The TPS bioreactor is easily reproducible allowing for more standardized experimentation and greater opportunity for clinical use which would require consistency [241]. The system may be easily modified to accommodate larger or smaller scaffold numbers and sizes through adjustment of growth chamber and media reservoir size. Media flow rate in this system may be accurately adjusted between 0.16 and 47.00 mL per minute. This large flow rate range will allow for experimentation on the effect of flow rate on cell proliferation and differentiation. The bioreactor system is fully autoclavable to allow for easy sterilization. Bacterial contamination is a significant problem faced by perfusion bioreactor systems and efficient sterilization will reduce this risk [226]. Furthermore this sterilization

method allows for easy reuse of tubing components. Mathematical modeling revealed the TPS bioreactor exposed the surface of the beads to shear stresses and subsequent calculations indicated that mass transfer in the TPS bioreactor is dominated by convection rather than diffusion. Diffusion models indicated minimum oxygen concentrations to be over 5 fold higher in bioreactor culture as compared to static culture. Oxygen concentrations similar to those calculated for static culture were shown to reduce the osteoblastic differentiation of rat osteoblasts [242]. Oxygen concentrations in the TPS bioreactor remain high throughout the alginate constructs as a homogenous oxygen concentration exists at the surface of the beads. Diffusion still dominates transport which could result in low interior oxygen concentrations, especially if a different material or a higher cell seeding density is used. Bone growth requires aerobic growth conditions and though the TPS bioreactor improves oxygen transport over static culture continued investigation should be completed to improve oxygen transport [182]. As an example of the potential for hypoxic conditions Volkmer et al demonstrated that oxygen concentration in 9 mm static bone tissue engineering constructs dropped to 0% at the center of the scaffold and 4% at the edge of the scaffold after five days of static culture, indicating diffusion is insufficient for oxygen transport. Perfusion culture was able to mitigate this effect [21]. Furthermore increased flow in bioreactor systems has been shown to increase oxygen content in media exiting the growth chamber [235]. Thus it is concluded that the TPS bioreactor both exposes the cell containing beads at the surface of the construct to shear stresses and provides for transport of oxygen and nutrients to cells in the scaffolds.

Our second objective of the study was to demonstrate the ability of the TPS bioreactor to support the growth and differentiation of hMSCs. Based on results from this study, the TPS bioreactor was shown to be effective in the culture of human mesenchymal stem cells. Over early time points bioreactor culture was shown to support proliferation of the cells. Bioreactor culture was shown to support osteogenic differentiation, but did not have a significant effect on the mRNA expression of early osteoblastic marker ALP. This is consistent with bioreactor studies that report minimal effects of flow on ALP expression [28]. Other studies report increased amounts of ALP expression with flow rate, indicating that specific parameters such as the shear stresses experienced by the cells could influence ALP expression [20, 23]. Based on the mathematical analysis the average shear stresses at the surface of the beads in this study were 0.98 ± 0.08 and 2.98 ± 0.22 dynes/cm^2 for the 3 mL/min and 10 mL/min flow group, respectively. This model provides an estimate for surface shear stresses, though several assumptions are made in the creation of the model. First it is assumed that all the alginate beads are spherical in shape with a fixed diameter, when in reality there is some minor observed variation between the exact size and shape of a bead. Second the beads are stacked in an ideal manner in the model, whereas there are often changes in the alignment of the beads in the TPS bioreactor. Finally both the fluid flow and diffusion model are completed in two dimensions. Additional math models should be completed in future work to determine if fluid shears affect cells on the interior portions of the scaffold as current models only describe shear on the exterior portion of the bead. Fluid shear stresses of 1.6 dynes/cm^2 have been shown to upregulate osteopontin expression, while shear stresses of 12 and 20 dynes/cm^2 have been shown to increase ALP expression [36, 38, 39]. In long term

bioreactor culture, shear stresses of 0.15 dynes/cm^2 have been shown to increase osteocalcin expression [80]. Shear stresses in this system are in the range to enhance osteoblastic differentiation but it is hypothesized that in the TPS bioreactor encapsulation of the hMSCs in the alginate leads to only a portion of the cell population being exposed shear stresses as opposed to cells seeded on the surface of a porous scaffold. Thus shear stresses could be too low to influence early osteoblastic differentiation, but high enough to affect late term differentiation and matrix deposition.

Our final objective was to evaluate the effects of flow rate on late osteoblastic differentiation and matrix production. Expression of osteocalcin and osteopontin, both late term markers of osteoblastic differentiation was shown to be significantly upregulated in bioreactor culture as compared to a static osteogenic control. The 10 mL per minute group showed higher expression of osteocalcin than 3 mL/min group on day 14, indicating that 14 days is sufficient for the higher flow rate to begin influencing the osteoblastic differentiation. By day 28 both flow groups showed significant increases in expression as compared to the static control, with the 10 mL/min group having over a two fold increase in expression levels as compared to the 3 mL/min group. Similar results are seen in osteopontin signal expression levels. This result is significant as though upregulation of late osteogenic markers has been previously demonstrated in perfusion bioreactors, our bioreactor uses a unique design in which cells are encapsulated in bulk scaffolds and media is not perfused directly through the pores of the scaffolds [53, 59]. Thus it is noteworthy that such dramatic increases in late term osteogenic signals are observed. Significant upregulation of BMP-2 was also observed during the long term study in the bioreactor groups. BMP-2 is an early osteoblastic marker that has been

shown to enhance to stem cell differentiation and promote osteogenesis in a scaffold [66-68]. As cells in the TPS bioreactor are already expressing high levels of late osteogenic markers, indicating terminal osteoblastic differentiation is occurring, the increased BMP-2 production observed with increasing flow may be effective in enhancing bone growth following implantation of the construct from the bioreactor system. Further investigation is necessary to completely elucidate the effect flow rate has on BMP-2 expression in this system and the effect this has on differentiation.

The clinical relevance of hMSCs cultured in alginate in the TPS bioreactor is two fold. First the alginate beads could be removed from the bioreactor and directly implanted into bone defects that do not have a load bearing requirement. For example certain types of craniofacial bone fractures heal poorly due to lack of neighboring bone and patients often have reported long term sequelae even after currently available treatments [243-246]. Second the alginate beads cultured in the TPS bioreactor could be loaded into a load bearing carrier scaffold after cultivation for implantation into load bearing defects such as long bones. This carrier scaffold would be constructed of a hard synthetic material such as poly(propylene fumarate), could be fabricated using stereolithography and would feature a hollow interior to load the beads [62]. Alternatively future work will investigate the use of cylindrical or spherical synthetic scaffolds in the system. It is thought that these scaffold materials would also function in the system, though additional modeling and investigation would be necessary to account for changes in the flow dynamics. Alginate is used in the system as cells can easily be encapsulated, avoiding complications occurring with the loading of some large 3D synthetic scaffolds. The alginate can also be easily dissolved allowing for creation of tissue without the presence of a scaffold [108,

109, 218]. This could lead to the production of a section of engineering tissue that could be extracted and implanted into a patient. Based on results, a longer culture period would be required to see these results, but in images taken at day 28, macroscopic differences could be seen between static and flow cultured constructs. White nodules can be seen on the periphery of scaffolds removed from the bioreactor, while minimal formations were observed in static osteogenic control groups. After dissolution of the scaffold, extracellular matrix depositions of nearly the same size as the original cell-scaffold construct were observed in the bioreactor group. These depositions were larger and more intact than the osteogenic static control. Despite the higher expression of osteogenic markers the 10 mL/minute flow rate was shown to be too high for successful long term culture in the TPS bioreactor as much of the cell-scaffold construct broke apart prior to the final time point. This would indicate that though the 10 mL/min flow rate stimulated the osteoblastic differentiation of the cells, it was too high to support the macroscopic growth of tissue. Thus an optimal flow rate likely exists between 3 mL/min and 10 mL/min, in which matrix deposition is enhanced but scaffold dissolution does not occur too quickly. Late term differentiation was confirmed by visualizing the production of calcium by completing Von Kossa staining. Higher amounts of calcium deposits were observed throughout the scaffold in the bioreactor groups as compared to the controls. On day 28 uniform dense mineralization is observed while day 14 mineralization appears to be restricted to the edges of the scaffold in all groups. The upregulation of late osteoblastic markers observed in tandem with macroscopic differences in bead appearance and Von Kossa staining indicate significant differences in late osteoblastic differentiation between static and bioreactor cultured cells.

5.5 Conclusions

In order to enhance the clinical relevance of cell based tissue engineering utilizing three dimensional scaffolds, *in vitro* culture techniques must be improved. We have developed a bioreactor system that can enhance the *in vitro* proliferation of human mesenchymal stem cells and the differentiation of these cells into osteoblasts. This system could be utilized to produce clinically relevant tissue amounts through extended *in vitro* culture. The findings in this study reveal that dynamic culture supports proliferation of hMSCs and enhances late osteoblastic differentiation. Other bioreactor systems have been developed but the TPS bioreactor utilizes a unique design, allowing for an alternative way to dynamically culture cells.

Chapter 6: Human Mesenchymal Stem Cell Position within Scaffolds Influences Cell Fate During Dynamic Culture[3]

6.1 Introduction

Tissue engineering exists as a promising treatment for bone injuries that fail to heal through endogenous repair mechanisms however *in vitro* culture of three dimensional tissue engineering constructs remains a challenge. Bioreactor systems are an important technology to improve this *in vitro* culture and increase the feasibility of cell based tissue engineering strategies. Many different bioreactors systems have been previously studied for bone tissue engineering including spinner flasks [22, 24, 42, 43], rotating wall bioreactors [42, 47], and perfusion systems [15, 17, 27]. In this study we utilize a tubular perfusion system (TPS) bioreactor, a simple, modular bioreactor system, which has previously been demonstrated to enhance proliferation and late osteoblastic differentiation of human mesenchymal stem cells (hMSCs) [112].

In traditional static culture of three dimensional scaffolds nutrient gradients arise leading to non homogenous cell growth and differentiation [21]. Bioreactor systems enhance cell culture through the creation of a dynamic environment that delivers oxygen and nutrients to cells while exposing them to shear stress. Advantages to using bioreactors for the culture of three dimensional scaffolds are two fold. First through increased nutrient transfer bioreactor systems can support increased cell growth. Cell death can be observed on the interior of scaffolds as little as 200 μm from the scaffold surface [21, 25, 28, 215,

[3]As published in Yeatts, A.B., et al., *Human mesenchymal stem cell position within scaffolds influences cell fate during dynamic culture.* Biotechnol Bioeng, 2012.

216]. This cell death occurs as oxygen and other nutrients do not diffuse into scaffolds quickly enough to replace those being used in cell respiration. Lack of oxygen (hypoxia) and lack of nutrients limit both the ability of cells to survive and to differentiate, which leads to a nonhomogeneous cell and matrix distribution [182]. Bioreactor culture has been used to overcome these limitations [111, 118]. Second, bioreactors typically expose cells to fluid shear stress, an important stimulus for hMSC osteoblastic cell differentiation [16, 18, 28, 29, 38, 39, 80, 89, 110, 111].

While bioreactors can regulate shear stress and oxygen concentration to some extent, it is possible exposure varies between cells in different regions of the scaffold. Differing oxygen and shear levels could influence stem cell proliferation and differentiation. While shear is commonly thought to stimulate osteoblastic differentiation, the role of oxygen is less clear. Low oxygen and nutrient levels lead to significant cell death [207] however hMSCs cultured at 2% oxygen levels had increased proliferation and differentiation levels compared to hMSCs cultured at 20% oxygen [196]. Other studies found low oxygen levels to have inhibitory effects on osteoblastic differentiation [182, 191, 242, 247].

Based on the influence of oxygen and shear on stem cell development we investigate in this study how spatial positioning of hMSCs within a scaffold influences cell fate. To this end the study first aims to evaluate the effect of shear stress on osteoblastic differentiation in the TPS bioreactor. Second the study aims to evaluate the effect of dynamic culture on the proliferation of human mesenchymal stem cells as a function of radial distance in the scaffold. The final aim of the study is then to compare osteoblastic

differentiation of cells present on the exterior annulus of the scaffold to cells on the interior annulus.

6.2 Materials and Methods

6.2.1 Human Mesenchymal Stem Cell Culture

Human mesenchymal stem cells (Lonza, Walkersville MD) were expanded prior to the study in control media consisting of DMEM (Gibco, Carlsbad, CA) supplemented with 10% fetal bovine serum (Gibco), 1.0 % v/v penicillin/ streptomycin (Gibco), 0.1 mM non essential amino acids (Gibco), and 4 mM L-glutamine (Gibco) using protocols set forth by the manufacture and previously described [69, 112, 113, 232]. hMSCs were expanded on tissue culture polystyrene flasks with media changes every three days according to the manufacture's specifications. Cells were stored in a cell culture incubator at 37º C and 5% CO_2 and passaged every 6-7 days using trypsin/EDTA (Lonza). Osteogenic media was formulated as described in the literature by supplementing control media with 100 nM dexamethasone (Sigma), 10mM β-glycerophosphate, and 173 μM ascorbic acid (Sigma) [69, 232].

6.2.2 Alginate Bead Fabrication and Cell Seeding

Alginate beads were fabricated as described previously in the literature [108, 109]. Alginate solution (Sigma, St. Louis MO) was sterilized via sterile filtration then mixed with a cell pellet containing hMSCs. Beads were seeded at a concentration of 4 x 10^6 cells per mL. This solution was added dropwise by syringe to a 0.10 M calcium chloride solution, in which the alginate was ionically crosslinked into beads. A 20 gauge syringe

was used to create large beads and beads for shear stress study while a 30 gauge syringe was used to create small control beads. The solution was stirred for 15 minutes. The calcium chloride solution was then removed and the beads rinsed in control media. Beads were then transferred to six well plates for control groups or TPS bioreactor growth chambers for experimental groups.

6.2.3 Identification of Discrete Bead Layers

In order to develop a calibration curve for annuli isolation beads were immersed in 3 mL of 0.025 M EDTA. Cross sectional areas were measured at five minute time points using Image J software (NIH, Bethesda MD) based on an image taken of a bead with an Axiovert 40 CFL with filter set 23, (Zeiss, Thornwood, NY) equipped with a digital camera (Diagnostic Instruments 11.2 Color Mosaic, Sterling Heights, MI). A calibration curve was constructed in order to determine the dissolution time to divide the scaffold into two annuli equal in radius. The calibration curve had an R^2 value of 0.98. Based on the calibration curve 18 minutes was determined as the dissolution time to achieve two equal radii as the dissolution value was 49.4 ± 4.9 % at 18 minutes.

6.2.4 hMSC Isolation from Discrete Bead Layers

In order to isolate beads from specific annuli beads were placed into a twelve-well plate and 1.0 mL of 0.025 M EDTA was added. Beads were dissolved for 18 min as determined by the calibration curve. EDTA, now with suspended cells, was removed and placed into a centrifuge tube (Figure 6.1). The well was washed with 1.0 mL of phosphate buffered saline (PBS). Beads were moved to a new well containing 1.0 mL of 0.025 M EDTA for the next dissolution. Centrifuge tubes were spun at 5000 xg for 5

minutes to isolate the cell pellet. To isolate cells from entire scaffold 0.025 M EDTA was added and beads were entirely dissolved and pellets isolated as previously described.

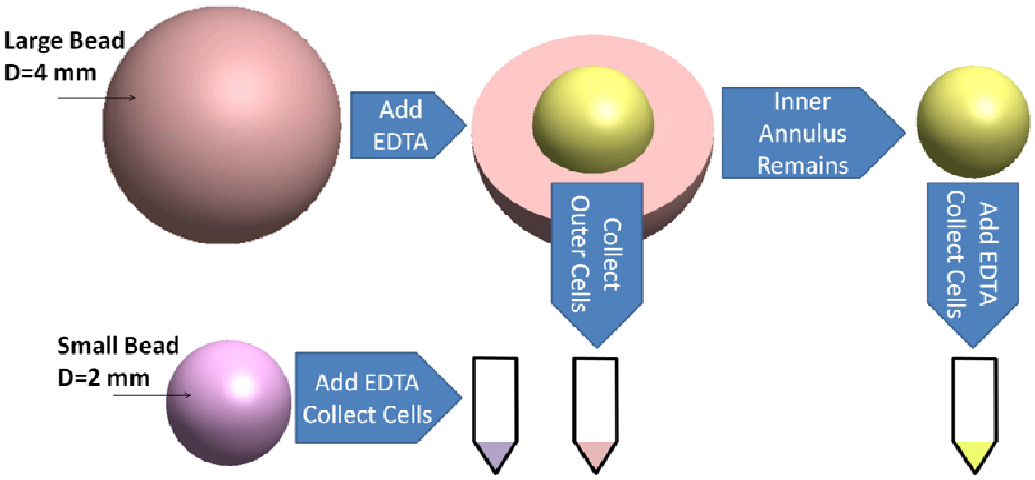

Figure 6.1: Schematic of cell removal from annuli of alginate beads. Diameters of small beads and inner annulus are equal.

6.2.5 Bioreactor Design

Bioreactor culture was completed in the TPS bioreactor as described previously [112, 113]. Briefly a tubing circuit comprised primarily of platinum-cured silicone tubing (Cole Parmer, Vernon Hills, IL) and PharMed BPT tubing (Cole Parmer) for the section that passes through the pump connected a growth chamber to a media reservoir (Figure 6.2). The entire tubing circuit was sterilized via autoclave. The growth chamber was composed of platinum-cured silicone (ID of 1/4") and contained the tightly packed alginate scaffolds. Media was pumped through the recirculating system using a peristaltic pump (Cole Parmer) at 1.0 mL/min for annuli studies and 3.0 mL/min for shear stress studies. The entire system was placed in an incubator at 37^{o}C for the duration of

the study. Forty mL of osteogenic media was loaded into separate 125 mL Erlenmeyer flask reservoirs for each growth chamber topped with rubber stoppers. Media was withdrawn and replaced from the reservoir through two tubes that penetrate the stopper and changed every three days.

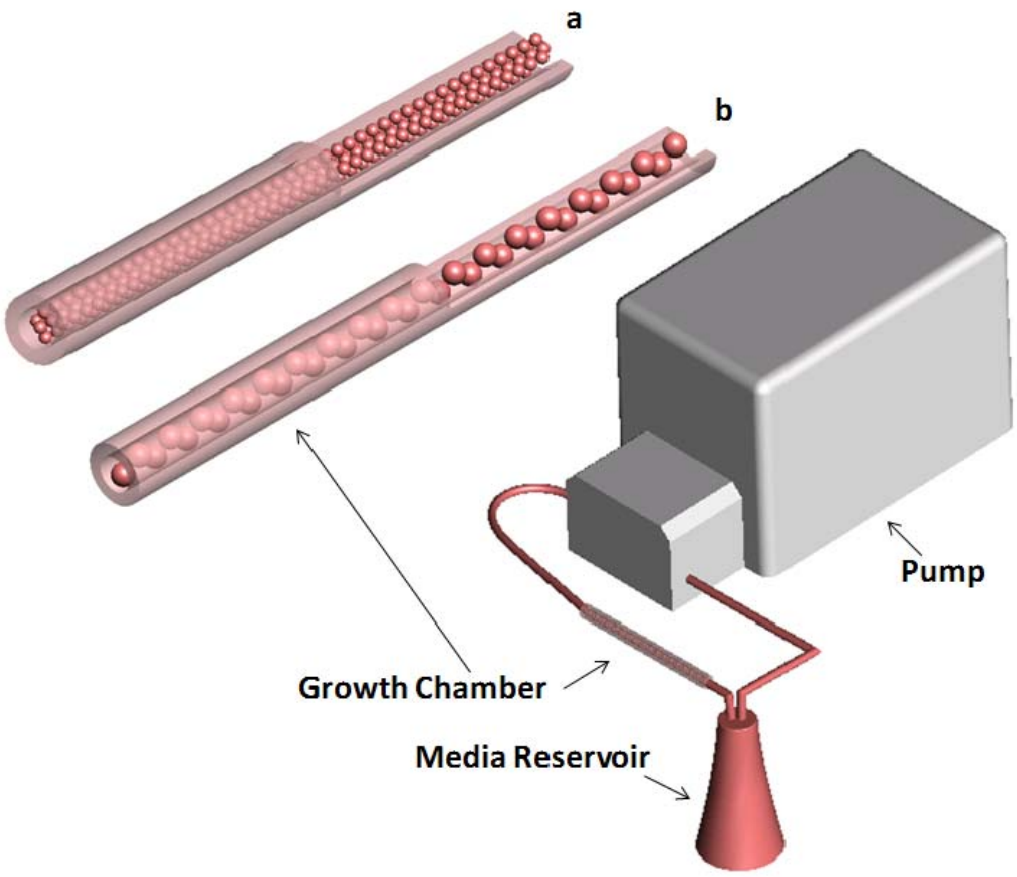

Figure 6.2: Schematic of TPS bioreactor. Bioreactor consists of media reservoir, growth chamber, and pump. Enlargement of this growth chamber can be seen with (a) small beads (2 mm diameter) and (b) large beads (4 mm diameter).

6.2.6 Modification of Shear Stress

In order to analyze shear stress in the system 70,000 MW dextran (Sigma) was added to the media. Dextran was chosen as a thickening agent as it has previously been shown to not affect hMSC proliferation and differentiation [80, 90]. The shear stress study

consisted of three groups all cultured in osteogenic media. The first group with zero shear was cultured in static culture. The second group was cultured in the TPS bioreactor at 3 mL/min in media supplemented with 3% dextran yielding a media viscosity of 1.66 ± 0.05 mPA · S. The third group was cultured in the TPS bioreactor at 3 mL/min in media supplemented with 9% dextran yielding a media viscosity of 4.21 ± 0.03 mPA · S. Surface shear stress was then calculated using a two-dimensional steady state Navier-Stokes model of the tubular perfusion system developed using COMSOL Multiphysics Version 3.5 (COMSOL, Burlington MA) [112].

6.2.7 Experimental Setup

In order to determine the effect of shear stress on hMSC osteoblastic differentiation a shear stress study was completed using the entire 4 mm bead. This study consisted of 3 groups, a static group and two bioreactor groups with dextran added as a thickening agent to change shear while not affecting nutrient transfer. The samples were analyzed for late osteoblastic marker osteopontin (OPN) at days 14 and 21 and osteogenic signaling protein bone morphogenetic protein-2 (BMP-2) on days 1, 4, 8, 14, and 21.

In order to determine hMSC growth and osteoblastic differentiation in relation to radial position the cells were isolated from the outer 2 mm radius (outer) and inner 2 mm radius (inner) of alginate beads. These beads were cultured in the TPS bioreactor and compared to a static control. In addition small beads equal to the inner bead size were cultured in the TPS bioreactor and static culture as a control. All samples were cultured in osteogenic media. These samples were analyzed at days 1, 7, 14, and 21 for ALP and

mineralization and at days 7, 14, and 21 for proliferation and late osteoblastic differentiation using marker osteopontin.

6.2.8 Live Dead Assay

Five beads each cultured in control media were dissolved for 18 min as determined previously in order to isolate cells from discrete layers. After each time point, beads were immediately removed from the EDTA solution and immersed in live dead solution containing 2 μM ethidium homodimer and 4 μM calcein AM (Invitrogen, Carlsbad, CA) for thirty minutes. Fluorescent images were then taken using a fluorescent microscope (Axiovert 40 CFL with filter set 23, Zeiss, Thornwood, NY) equipped with a digital camera (Diagnostic Instruments 11.2 Color Mosaic, Sterling Heights, MI) for the live/dead assay, as described previously [112, 113].

6.2.9 DNA Quantification

DNA was extracted at each time point and quantified using pico green as previously described [112]. Cell pellets were isolated from the two annuli as well as from small beads cultured as a control. Isolated cell pellets were resuspended in PBS and DNA isolated using a DNeasy Tissue Kit (Qiagen, Valencia CA) following standard protocols. Double stranded DNA was then quantified using Quant-iT PicoGreen dsDNA reagent (Molecular Probes, Carlsbad, CA), incubated for five minutes in the dark and fluorescence measured using an M5 SpectraMax plate reader (Molecular Devices, Sunnyvale, CA) with excitation/emission of 480/520 nm. All samples were performed in triplicate (n=3).

6.2.10 Histomorphometric Analysis

At each timepoint beads were collected and fixed in 4% paraformaldehyde (Sigma-Aldrich) and 0.1 M sodium cacodylate (Sigma-Aldrich) buffer containing 10mM $CaCl_2$ at pH 7.4 for 4 hours at room temperature. Following fixation, the beads were placed in cassettes and washed with 0.1 M sodium cacodylate buffer and 10 mM $CaCl_2$ at pH 7.4 at room temperature for 24 hours. The beads were then dehydrated for histological processing by ethanol washes followed by two citrisolv (Fisher) washes. The samples were then embedded in paraffin (Fisher) and sectioned to 5 μm thickness sections and placed on glass slides. Sections were taken from the same position in each sample for histomorphometric analysis. Sections were oven dried at 64° C for 2 hours, deparaffinized in citrisolv and rehydrated in ethanol. Von Kossa staining was performed to visualize mineralization using a Nuclear Fast Red (Poly Scientific, Bay Shore, NY) counterstain using standard protocols. For histomorphometric analysis images the entire sample were taken using the Axiovert 40 CFL microscope equipped with a digital camera. Images were divided into inner and outer annuli for large beads using diameter measurements. Using Image J 1.44p (NIH, Bethesda MD) images were converted to binary where the dark Von Kossa stain represented mineralized area. Black area was calculated as percent of total area to represent mineralization percent.

6.2.11 Quantitative Reverse Transcriptase Polymerase Chain Reaction (qRT-PCR)

Cell pellets were isolated as described previously. RNA was extracted using an RNeasy mini plus kit (Qiagen) following standard protocols. The isolated RNA was then reverse transcribed to cDNA using a High Capacity cDNA Archive Kit (Applied Biosystems,

Foster City, CA). The expression of bone morphogenetic protein-2 (BMP-2, Taqman Assay ID: Hs00154192_m1) (only shear study), osteopontin (OPN, Hs00960641_m1) (all studies) and alkaline phosphatase (ALP, Hs00758162_m1) (only for annuli study) was analyzed with glyceraldehyde-3-phosphate dehydrogenase (GAPDH, Hs00960641_m1) as an endogenous control gene for all samples. The sequences are propietary. Gene expression assays (Applied Biosystems) were combined with the cDNA to be analyzed and Taqman PCR master mix (Applied Biosystems). The reaction was performed on a 7900HT real time PCR System (Applied Biosystems) using thermal conditions of 2 minutes at 50°C, 10 minutes at 95°C, and 40 cycles of 15 seconds at 95°C and 1 minute at 60°C. The relative gene expression level of each target gene was then normalized to the mean of the GAPDH in each group. Fold change was calculated using the ΔΔCT relative comparative method as described previously [218, 240]. Samples were evaluated in triplicate and standard deviations are reported (n=3).

6.2.12 Statistical Analysis

All samples were completed in triplicate (n=3). Data was analyzed using single factor ANOVA followed by Tukey's Multiple Comparison Test assuming normal data distribution with a confidence of 95% ($p < 0.05$). Mean values of triplicates and standard deviation error bars are reported on each figure as well as relevant statistical relationships.

6.3 Results

6.3.1 Effect of Shear Stress on Late Osteoblastic Differentiation and BMP-2 Expression

An investigation was completed to determine the effect of shear on osteoblastic differentiation. Osteogenic signaling protein BMP-2 was analyzed at days 1, 4, 8, 14 and 21 (Figure 6.3a). On days 1, 4, and 8 a weak correlation was observed between shear stress and BMP-2 expression. Specifically on day 4 BMP-2 fold change increased an average of 0.19 per dyne/cm^2. On day 8 the fold change was 0.44 per dyne/cm^2. By day 14 a strong correlation began to emerge between shear stress and BMP-2 expression. Specifically BMP-2 fold change increased 0.95 per dyne/cm^2. By day 21 this correlation was stronger with an average fold change of 1.64 per dyne/cm^2. Following this analysis late osteoblastic marker osteopontin was evaluated to determine the effect of shear on late osteoblastic differentiation. As OPN expression was not observed at early timepoints, it was analyzed at day 14 and 21. By day 14 the fold change of OPN increased 0.46 per dyne/cm^2 (Figure 6.3b). This trend strengthened by day 21 when a fold change of 1.26 per dyne/cm^2 was observed. These results demonstrate a strong time dependent effect of shear stress. Following this study, an investigation was completed to analyze the effect of hMSC radial position in scaffolds on hMSC osteoblastic differentiation and proliferation.

a)

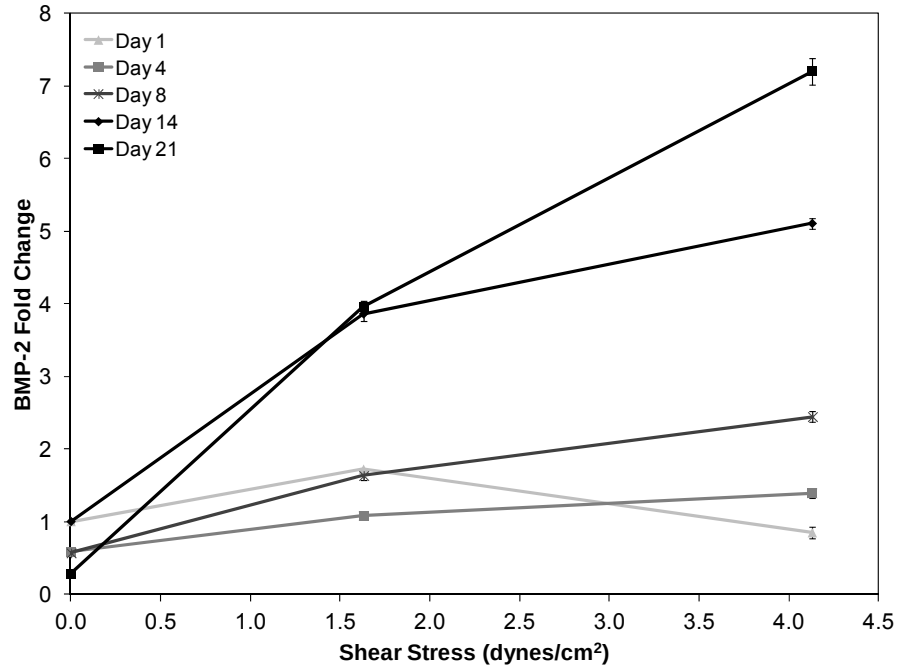

b)

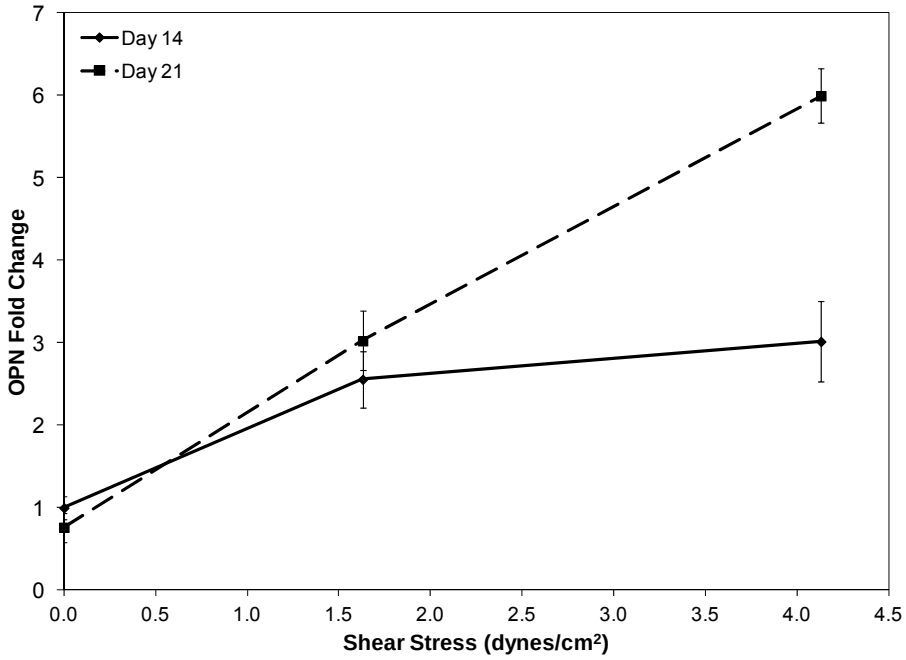

Figure 6.3: RT-PCR analysis for BMP-2 (a) and osteopontin (b) mRNA expression versus shear stress for timepoints 1, 4, 8, 14, and 21 (a) and 14 and 21 (b). Day 1, 4, and 8 BMP-2 data is normalized to day 1 zero shear, day 14 and 21 BMP-2 and OPN data is normalized to day 14 zero shear. Expression levels of BMP-2 and osteopontin are dependent on shear stress with higher shear stresses correlating to greater expression levels. The magnitude of this increase becomes stronger at later timepoints.

6.3.2 hMSC Proliferation in Discrete Layers

Based on live dead staining of entire bead, inner annuli, and small bead nearly all cells were viable throughout the alginate beads after 1 day of culture. Dead cells were not observed (Figure 6.4).

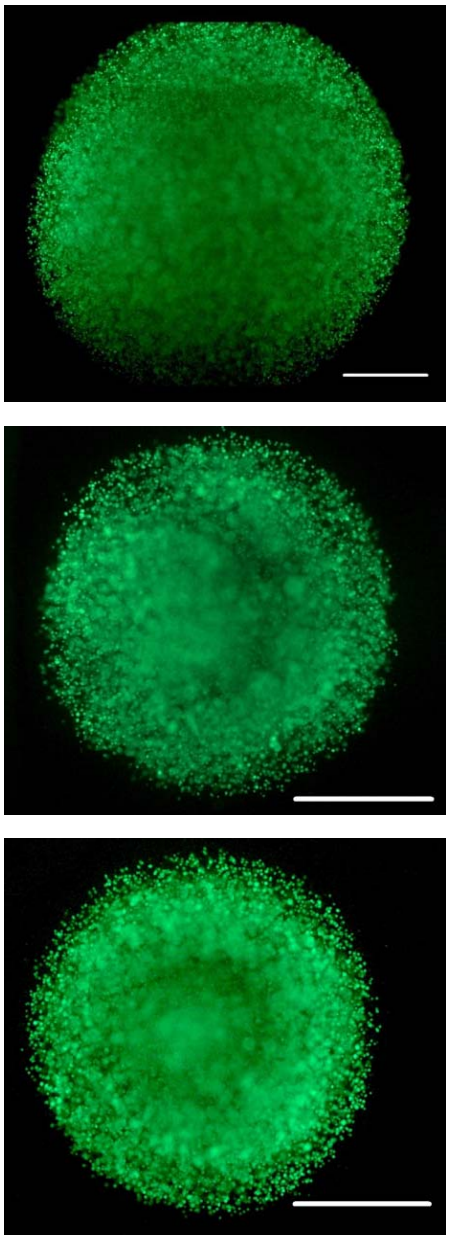

Figure 6.4: Live Dead Images of entire bead (top), inner annuli (middle), and small bead (bottom) after one day of bioreactor culture. Scale bar represents 1000 μm. Note small bead and inner annuli are approximately the same size and half that of the entire bead. Cells appear viable in all groups throughout the bead.

On day 7 proliferation remained comparable in all groups except for bioreactor cultured small beads which had significantly higher ($p < 0.05$) levels of DNA (Figure 6.5). By day 14 a sharp decrease in proliferation could be observed in the inner annulus of control beads while the highest proliferation continues to be observed in the bioreactor small beads. On day 21 significantly ($p < 0.05$) higher proliferation was observed in bioreactor cultured beads as compared to control beads of the same size. DNA concentration in the outer and inner annuli of bioreactor cultured beads was 3.82 ± 0.31 and 3.33 ± 0.58 ng/mm^3 respectively. This was significantly higher ($p < 0.05$) compared to the outer and inner annuli of statically cultured beads which were 1.59 ± 0.34 and 1.24 ± 0.22 ng/mm^3 respectively. Bioreactor small beads had the highest DNA amount at 5.55 ± 0.82 ng/mm^3. Statically cultured small beads had a lower DNA amount at 3.15 ± 0.64 ng/mm^3. This amount is lower but statistically similar ($p > 0.05$) to bioreactor cultured large beads.

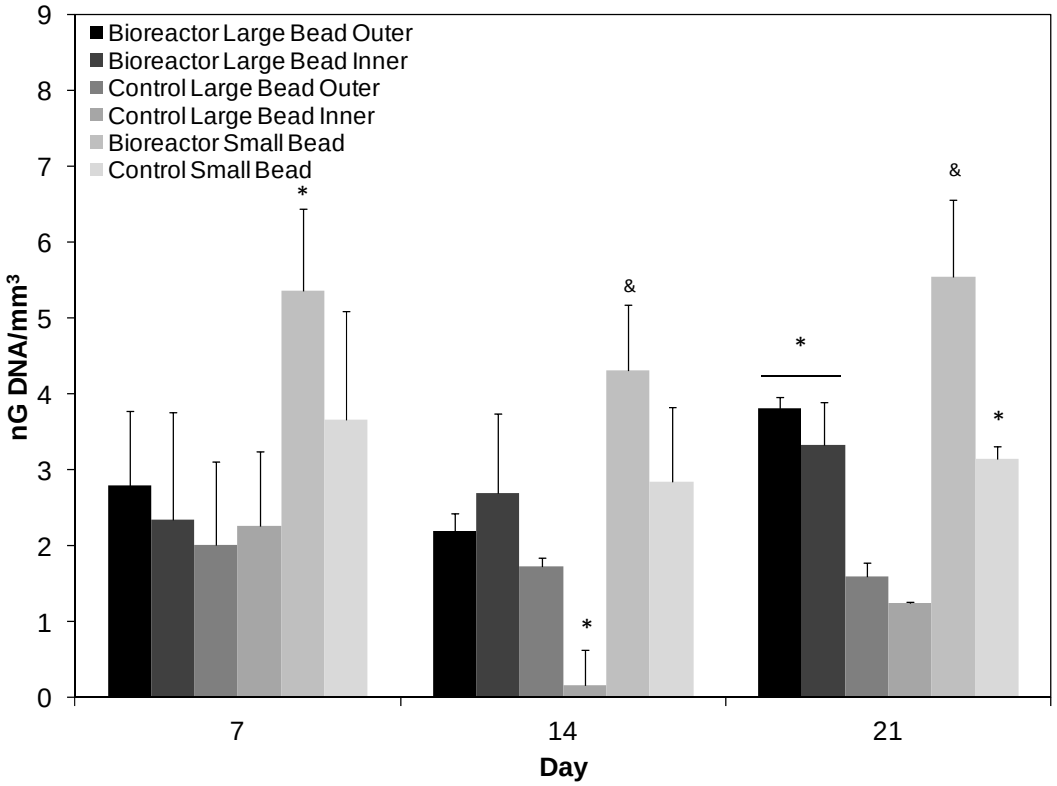

Figure 6.5: DNA amount normalized to scaffold volume for days 7, 14, and 21. On day seven similar proliferation is observed in all groups except bioreactor small bead. By day 14 control inner exhibits decreased proliferation. On day 21 note significantly higher DNA amounts in bioreactor cultured large beads as compared to static cultured large beads. The symbols (*, &) represent statistical significance within a timepoint ($p < 0.05$). Groups with symbol * or & are statistically different from all groups except those groups with the same symbol. Groups with the same symbol are statistically similar to each other.

6.3.3 hMSC Differentiation and Matrix Production in Discrete Layers

ALP was used as a marker of early osteoblastic differentiation. The earliest peaks in ALP expression were observed in the control beads indicating they may be differentiating more rapidly than bioreactor cultured beads (Figure 6.6). By day 21 the highest expression levels were observed in the inner annuli of bioreactor cultured beads with a fold change of 5.85 ± 0.41 as compared to day one control inner. The inner annuli of control beads also exhibited high expression levels with a 3.54 ± 0.08 fold change

compared to the same group. Interestingly low expression was observed in the bioreactor outer and bioreactor small groups with expression levels of 0.34 ± 0.04 and 0.82 ± 0.06 respectively.

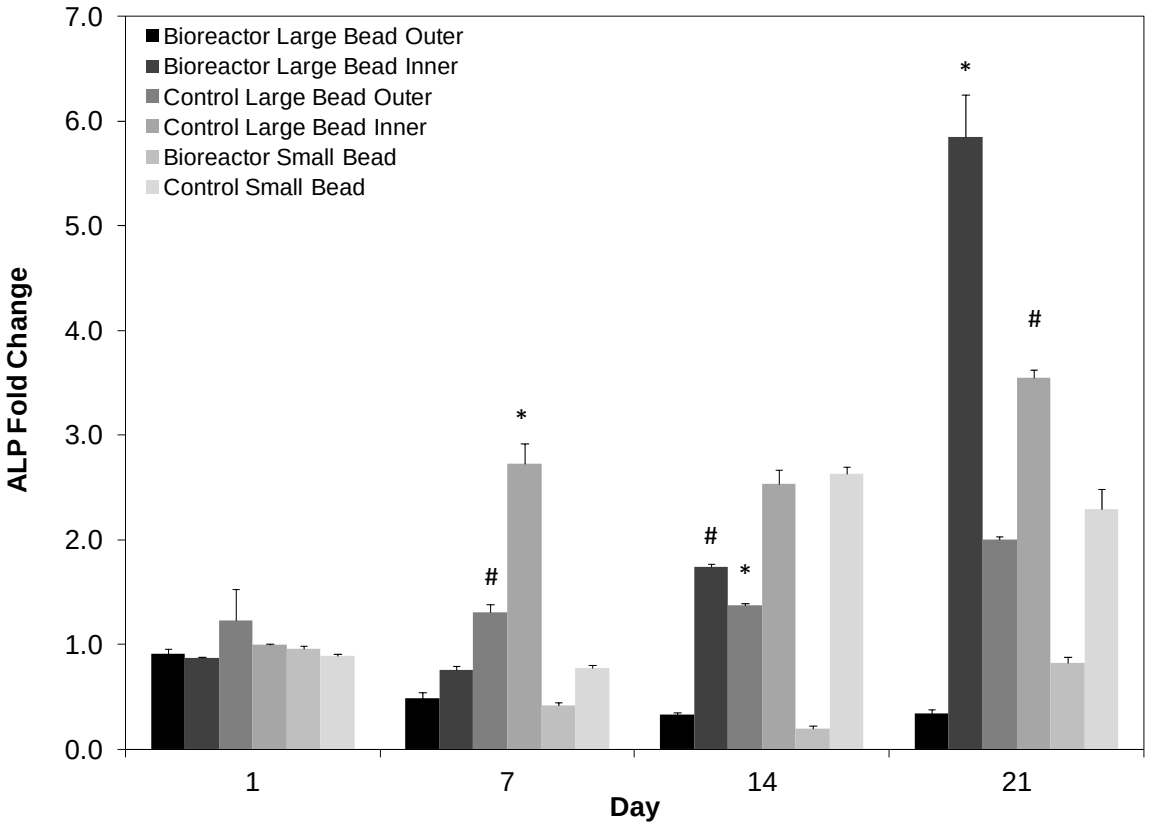

Figure 6.6: Quantitative reverse transcriptase polymerase chain analysis for days 1, 7, 14, and 21 for early osteoblastic marker ALP. Values are normalized to day one control large bead inner. All groups are cultured in osteogenic media. On day 21 ALP expression levels are significantly higher in bioreactor large bead inner cells than all other groups. The symbols (*, #) indicate statistical significance from all other groups within a timepoint ($p < 0.05$). Groups with symbol * or # are statistically different from all groups except those groups with the same symbol. Groups with the same symbol are statistically similar to each other.

Following this an analysis of osteoblastic differentiation marker OPN was completed. As OPN is a late osteoblastic marker low levels were observed on days 7 and 14 (Figure 6.7). By day 21 expression of OPN began to increase in some groups with the highest levels observed in the inner annuli of bioreactor cultured beads. This group exhibited a

fold change of 12.31 ± 1.47 as compared to day 7 control inner. The outer annuli of the bioreactor cultured beads exhibited a significantly ($p < 0.05$) lower fold change of 4.55 ± 0.32. Control groups exhibited low day 21 levels of 1.45 ± 0.41 and 1.37 ± 0.54 for the outer and inner annuli respectively. The control small group was slightly but statistically significantly higher ($p < 0.05$) at a fold change of 1.65 ± 0.33. The bioreactor small group was significantly higher ($p < 0.05$) at a fold change of 7.21 ± 1.24.

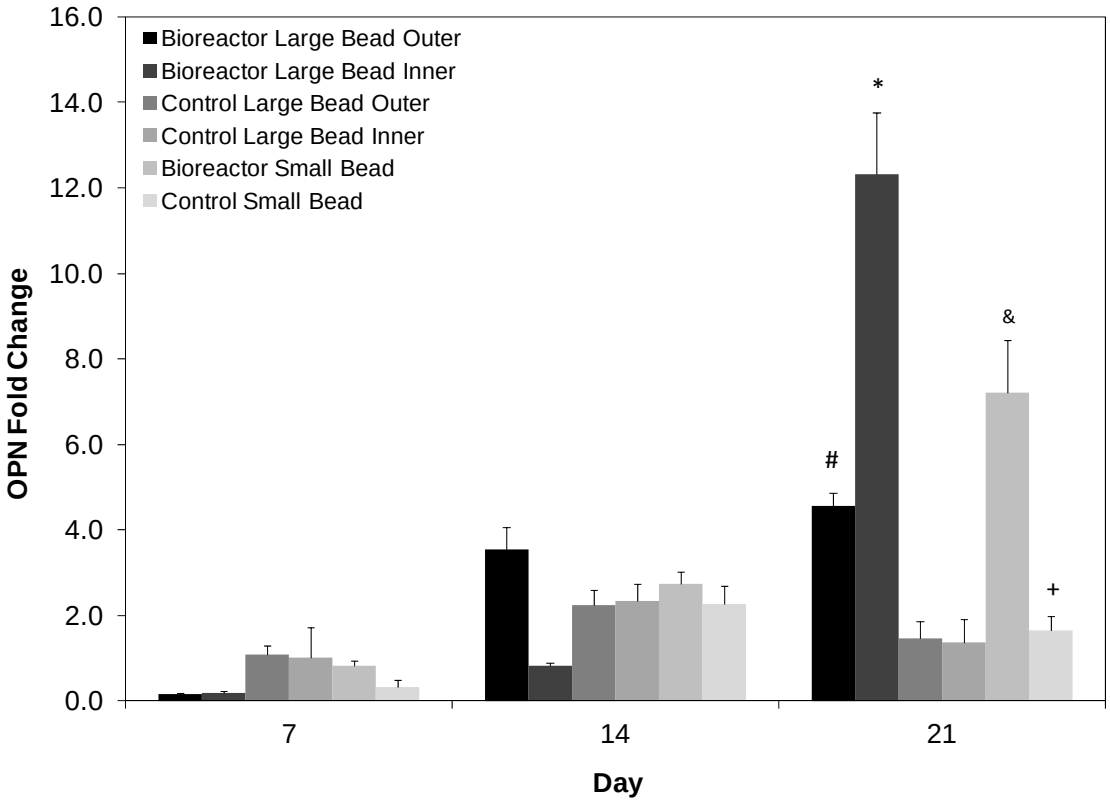

Figure 6.7: RT-PCR analysis for days 7, 14, and 21 for late osteoblastic marker osteopontin. Values are normalized to day seven control large bead inner. All groups are cultured in osteogenic media. On day 21 expression levels are significantly greater in bioreactor inner than all other groups. The symbols (*, #, &, +) indicate statistical significance from all other groups within a timepoint ($p < 0.05$). Groups with symbol *, #, + or & are statistically different from all groups except those groups with the same symbol. Groups with the same symbol are statistically similar to each other.

To analyze mineralized matrix production, another marker of late osteoblastic differentiation Von Kossa staining was quantified using a histomorphometric analysis (Figure 6.8).

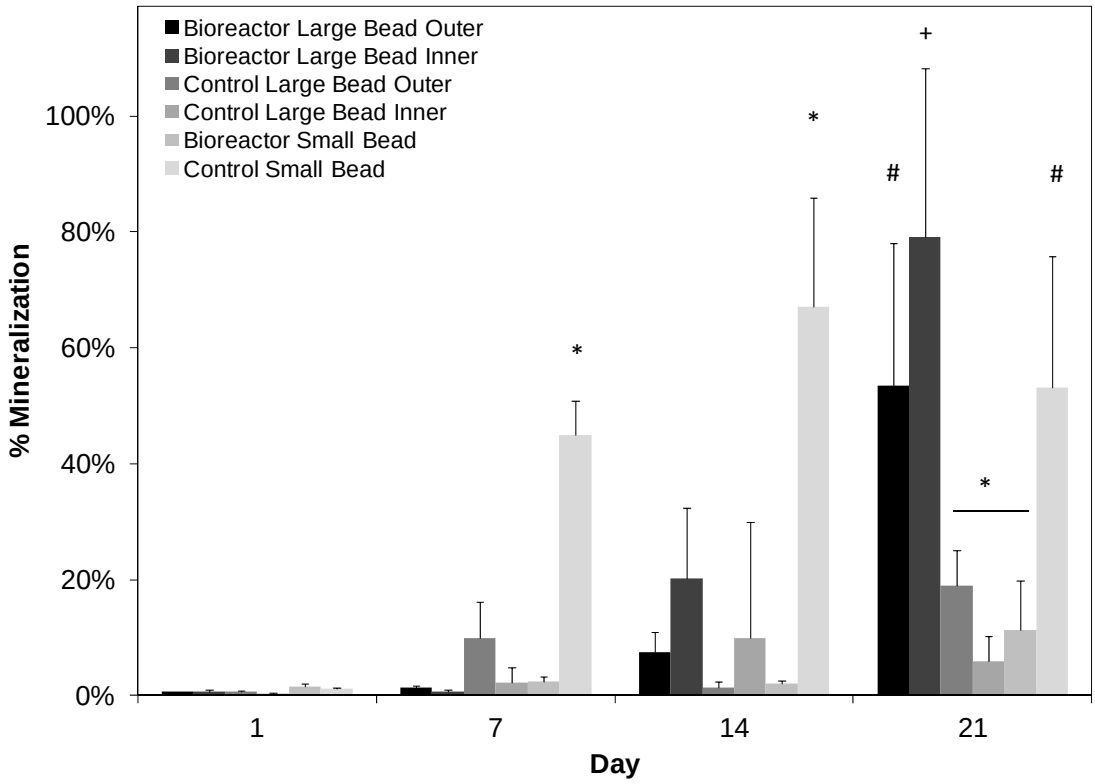

Figure 6.8: Percent mineralization based on histomorphometric analysis of Von Kossa stain of beads on days 1, 7, 14, and 21. Highest mineralization can be observed on day 21 in the inner annuli of bioreactor cultured beads. The outer annuli of bioreactor cultured beads and statically cultured small beads exhibit high mineralization on day 21. The symbols (*, #, +) indicate statistical significance within a timepoint ($p < 0.05$). Groups with symbol *, #, or + are statistically different from all groups except those groups with the same symbol. Groups with the same symbol are statistically similar to each other.

Surprisingly higher levels of staining were observed in the control small group on days 7 and 14 while other groups do not show large increases in mineralization until day 21. On day 21 significantly higher ($p < 0.05$) amounts of mineralization were observed in the inner annuli of bioreactor cultured beads with 79 ± 29% percent mineralization. High

levels of mineralization were also observed in the outer annuli of bioreactor cultured beads with 53 ± 25% mineralization. The control small exhibited similar levels of mineralization at 53 ± 22% mineralization. Low levels of mineralization were observed in the large control beads with only 19 ± 6% and 6 ± 4% mineralization area for the outer and inner sections respectively. Surprisingly the bioreactor small beads also had low levels of mineralization with 11 ± 9% mineralization. Representative images in Figure 6.9 illustrate these trends.

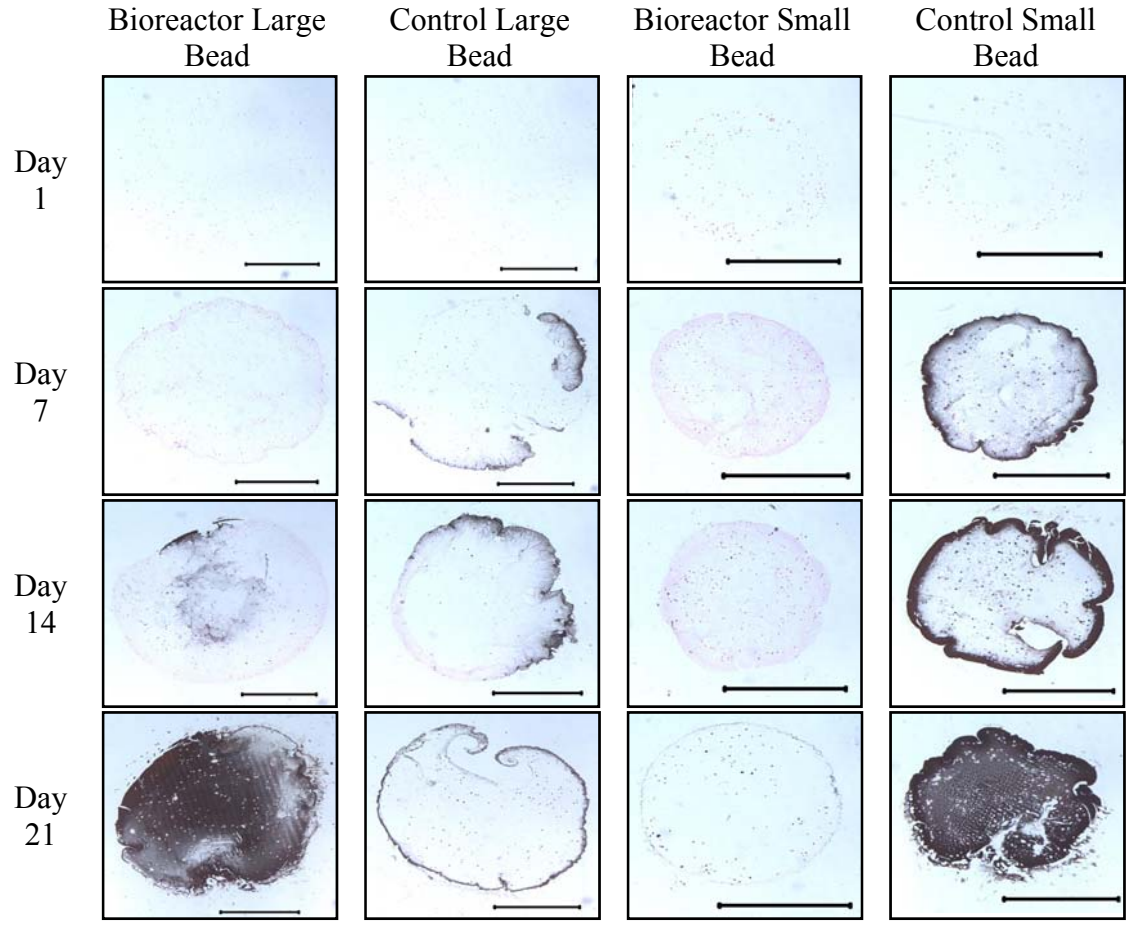

Figure 6.9: Representative images of bioreactor cultured large beads, statically cultured large beads, bioreactor cultured small beads, and statically cultured small beads. Scale bar represents 1000 μm. Note increased calcium staining on day 21 and the highest overall percentage of calcified area in the bioreactor large bead on day 21.

6.4 Discussion

The overall goal of this study was to determine how external culture conditions including shear stress and nutrient transfer affect hMSCs proliferating and differentiating in the TPS bioreactor as compared to static controls. The first part of the study focused on the role of shear stress in the osteoblastic differentiation of bioreactor cultured beads. Shear stress is commonly thought to induce osteoblastic differentiation in perfusion systems [16, 18, 28, 29, 38, 39, 80, 89, 110, 111]. Shear can be isolated from mass transport in a perfusion system using a thickening agent to change media viscosity. In this manner increasing shear has been demonstrated to increase mineralization in rat BMSCs [17] and upregulate osteoblastic differentiation in hMSCs [80]. Though increasing flow rate was previously shown to upregulate osteoblastic markers in the TPS bioreactor, shear stress was not isolated and specifically investigated [112]. In addition the TPS bioreactor utilizes bulk hydrogels rather than porous scaffolds used in previous bioreactor shear studies. Thus the direct effect of surface shear stress on encapsulated cells was previously unknown. It was discovered that increasing shear in the system led to an increase in late osteoblastic marker osteopontin and osteogenic signaling protein BMP-2 (Figure 6.3). Interestingly the effect of shear on osteopontin expression was temporal in nature with a greater correlation occurring at day 21 than on day 14. Though shear has previously been observed to upregulate osteoblastic differentiation of hMSCs, to our knowledge this is the first observation of a temporal correlation of this effect in a bioreactor system. This result was also observed when analyzing BMP-2 expression as minimal correlation is observed at days 1, 4, and 8, but a strong correlation is observed on day 21. Following previous work, shear stresses were calculated at the surface of the

bead equaling 1.63 ± 0.13 dynes/cm^2 for the 3% dextran media and 4.13 ± 0.34 dynes/cm^2 for the 9% dextran media [112]. Flow rate through the bead can be related to the permeability of alginate (1.2 ± 0.1 x 10^{-12} cm^2) [248] using Darcy's law in permeability [236, 248] where $Permeability = (QuL)/\big(A(\Delta P)\big)$ where Q is flow rate, u is dynamic viscosity of the media, L is the diffusion length, A is the surface area of the bead, and ΔP is change in pressure across the bead. Using the pressures in the system calculated from the COMSOL model [112] and assuming bead homogeneity, flow rate through a 4 mm cross section of the large bead was calculated to be approximately 3 x 10^{-7} ml/min. As shear is proportional to the change in velocity and the flow rate in the bead (3 x 10^{-7} mL/min) is 10^7 lower than the flow rate at the surface (3 mL/min), we can conclude that shear stresses will be reduced by similar amounts on the interior portions of the bead assuming a no slip condition at the surface. Therefore we speculate the effects of shear stress likely result from cells in the inner core of the bead responding to paracrine signals released from cells on the surface of the bead, however prolonged exposure of cells in the core of the bead to these small shear stresses could also impact cellular responses.

In the second part of the study the role of the cellular position in a scaffold as it relates to cell proliferation was investigated. The objective of this part of the study was to determine if nutrient transfer limitations were occurring and what role the TPS bioreactor had on these limitations. Nutrient and oxygen levels must be kept at sufficient levels throughout a three dimensional construct in order for cells to remain viable. The effect of oxygen concentration on hMSC proliferation has been previously investigated [207]. It was reported that hMSCs can survive low oxygen levels for up to 48 hours, but if the low

oxygen levels are combined with nutrient deprivation, significant cell death occurs. Based on proliferation data in this study it can be concluded that hMSCs in large (4 mm diameter) static cultured scaffolds are proliferating at lower rates than cells in bioreactor culture (Figure 6.5). This was likely caused by a deprivation of nutrients and oxygen to cells in these scaffolds. Day 21 DNA amount is over twice as high in bioreactor groups as compared to static control groups. The decrease in proliferation was most significant in the inner annuli of statically cultured large beads in which nearly a 50% drop in DNA amount is observed from day 7 to 21. These results are further supported when the small bead control is taken into account. Just as dynamic culture mitigates diffusion limitations, increasing the surface area to volume ratio of scaffolds through decreased size also mitigates this limitation. Thus small (2 mm diameter) static control beads had increased proliferation as compared to large statically cultured beads. Bioreactor cultured small beads had the highest levels of proliferation. These results highlight the need for bioreactor systems for the culture of tissue engineering constructs to avoid cell death resulting from hypoxia.

Finally, *in vitro* osteoblastic differentiation was analyzed as another key aspect of a cell based tissue engineering strategy. The objective of this final part of the study was to determine if scaffold radial position influenced hMSC osteoblastic differentiation. It is hypothesized that radially dependent differentiation will be influenced by two factors, shear stress (as discussed earlier) and oxygen content. The effect of oxygen content on stem cell osteoblastic differentiation is conflicted in the literature as increased proliferation and differentiation of hMSCs have been reported upon exposure to low (2% oxygen) conditions [196]. A similar result has been observed in rat MSCs as cells

cultured under 5% oxygen conditions increased in proliferation and differentiation as compared to 20% oxygen conditions. However it has been demonstrated previously that low oxygen concentrations can inhibit bone formation and *in vitro* osteoblastic differentiation [182, 191, 242, 247]. In hMSCs it was observed that even short term (48 hr) hypoxia caused a down regulation in several osteoblastic factors and markers [191]. In a study with rat osteoblasts sufficient oxygen was found as a requirement for bone growth as hypoxic conditions (2% oxygen) resulted in a downregulation of ALP and osteocalcin as well as an 11 fold decrease in mineralized bone [242]. Knowledge of the culture environment is critical as divergent cellular pathways of MSC differentiation and proliferation have previously been reported in the literature [101, 249, 250]. MSCs may directed down a specific pathway by physical factors in their environment [250]. Wnts have been demonstrated to be crucial in the modulation of these pathways [101, 165] and may be regulated via other signaling pathways including BMP-2 [166]. BMP-2 has been shown to enhance to stem cell differentiation and promote osteogenesis [66-68] and was measured in the first part of the study because of its strong association with bone formation.

This work supports findings that static culture of large constructs leads to reduced osteoblastic differentiation as large bead static control groups failed to express elevated levels of late osteoblastic marker osteopontin (Figure 6.7). These groups also produced low levels of mineralization further indicating an inhibition of osteoblastic differentiation in these groups. It is likely the observed decrease in proliferation in large control groups also results in less mineralization. These findings demonstrate the critical need for sufficient oxygen and nutrient transport during the three dimensional culture of hMSCs.

Interestingly low levels of mineralization were observed in the bioreactor cultured small beads. These beads exhibited the highest levels of proliferation, but mineralization levels were similar to that of large control beads. In addition osteopontin levels and mineralization percent were higher on the interior annulus of bioreactor cultured beads than the exterior annulus. The combination of these results with the observed increases in proliferation of cells in the exterior annulus of large beads and small beads of bioreactor cultured scaffolds could indicate the hMSCs being directed toward a proliferative pathway when more directly exposed to shear stress at the scaffold surface. In this manner the scaffold position could be altering the time course of differentiation by promoting a longer proliferation stage rather than differentiation and subsequent mineralization. Though the bioreactor smalls bead are not significantly mineralized in 21 days, osteopontin expression begins to rise on day 21 indicating these cells are undergoing late osteoblastic differentiation. This effect could result from two factors or a combination thereof. First, oxygen levels and shear vary throughout the scaffold [112] and the oxygen content and shear levels could be optimal for proliferation closer to the surface of the scaffold and differentiation closer to the center. Second the higher level of mineralization observed on the interior of bioreactor cultured large beads could result from signaling molecules released by cells on the exterior portions of scaffolds. We speculate exposure to shear stress may be inducing these cells to release factors that signal cells on the interior portion of the scaffolds to differentiate, while the cells directly exposed to shear and higher nutrient concentration follow a proliferative pathway. These results demonstrate the ability of the TPS bioreactor to both promote an osteoblastic

differentiation pathway or a proliferative pathway prior to osteoblastic differentiation depending on culture conditions.

This study demonstrates the critical need for bioreactor systems in three dimensional cell culture. Reduced proliferation and differentiation were observed in 4 mm statically cultured constructs and the ability of the TPS bioreactor to mitigate these results in three dimensional scaffolds was demonstrated. Osteoblastic differentiation and shear results demonstrate shear stress to induce a temporal and potentially indirect effect on hMSC osteoblastic differentiation. Bioreactor systems provide a complex environment and when evaluated on a cellular level can deliver an array of culture conditions to cells cultured in the same macro environment. This can lead to a multitude of outcomes on the individual cell level. Thus while bioreactor systems are vital to provide sufficient nutrients to prevent cell death they must be thoroughly evaluated to identify optimal culture conditions for the desired differentiation level prior to implantation.

6.5 Conclusions

This study demonstrated shear stress as a potent and temporal stimulus of hMSC osteoblastic differentiation within bulk scaffolds. Mineralization and proliferation levels were decreased in statically cultured constructs highlighting a need for bioreactor systems. In addition it was discovered that hMSC spatial position within scaffolds had an effect on both the osteoblastic differentiation and proliferation of these cells. These results could be used to tailor a flow and shear regime for either expansion or differentiation of a stem cell population to dictate the desired outcome of *in vitro* culture

Chapter 7: Formation of an Aggregated Alginate Construct in a Tubular Perfusion System[4]

7.1 Introduction

A significant challenge in the implementation of cell based tissue engineering strategies remains the inability to successfully culture large constructs *in vitro*. One approach to overcoming this difficulty is a bottom up approach to creating a tissue engineering construct. In the traditional tissue engineering approach a polymer scaffold is constructed in its final shape and seeded with cells. The cells are then cultured *in vitro* to allow for proliferation and matrix deposition throughout the scaffold. This approach is limited by the scaffold size and cell density that will allow for homogenous growth and matrix production throughout the scaffold. For example, central oxygen concentration of cells cultured in scaffolds 9 mm by 5 mm were shown to drop to 0% after just five days of culture [21]. Bioreactor culture was shown to mitigate this effect, however central oxygen concentration of the same constructs cultured in a perfusion bioreactor were only 4%. This work underscores the difficulty of culturing larger, clinically relevant three dimensional scaffolds *in vitro* using a traditional top down tissue engineering approach.

In a bottom up tissue engineering approach small scale tissue engineering building blocks are created. These tissue building blocks are then assembled into a large tissue engineering construct [251]. For example, using endothelial cell coated collagen gel constructs a modular tissue engineering approach has been used to create a multicell

[4] As published in Yeatts, A.B., C.N. Gordon, and J.P. Fisher, *Formation of an aggregated alginate construct in a tubular perfusion system.* Tissue Eng Part C Methods, 2011. **17**(12): p. 1171-8.

microvascularized tissue engineering construct [214]. These endothelial coated gels contained an encapsulated hepatoma cell line and following perfusion culture in a bioreactor system the individual modules assembled to form a construct with interconnected channels [252, 253].

The goal of this work is to create an engineered tissue aggregated from many small alginate beads that are cultured individually prior to aggregation. This will allow for the *in vitro* development of tissue engineering constructs on size scales not easily possible with previous culture methods. The system involves the culture of human mesenchymal stem cells (hMSCs) in alginate beads in the tubular perfusion system (TPS) bioreactor. The tubular perfusion system uses an elegant bioreactor design in which alginate scaffolds are tightly packed in a tubular growth chamber and media is pumped through the growth chamber from a reservoir by a peristaltic pump. The TPS bioreactor has been shown to support the growth and osteoblastic differentiation of hMSCs as well as enhance late osteoblastic differentiation and calcium matrix production [112]. hMSCs are utilized in this study as a promising cell source for both bone and cartilage tissue engineering as they can be isolated from the bone marrow and readily differentiated into both osteoblasts and chondrocytes [6, 112]. The hMSCs are encapsulated in alginate, a natural biomaterial derived from algae that is frequently utilized in cartilage tissue engineering [108, 109, 218, 219] as well as some bone tissue engineering applications [221-224]. Alginate is composed of mannuronic acid and guluronic acid chains [219]. When a divalent ion such as calcium is added to an alginate solution the calcium binds between guluronic acid blocks of the alginate chain ionically crosslinking the alginate chains and gelling the alginate solution [254]. Thus cells can be easily encapsulated in an

alginate hydrogel by mixing an alginate cell solution and adding the solution dropwise into a calcium chloride solution. The size of these beads can be controlled by changing the size of the needle. The beads can then be dissolved through the addition of a calcium chelating agent such as ethyldiaminetetraacetic acid (EDTA) which sequesters the crosslinking calcium ions. This makes alginate advantageous for *in vitro* experimentation as cells can easily be removed and analyzed.

In this work these properties are utilized to create an aggregated construct where cells are cultured in smaller beads which are joined to form a single, mechanically intact large construct. The objectives of this study are to first develop this aggregated construct in the TPS bioreactor. Following this the mechanical properties of the construct will be tested. Finally, hMSCs will be encapsulated in the construct and the viability of these cells will be demonstrated throughout the creation of this construct.

7.2 Materials and Methods

7.2.1 Bioreactor Design

Dynamic culture is completed in the TPS bioreactor as previously described [112]. Briefly, the bioreactor system consists of a tubular growth chamber and media reservoir connected via a tubing circuit which consists of platinum cured silicone tubing (Cole Parmer, Vernon Hills, IL) for all areas except the area that passes through the pump which is composed of Pharmed BPT tubing (Cole Parmer) (Figure 7.1). Media flow was driven by an L/S Multichannel Pump System (Cole Parmer) at 3 mL/min. Following loading with cell containing beads the tubing was fully assembled inside a cell culture hood and then placed in a cell culture incubator at 37º C and 5% CO_2. Fifty mL of

osteogenic media was loaded into separate 125 mL Erlenmeyer flasks for each growth chamber topped with rubber stoppers. Media is withdrawn and replaced from the reservoir through two tubes that penetrate the stopper and changed every three days.

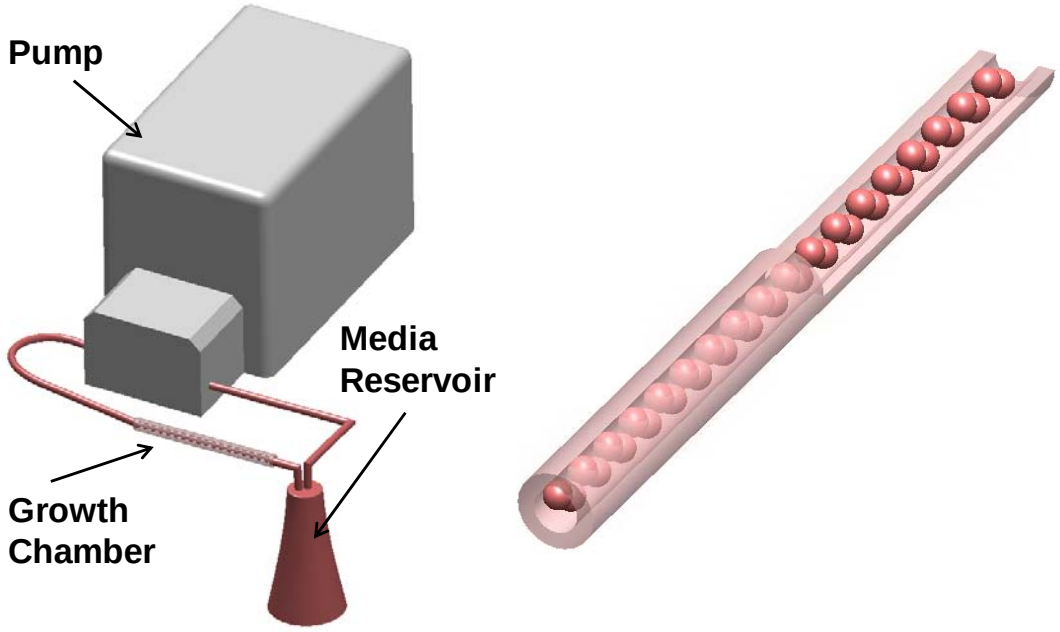

Figure 7.1: Schematic of TPS bioreactor (left) and enhanced view of growth chamber (right). Aggregated alginate constructs are formed in the growth chamber.

7.2.2 Fabrication of Aggregated Alginate Constructs (AACs)

Alginate solutions of 2.0% w/v were prepared as previously described by adding alginic acid sodium salt from brown algae (Sigma, St. Louis, MO), into 0.15M NaCl (Sigma), and 0.025M HEPES (Sigma) in deionized water [106, 108, 109]. Alginate beads were fabricated by dropwise addition of this solution into a stirred solution of 0.1 M calcium chloride (Sigma). The beads were stirred for 15 minutes using a magnetic stir bar and stir plate set to 60 rotations per minute. The beads were then removed from the calcium chloride solution and rinsed in a phosphate buffered saline (PBS) solution for 15 minutes.

Bead size was varied by changing the needle gauge size. Gauges of 16, 18, 20, 27, and 30 were used. To make aggregated constructs beads were loaded into a growth chamber to make an aggregated construct approximately 2 cm in length. A 0.025M solution of ethyldiaminetetraacetic acid (EDTA) (Sigma) was flowed through the growth chamber at 1.8 mL/min for five minutes. Allowing the EDTA to flow through the growth chamber for five minutes permits all the beads to be in full contact with the EDTA solution, and causes the alginate beads to expand in size and overlap. Following this step, the EDTA solution was replaced with a 0.5 M solution of calcium chloride. This solution was flowed into the TPS for 5 minutes at 1.8 mL/min to remove EDTA, then perfused through the growth chamber at 10 mL/minute for 20 minutes to form aggregated constructs by ionically crosslinking the alginate chains with the calcium ions. The five minute calcium chloride step is important to wash all remaining EDTA, while the 20 minute calcium chloride step distributes calcium ions to all beads. Aggregated alginate constructs were then removed from the TPS bioreactor for experimentation.

7.2.3 Measurement of Tensile Mechanical Strength

Prior to mechanical testing the dimensions of the AACs were measured using calipers and the mass of the sample measured using an Ohaus Analytic Plus analytical balance. Constructs were placed using forceps into custom fit clamps attached to the clamps provided by the manufacture and the tensile strength measured using a Tensilon RTF-1310 mechanical tester outfitted with a 50N load cell and MSAT0002 materials testing software. The AAC samples were stretched with a constant crosshead speed of 1.0 mm/min, with the software constantly recording the stress and strain. The test ended with sample fracture. Young's modulus, tensile strength, and yield strength of the AACs were

calculated. The Young's modulus was calculated as the slope of the initial linear portion of the stress-strain curve. The ultimate tensile strength was identified as the maximum stress reached by each sample. The tensile strength at 0.2% yield was calculated by locating the intersection of the stress-strain curve and a line with the Young's modulus slope at 0.2% strain offset [255].

7.2.4 Measuring Rate of Bead Dissolution

To determine the dissolution rates of beads in EDTA beads were fabricated as described previously in the methods using an 18 gauge needle. Initial bead size was then measured by calculating the cross sectional area using Image J software (NIH, Bethesda MD) of a bead based on a image taken with an Axiovert 40 CFL with filter set 23, (Zeiss, Thornwood, NY) equipped with a digital camera (Diagnostic Instruments 11.2 Color Mosaic, Sterling Heights, MI). Alginate beads were loaded into TPS growth chamber and perfused with EDTA with concentrations ranging from 0.008M to 0.1M at 1.8 mL/min. At each time point, five beads were removed from the bioreactor and photographed. Cross sectional areas were normalized to initial cross sectional areas to determine bead dissolution at each time point.

7.2.5 Human Mesenchymal Stem Cell Culture

Human mesenchymal stem cells ($p \leq 5$) from a single donor were purchased from Lonza (Walkersville, MD). Single donor cells were used to minimize variability associated with a primary cell population. Cells were cultured prior to the study in control media consisting of DMEM (Gibco, Carlsbad, CA) supplemented with 10% fetal bovine serum (Gibco), 1.0 % v/v penicillin/ streptomycin (Gibco), 0.1 mM non essential amino acids

(Gibco), and 4 mM L-glutamine (Gibco) using protocols set forth by the manufacture and previously described [69, 112, 232]. Cells were cultured on tissue culture polystyrene flasks with media changes every three days according to the manufacture's specifications. Cells were stored in a cell culture incubator at 37º C and 5% CO_2 and passaged every 6-7 days using trypsin/EDTA (Lonza). Osteogenic media was formulated as described in the literature by supplementing control media with 100 nM dexamethasone (Sigma), 10mM β-glycerophosphate, and 173 μM ascorbic acid (Sigma) [69, 233].

7.2.6 hMSC Encapsulation in Alginate

Alginate solutions were sterilized via sterile filtration. hMSCs were removed from tissue culture flasks using trypsin/EDTA and pelleted via centrifugation at 500 xg for five minutes. The cell pellet was resuspended in the alginate solution at a density of 1.25-2.5 x 10^6 cells/mL. The alginate cell solution was added drop wise through a 20 gauge needle into a stirred solution of 0.1 M calcium chloride (Sigma) which immediately crosslinked the alginate to form beads. Beads were allowed to stabilize for 15 min and were loaded into the bioreactor. Cells were cultured in control media for use in live dead staining and osteogenic media in order to differentiate the hMSCs into osteoblasts and determine if calcium is produced as measured using Von Kossa staining. Control media was used for live dead and metabolic activity assays to observe the growth process when cells are not differentiating. Media was changed every three days.

7.2.7 Metabolic Activity

hMSCs were encapsulated in alginate beads at 100,000 cells per bead. After stabilizing for 24 hours in control media in static culture, beads were exposed to either 35 minutes of

control media with FBS (control group), 5 minutes of 0.1 M calcium chloride, 5 minutes of 0.025 M EDTA, and 25 minutes of 0.5 M calcium chloride (AAC treatment group), or 35 minutes of 70% methanol (Sigma) (dead control group). Metabolic activity was then assessed using a dimethylthiazolyldiphenyltetrazolium bromide (MTT) based *in vitro* toxicology kit (Sigma) as previously described [239]. Briefly 200 µL of 5 mg/mL of reconstituted MTT was added to each well with 2 mL of control media with 10% FBS. Beads were then incubated for 150 minutes to allow for the formation of formazan crystals. Crystals were dissolved in 2 mL of MTT solubilization solution (Sigma) and allowed to dissolve out of alginate beads overnight. 200 µL of supernatant was then transferred to a 96 well plate to record the optical density in triplicate at 570 nm using an M5 SpectraMax microplate reader (Molecular Devices, Sunnyvale, CA).

7.2.8 Live Dead Assay

Cell viability was assessed using a live dead assay following standard protocols as described previously [239]. Viability tests were completed on three groups. In the control group cells were cultured in static culture in control media. In the AAC group cells were cultured in the bioreactor at a 3 mL/min flow rate for 10 days. AACs were formed from bioreactor cultured beads and removed from the bioreactor. In the final group the AAC was cultured in a static culture plate to determine if the hMSCs could remain viable for 24 hours. AACs were either soaked in PBS to remove FBS and media for 30 minutes or moved to six well plate for 24 hour culture. Control beads were also first soaked in PBS for 30 minutes to remove FBS and media. Beads and AACs were then placed in well plates and incubated in 2 µm ethidium homodimer and 4 µm calcein AM (Invitrogen, Carlsbad, CA) for thirty minutes. Fluorescent images were then taken

using a fluorescent microscope (Axiovert 40 CFL with filter set 23, Zeiss, Thornwood, NY) equipped with a digital camera (Diagnostic Instruments 11.2 Color Mosaic, Sterling Heights, MI). AACs cultured in well plate were removed 24 hours later and stained following the same procedures as other groups.

7.2.9 Histological Analysis

Experimental hMSCs were cultured in individual alginate beads in osteogenic media in the TPS bioreactor for 21 days. On day 21, alginate beads were aggregated into AACs and were collected and fixed in 4% paraformaldehyde (Sigma) and 0.1 M sodium cacodylate (Sigma) buffer containing 10 mM calcium chloride at pH 7.4 at 4° C for 4 hours. Following fixation, the beads were placed in cassettes and washed with 0.1 M sodium cacodylate buffer and 10mM calcium chloride at pH 7.4 at room temperature for 24 hours. The beads were then dehydrated for histological processing by ethanol washes followed by two Citrisolv (Fisher Scientific) washes. The samples were then embedded in paraffin (Fisher Scientific) and sectioned to 5 μm thickness sections and placed on glass slides. Sections were oven dried at 64° C for 2 hours, deparaffinized in Citrisolv and rehydrated in ethanol. Von Kossa staining was performed using standard protocols to visualize mineralization with a Nuclear Fast Red (Poly Scientific, Bay Shore, NY) counterstain.

7.2.10 Statistical Analysis

All samples were completed in triplicate (n=3). Data was analyzed using single factor ANOVA followed by Tukey's Multiple Comparison Test assuming normal data distribution with a confidence of 95% ($p < 0.05$). Mean values of triplicates and standard

deviation error bars are reported on each figure as well as relevant statistical relationships.

7.3 Results

7.3.1 Formation and Dissolution of Alginate Beads

Alginate beads were fabricated to consistently different sizes using needle gauges of 16, 18, 20, 27, and 30 (Table 7.1). By using a needle gauge of 30 an average bead diameter of 2.15 ± 0.07 mm was obtained. Sixteen gauge needles resulted in average bead diameters of nearly twice this magnitude with an average diameter of 3.90 ± 0.09 mm. Needles with gauges in between these two resulted in bead diameters inside this range with each gauge needle producing beads significantly different in diameter from all other gauges ($p<.05$). Based on these results beads of discrete diameters can be fabricated using different needle sizes.

Table 7.1: Alginate bead cross sectional area. Data are reported as mean ± standard deviation. All groups are statistically different ($p<0.05$).

Needle Gauge	Bead Diameter (mm)
16	3.90 ± 0.09
18	2.97 ± 0.02
20	2.65 ± 0.07
27	2.46 ± 0.06
30	2.15 ± 0.07

Dissolution curves of beads were then generated using 0.1 M, 0.05 M, 0.025 M, and 0.008 M concentrations of EDTA. This analysis was performed with 2.97 mm diameter beads. Results of bead dissolution experiments revealed that 0.008 M EDTA did not

dissolve alginate beads over the thirty minute experiment (Figure 7.2). Cross sectional area was shown to increase slightly over the time points. For groups dissolved in 0.025 and 0.050 M EDTA bead size initially increased but decreased over later time points until complete dissolution in the 0.05 M group and near complete dissolution in the 0.025 M group. The 0.025 EDTA group increased to 127% of original bead diameter after 5 minutes before dissolving to 11% of original area after 30 minutes. The 0.05 M group increased to 108% its original diameter before completely dissolving after 30 minutes. The 0.100 M was shown to completely dissolve in 10 minutes without an increase at the 5 minutes timepoint. These observed results in 0.025 M and 0.05 M EDTA likely occur as EDTA decreases the crosslink density of the alginate causing the bead to grow in size before the bead is dissolved.

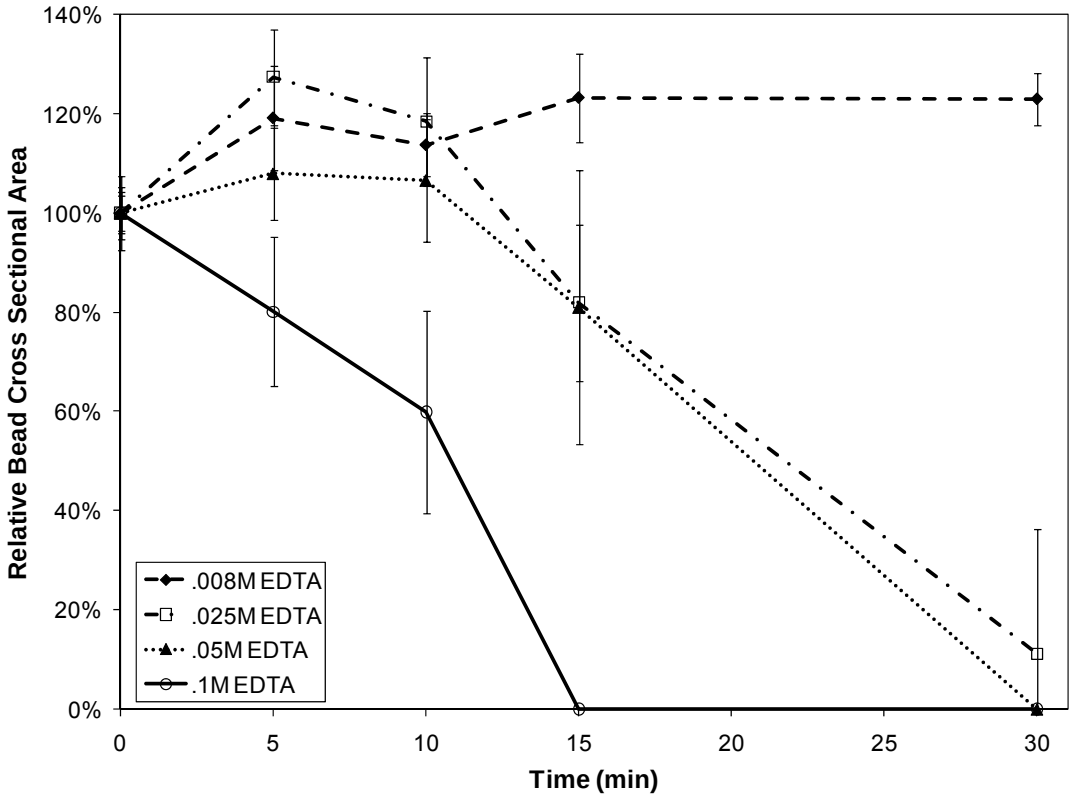

Figure 7.2: The dissolution of alginate beads at varying EDTA concentrations at 1.8mL/min flow rate. Bead sizes are reported as cross sectional areas in relation to initial area.

7.3.2 Mechanical Properties of Aggregated Alginate Constructs

The initial increase in size of beads in the 0.025 M EDTA group was used to develop a protocol to make aggregated alginate constructs. Using this protocol these constructs were successfully created and shown to be easily transported and manipulated (Figure 7.3).

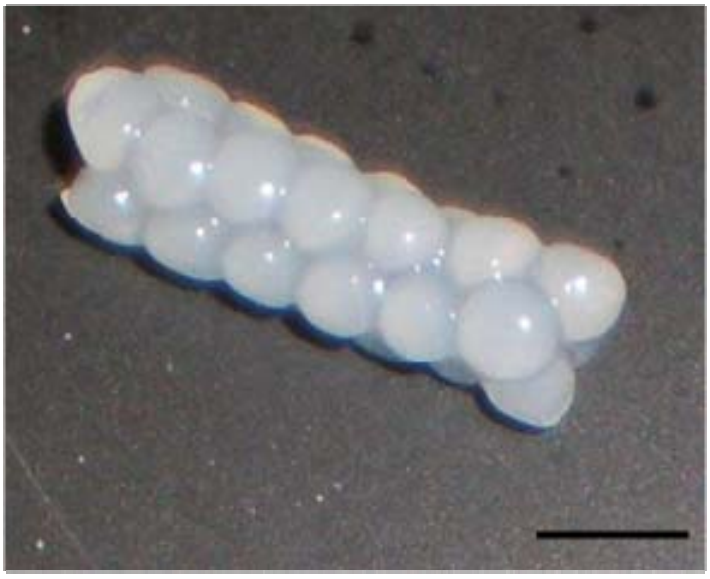

Figure 7.3: Image of aggregated alginate construct. Owing to the simplicity of the design, the construct can be easily moved and manipulated. Scale bar represents five millimeters.

Mechanical testing of these constructs revealed that smaller diameter beads resulted in stronger aggregated constructs (Figure 7.4). Aggregated constructs made from beads with 2.15 mm diameters had a Young's modulus of 85.6 ± 15.8 kPa, a tensile strength of 3.24 ± 0.55 kPa and a yield strength of 1.44 ± 0.27 kPa. These values were statistically similar ($p>0.05$) to constructs made from beads with 2.46 mm diameter. Increase of bead diameter slightly to 2.65 mm resulted in a relatively large and statistically significant change ($p<0.05$) in mechanical properties producing constructs with a Young's modulus of 39.2 ± 10.6 kPa, a tensile strength of 0.85 ± 0.25 kPa and a yield strength of 0.52 ± 0.15 kPa. These mechanical properties were statistically similar ($p>0.05$) to constructs made from beads with 2.97 mm and 3.90 mm diameters though beads with the largest diameter, 3.90 mm, exhibited the weakest mechanical properties. These samples had a Young's modulus of 18.2 ± 5.6 kPa, a tensile strength of 0.45 ± 0.04 kPa and a yield

strength of 0.27 ± 0.03 kPa. AAC fracture was typically observed on the periphery of beads aggregated together, however no other preferential breaking point was noted.

(a)

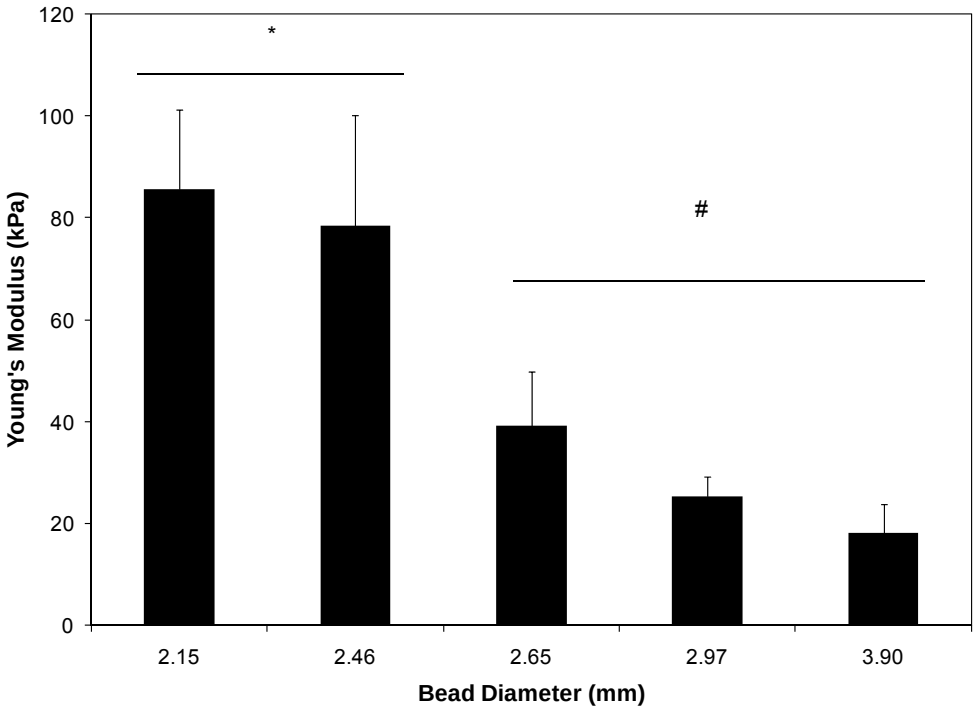

(b)

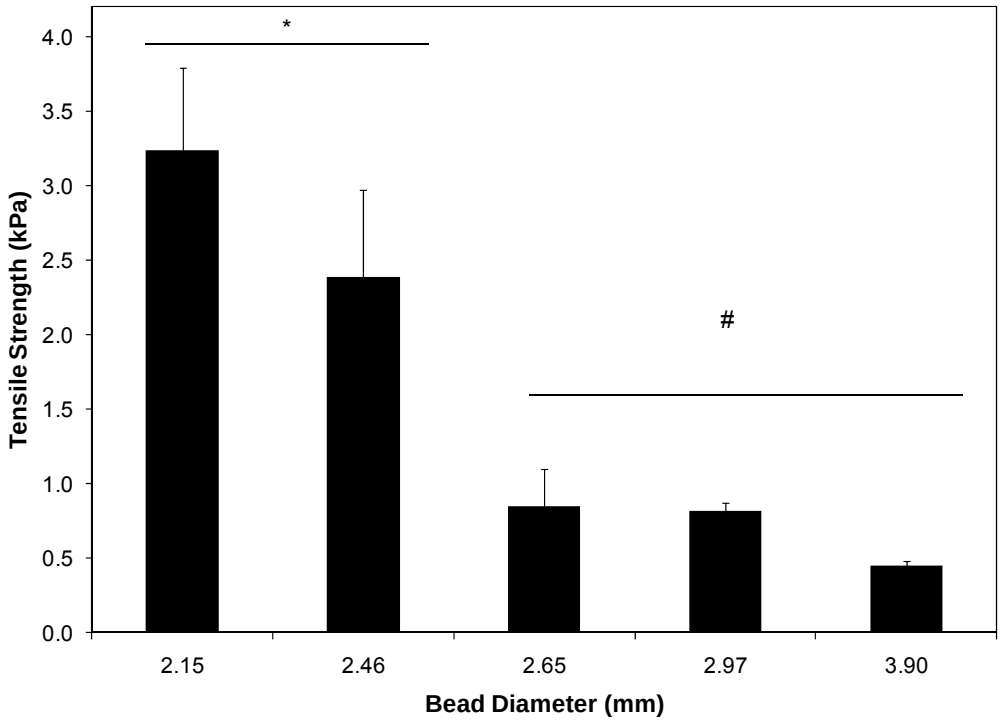

(c)

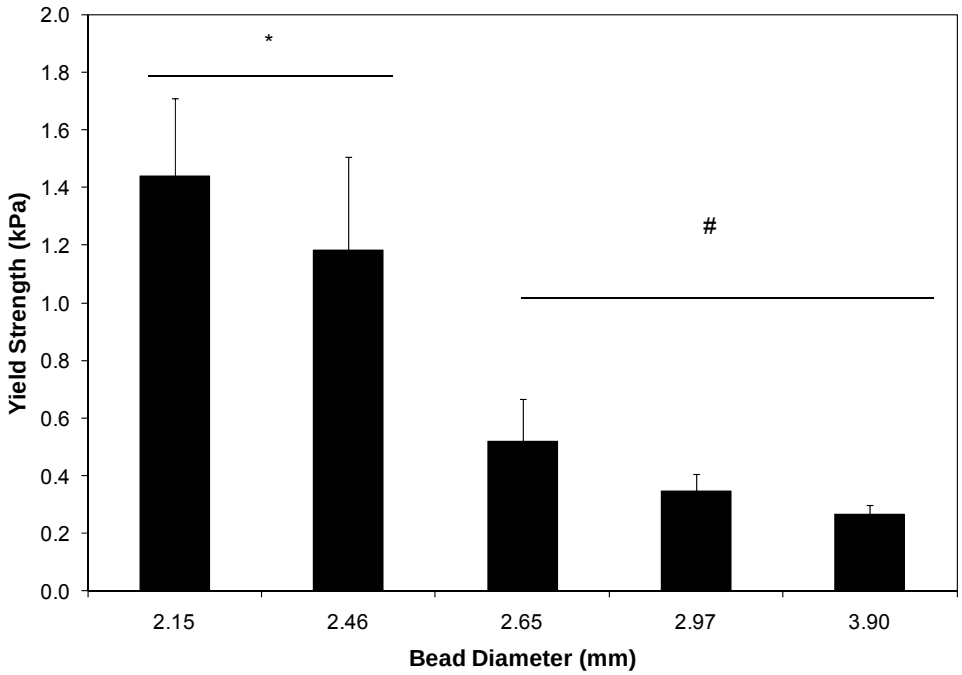

Figure 7.4: Mechanical properties of aggregated alginate construct including Young's Modulus (a), tensile strength (b) and yield strength (c). Note 2.15 and 2.46 mm groups are statistically greater than other groups but statistically similar to each other. All other groups are statistically similar. The symbols (*, #) indicates statistical significance ($p < 0.05$).

7.3.3 hMSC Viability and Calcium Deposition in Aggregated Alginate Constructs

Results of MTT assay indicate AAC treatment has no effect on the metabolic activity of encapsulated hMSCs (Figure 7.5).

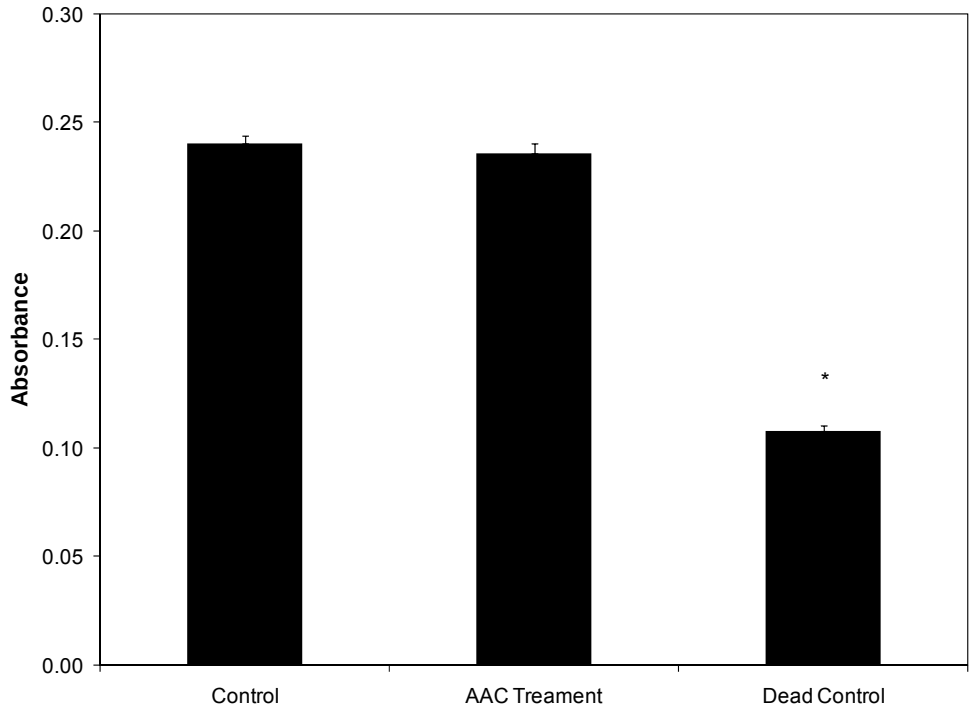

Figure 7.5: Metabolic activity of cells in alginate bead in control media, AAC treatment, and dead control. Dead control is significantly lower than control bead and AAC treatment, which are statistically similar. The symbol (*) indicates statistical significance ($p < 0.05$).

Cells in alginate beads exposed to AAC treatment had statistically similar metabolic activity to control hMSCs. Both these groups had significantly greater metabolic activity than hMSCs in beads exposed to methanol as a dead control. Microscopic images of the AAC reveal that hMSCs are homogenously distributed throughout the construct (Figure 7.6).

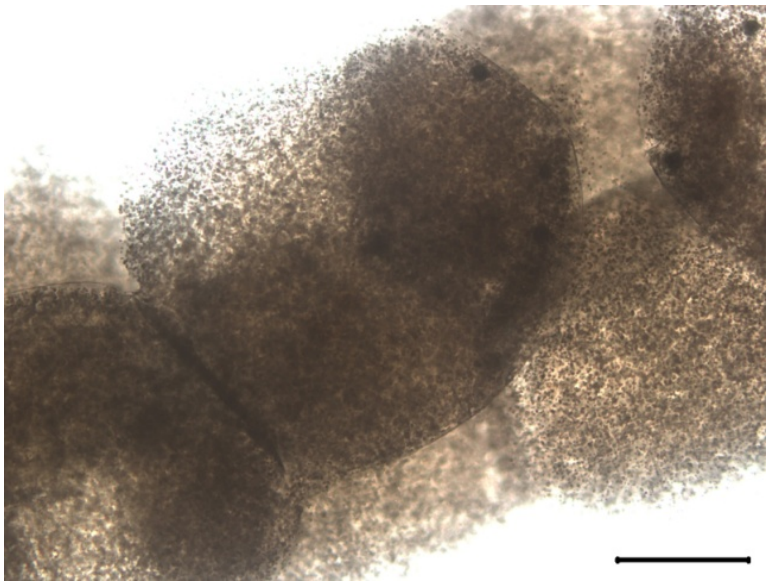

Figure 7.6: Image of cell containing AAC. Cells can be observed throughout construct. Scale bar represents 1000 μm.

Upon live dead staining images reveal that the majority of these cells are viable after ten days of culture and AAC formation (Figure 7.7). Live dead images of cells 24 hours after AAC treatment reveal that cells remain viable following the treatment.

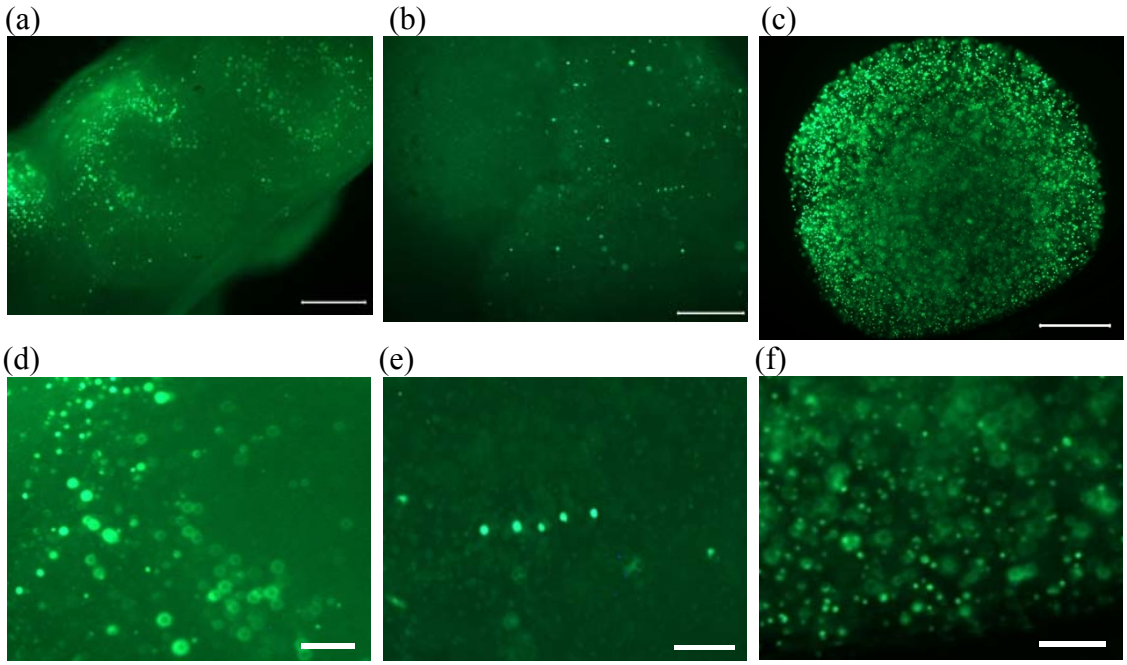

Figure 7.7: Live dead stain of AAC (a,d) after 10 days of individual bead TPS culture and formation. Live dead stain of AAC after 10 days of individual bead TPS culture and 24 hours of static culture following AAC treatment (b,e) Live dead staining of control (c,f) after ten days of static culture. Cells appear viable in all groups. Scale bar represents 1000 μm (a,b,c) and 200 μm (d,e,f).

Following demonstration that hMSCs are viable in AACs, beads were cultured for 21 days in osteogenic media to demonstrate if calcium production was occurring as previously observed and if this calcium deposition would remain present throughout the AAC treatment [112]. Images of AAC sections stained using Von Kossa staining indicate that hMSCs produce calcium while being cultured prior to AAC formation and that AAC treatment does not eliminate these calcium deposits (Figure 7.8). Calcium is stained black in these images and can be seen surrounding cells in AACs.

(a) (b)

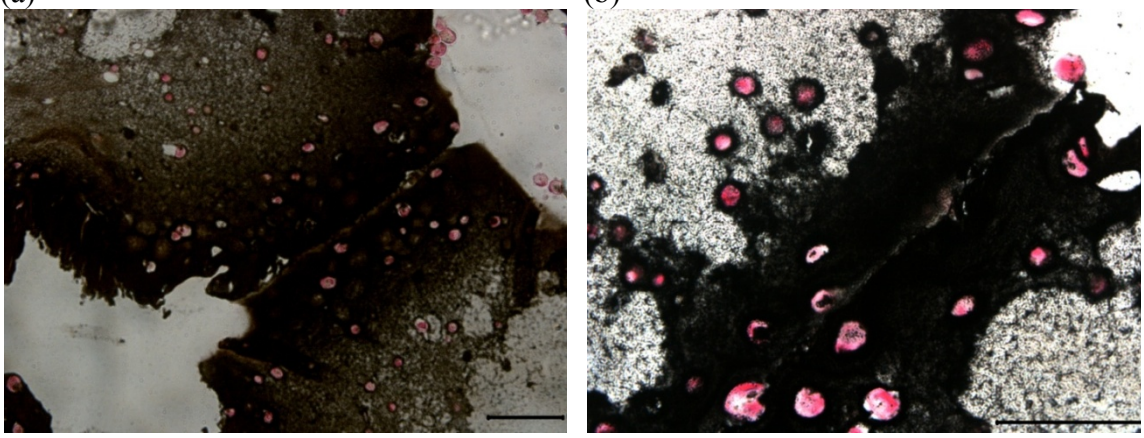

Figure 7.8: Von Kossa staining of AAC formed after 21 days of *in vitro* TPS culture of individual beads in osteogenic media at 20x objective (a) and 40x objective (b). Images show cells (pink) at the juncture of two beads in the AAC surrounding by calcium deposits (black). Scale bars represent 100 μm.

7.4 Discussion

A tissue engineering treatment option for bone, cartilage and skeletal muscle represents a promising alternative to current clinical options. Despite the promise of tissue engineering, several significant hurdles exist. A central limitation is the culture of three dimensional tissue engineering constructs *in vitro*. In static culture, nutrients and oxygen are replenished via diffusion. A nutrient gradient develops where cells on the exterior portions of scaffolds receive sufficient nutrients, while cells on the interior of scaffolds are deprived of nutrients and are exposed to hypoxic conditions [111, 182]. In a study analyzing oxygen concentration in three dimensional scaffolds, a preosteoblast cell line was seeded on demineralized bone matrix scaffolds at 5 x 10^4 cells/scaffold [21]. These scaffolds were 9 mm in diameter and 5 mm in height and cultured in static and dynamic conditions. In static culture central oxygen concentrations dropped quickly, below 10% in just two days and to 0% in just five days. Cell death was observed in areas where the central oxygen concentration was low. Dynamic culture in a bioreactor significantly

improved oxygen transport and though central oxygen concentrations dropped to 4% cell death was not observed. Here we create aggregated constructs as large as 6 mm in diameter and 30 mm in height seeded at 3 x 10^6 cells/scaffold. Prior to scaffold aggregation the individual alginate beads are cultured in the TPS bioreactor to enhance the growth of cells in the scaffolds. Following aggregation the cells will no longer be cultured in the TPS bioreactor and are ready for implantation into a defect. By not attempting to culture such a large construct *in vitro* this method avoids nutrient transfer limitations, a major obstacle to three dimensional cell culture. To the best of our knowledge this is the first time an aggregated alginate scaffold has been created from many smaller cell containing scaffolds in a bioreactor system. Cells were viable throughout the scaffold as these constructs were rapidly fabricated.

A modular tissue engineering approach previously has been used to create a perfusable cell containing construct [214], a cardiac sheet like construct [256], and dermal equivalent tissue [257]. Previously used modular techniques have relied either on cell aggregation or a more complex approach such as tissue printing. Here we use a new approach where individual alginate beads are assembled together prior to implantation. This approach creates a controlled aggregated construct within a bioreactor system quickly with no major fabrication steps.

The method for fabricating these aggregated scaffolds was developed following analysis of alginate bead dissolution curves in EDTA, where it was discovered that alginate beads first increase in diameter prior to dissolution. When using EDTA concentrations ranging from 0.008-0.05 M this initial expansion occurs over a sufficiently long period to manipulate beads prior to dissolution. The goal of this experiment was to find an optimal

EDTA concentration that could be used to form aggregated alginate constructs. Results indicated that dissolution in 0.025 M EDTA would be optimal as this concentration resulted in the largest initial increase in bead diameter. It should be noted that these dissolution curves may not me applicable to dissolution of alginate beads in other systems as bead size can vary significantly due to swelling [258]. This swelling results from ion exchange between the calcium crosslinking ions and monovalent ions in the environment of the bead [259, 260]. In order to fabricate the AACs, the alginate beads were tightly packed in the tubular growth chamber and were perfused with 0.025 M EDTA for 5 minutes to allow for expansion. Following this expansion, exterior edges of the beads overlapped with one another. Beads were then perfused with calcium chloride to ionically crosslink the overlapping edges, creating one aggregated construct from many beads.

Mechanical testing of this aggregated construct was then completed. Beads with different initial sizes were used in the study. AACs composed of beads with initial diameters of 2.15 and 2.46 mm had significantly higher Young's Moduli, Ultimate Tensile Strength and Yield Strength than AACs composed of beads with initial diameters of 2.65, 2.97, and 3.90. Young's modulus, Ultimate Tensile Strength, and Yield Strength all decreased with increasing bead size. It is hypothesized that this occurs as beads with larger diameters are not able to pack as closely and create a less dense aggregated construct. Compression testing was not completed on the construct the primary goal was to measure the strength of bead aggregation. Alginate compression testing has been previously reported in the literature [261, 262].

Previous studies to determine the mechanical strength have shown large variations based upon the specific alginate polymer used; however our results revealed AACs have tensile properties in the lower range of alginates tested and Young's Moduli similar to previously described results [263]. This demonstrates AACs to be of sufficient strength for the engineering of tissue such as cartilage [108, 109, 204, 264], non load bearing bone [220, 221], skeletal muscle [265], and other tissues that are commonly engineered using alginate. Specifically AACs provide an advantage over typical alginate constructs, as individual alginate beads can be cultured in a bioreactor and then fabricated into one large construct. Thus a large construct will be created without nutrient transfer problems that occur in statically cultured large constructs. Metabolic activity assays indicate that the AAC treatment does not have a negative effect on the metabolic activity of hMSCs encapsulated in alginate beads. This result is expected as the AAC treatment utilizes chemicals that are widely used in alginate bead fabrication and usage [108, 109, 264]. This result was further confirmed by live dead staining which indicated cells in AACs were viable immediately and 24 hours after AAC fabrication.

In a prior study utilizing the TPS bioreactor hMSCs were shown to express much higher levels of osteogenic markers osteocalcin and osteopontin than static controls [112]. In addition to this mineralization was shown to be greatly increased throughout the bioreactor cultured beads. A goal of this study was to determine if this mineralization would remain following AAC treatment. Von Kossa staining for calcium was performed to examine this. This stain revealed that hMSCs in the AACs had deposited calcium and this calcium remained present throughout the AAC treatment. *In vitro* calcium

deposition indicates that the hMSCs are able to differentiate into osteoblasts after 21 days and this calcium deposition remains present following AAC treatment.

The clinical strategy for use of this construct is to first extract bone marrow from the patient and isolate the mesenchymal stem cells. These stem cells will then be encapsulated in the alginate beads and cultured in the TPS bioreactor. When the tissue is ready to be implanted into the defect site the beads will be aggregated in the bioreactor, removed and the construct implanted into the patient. This follows the same strategy as traditional tissue engineering however will allow for the production of larger cell containing constructs than previously possible.

7.5 Conclusions

Through the course of this study a protocol has been developed and evaluated for the fabrication of a cell containing tissue engineering construct from many smaller scaffolds in a bioreactor system. Results demonstrate this construct can be elegantly fabricated and has mechanical properties similar to traditionally fabricated alginate scaffolds. This aggregated alginate construct has many potential applications including non load bearing bone, cartilage and skeletal muscle tissue engineering. By allowing cells to proliferate in smaller beads within the TPS bioreactor prior to aggregation, a large tissue engineering construct is created ready for implantation into a defect site.

Chapter 8: Tubular Perfusion System Culture of Human Mesenchymal Stem Cells on PLLA Scaffolds Produced Using a Supercritical Carbon Dioxide Assisted Process[5]

8.1 Introduction

Despite recent advances, commonly used techniques for the treatment of bone defects have significant disadvantages and cell based tissue engineering (TE) represents a promising alternative treatment [2, 3]. An objective of TE is to create interactions between an artificial component and cellular components to ensure tissue regeneration. The artificial component needs to support cellular growth and three dimensional organization, which requires the coexistence of micro and nano-structures, mimicking the extracellular matrix (ECM). In this study micro-structure is defined as scaffold features with a size scale between 1 and 1000 μm and nano-structure is defined as scaffold features between 1 and 200 nm. The cells growing in a structural environment similar to their natural medium are driven to colonize the polymeric structure and to differentiate; thus, the porosity of scaffolds must have a specific size for the type of tissue to be replicated [61, 62, 266]. In addition to the micro-structure, the nano-structure is necessary to ensure the roughness of the pore walls that provide for cell adhesion, growth, migration, and differentiation [51].

[5]As published in Pisanti, P., A.B. Yeatts, S. Cardea, J.P. Fisher and E. Reverchon. *Tubular Perfusion System Culture of Human Mesenchymal Stem Cells on PLLA Scaffolds Produced Using a Supercritical Carbon Dioxide Assisted Process.* Journal of Biomedical Materials Research Part A, 2012.

Several techniques have been proposed in the literature to obtain TE scaffolds [267], including solvent casting, particulate leaching [69, 268], freeze drying [267, 268], phase separation [269], rapid prototyping [62, 107, 270], foaming [270, 271], sintering, or a combination of these techniques.

Solvent casting is relatively simple and it is possible to obtain controlled porosity and interconnection between pores using this method. However, post-treatments to eliminate the residual solvent and long processing times are necessary. Electrospinning and similar techniques can yield nano-structures, but are limited to primarily two dimensional products and the scaffolds exhibit low mechanical strength. Gas foaming can be used to fabricate highly porous polymer foams without the use of organic solvents but the samples obtained lack a nano-structure.

As an alternative to overcome the limitations of these methods the adoption of supercritical carbon dioxide (SC-CO_2) based techniques has been proposed. These techniques take advantage of specific properties of gases at supercritical conditions including modifiable solvent power, high diffusivities, and solvent elimination [272-274]. However, the general limitation of supercritical and non-supercritical techniques is the absence of nano-structure in scaffolds. Therefore, in this work a new supercritical CO_2 based process is used that, in contrast to other techniques, allows for the reproduction of micro and nano-structure. Termed supercritical gel drying it has no limitations in the size and shape of the structures that can be produced [275-277]. Supercritical gel drying can be combined with porogen leaching in a process that consists of four steps:

1. Formation of a PLLA solution in an organic solvent, loaded with a solid, water soluble, leaching agent.
2. Formation of a gel by thermally induced phase separation.
3. Drying of the gel using SC-CO_2, forming a supercritical solution between the supercritical fluid and the organic solvent and flushing it away.
4. Porogen leaching in distilled water.

To the best of our knowledge this work represents the first time scaffolds fabricated by this technique have been tested for a cellular response.

In addition to the key role of scaffold micro and nano-structure in hMSC proliferation and osteoblastic differentiation, the environment in which the cells are cultured also has a dramatic impact. hMSCs have been shown to respond to both mechanical stresses in the surrounding environment leading to an enhancement of osteoblastic differentiation [111, 118]. Thus, bioreactor culture is advantageous for three dimensional bone tissue engineering constructs. In this study scaffolds are cultured in the tubular perfusion system (TPS) bioreactor. In this bioreactor system, scaffolds are loaded into a tubular growth chamber and media is perfused through the growth chamber using a pump. This system has previously been demonstrated to enhance hMSC osteoblastic differentiation using alginate scaffolds [112], but has not previously been used for synthetic microporous scaffold culture.

Therefore this study aims to use the PLLA structures produced by supercritical gel drying with porogen leaching to culture human mesenchymal stem cells (hMSCs) and analyze cell response to this artificial environment. Different micropore size ranges were tested

using the same nano-structure to select the most suitable range for hMSC culture in these scaffolds in the TPS bioreactor. To this end, the objectives of this study are first to evaluate hMSC response to PLLA scaffolds fabricated using supercritical gel drying with porogen leaching, second to demonstrate cell viability on these scaffolds cultured in the TPS bioreactor, and finally to evaluate the cellular response to dynamic culture and pore size.

8.2 Materials and Methods

8.2.1 Scaffold Preparation

Scaffolds were prepared according to the following procedure. Poly(l-lactic acid) (PLLA) L210 (MW 210000) with an inherent viscosity ranging between 2.6 and 3.2 dl/g (0.1% in chloroform, 25°C) was purchased from Boehringer Ingelheim (Ingelheim, Germany). A solution of PLLA 15% w/w in dioxane (Sigma Aldrich, St. Louis, MO) was prepared and 99.8% pure ethanol (Sigma Aldrich) as the non-solvent was added at dioxane/ethanol ratio of 1.7. The solution was stirred and heated at 60°C until it became homogeneous. Scaffolds with different average microporosity were produced through the addition of D-fructose (m.p. 119–122°C) (Sigma Aldrich) particles with average diameters of 100, 250 and 500 μm.

The solution was enriched with the leaching agent (fructose), homogenized, and poured into steel cylindrical containers with the diameter of 4 mm and the height of 3.5 cm. The solution was then compressed to 10 bar in order to obtain uniform contact between the leaching agent particles and the polymer and produce interconnected pores. The solution

was then incubated at -18 °C for 1 hour to obtain a gel that was subsequently dried using SC-CO_2 (99% purity) (SON, Società Ossigeno, Napoli, Italy).

The drying vessel was filled from the bottom with SC-CO_2 up to the desired pressure using a high pressure pump (Milton Roy-Milroyal B, Pont-Saint-Pierre, France). Optimized supercritical CO_2 extraction conditions of the solvent from the polymeric gel (200 bar and 35 °C) were selected and extraction was completed in 4 hours [277]. A depressurization time of 10 minutes was used to bring the system to atmospheric pressure.

The dried samples were cut to obtain plug scaffolds of 4 mm in diameter and 5 mm height. To avoid the shrinkage of the nano-structure of the surface, the samples were cut using a blade previously immersed in liquid nitrogen. The samples were then soaked in distilled water to remove porogen, sterilized in 70% ethanol and rinsed with PBS.

8.2.2 Mechanical Tests

Compressive mechanical properties of the scaffolds were measured using an INSTRON 4301 (Instron Int. Ltd, High Wycombe, UK). The compressive modulus is defined as the initial linear modulus on the stress-strain curves. Cylindrical samples with a diameter of 4 mm and a thickness of 5 mm were compressed at a crosshead speed of 1 mm/min. Seven specimens were tested for each sample (n=7).

8.2.3 Solvent Residue Analysis

Dioxane residue was measured by a headspace (HS) sampler (model 7694E, Hewlett Packard, Palo Alto, CA) coupled to a gas chromatograph (GC) interfaced with a flame

ionization detector (GC-FID, model 6890 GC-SYSTEM, Hewlett Packard). Dioxane was separated using two fused-silica capillary columns connected in series by press-fit: the first column (model Carbowax EASYSEP, Stepbios, Italy) connected to the detector, 30 m length, 0.53 mm i.d., 1 µm film thickness and the second (model Cp Sil 5CB CHROMPACK, Stepbios, Italy) connected to the injector; 25 m length, 0.53 mm i.d., 5 µm film thickness. GC conditions were the one described in the USP 467 Pharmacopoeia with some minor modifications (oven temperature from 45°C to 210°C for 15 min). The injector was maintained at 135°C (split mode, ratio 4:1), and Helium was used as the carrier gas (5 mL/min). Head space conditions were: equilibration time, 30 min at 95°C; pressurization time, 0.15 min; and loop fill time, 0.15 min. Head space samples were prepared in 20 mL vials, filled with internal standard DMI (3ml) and 500mg of NaCL and water (0.75 ml) in which samples of PLLA scaffold were suspended.

8.2.4 Scaffold Porosity

The porosity (ε) represents the "void space" of the scaffold and was calculated from the density of the scaffold $\left(\rho_S = \frac{ScaffoldWeight}{ScaffoldVolume}\right)$ and the density of untreated PLLA $\left(\rho_P = 1.24 \frac{g}{cm^3}\right)$: $\varepsilon = 1 - \frac{\rho_S}{\rho_P}$

The scaffold density was determined by measuring its dry volume and weight.

8.2.5 Experimental Setup

Following scaffold fabrication and characterization, cellular studies were completed. The first short term study aimed to evaluate proliferation and osteoblastic differentiation of

hMSCs cultured on the scaffolds in a dynamic culture environment. Six experimental groups were used including scaffolds with pore sizes of 100 μm, 250 μm, and 500 μm cultured in both static (six well plates) and dynamic (TPS bioreactor) conditions. In addition two monolayer control groups were completed, a control cultured in control media and a control cultured in osteogenic media. Timepoints were taken at days 1, 4, 8, and 12 and samples analyzed for alkaline phosphatase (ALP) protein and deoxyribonucleic acid (DNA) content. Following this, a long term study was completed. The same six experimental groups were used and monolayer control groups were not used. Timepoints were taken at days 1, 8, 16, and 24 and samples were analyzed for ALP and bone morphogenic protein-2 (BMP-2) gene expression. In addition to visualize cells histological staining was completed and SEM images were taken.

8.2.6 Human Mesenchymal Stem Cell Culture

hMSCs were purchased from Lonza (Walkersville, MD) and were expanded on tissue culture polystyrene flasks in control media composed of high glucose DMEM (Gibco, Carlsbad, CA) with 4 mM L-glutamine (Gibco), 0.1 mM nonessential amino acids (Gibco), 1.0% penicillin/streptomycin (v/v) (Gibco), and 10% mesenchymal stem cells qualified FBS (Gibco) as described previously [69, 112, 113, 232]. Media was changed every 3-4 days, according to manufacture specifications. Cells were stored in a cell culture incubator at 37 °C and 5% CO_2 and passaged into a new flask every 7 days ($p < 6$) using trypsin/EDTA (Lonza). To obtain the osteogenic media, 100 nM β-dexamethasone (Sigma-Aldrich), 10 mM β-glycerophosphate (Sigma-Aldrich), and 50 mg/L ascorbic acid (Sigma-Aldrich) were added to the control media [69, 112, 113, 232].

8.2.7 hMSC Seeding on PLLA Scaffolds

Sterilized and rinsed scaffolds were soaked in DMEM supplemented with 10% fetal bovine serum for 4 hours. hMSCs were removed from tissue culture and pelleted. The cell pellet was then resuspended at a density of 1.2 x 10^7 cells/mL to prepare the solution for seeding. Scaffolds were removed from DMEM and seeded with 10 μL of the solution (1.2 x 10^5 cells/scaffold) via pipetting directly on the scaffold surface. The scaffolds were then put in the incubator for 4 hours without media to allow cell attachment on the scaffolds surface. In order to measure attachment efficiency cells not attached to scaffold were removed after four hours and mixed with trypan blue (Sigma-Aldrich) and counted on a standard hemocytometer. Four counts were made for each sample (n=4). Attachment efficiency was then calculated by the following formula: $Effeciency = \frac{Unattached\ Cells}{Total\ Cells\ Added\ to\ Scaffold}$. On study day -1 (cell seeding day), all cell seeded scaffolds were cultured in static into six well plates using control media for 24 hours, to facilitate the cell adhesion. On study day 0 dynamically cultured scaffolds were loaded into the TPS growth chambers while six static scaffolds were placed in osteogenic media in each well of six well plates. In addition, two control groups were performed: monolayer hMSCs grown on tissue culture polystyrene six well plates in control media and monolayer of hMSCs grown on tissue culture polystyrene six well plates in osteogenic media. Control group cells, used to demonstrate the osteoblastic differentiation of seeded samples, were cultured in 5 mL of media, for the duration of the study with media changes every three days for all groups.

8.2.8 Bioreactor for Dynamic Culture

The bioreactor system consists of a tubular growth chamber and media reservoir connected via a tubing circuit as described previously [112, 113]. Media flow was driven by an L/S Multichannel Pump System (Cole Parmer, Vernon Hills, IL) at 0.3 mL/min for all studies. The tubing circuit was sterilized via autoclave and consisted of platinum cured silicon tubing (Cole Parmer) for all areas except the one that passes through the pump which was composed of Pharmed BPT tubing (Cole Parmer) chosen for its high mechanical durability. The growth chamber was packed with cell seeded PLLA scaffolds using a sterile spatula. The TPS bioreactor was then kept in the incubator for the duration of the study with media changes every three days.

8.2.9 Scanning Electron Microscopy (SEM)

PLLA scaffolds were analyzed using two scanning electron microscopes. In the first part of the work, scaffolds were cryofractured using liquid nitrogen and then were sputter coated with gold (Agar Auto Sputter Coater mod. 108 A, Stansted, UK) at 30 mA for 180 s (SEM mod. LEO 420, Assing, Italy) to analyze cell and pore size and the overall scaffold structure.

Following cell culture, the scaffolds were analyzed to evaluate cell adhesion, diffusion, and proliferation inside the PLLA structures. Scaffolds were soaked 12 hours in 4% paraformaldehyde to fix the biological material on the polymeric surface, then were dried for 24 hours at room temperature. The samples were then sputter coated with carbon at 30 mA for 180 s and then analyzed by SEM (SU-70 Hitachi).

8.2.10 Protein Assays

Protein was extracted using the M-PER (Pierce, Rockford, IL) mammalian protein extraction reagent, following standard protocols [69, 278]. A p-nitrophenyl phosphate liquid substrate system (pNPP) (Sigma-Aldrich) was used to analyze intracellular ALP concentrations from the extracted protein. The extracted protein sample was suspended in PBS and added to 100 µL of pNPP and incubated at room temperature for 30 min in the dark. The absorbance was read using a M5 SpectraMax plate reader (Molecular Devices, Sunnyvale, CA) at 405 nm by the PicoGreen assay. Data were normalized to scaffold weight and DNA. All samples were analyzed in triplicate (n=3).

8.2.11 DNA Quantification

Deoxyribonucleic acid (DNA) was isolated from samples to normalize the alkaline phosphatase (ALP) assay and to relate to cell proliferation [69, 278]. Cell pellets or scaffolds were resuspended in 200 µL of PBS. Scaffolds were mechanically agitated following resuspension and the supernatent was retreived. DNA was isolated using a DNeasy Tissue Kit (Qiagen, Valencia CA) following the kit standard protocols into 400 µL of eluate. DNA was then quantified by mixing 100 µL of DNA eluate with 100 µL of diluted Quant-iT PicoGreen dsDNA reagent (Molecular Probes, Carlsbad, CA), incubating for 5 minutes in the dark and measuring fluorescence using an M5 SpectraMax plate reader with excitation/ emission of 480/520 nm. All samples were analyzed in triplicate (n = 3).

8.2.12 Gene Expression

RNA was isolated using trizol (Invitrogen, Carlsbad, CA) and mechanical agitation and purified using an RNeasy mini plus Kit (Qiagen, Valencia, CA) following standard protocols [69, 278]. Then isolated RNA was reverse transcribed to cDNA using a High Capacity cDNA Archive Kit (Applied Biosystems, Foster City, CA). The expression of bone morphogenetic protein-2 (BMP-2, Taqman Assay ID: Hs00154192_m1) and alkaline phosphatase (ALP, Hs00758162_m1) was analyzed with glyceraldehyde-3-phosphate dehydrogenase (GAPDH, Hs00960641_m1) as an endogenous control gene for all samples. Gene expression assays (Applied Biosystems) were combined with the cDNA to be analyzed and Taqman PCR master mix (Applied Biosystems). The reaction was performed on a 7900HT real time PCR System (Applied Biosystems) using conditions of 2 min at 50°C, 10 min at 95°C, and 40 cycles of 15 sec at 95°C and 1 min at 60°C. The relative gene expression level of each target gene was, then, normalized to the mean of the GAPDH in each group. Fold change was calculated using the ΔΔCT relative comparative method. Samples were analyzed in triplicate and standard deviations were reported (n=3).

8.2.13 Histological Analysis

PLLA scaffolds were collected and fixed in 4% paraformaldehyde (Sigma) and 0.1 M sodium cacodylate (Sigma) buffer, containing 10mM $CaCl_2$ (Sigma) at pH 7.4 at 4° C for 4 hours. After, fixing, the scaffolds were placed in cassettes and washed with 0.1M sodium cacodylate buffer and 10mM $CaCl_2$ at pH 7.4 at room temperature, for 24 hours. The scaffolds were then dehydrated for histological processing washing with ethanol,

followed by two Citrisolv (Fisher Scientific) washes. The samples were then embedded in paraffin (Fisher Scientific) and sectioned to 5 μm thickness sections and placed on glass slides. Sections were oven dried at 64° C for 2 hours, deparaffinized in Citrisolv and rehydrated in ethanol. Hematoxylin and Eosin (H&E) staining was performed to visualize the cells using standard protocols.

8.2.14 Statistical Analysis

All samples were performed in replicates (n = 3-7). Data were analyzed first using ANOVA single factor analysis and then using Tukey multiple comparison test to demonstrate differences between groups assuming a normal data distribution with a confidence of 95% ($p < 0.05$). Mean values of triplicates and standard deviation error bars are reported on each figure as well as relevant statistical relationships.

8.3 Results

8.3.1 Scaffold Fabrication

PLLA scaffolds were readily and reliably fabricated with micro and nano-structure in a short time (8hr) to set specifications. Following porosity analysis of PLLA samples, all samples had porosity values higher than 90% as reported in Table 8.1.

Table 8.1: Effect of leaching agent size on porosity and compressive modulus of gel dried PLLA scaffolds. Means ± standard deviation presented (n = 9)

Average fructose particles size range [µm]	Polymer Concentration [%]	Compressive Modulus [kPa]	Porosity [%]
100	15	120 ± 1	95.5 ± 0.2
250	15	117 ± 0	96.0 ± 0.2
500	15	100 ± 1	96.3 ± 0.1

Porosity values were 95.5 ± 0.1%, 96.0 ± 0.2% and 96.3 ± 0.1% for the 100, 250 and 500 µm pore size scaffolds respectively. Micropores were successfully produced using porogens of 100 µm, 250 µm and 500 µm in average diameter. The size difference in these pores can be observed in SEM images (Figure 8.1).

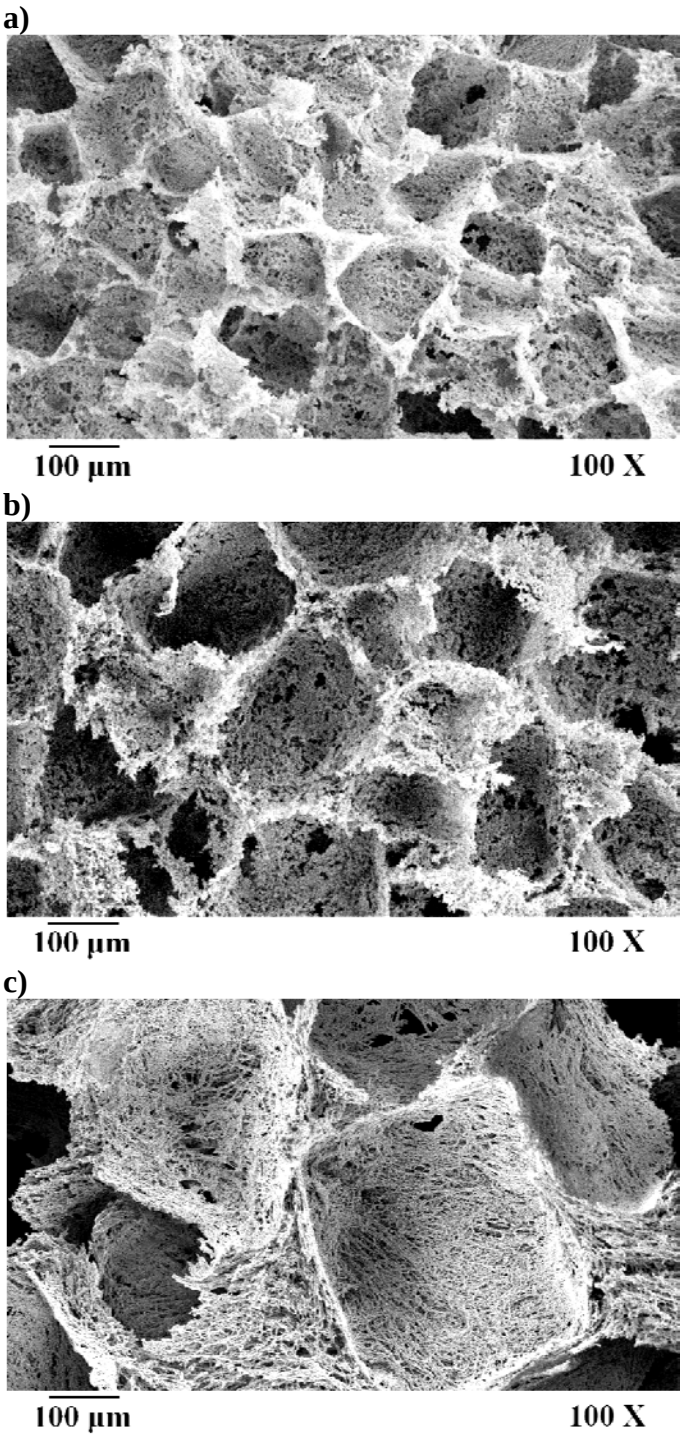

Figure 8.1: 3D PLLA scaffolds structures obtained with pore sizes of (a) 100 µm, (b) 250 µm, and (c) 500 µm.

In addition to this microporous structure, a nano-structure is formed by a continuous network of nanofilaments originating during the gelation step. Nanofilaments located on

the wall of a micropore with a diameter of approximately 200 nm are observed in Figure 8.2.

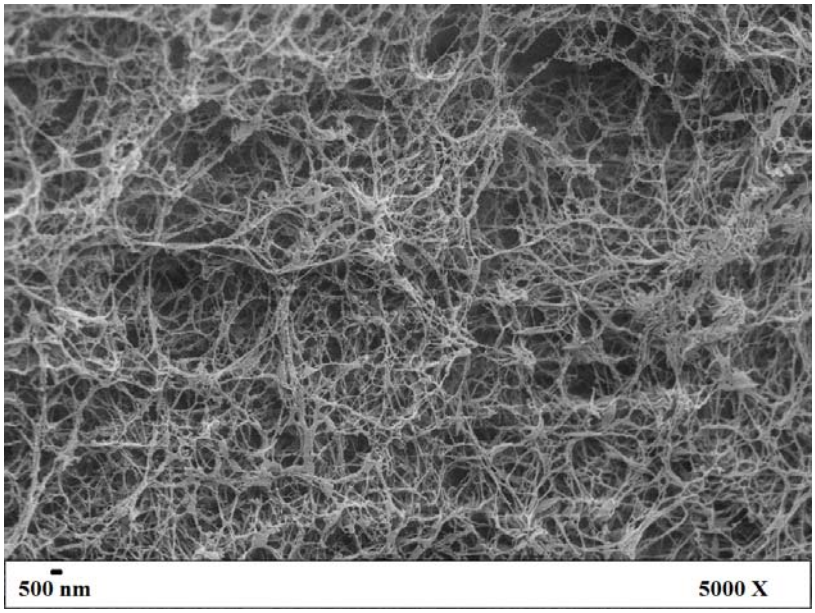

Figure 8.2: Nanofilaments on the walls of a micropore in a PLLA scaffold.

The compressive modulus of these samples was then determined to demonstrate sufficient mechanical strength for bone tissue engineering. The compressive modulus was found to range between 100 ± 1 and 120 ± 1 kPa for the scaffolds tested (Table 8.1). Specifically, scaffolds with 100 μm pore size had a higher modulus of 120 ± 1 whereas the 500 μm pore size scaffolds had a lower modulus of 100 ± 1. The 250 μm pore size modulus had a compressive modulus more similar to that of the 100 μm pore size at 117 ± 0 kPa.

A solvent residue analysis was then performed, to verify the successful elimination of the solvent from the scaffolds. For all samples tested, a residue solvent value was found, which approached the detection limit of the instrument of 5 ppm.

8.3.2 hMSC Growth and Osteoblastic Differentiation

After a four hour incubation, approximately 70% of the total cells seeded were attached to the scaffolds based on cell counts, indicating hMSCs readily adhere to the PLLA scaffolds. SEM images indicated that by day 8 cells had spread and infiltrated scaffolds (Figure 8.3).

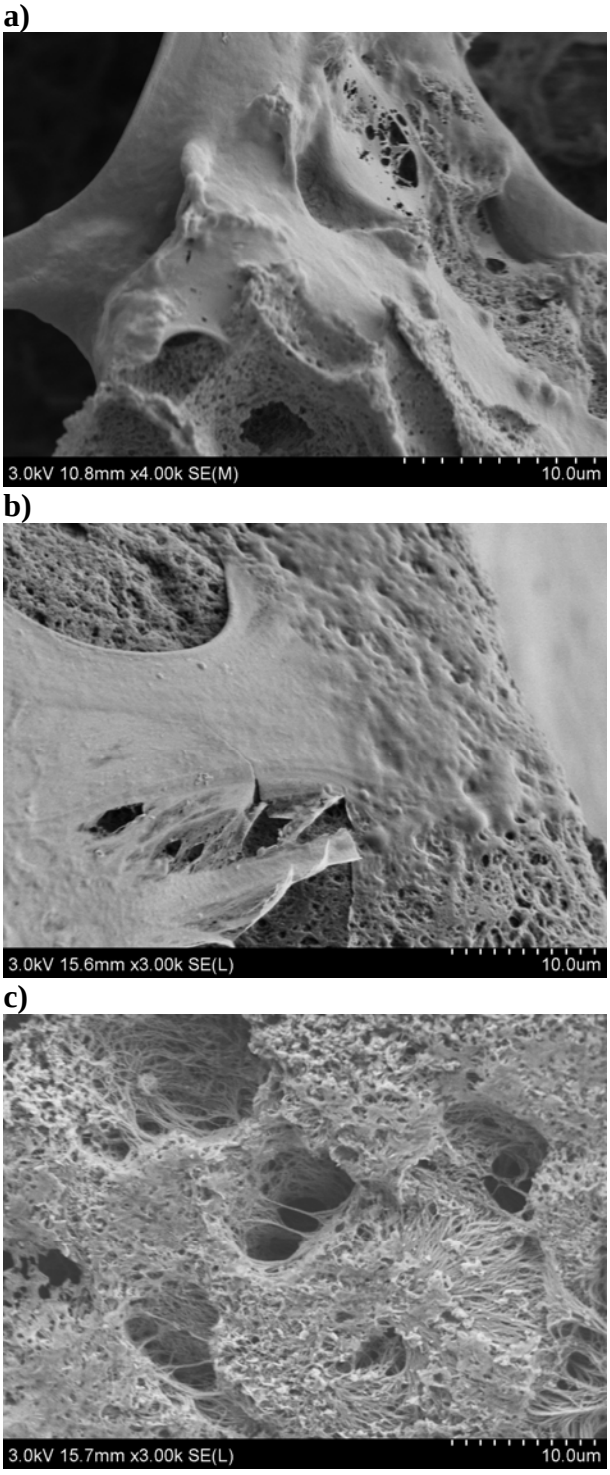

Figure 8.3: SEM images of hMSCs growing on PLLA scaffolds following 8 days of static culture. Cells aggregates can be observed growing homogenously on (a) 100 µm (b) 250 µm, and (c) 500 µm synthetic scaffolds.

hMSCs can be observed covering pores demonstrating continued cell adhesion to the samples. This observation can also be made in histological sections in which the cells are stained using hematoxylin and eosin (Figure 8.4). In all groups cells appear both lining and infiltrating the pores of the scaffolds by day 8.

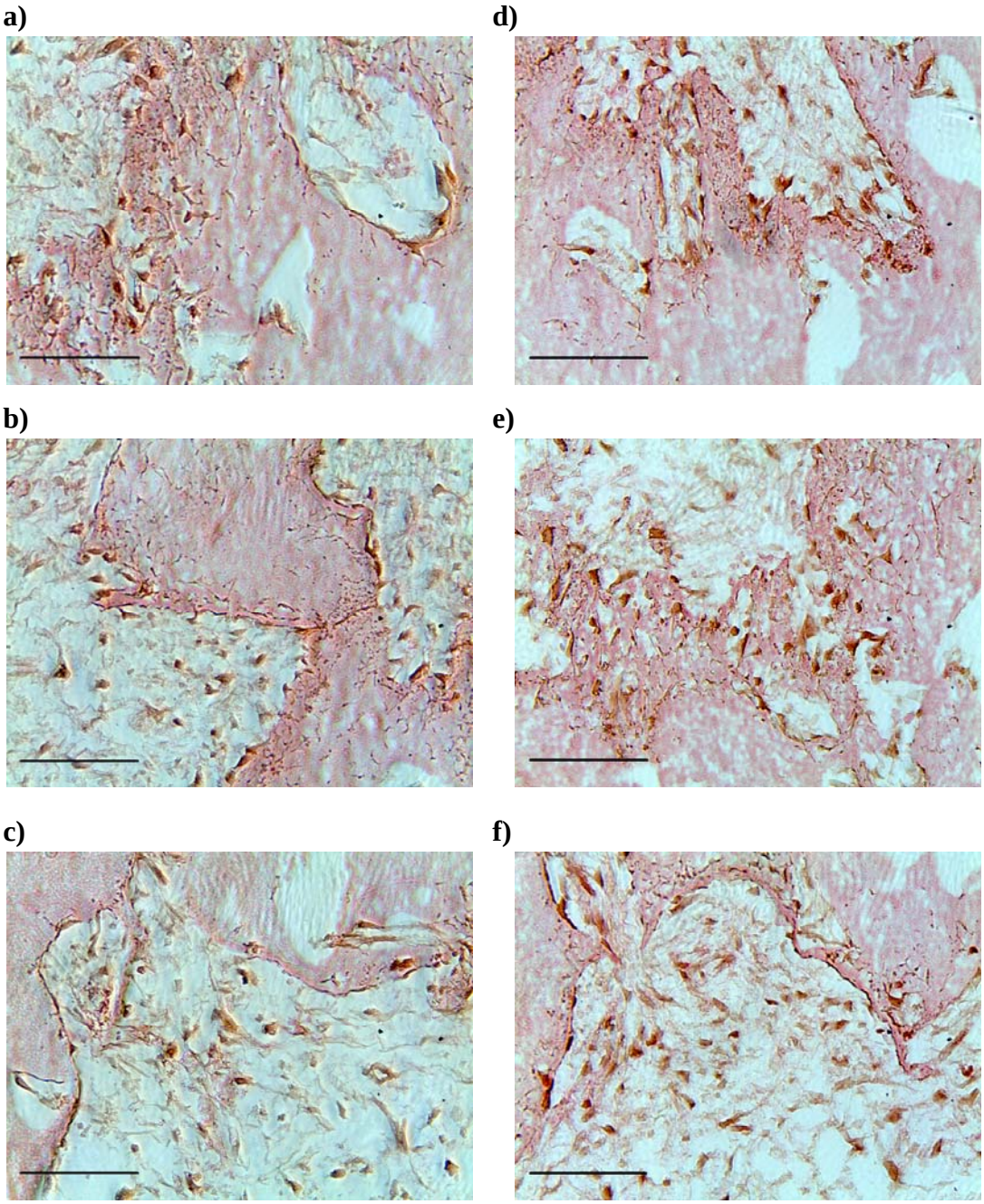

Figure 8.4: Hematoxylin and Eosin staining of 100 µm (a,d), 250 µm (b, e), and 500 µm (c, f) PLLA scaffolds after 8 days of static (a-c) and dynamic culture (d-f). Cells have infiltrated pores of scaffolds in all groups by day 8. Scale bar represents 100 µm.

Following an investigation of cell adhesion, DNA quantification was completed to determine the proliferation of seeded cells (Figure 8.5). In order to account for any seeding difference all values were normalized to the respective day 1 sample. Through

12 days both the monolayer control groups proliferated at a steady rate with a day 12 increase of 5.56 ± 1.5 μg/μg and 14.28 ± 7.30 μg/μg fold for the control media and osteogenic media groups, respectively. Cell growth varied between static and dynamic culture and pore size; however, all day 12 samples maintained at least 70% of the cell number from day 1. The lowest day 12 relative cell numbers were observed in the 250 μm statically cultured group with a DNA decrease of 0.70 ± 0.24 μg/μg fold compared to day 1. Slightly higher proliferation was observed in the 500 μm static groups with a day 12 increase of 1.14 ± 0.45 μg/μg fold. The highest day 12 proliferation of the static groups was the 100 μm pore size with an increase of 2.94 ± 0.67 μg/μg fold compared to day 1. Interestingly the 100 μm had the lowest day 12 relative cell number among the TPS cultured group with a decrease of 0.75 ± 0.21 μg/μg fold compared to day 1. The 500 μm TPS cultured group had a nearly 2 fold higher proliferation with an increase of 1.49 ± 0.35 μg/μg fold. The highest day 12 scaffold proliferation was observed in the 250 μm bioreactor groups with an increase of 3.69 ± 2.84 μg/μg fold.

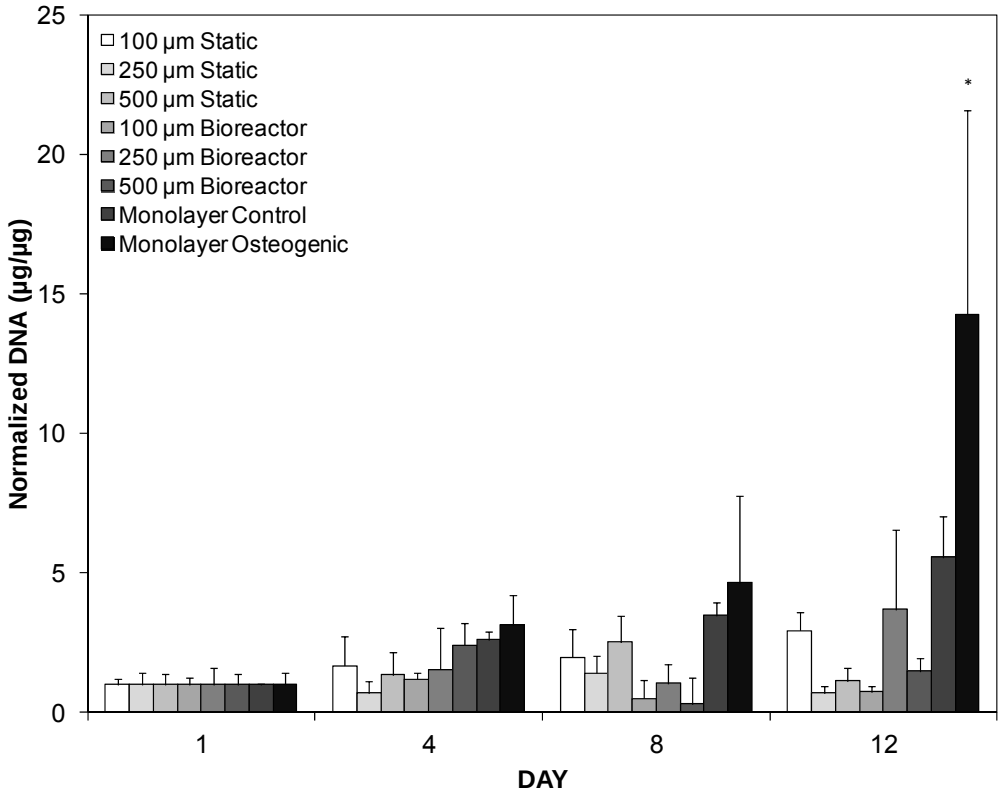

Figure 8.5: Fold change of DNA content normalized to day one based on DNA quantification from pico green. The symbol (*) denotes statistical significance within a timepoint ($p<0.05$).

Following quantification of proliferation, intracellular ALP protein was measured as a marker of early osteoblastic differentiation (Figure 8.6). On day 4 statically cultured groups and the monolayer osteogenic control showed slightly elevated levels as compared to day 1 levels. The 100 µm, 250 µm and 500 µm statically cultured groups exhibited ALP values of 0.11 ± 0.05, 0.20 ± 0.16, and 0.22 ± 0.20 µM 4-nitrophenol/µg DNA, respectively. These values represent an approximate 2 fold increase from day 1 numbers for the 100 µm and 500 µm scaffolds and approximately a 4 fold increase for the 250 µm scaffolds. The osteogenic control also increased approximately 3 fold, while the bioreactor cultured groups and control media group maintained ALP levels close to day 1 values. By day 8, the statically cultured scaffolds decreased back to approximately day 1

levels while the bioreactor cultured scaffolds and the osteogenic control increased significantly. The 100 μm, 250 μm, and 500 μm had ALP values of 0.50 ± 0.26, 1.67 ± 0.87, and 1.00 ± 0.57 μM 4-nitrophenol/μg DNA respectively. The osteogenic control also exhibited an increase to 1.17 ± 0.54. This represented an approximate 13 fold increase compared to day 1 numbers. Bioreactor groups also increased from day 1 numbers with fold changes of approximately 4, 11, and 6 for the 100 μm, 250 μm, and 500 μm groups respectively. The control group remained at baseline level as expected. By day 12, dynamically cultured scaffold groups returned to a lower ALP level while the osteogenic control decreased, but to a level higher than other groups.

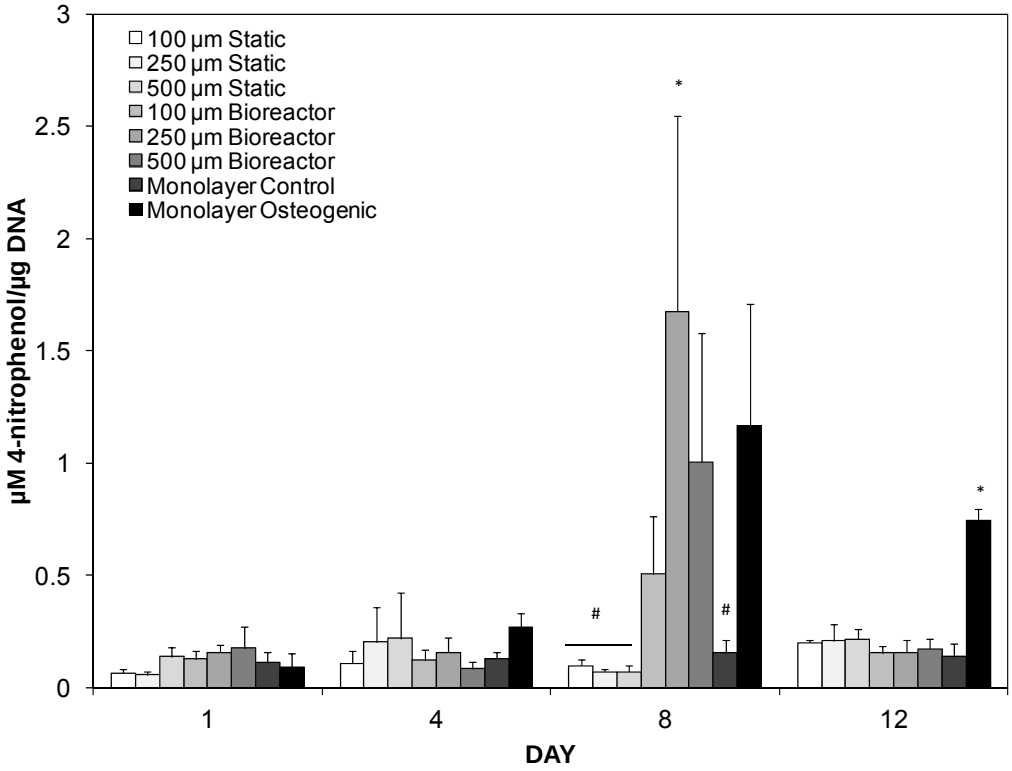

Figure 8.6: Intracellular alkaline phosphatase protein normalized to DNA. Note increased day 8 ALP amounts in bioreactor groups and osteogenic control. Day 8 250 μm pore size bioreactor group is statistically different from all static scaffold groups and monolayer control group. All other day 8 groups are statistically similar. The symbols (*, #) denote statistical significance within a timepoint ($p<0.05$).

ALP was also analyzed in the long term study at the mRNA level (Figure 8.7a). All groups underwent a peak at day 8 but no significant differences were detected between the groups at this day. This could be due to an earlier peak of ALP mRNA in these groups. In addition to ALP, osteogenic signaling molecule BMP-2 (Figure 8.7b) was analyzed at days 1, 8, 16, and 24. BMP-2 expression levels on day 1 were elevated in the bioreactor groups as compared to the statically cultured scaffolds. This trend continued on Day 8, where the 500 μm and 250 μm bioreactor cultured scaffolds exhibited statistically significant increased fold changes of 13.65 ± 1.67 and 6.93 ± 0.96 respectively. On day 16 BMP-2 expression levels increased with increasing pore size and with dynamic culture. Static cultured samples exhibited fold changes of 0.29 ± 0.02, 0.62 ± 0.07, and 0.72 ± 1.2 respectively for the 100 μm, 250 μm, and 500 μm groups. TPS cultured scaffolds exhibited higher BMP-2 expression levels with fold changes of 1.40 ± 0.28, 3.73 ± 1.01, and 6.04 ± 0.28 for the 100 μm, 250 μm, and 500 μm pore sizes respectively. On day 24, the significantly higher expression levels were observed in the 250 μm and 500 μm bioreactor cultured groups. Lower BMP-2 expression levels continued to be observed in the 100 μm bioreactor group and the statically cultured groups including no BMP-2 being detected in the 500 μm statically cultured group.

a)

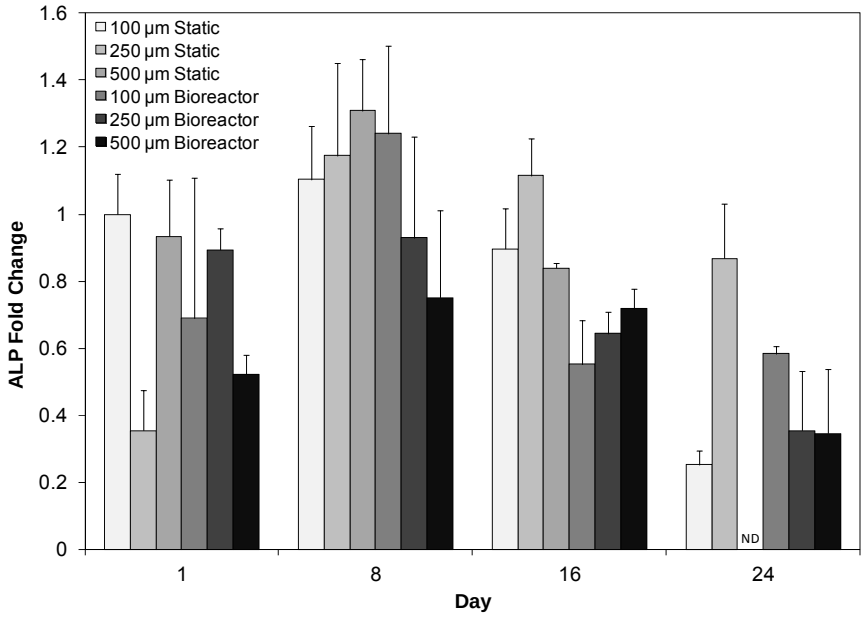

b)

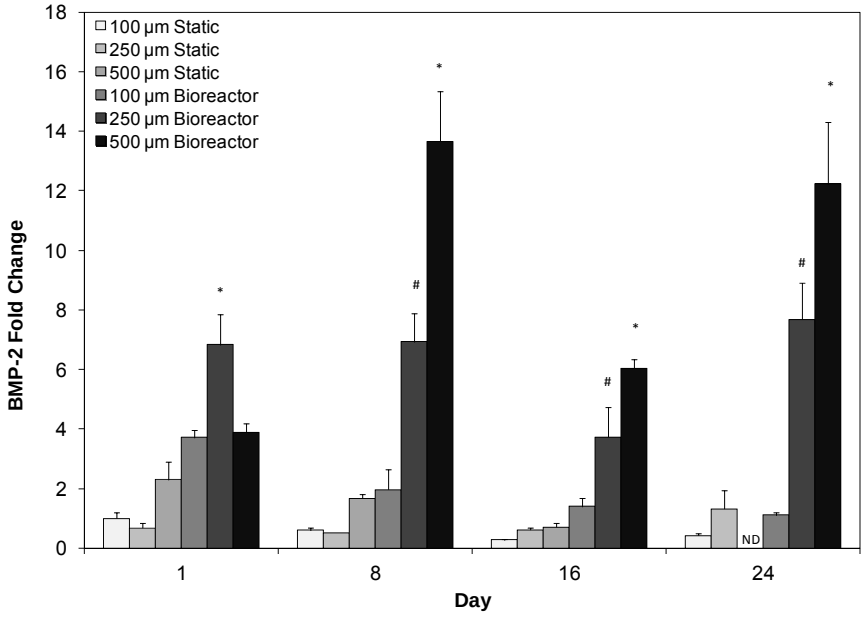

Figure 8.7: Quantitative reverse transcriptase polymerase chain reaction analysis on days 1, 8, 16, and 24 of (a) alkaline phosphatase and (b) bone morphogenetic protein-2. All groups are normalized to day 1 100 µm static. In ALP data note no relevant significant difference between groups. In BMP-2 data note statistically significant increases of expression levels in 250 µm and 500 µm bioreactor groups on days 8, 16, 24. The symbols (*, #) indicate statistical significance from all other groups within a timepoint ($p < 0.05$). The abbreviation ND refers to no gene detected within 40 cycles.

8.4 Discussion

The objectives of this study were to evaluate hMSC response to PLLA scaffolds fabricated using supercritical gel drying, to demonstrate cell viability on these scaffolds cultured in the TPS bioreactor, and to evaluate the cellular response to dynamic culture and pore size. In order to accomplish these objectives PLLA scaffolds were first fabricated using supercritical gel drying with porogen leaching; thus producing gels characterized by high porosity and distinct nano-structure [277]. The nano-structure was formed by a continuous network of nanofilaments formed during the gelation step in micro-structure derived from porogen leaching. This nano-structure is fundamental to guide cell adhesion, proliferation and migration [279]. Nano-structure of 50 and 24 nm was shown to reduce the adhesion of hMSCs compared to 200 or 1500 nm [280]. In addition to affecting proliferation and adhesion surface topography can affect hMSC differentiation and matrix production [281, 282]. Comparing titanium scaffolds without surface texture to those that do hMSCs produced significantly more mineralization and collagen on the scaffolds with surface topography [281]. Thus surface nano-structure is important to support hMSC attachment and proliferation as well as differentiation. Because of the well documented effects of scaffold nano-structure, this study focuses primarily on the effect of bioreactor culture and microporosity with this nano-structure present.

Solvent residue analysis was performed on PLLA scaffolds to verify the successful elimination of the solvents from the polymeric gels; for all PLLA scaffolds, a residue solvent value lower than 5 ppm was found, lower than the limits of USP 467

Pharmacopeia (380 ppm for Dioxane). Mechanical testing indicated these scaffolds to have compressive moduli from 100-120 kPa.

Following fabrication and characterization of scaffolds, hMSC attachment to scaffolds and long term viability was tested. Efficient seeding was accomplished with a seeding efficiency of over 70%. SEM and histological images indicated cells were readily able to infiltrate the scaffolds and attach to the nano-structure lining the pores. DNA quantification indicated the majority of the hMSC population remained viable throughout the twelve day study. In statically cultured scaffolds the highest proliferation was observed on the 100 μm pore size scaffolds. It is hypothesized that this scaffold provided for closer cell interactions leading to increased cell proliferation. Cell density is a potent regulator of hMSC proliferation rate with low cell densities leading to reduced proliferation due to poor cell communication and high cell densities leading to reduced proliferation due to contact inhibition [240, 283]. Smaller pores permit for closer cell interactions[284], thus it is hypothesized in larger pore scaffolds cell-cell distance may have been too great for optimal proliferation, thus leading to the modest proliferation in the 500 μm static culture group and the slight decrease in cell number in the 250 μm group. Another potent regulator of cell proliferation is nutrient transport and waste removal. Nutrient transfer and waste removal are limited to hundreds of microns, thus culturing three dimensional scaffolds in a static environment can lead to nutrient gradients and non-homogenous cell distributions [21, 111]. In the bioreactor the 250 μm and 500 μm pore size groups exhibited the higher proliferation levels compared to static cultures of the same pore sizes. It is hypothesized that in dynamic culture these pore sizes group allowed for greater infiltration of media flow into the scaffold, resulting in

higher proliferation from increased nutrient transport. The highest proliferation was observed in the monolayer control groups, however monolayer culture of hMSCs lacks a scaffold to support the cells upon *in vivo* implantation. Furthermore upon reaching confluence in monolayer proliferation would no longer continue.

In addition to cell proliferation, osteoblastic differentiation was evaluated. ALP was used as an early osteoblastic marker and BMP-2 was evaluated as an important osteogenic signalling molecule. Statically cultured samples exhibited elevated ALP levels on day 4 indicating these samples may be undergoing differentiation more rapidly than bioreactor cultured samples. Only small differences were observed for different pore sizes of statically cultured groups with slightly higher day 4 levels observed in the 250 μm and 500 μm groups. Though bioreactor cultured samples did not exhibit a peak in ALP expression until day 8, the peak had a higher magnitude than the statically cultured samples. It was also much more dependent on pore size as no significant differences were observed between pore sizes of statically cultured constructs but with higher ALP levels again in the 250 μm and 500 μm groups in dynamically cultured constructs. It is hypothesized that dynamic culture magnifies the cellular response to pore size by stimulating the cells via fluid shear stress. Fluid shear stress has been widely demonstrated to enhance osteoblastic differentiation [20, 80, 89, 110, 111], and it is hypothesized that a greater percent of cells in larger pore size scaffolds are directly exposed to fluid shear stresses. ALP mRNA levels peaked at day 8, but did not show significant differences between groups. It is hypothesized this is because ALP mRNA peaked previous to day 8 in order to stimulate downstream protein production. BMP-2 expression levels follow a similar trend as ALP protein levels with higher levels in the

bioreactor samples as compared to static controls. In addition, BMP-2 expression was shown to be dependent on pore size in dynamic culture with larger pore sizes corresponding to higher expression levels after day one. This further demonstrates the ability of the bioreactor culture to enhance osteogenic signal expression. Pore size and porosity have previously been shown to be powerful mediators of hMSC osteoblastic differentiation through facilitation of autocrine and paracrine signalling pathways [69]. Previous studies have analyzed the effect of pore size *in vitro* including findings that pore sizes greater than 500 μm increased osteogenic signal expression as compared to 180-300 μm pore sizes [107]. Larger pore size (500 μm compared to 200 μm) has also been demonstrated to increase cell proliferation [11]. It is hypothesized that this effect is due to increased nutrient transport throughout the scaffolds with larger pore sizes [11, 62, 107]. Though the effect of pore size has been fairly widely investigated in static culture, relatively few studies have investigated the effect in dynamic culture. Focusing on porosity rather than pore size, it has previously been demonstrated that osteoblastic differentiation of rat BMSCs was influenced by scaffold geometry in a perfusion system [57]. A more recent study found that though scaffold pore size influenced osteoblastic differentiation in static culture, bioreactor culture was detrimental to both proliferation and differentiation of hMSCs [285]. This was not found to be true in this as study as proliferation and differentiation tended to increase during bioreactor culture. The difference could be due to the difference in bioreactor design. In the study demonstrating decreased hMSC proliferation, the flow perfusion system used was a direct perfusion system forcing media through the pores of the scaffold. Depending on the pore size, overall porosity and interconnectivity of a scaffold, this method can result in high shear

stresses on cells lining the pores of the scaffold. In the tubular perfusion system, media is perfused in and around the scaffolds, thus the magnitude of shear stresses placed on cells is much less than forced perfusion systems of the same flow rate. Despite media not being directly perfused through the scaffolds tubular perfusion system culture still was able to increase both proliferation and osteoblastic differentiation. Based on these results, it can be concluded that scaffold micro-structure greatly influences hMSC proliferation and differentiation in perfusion culture and scaffold geometry and flow rates must be tailored in tandem to optimize culture conditions.

8.5 Conclusions

This work demonstrated that 3D PLLA scaffolds could be produced by supercritical gel drying with porogen leaching and possessed mechanical strength for use as bone tissue engineering scaffolds. hMSCs were able to adhere, proliferate, and differentiate into the scaffold structure in both static and dynamic culture. Effects of the architecture of the scaffold were magnified in dynamic culture leading to increased proliferation and osteoblastic differentiation. Thus, we conclude that PLLA scaffolds produced by supercritical gel drying with porogen leaching are effective scaffolds for bone tissue engineering using hMSCs and can be cultured in the tubular perfusion system to enhance hMSC proliferation and differentiation.

Chapter 9: *In Vivo* Bone Regeneration Using Three Dimensional Tubular Perfusion System Bioreactor Cultured Constructs

9.1 Introduction

Cell based tissue engineering of three dimensional constructs is limited by the ability to culture these constructs *in vitro*. During this culture oxygen transport and waste removal are limited to as little as hundreds of microns [21, 216, 286]. This leads to the development of a nutrient gradient which can lead to a non homogenous cell distribution. Bioreactors can be used as a culture tool to improve *in vitro* cell culture [110, 111, 117, 118]. Bioreactor systems have frequently been used in bone tissue engineering applications with designs including spinner flask [23, 24], rotating wall [42, 52, 114], and perfusion [14, 17, 20, 23, 29, 58, 78, 217] bioreactor systems. In this study we utilize a tubular perfusion system (TPS) bioreactor which consists of a packed scaffold design. In the system scaffolds are tightly packed in a tubular growth chamber and media perfused through the growth chamber using a pump. TPS culture has previously been shown to enhance the proliferation and differentiation of human mesenchymal stem cells (hMSCs) [112]. hMSCs are used as a cell source in this study as they are readily extracted from bone marrow and have the potential to form bone *in vivo* [5, 287].

Bioreactor systems are frequently used in the *in vitro* culture of MSCs, however *in vivo* studies involving perfusion bioreactor systems are relatively few in number. In subcutaneous models bioreactor cultured human bone marrow stromal cells were shown to generate bone like tissue in mice [16]. In a bone defect model bone marrow stromal osteoblasts were shown to have the greatest ability to form bone in a rat critical size

cranial defect when cultured for one day in flow perfusion culture however these differences were not statistically significant [78].

In this study we evaluate the ability of TPS cultured hMSC containing constructs to aid in bone regeneration in a rat femoral condyle defect. Two different scaffold types will be evaluated in this study, a synthetic electrospun poly(lactic-co-glycolic acid) (PLGA)/ poly(ε-caprolactone) (PCL) scaffold and a natural bulk alginate scaffold. PCL scaffolds have previously been used to support MSC bone grafts for *in vivo* bone regeneration [12]. In this study PLGA is added to the PCL to accelerate degradation and scaffolds were fabricated using a new method to create cylindrical electrospun scaffolds. In addition to the PLGA/PCL scaffolds, alginate, a natural polysaccharide is used as a scaffold. hMSCs cultured in alginate scaffolds in the TPS bioreactor have previously been shown to undergo enhanced osteoblastic differentiation and improved mineralization as a result of bioreactor culture [112, 286] however *in vivo* testing has not previously been completed. This study aims to evaluate the effect statically and TPS cultured hMSCs have on bone regeneration in a rat femoral condyle defect and to compare bone in growth and regeneration between the two scaffold types.

9.2 Materials and Methods

9.2.1 Human Mesenchymal Stem Cell Culture

Human mesenchymal stem cells (Lonza) were expanded prior to the study in control media consisting of DMEM (Gibco) supplemented with 10% fetal bovine serum (Gibco), 1.0 % v/v penicillin/ streptomycin (Gibco), 0.1 mM non essential amino acids (Gibco), and 4 mM L-glutamine (Gibco) using protocols set forth by the manufacture and

previously described [69, 112, 113, 232, 286]. hMSCs were expanded on tissue culture polystyrene flasks with media changes every three days according to the manufacture's specifications. Cells were stored in a cell culture incubator at 37º C and 5% CO_2 and passaged every 6-7 days using trypsin/EDTA (Gibco). hMSCs (p=4) were then seeded on scaffolds and cultured in osteogenic media formulated as described in the literature by supplementing control media with 100 nM dexamethasone (Sigma), 10mM β-glycerophosphate, and 173 μM ascorbic acid (Sigma) [69, 232].

9.2.2 Alginate Bead Fabrication and Cell Seeding

Alginate beads were fabricated as described previously [108, 109]. Alginate solution (Sigma, St. Louis MO, USA) was sterilized via sterile filtration then mixed with a cell pellet containing hMSCs. Beads were seeded at a concentration of 4 x 10^6 cells per mL or approximately 80,000 cells/bead. This solution was added dropwise via a 30 gauge needle to a 0.10 M calcium chloride solution, in which the alginate was ionically crosslinked into beads. The solution was stirred for 15 minutes. The calcium chloride solution was then removed and the beads rinsed in control media. This created beads of approximately 3 mm in diameter, which could be press fit into the 3 mm diameter defect. Beads were then transferred to 24 well plates for control groups or TPS bioreactor growth chambers for experimental groups. All groups were cultured for 10 days in osteogenic media which was changed every three days. Beads for no cell groups were fabricated following a similar manner without cellular incorporation and were also cultured in osteogenic media.

9.2.3 PLGA/PCL Scaffold Fabrication

The polymers used for electrospinning, poly(lactic-co-glycolic acid) (PLGA, Purasorb® PDLG 5010) and poly(ε-caprolactone) (PCL from LACTEL® Absorbable Polymers, inherent viscosity range: 1.0 – 1.3 dl/g) were purchased from Purac Biomaterials BV (Gorinchem, The Netherlands) and DURECT Corporation (Pelham, AL, USA), respectively. The electrospinning solution was prepared by dissolving PLGA/PCL (3:1 weight ratio) in TFE/HFIP (9:1 volume ratio) at a concentration of 20% w/v. The experimental 3D scaffolds were fabricated using a modified electrospinning technique. Briefly, the electrospinning process was implemented by Esprayer ES-2000S (Fuence Co., Ltd, Japan) under an optimal condition. The prepared solution was loaded into a syringe and fed into the nozzle at the tip of the syringe with a speed of 25 µl/min. A high voltage of 15 kV was applied at the nozzle to generate a stable polymer jet. A grounded bath filled with 100% ethanol was positioned 14 cm under the nozzle for fiber deposition. As ethanol is a wetting agent for both PLGA and PCL, the resulted PLGA/PCL fibers formed a loosen cotton ball shape in the ethanol bath. Every 5 minutes, the 2 µm diameter fibers were collected and inserted into a Teflon mold with 3 mm in diameter and 3 mm in depth. Subsequently, they were washed thoroughly in MilliQ water and freeze-dried for 3 days. Prior to the cell culture and animal experiment, all scaffolds were sterilized by γ-irradiation (Isotron, Ede, The Netherlands).

9.2.4 hMSC Seeding on PLGA/PCL Scaffolds

hMSCs were removed from tissue culture flasks and resuspended in media at a concentration of 1.25 x 10^6 cells/mL. Concentrated cell solution was added to the

scaffold resulting in the seeding of 250,000 cells/scaffold. Scaffolds were briefly exposed to vacuum and put in a rotary seeder for 3 hours. Scaffolds were then moved to a 24 well plate. Unseeded cells were captured via centrifugation and reseeded on scaffolds. Following an additional 2 hour incubation, control media was added to scaffolds. Cell containing scaffolds were incubated overnight and moved to 24 well plates or TPS bioreactor growth chambers. All groups were cultured in osteogenic media which was changed every three days. Scaffolds for no cell groups were fabricated following a similar manner and placed in 24 well plates in osteogenic media without the seeding of a cell population.

9.2.5 Bioreactor Design

Dynamic culture was completed in the TPS bioreactor as described previously in the literature [112, 113, 286]. Briefly a tubing circuit comprised primarily of platinum-cured silicone tubing (Cole Parmer, Vernon Hills, IL) and PharMed BPT tubing (Cole Parmer) for the section that passes through the pump connected a growth chamber to a media reservoir (Figure 9.1a). The entire tubing circuit was sterilized via autoclave. The growth chamber was composed of platinum-cured silicone tubing (ID of 1/4") and contained the tightly packed scaffolds. Media was pumped through the recirculating system using a peristaltic pump (Cole Parmer) at 1.0 mL/min. The entire system was placed in an incubator at 37^{o}C for the duration of the study. Forty mL of osteogenic media was loaded into separate 125 mL Erlenmeyer flasks reservoirs for each growth chamber topped with rubber stoppers. Media was withdrawn and replaced from the reservoir through two tubes that penetrate the stopper and changed every three days.

9.2.6 Surgical Procedure for Femoral Condyle Defect

Thirty two 7-11 week old nude rats (Charles River Labs) were used in the study. The animal experiment was approved by the animal ethics committee of the Radboud University Nijmegen Medical Centre. All surgeries were performed under general inhalation anesthesia (Isoflurane®) and sterile conditions. Pre-operative, Rimadyl® (5.0 mg/kg) and Morphine® (1.0 mg/kg) were administered to reduce postoperative pain. Subsequently, each animal was immobilized supine with the knee joint in a maximally flexed position and the hind limbs were shaved, washed and disinfected with 10% Povidone-iodine.

A mid-line longitudinal para-patellar incision was made. The knee joint capsule was incised longitudinally, and by lifting the patellar ligament gently and moving it laterally, the knee joint became fully exposed. This maneuver was facilitated by a slight extension of the knee. At the femoral inter-condylar notch, a cylindrical hole defect (2.5 mm in diameter and 3 mm in depth) was prepared parallel to the long axis of the femur, using a dental bur (Elcomed 100,W&H Dentalwerk Burmoos, Austria) with low rotational drill speeds (1200 rpm) and continuous external cooling with saline (Figure 9.2a).

a)

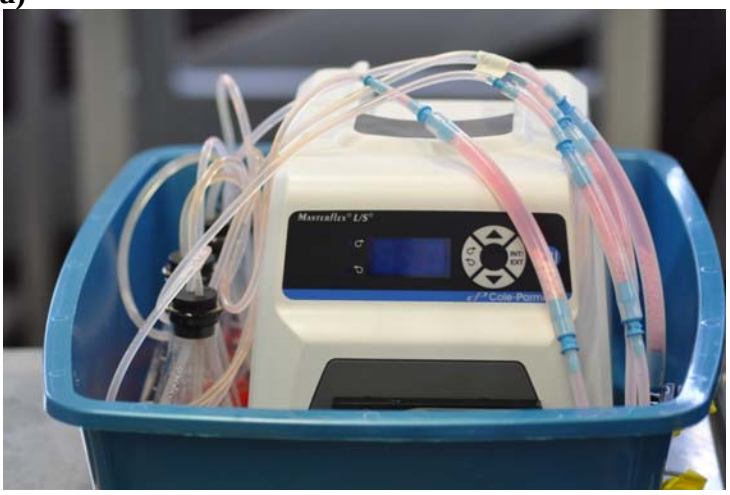

b)

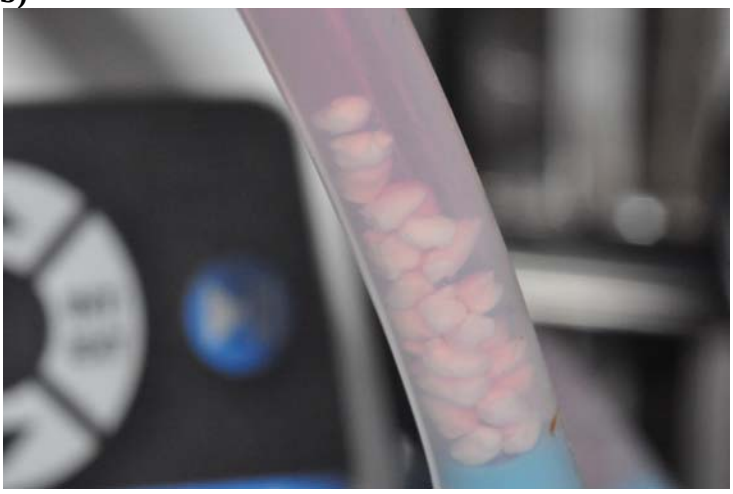

c)

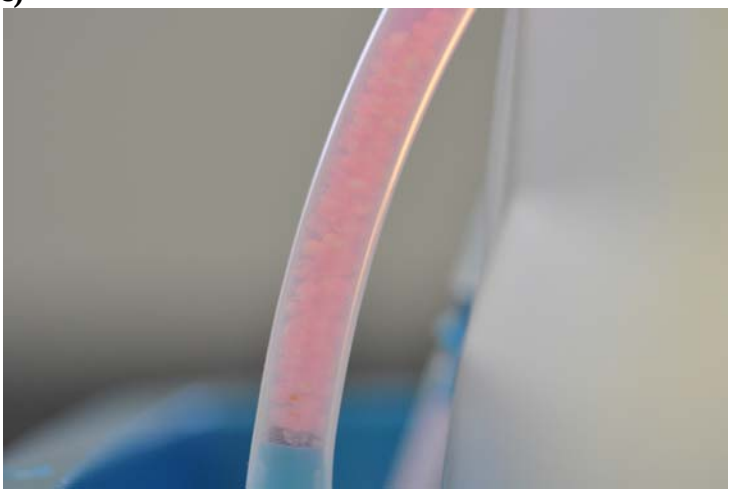

Figure 9.1: Image of TPS system (a) with tightly packed PLGA/PCL scaffolds (b) and alginate beads (c)

Implanted scaffolds were placed bilaterally into the predrilled bony defects, resulting in two implants per rat. PLGA/PCL scaffolds were rinsed in saline and one scaffold was press fit into each defect (Figure 9.2b-c). Alginate scaffolds were rinsed in calcium chloride and saline and 2 beads were placed in each defect (Figure 9.2d).

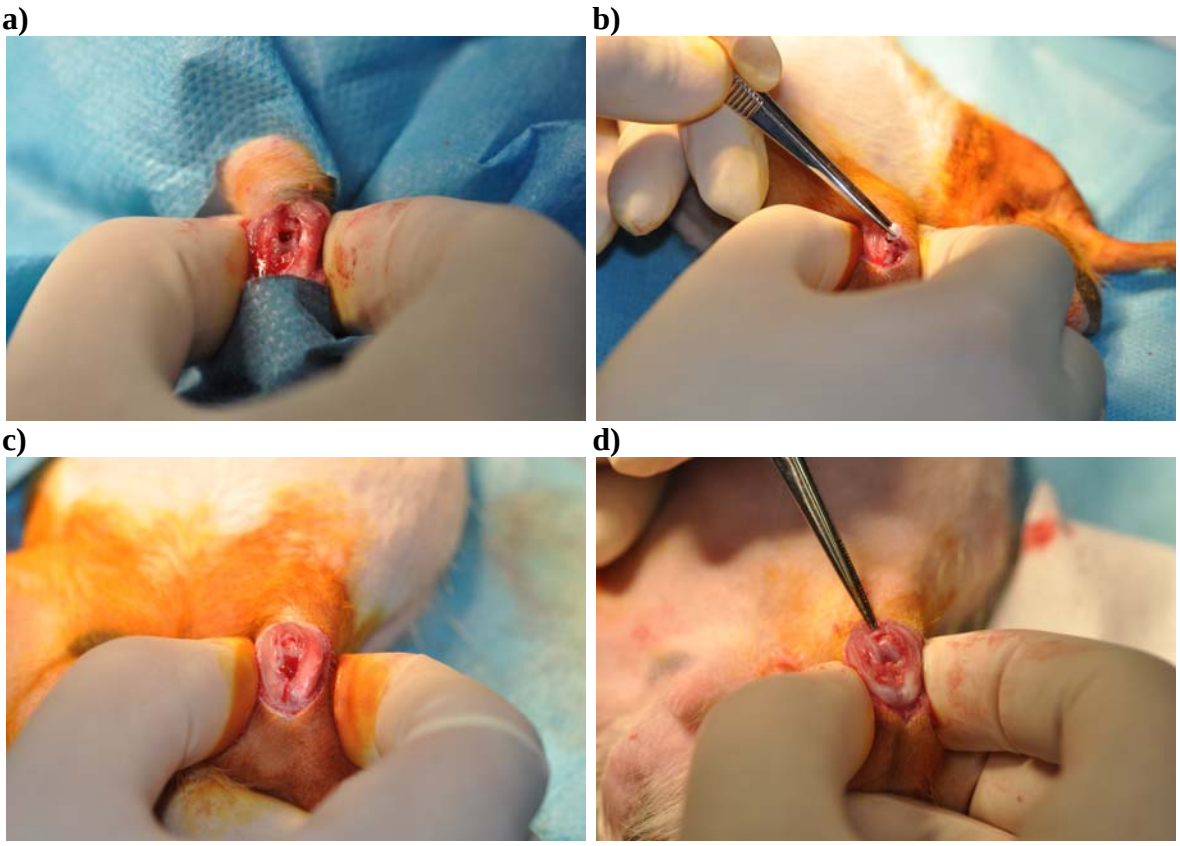

Figure 9.2: Image of femoral condyle defect (a) with a cylindrical PLGA/PCL scaffold being press fit into the defect (b), defect filled with PLGA/PCL (c) and alginate scaffolds (d)

After insertion of the implants, the soft tissue layers were closed with resorbable sutures (Vicryl® 4.0, Ethicon Products, Amersfoort, the Netherlands) and the skin with Vicryl® 3.0, (Ethicon Products, Amersfoort, the Netherlands). To reduce post-operative pain, Temgesic® (0.02mg/kg) was administered subcutaneously for 2 days postoperatively. After 3 and 6 weeks rats were sacrificed using carbon dioxide and condyles were retrieved and fixed in formalin.

9.2.7 Histomorphometric Analysis

Samples were decalcified in EDTA, dehydrated using graded ethanol washes, and embedded in paraffin. 5 µm sections were sectioned transversely using a microtome (RM 2165; Leica). Sections were mounted on glass slides and stained with hematoxylin and eosin (HE) stain using standard protocols. Images of stained sections were acquired by optical light microscopy (Axio Imager Microscope Z1; Zeiss, Göttingen, Germany). 10x images on entire defect region were analyzed quantitatively by defining a region of interest (ROI) to the size (2.5 mm diameter) of the original defect using Adobe Photoshop (Figure 9.3). ROI images were then evaluated using an image analysis system (Leica Qwin; Leica) to select and measure bone area and distance of bone in growth.

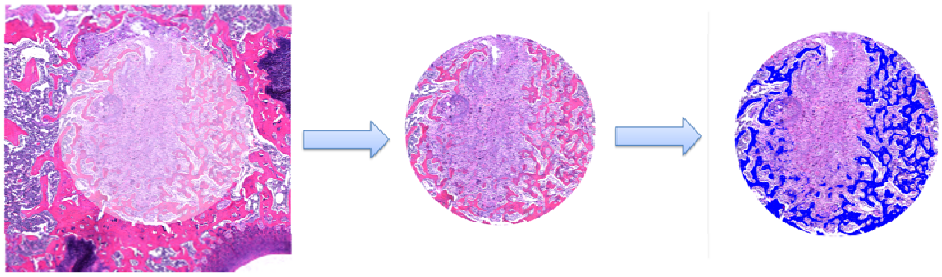

Figure 9.3: Schematic illustrating method to measure bone area. A region of interest was defined to the size of the original 2.5 mm diameter defect. After this region of interest was created bone area was identified and measured

9.2.8 Statistical Analysis

Five replicate defects were created for each group and timepoint (n=5) with the exception of two groups in which animals were lost during surgery (n=3,4) Images were analyzed in triplicate (n=3). Data was analyzed using single factor ANOVA followed by Tukey's Multiple Comparison Test assuming normal data distribution with a confidence of 90%

($p < 0.10$). Mean values of triplicates and standard deviation error bars are reported on each figure as well as relevant statistical relationships.

9.3 Results

9.3.1 Scaffold Properties Following Culture

PLGA/PCL scaffolds were fabricated using a new method to produce a cylindrical design that could be press fit into the defect (Figure 9.2b-c). Scaffolds were fabricated to be cylinders 3 mm in diameter and 3 mm in length. Scaffolds maintained size and shape following 10 days of culture. Two alginate scaffolds could be placed into the defect also resulting in a scaffold filled defect (Figure 9.2d). Both these scaffold types could be manipulated using forceps.

9.3.2 Bioreactor Culture and Surgery

Both PLGA/PCL and alginate scaffolds were successfully cultured in the TPS bioreactor. Samples were easily loaded into the tubular growth chamber. Scaffold implantation was without complication. A defect 2.5 mm wide and 3 mm deep was successfully created using a frontal approach as not to penetrate the medullary space. Although a non critical size defect, this defect did not naturally heal following 21 days. Two animals were lost in surgery unrelated to scaffold implantation. Soft tissue covered defect within days and by day 21 no noticeable inflammation was observed. No gross observation could be made on bone regeneration between groups.

9.3.3 Bone Growth Following Implantation of PLGA/PCL Scaffolds

Light microscopy analysis using histological images indicated some regeneration of the defect following 21 days of culture (Figure 9.4). PLGA/PCL scaffolds containing no hMSC population exhibited minimal bone regeneration largely originating from the original bone on the edge of the defect (Figure 9.4c). Increased bone regeneration was observed in cell containing scaffolds with bone regeneration occurring both at the edge and center of scaffolds (Figure 9.4a-b). Bone could be observed mineralizing within PLGA/PCL scaffolds (Figure 9.5). By day 42 PLGA/PCL scaffold area has been reduced through scaffold degradation and largely replaced with newly formed bone (Figure 9.4d-f). Differences in bone in growth between implant groups were less apparent than on day 21. Blood vessels are observed penetrating the PLGA/PCL scaffold in all groups (Figure 9.5). There appears to be minimal tissue response to PLGA/PCL scaffolds as there is not a significant presence of inflammatory cells.

Histomorphometric analysis of new bone growth area within the PLGA/PCL implanted defects indicated that on Day 21 new bone area was significantly ($p < 0.10$) higher in rats implanted with cell containing scaffolds than those implanted with acellular scaffolds (Figure 9.6). Defects implanted with scaffolds containing TPS bioreactor cultured constructs had the highest overall new bone area with 1.23 ± 0.37 mm^2 at 21 days of the PLGA/PCL groups. This was higher but statistically similar ($p > 0.10$) to statically cultured hMSC containing PLGA/PCL scaffolds which had 0.99 ± 0.40 mm^2 of bone area in the original defect site. Both these groups had a statistically significant ($p < 0.10$) increase in new bone area as compared to defects implanted with a PLGA/PCL scaffold that did not contain cells. New bone area in this group was 0.50 ± 0.28 mm^2. Total

defect area was 4.9 mm^2 however because the native bone in this region is trabecular and bone marrow was not quantified, a fully healed defect would have a bone area less than 4.9 mm^2. By day 42 all groups had increased amount of bone area as compared to day 21 PLGA/PCL scaffolds. Defects implanted with bioreactor cultured PLGA/PCL scaffolds again had a higher level of bone area in the original defect site with 1.72 ± 0.41 mm^2 of new bone area as compared to day 42 static and no cell groups. This was significantly higher ($p < 0.10$) than defects implanted with PLGA/PCL scaffolds that did not contain hMSCs which had a new bone area of 1.19 ± 0.32 mm^2. Defects implanted with statically cultured hMSC containing scaffolds had a new bone area of 1.26 ± 0.40 mm^2 this was statistically similar ($p > 0.10$) to other PLGA/PCL treatment groups at this timepoint.

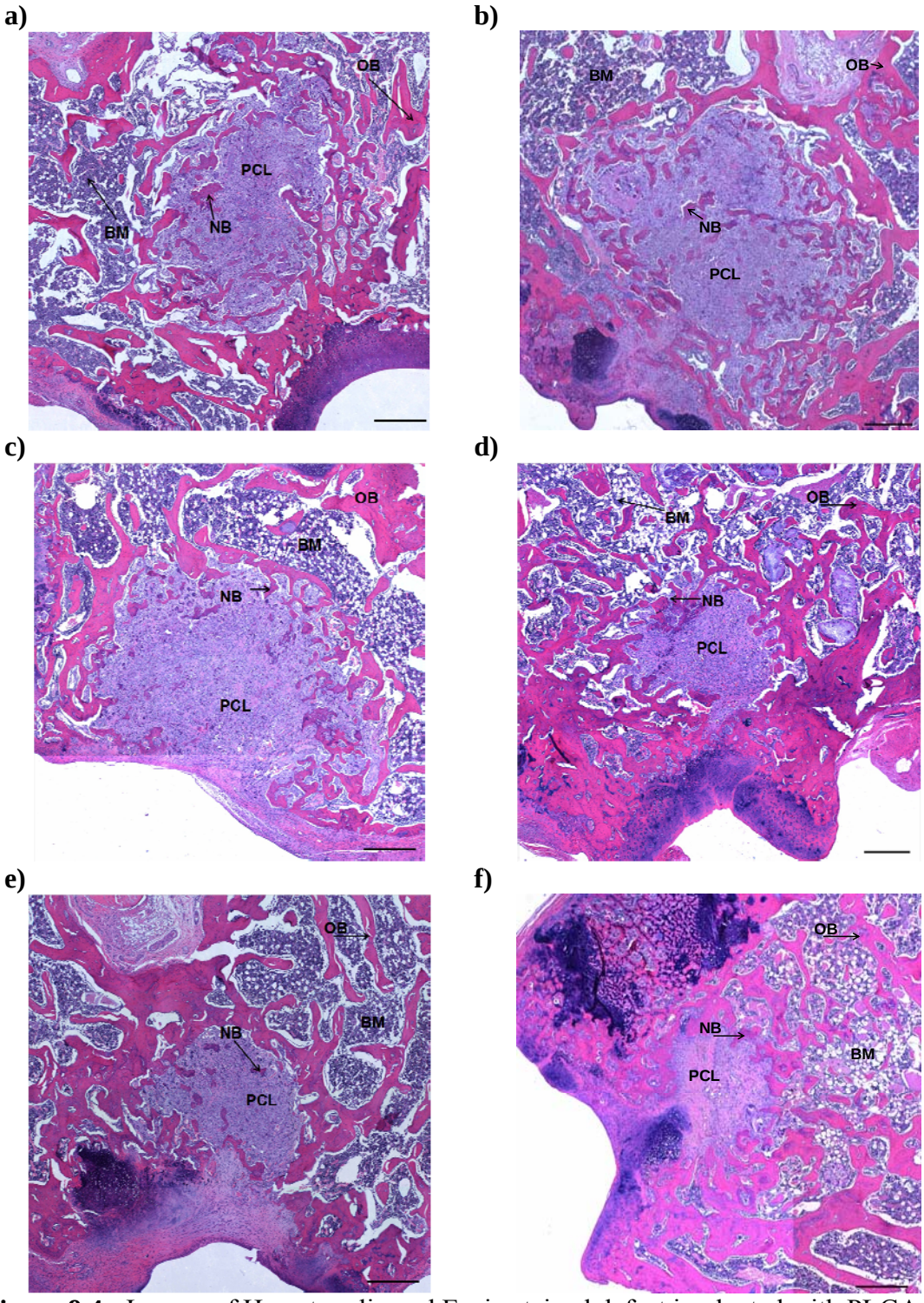

Figure 9.4: Images of Hematoxylin and Eosin stained defect implanted with PLGA/PCL scaffolds after 3 weeks (a-c) and 6 weeks (d-f) of *in vivo* implantation. Prior to implantation scaffolds were cultured *in vitro* in the TPS bioreactor with an hMSC population (a, d), in static culture with an hMSC population (b, e), or in static culture with no cell population (c, f). Scale bar represents 500 µm. PCL=PLGA/PCL Scaffold, NB=New Bone, OB=Original Bone, BM=Bone Marrow

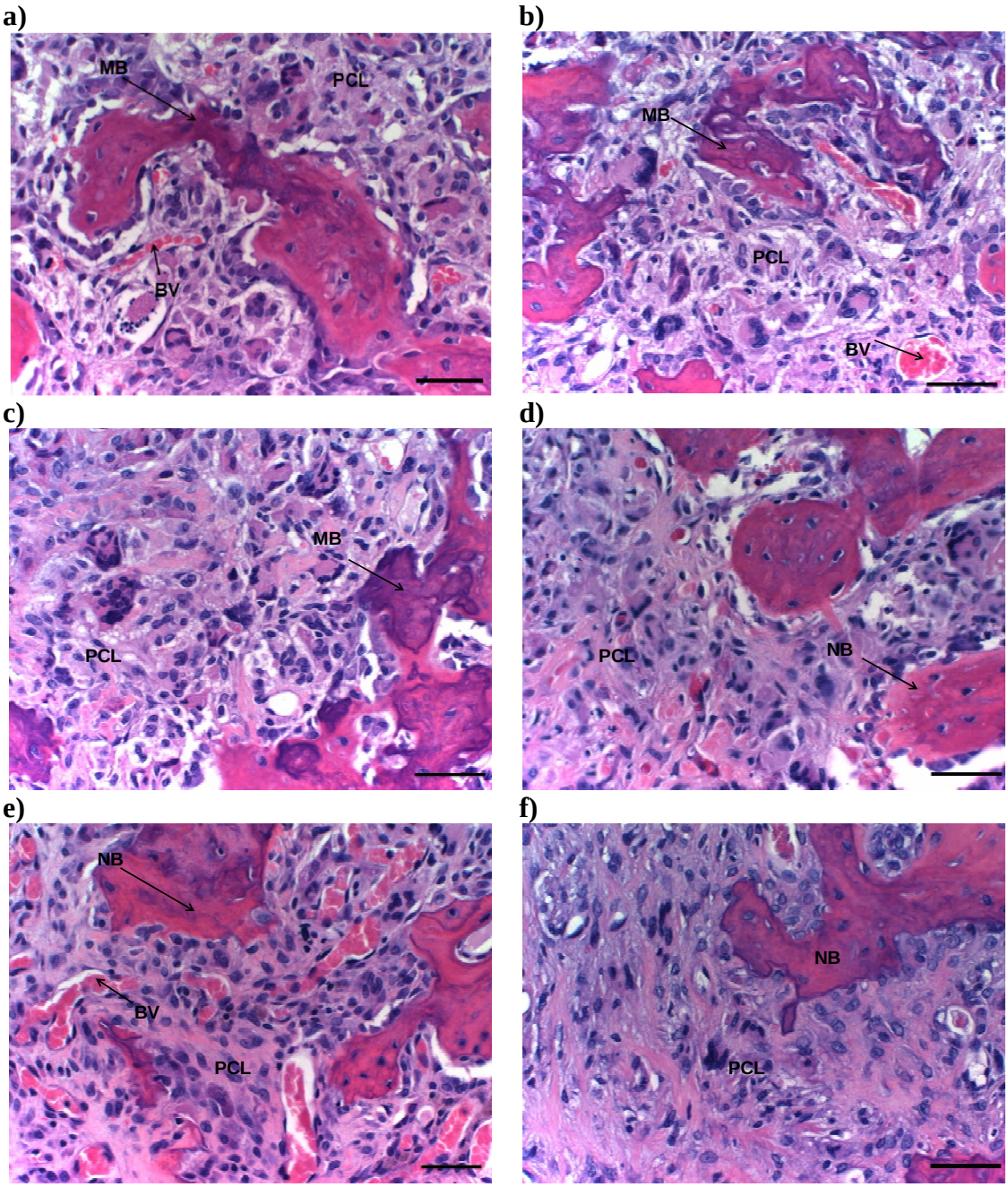

Figure 9.5: Magnified images of Hematoxylin and Eosin stained defect implanted with PLGA/PCL scaffolds after 3 weeks (a-c) and 6 weeks (d-f) *of in vivo* implantation. Prior to implantation scaffolds were cultured *in vitro* in the TPS bioreactor with an hMSC population (a, d), in static culture with an hMSC population (b, e), or in static culture with no cell population (c, f). In images (a,b) note mineralization formation and blood vessel infiltration within PLGA/PCL scaffold. In image (c) note mineralized bone formation around the edge of the scaffold. Bone in growth continues to penetrate scaffold after 42 days (d-f). Note minimal tissue response to material. Scale bar represents 50 µm. PCL=PLGA/PCL Scaffold, NB=New Bone, MB=Mineralized Bone, BV=Blood Vessel

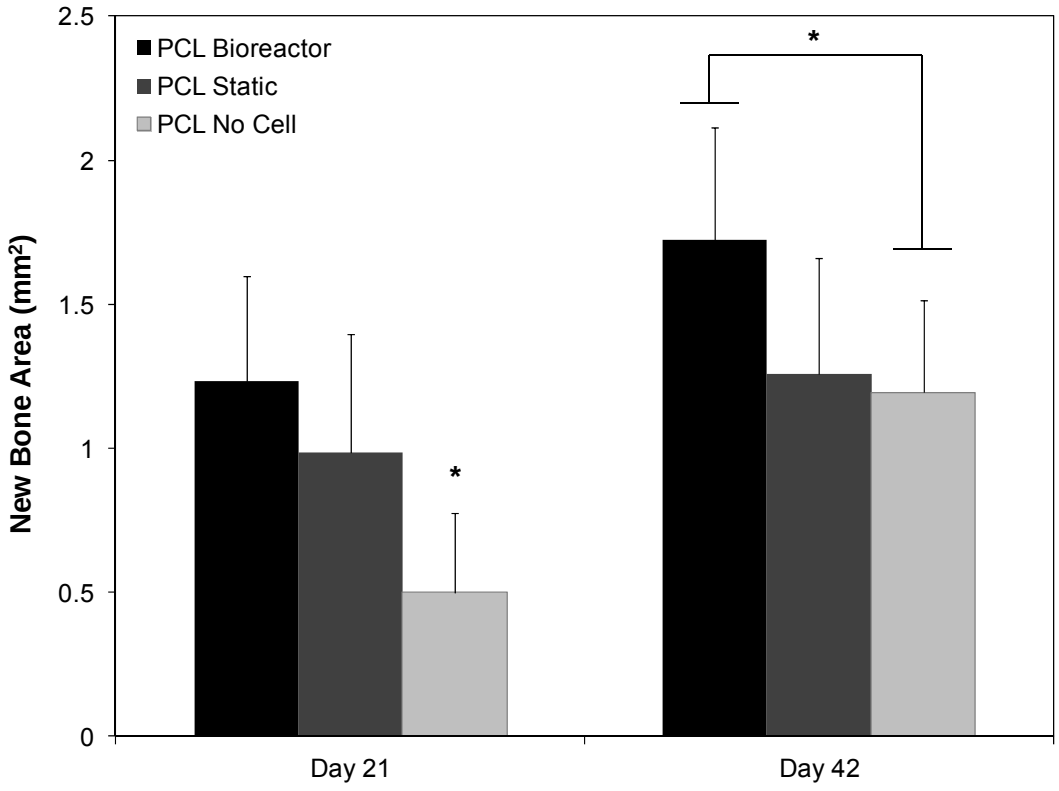

Figure 9.6: New bone area occurring in original defect area following implantation of PLGA/PCL scaffold as calculated by histomorphometric analysis. The symbol (*) indicates statistical significance within a timepoint ($p < 0.10$)

9.3.4 Bone Growth Following Implantation of Alginate Scaffolds

Light microscopy analysis of defects implanted with alginate scaffolds revealed limited bone growth in the center of the scaffold after 21 days (Figure 9.7a-c). Bone regeneration primarily occurred at the periphery of the defect. It should be noted that observed gaps between tissue and alginate often result as a histological artifact as alginate shrinks following dehydration. Some cartilage like tissue indicated by round cells in lacunae can be observed in the defect (Figure 9.8a). Observation of bone growth within alginate is limited however as bone alginate contact at the edge of the defect is observed (Figure 9.8b). In alginate groups containing no cells little bone alginate contact is

observed and alginate is largely absent of tissue invasion (Figure 9.7c). By day 42 increased bone growth is observed within the defect site and is observed in greater amounts in defects implanted with cell containing alginate scaffolds (Figure 9.7d-f). New bone can be observed lining the alginate scaffolds and some new bone can be observed inside remaining alginate. The scaffolds have dissolved and fractured into smaller pieces by day 42 allowing for greater bone in growth. Bone can be observed lining the edges and penetrating into alginate scaffolds (Figure 9.8d-e). Blood vessels are observed on the periphery of alginate scaffolds, but are not frequently observed within the alginate (Figure 9.8d). Less direct bone alginate contact was observed in alginate scaffolds implanted without an hMSC population (Figure 9.8f).

Histomorphometric analysis of bone growth in alginate scaffolds indicates significantly higher ($p < 0.10$) new bone area in defect sites implanted with cell containing alginate scaffolds than those without cells (Figure 9.9). Defects implanted with TPS cultured alginate scaffolds had a new bone area of 0.83 ± 0.26 mm^2. This was statistically similar ($p > 0.10$) to defects which were implanted with statically cultured hMSC containing constructs which had a new bone area of 0.82 ± 0.27 mm^2. Both of these groups had significantly higher ($p < 0.10$) new bone area than defects implanted with statically cultured no cell alginate constructs which had a new bone area of 0.39 ± 0.12 mm^2. By day 42 increased bone area was observed in all groups as compared to day 21 alginate scaffolds and significant differences in bone area did not exist between the groups. The highest overall new bone area was observed in the statically cultured cell containing scaffolds with a new bone area of 1.37 ± 0.31 mm^2. Bioreactor cultured scaffolds were

statistically similar with a new bone area of 1.27 ± 0.44 mm^2. Defects implanted with alginate without a cell population had the lowest new bone area with 0.89 ± 0.17 mm^2.

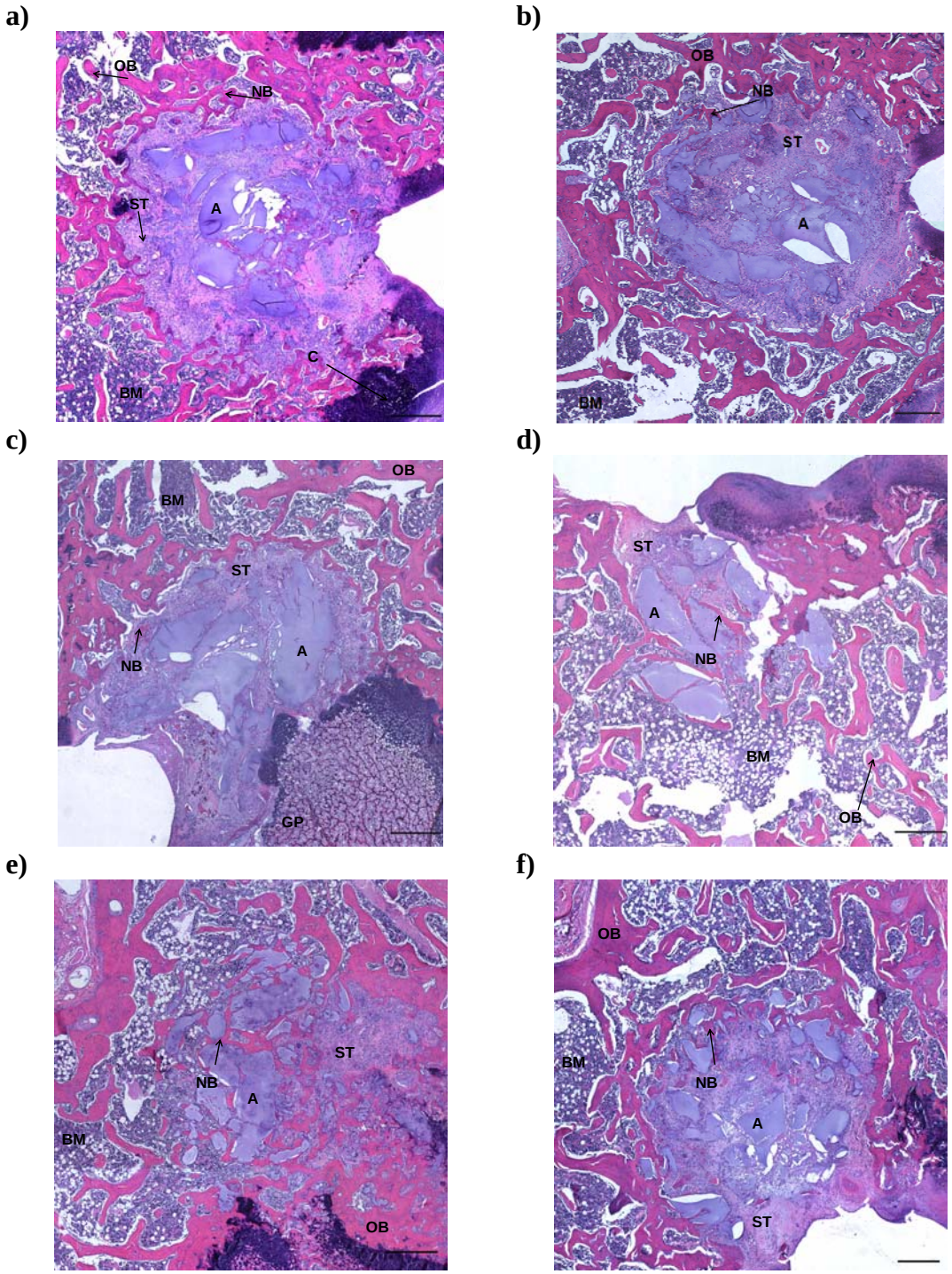

Figure 9.7: Images of Hematoxylin and Eosin stained defect implanted with alginate scaffolds after 3 weeks (a-c) and 6 weeks (d-f) of *in vivo* implantation. Prior to implantation scaffolds were cultured *in vitro* in the TPS bioreactor with an hMSC population (a, d), in static culture with an hMSC population (b, e), or in static culture with no cell population (c, f). Scale bar represents 500 µm. A=Alginate Scaffold, NB=New Bone, OB=Original Bone, BM=Bone Marrow, ST=Soft Tissue, C=Cartilage, GP=Growth Plate

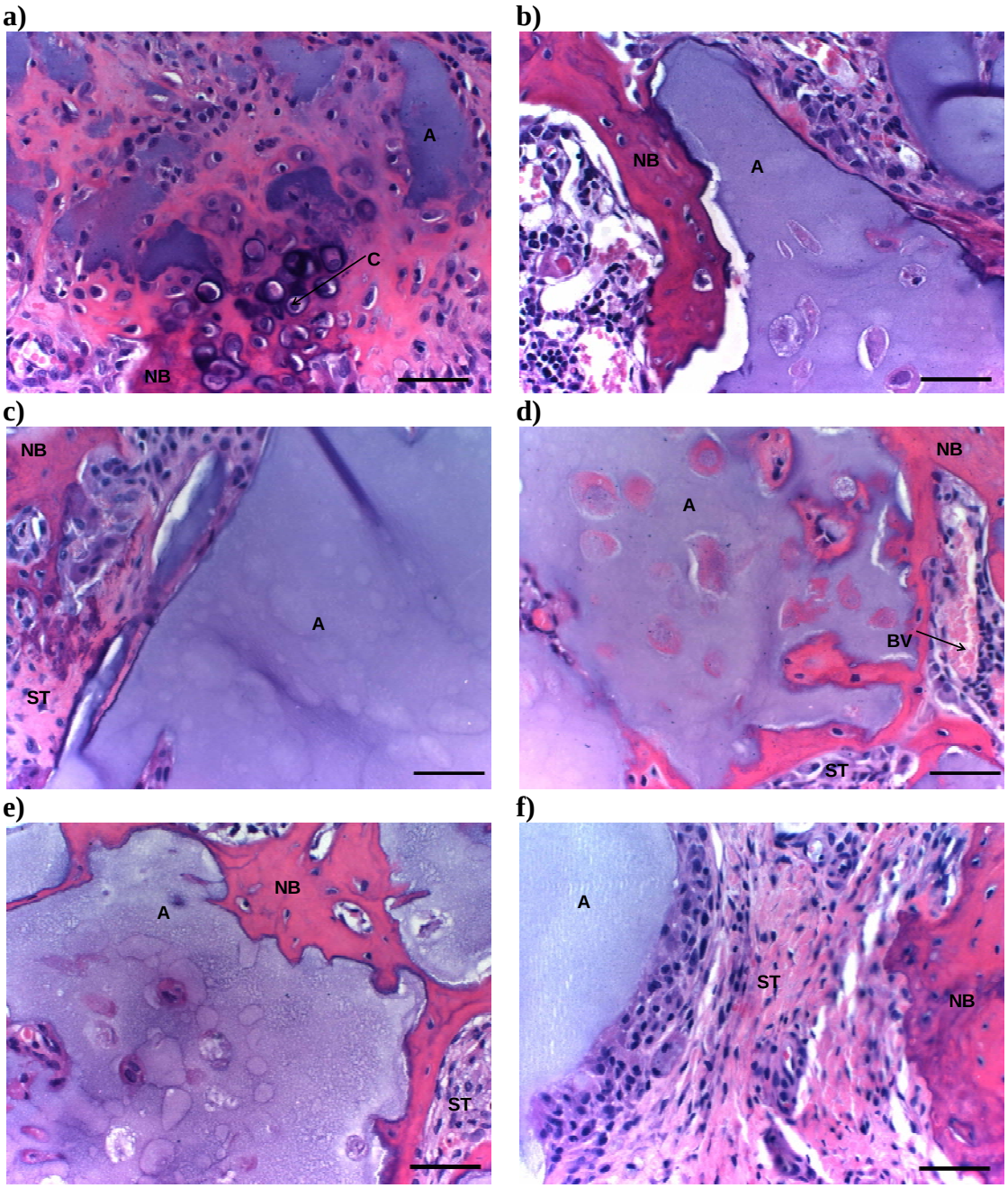

Figure 9.8: Magnified images of Hematoxylin and Eosin stained defect implanted with alginate scaffolds after 3 weeks (a-c) and 6 weeks (d-f) *of in vivo* implantation. Prior to implantation scaffolds were cultured *in vitro* in the TPS bioreactor with an hMSC population (a, d), in static culture with an hMSC population (b, e), or in static culture with no cell population (c, f). In (a) note some bone formation which may result from endochondral ossification. In (b) note some bone alginate contact, while no direct bone contact in (c). In six week samples (d,e) note direct bone alginate contact as well as some bone formation within alginate scaffolds. In no cell sample (f) limited bone alginate contact was observed and no bone formation was observed within the scaffold. Scale bar represents 50 µm. A=Alginate Scaffold, NB=New Bone, ST=Soft Tissue, C=Cartilage, BV=Blood Vessel

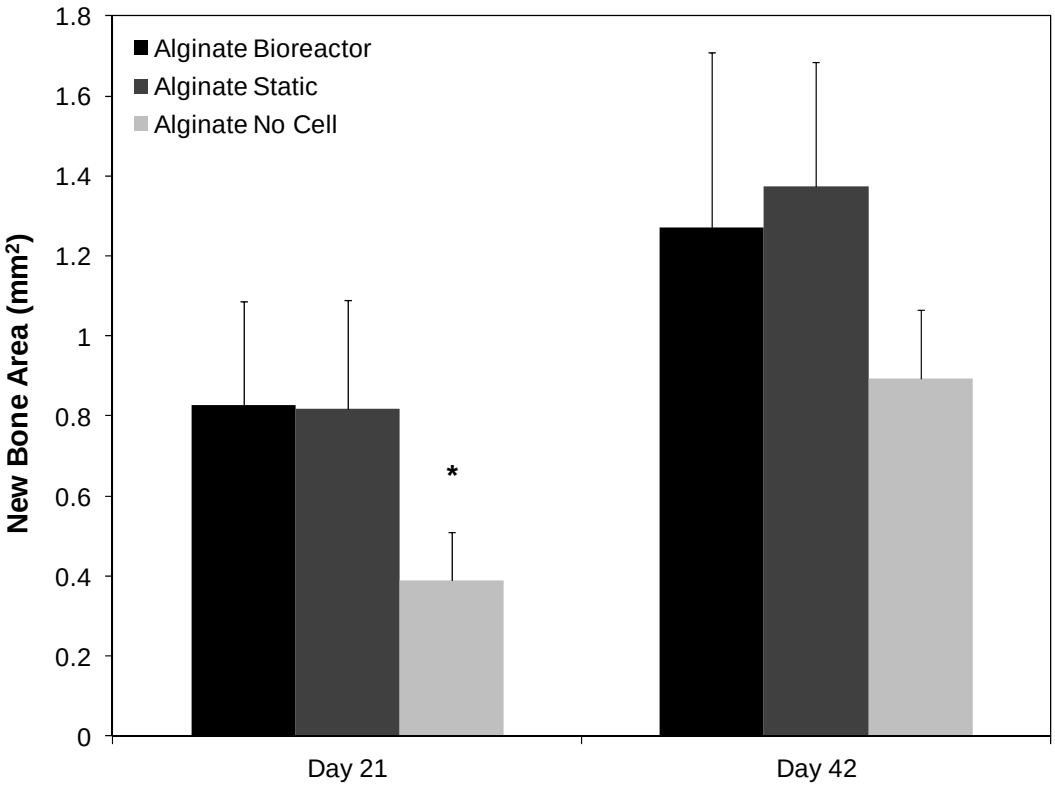

Figure 9.9: New bone area occurring in original defect following implantation of alginate scaffolds as calculated by histomorphometric analysis. The symbol (*) indicates statistical significance within a timepoint ($p < 0.10$)

9.4 Discussion

Bioreactor systems have frequently been used to improve *in vitro* culture of mesenchymal stem cells for bone tissue engineering purposes [16, 17, 20, 57]. The tubular perfusion system bioreactor utilized in this study has been previously shown to increase proliferation and enhance differentiation of hMSCs in alginate scaffolds as compared to static cultured controls [112, 286]. However, these *in vitro* findings do not necessarily correlate to improved *in vivo* bone regeneration [288] . In this study we compare the repair of a non critical size femoral condyle defect in nude rats following implantation of

two different scaffold materials, PLGA/PCL and alginate. Each of these scaffolds were cultured with and without a hMSC population. This cell population was cultured both under static and dynamic conditions to determine the effect of TPS bioreactor culture on *in vivo* repair capacities of hMSCs. Based on previous studies, hMSCs cultured in alginate scaffolds are viable after 10 days of bioreactor culture and have proliferated [112, 286]. After 10 days of osteogenic induction these cells have begun differentiating into osteoblasts but have not begun mineralizing *in vitro* [112, 286]. Both alginate and PLGA/PCL scaffolds had not undergone significant dissolution or degradation following ten days of *in vitro* and could be manipulated with forceps and easily implanted in the defect.

In PLGA/PCL scaffolds greater amounts of bone formation after 3 weeks were observed in cell containing scaffolds as compared to scaffolds without a cell population. This bone formation was highest in bioreactor cultured PLGA/PCL scaffolds. In cell containing groups new bone could be observed forming on the interior of PLGA/PCL scaffolds while in acellular scaffolds bone formation was primarily restricted to the exterior portions of the scaffold. This could indicate either increased bone formation directly from the implanted hMSC population, or an ability of this cell population to recruit native cells to the defect area. Mineralization can be observed in these scaffolds indicating formation of bone through an intramembranous ossification process.

By day 42 differences between groups are less obvious as this non critical bone defect has largely healed absent the PLGA/PCL scaffold area. The implanted scaffolds are visually reduced in area indicating significant scaffold degradation after 42 days. New

bone area was significantly higher in bioreactor cultured PLGA/PCL scaffolds than no cell scaffolds, possibly due to increased bone formation within scaffolds in this group.

Tissue response to the PLGA/PCL scaffolds appeared to be minimal on both day 21 and 42 as inflammatory cells were not frequently observed. Blood vessel infiltration into the defect, both on the periphery and interior of the PLGA/PCL scaffold was frequently observed. This is a significant observation as sufficient vascularization is a required for successful regeneration of a bone defect.

Similar to PLGA/PCL scaffolds increased new bone area was observed in alginate scaffolds which contained an encapsulated cell population compared to empty alginate scaffolds. However, compared directly to PLGA/PCL scaffolds, new bone area was lower at day 21 in alginate scaffolds. In addition light microscopy analysis indicated that bone was not frequently observed in the center of alginate scaffolds and rather was localized to the edge of the defect. Based on this observation it appears that the implanted hMSC population is not generating bone in these scaffolds. In addition new bone is unable to penetrate intact alginate scaffolds. However, increased bone growth is observed when comparing cell implanted scaffolds to acellular alginate scaffolds. Based on this observation it appears that the implanted hMSCs may be able to recruit cells from the native bone tissue to repair the defect. Unlike the PLGA/PCL scaffolds little difference was observed between bioreactor and statically cultured scaffolds. It is hypothesized that in bulk alginate scaffolds native tissue is only able to contact the cell population close to the surface of the scaffolds. Since only the cell population close to the surface is contributing to bone regeneration, bioreactor culture does not have an effect as cells closer to the surface can receive nutrients in both static and dynamic culture.

Though bioreactor culture increases the growth and osteoblastic differentiation of these hMSCs *in vitro*, following 10 days of *in vitro* culture these differences do not transfer into increased amounts of *in vivo* bone formation. Thus scaffolds must be able to support tissue and blood vessel infiltration to support the implanted cell population upon *in vivo* implantation. However by 42 days elevated new bone formation was still observed in cell containing alginate scaffolds and some bone formation was observed inside alginate scaffolds of cell containing groups. This demonstrates an ability of the implanted cell population to improve the bone formation through 42 days. In cell groups this new bone could be observed in direct contact with the alginate scaffolds. Negative tissue response to these scaffolds was also minimal as the area surrounding the defect did not appear inflamed in response to the alginate. Unlike the PLGA/PCL scaffolds vessel infiltration was not frequently observed inside the alginate scaffolds. Though vessels were often observed on the periphery of the defect, vessels did not seem to have the ability to penetrate the bulk alginate scaffolds. This lack of vessel infiltration could explain the reduced amount of bone formation in the center of the scaffold. Some cartilage formation was observed in the defect site indicating bone formation may be following an endochondral like pathway, however it could not be determined if the implanted cell population or scaffold had an influence on intramembranous versus endochondral bone formation.

Based on the results of this study it appears though beneficial for *in vitro* hMSC culture, bioreactor culture is only beneficial for *in vivo* bone growth under certain conditions. In alginate scaffolds that do not appear to be rapidly infiltrated by the host vasculature bioreactor culture does not have an influence on *in vivo* bone formation. This highlights

the need for a scaffold type that promotes rapid *in vivo* vascularization to maintain an implanted cell population. In contrast PLGA/PCL scaffolds were able to support vascular invasion and a greater amount of new bone formation was observed within these scaffolds as compared to the alginate scaffolds. In this case elevated levels of bone formation were observed as a result of bioreactor culture. Thus tubular perfusion system culture can be used to enhance *in vivo* bone regeneration using hMSCs, but scaffold type must support tissue infiltration to maximize this effect.

9.5 Conclusions

In this study we demonstrate the efficacy of using a tubular perfusion system bioreactor for the culture of hMSCs to aid in *in vivo* bone regeneration and repair. hMSCs enhanced bone regeneration in both alginate and PLGA/PCL scaffolds, however bioreactor culture was only shown to have a positive effect in PLGA/PCL scaffolds. This demonstrates the ability to utilize bioreactor systems for bone tissue engineering and the need for scaffold systems that can maintain a cell population following implantation.

10. Summary

The overall goal of this work was to develop and evaluate a new bioreactor system for bone tissue engineering. Human mesenchymal stem cells were used as a cell source and three different scaffold materials were evaluated in the system. The motivation for this work was to enhance the clinical relevance of cell based tissue engineering utilizing three dimensional scaffolds by improving *in vitro* culture techniques.

In the first part of the work a new bioreactor system was developed that was shown to enhance the *in vitro* proliferation of human mesenchymal stem cells in alginate beads and the differentiation of these cells into osteoblasts. Results of this study revealed that dynamic culture supports proliferation of hMSCs and enhances late osteoblastic differentiation of these cells.

Following this the second study evaluated shear stress in the TPS bioreactor as an important regulator of stem cell fate as well as the ability of hMSC scaffold position to affect differentiation. This study demonstrated shear stress as a potent and temporal stimulus of hMSC osteoblastic differentiation within bulk alginate scaffolds. Mineralization and proliferation levels were decreased in statically cultured constructs which highlighted a need for bioreactor systems to improve *in vitro* culture. In addition it was discovered that hMSC radial position within scaffolds had an effect on both the osteoblastic differentiation and proliferation of these cells. These results could be used to tailor a flow and shear regime for either expansion or differentiation of a stem cell population to dictate the desired outcome of *in vitro* culture.

In the next chapter of research an advanced implantation technique was developed for alginate scaffolds cultured in the TPS bioreactor. Through the course of this study a protocol was developed and evaluated for the fabrication of a cell containing tissue engineering construct from many smaller scaffolds in a bioreactor system. Results demonstrated the construct can be elegantly fabricated and has mechanical properties similar to traditionally fabricated alginate scaffolds. The scaffold, designated an aggregated alginate construct, has many potential applications including non load bearing bone, cartilage, and skeletal muscle tissue engineering. Through this method of culturing a large scaffold as individual small bead building blocks a large tissue engineering construct could be created ready for implantation into a defect site.

In the next chapter the utility of the bioreactor was demonstrated by using a synthetic PLLA scaffold. These scaffolds were fabricated by a new supercritical gel drying with porogen leaching process to create scaffolds with both a nano and microstructure. hMSCs were able to adhere, proliferate, and differentiate within the scaffold structure in both static and TPS culture. Effects of the architecture of the scaffold were magnified in dynamic culture leading to increased proliferation and osteoblastic differentiation.

In the final chapter of the work the efficacy of using the tubular perfusion system bioreactor for the culture of hMSCs to aid in *in vivo* bone regeneration and repair was demonstrated. hMSCs enhanced bone regeneration in both alginate and PLGA/PCL scaffolds. This work demonstrated the ability to utilize bioreactor systems for bone tissue engineering and the need for scaffold systems that can maintain the cell population following implantation.

These studies have demonstrated the effectiveness of the tubular perfusion system bioreactor for the culture of hMSCs for bone tissue engineering. This bioreactor was shown to increase the proliferation and osteoblastic differentiation of these cells which were dependent on both shear stress and cell radial position in the scaffold. This system was also demonstrated to be effective when using synthetic scaffolds including PLLA and PLGA/PCL to support the hMSC population. Finally, hMSC containing scaffolds cultured in the TPS bioreactor were implanted in a bone defect and results of this study demonstrated the efficacy of using this system for *in vivo* bone regeneration.

11. Future Work

This work highlighted the need for the effective use of bioreactor systems in cell based tissue engineering strategies. Though the TPS bioreactor was shown to be effective, design improvements could be made to further increase its utility. As discussed in Chapter 2, bioreactor systems can be automated to minimize difficultly of use. Significant hurdles in implementing a cell based tissue engineering strategy will include expense and manpower required to culture cells *in vitro* and risk of contamination. Bioreactor system automation could mitigate these two obstacles, streamlining the cell culture process.

Results from Chapter 9 revealed another area of future work to explore with the system. Though *in vivo* bone growth was improved using stem cells, histology images indicated that especially in alginate scaffold bone growth within scaffolds was limited. This highlighted the fact that *in vitro* stem cell differentiation and mineralization do not translate to *in vivo* bone generation unless the *in vivo* environment can support the implanted cell population. This requires a scaffold that can support infiltration from the host vasculature. To further improve *in vivo* vascularization an endothelial cell population could be cocultured in the TPS bioreactor to create a prevascular network that could integrate with the host vasculature. By developing a prevascular network, or improving vascularization through the use of growth factors essential nutrients can be delivered to the implanted cell population to enhance regeneration of a bone defect.

A final future direction for this research is the scaling up of the bioreactor system to create larger tissue engineering bone grafts. As a small animal study was completed through the course of this study, the TPS bioreactor can be scaled up to produce constructs that could fill a large animal bone defect model. The system design is scalable, so a size increase should not present too many difficulties. The completion of a critical size large animal defect model is essential to continue to demonstrate the effectiveness of the system for a bioreactor based bone tissue engineering strategy.

Bibliography

1. Laurencin, C.T., et al., *Tissue engineering: orthopedic applications.* Annu Rev Biomed Eng, 1999. **1**: p. 19-46.
2. Gitelis, S. and P. Saiz, *What's new in orthopaedic surgery.* J Am Coll Surg, 2002. **194**(6): p. 788-91.
3. Mistry, A.S. and A.G. Mikos, *Tissue engineering strategies for bone regeneration.* Adv Biochem Eng Biotechnol, 2005. **94**: p. 1-22.
4. Langer, R., *Tissue engineering.* Mol Ther, 2000. **1**(1): p. 12-5.
5. Pittenger, M.F., et al., *Multilineage potential of adult human mesenchymal stem cells.* Science, 1999. **284**(5411): p. 143-7.
6. Caplan, A.I., *Adult mesenchymal stem cells for tissue engineering versus regenerative medicine.* Journal of Cellular Physiology, 2007. **213**(2): p. 341-347.
7. Alvarez-Barreto, J.F., et al., *Flow perfusion improves seeding of tissue engineering scaffolds with different architectures.* Annals of Biomedical Engineering, 2007. **35**(3): p. 429-442.
8. Alvarez-Barreto, J.F. and V.I. Sikavitsas, *Improved mesenchymal stem cell seeding on RGD-modified poly(L-lactic acid) scaffolds using flow perfusion.* Macromolecular Bioscience, 2007. **7**(5): p. 579-588.
9. Wendt, D., et al., *Oscillating perfusion of cell suspensions through three-dimensional scaffolds enhances cell seeding efficiency and uniformity.* Biotechnology and Bioengineering, 2003. **84**(2): p. 205-214.
10. Grayson, W.L., et al., *Effects of Initial Seeding Density and Fluid Perfusion Rate on Formation of Tissue-Engineered Bone.* Tissue Engineering Part A, 2008. **14**(11): p. 1809-1820.
11. Mygind, T., et al., *Mesenchymal stem cell ingrowth and differentiation on coralline hydroxyapatite scaffolds.* Biomaterials, 2007. **28**(6): p. 1036-1047.
12. Shin, M., H. Yoshimoto, and J.P. Vacanti, *In vivo bone tissue engineering using mesenchymal stem cells on a novel electrospun nanofibrous scaffold.* Tissue Engineering, 2004. **10**(1-2): p. 33-41.
13. Yang, J.F., et al., *Proliferation and osteogenesis of immortalized bone marrow-derived mesenchymal stem cells in porous polylactic glycolic acid scaffolds under perfusion culture.* Journal of Biomedical Materials Research Part A, 2010. **92A**(3): p. 817-829.
14. Datta, N., et al., *In vitro generated extracellular matrix and fluid shear stress synergistically enhance 3D osteoblastic differentiation.* Proceedings of the National Academy of Sciences of the United States of America, 2006. **103**(8): p. 2488-2493.
15. Grayson, W.L., et al., *Engineering anatomically shaped human bone grafts.* Proceedings of the National Academy of Sciences of the United States of America, 2010. **107**(8): p. 3299-3304.
16. Janssen, F.W., et al., *Human tissue-engineered bone produced in clinically relevant amounts using a semi-automated perfusion bioreactor system: a preliminary study.* Journal of Tissue Engineering and Regenerative Medicine, 2010. **4**(1): p. 12-24.

17. Sikavitsas, V.I., et al., *Mineralized matrix deposition by marrow stromal osteoblasts in 3D perfusion culture increases with increasing fluid shear forces.* Proceedings of the National Academy of Sciences of the United States of America, 2003. **100**(25): p. 14683-14688.
18. Sikavitsas, V.I., et al., *Flow perfusion enhances the calcified matrix deposition of marrow stromal cells in biodegradable nonwoven fiber mesh scaffolds.* Annals of Biomedical Engineering, 2005. **33**(1): p. 63-70.
19. Wendt, D., et al., *Uniform tissues engineered by seeding and culturing cells in 3D scaffolds under perfusion at defined oxygen tensions.* Biorheology, 2006. **43**(3-4): p. 481-488.
20. Bancroft, G.N., et al., *Fluid flow increases mineralized matrix deposition in 3D perfusion culture of marrow stromal osteoblasts in a dose-dependent manner.* Proc Natl Acad Sci U S A, 2002. **99**(20): p. 12600-5.
21. Volkmer, E., et al., *Hypoxia in static and dynamic 3D culture systems for tissue engineering of bone.* Tissue Engineering Part A, 2008. **14**(8): p. 1331-1340.
22. Meinel, L., et al., *Bone tissue engineering using human mesenchymal stem cells: Effects of scaffold material and medium flow.* Annals of Biomedical Engineering, 2004. **32**(1): p. 112-122.
23. Stiehler, M., et al., *Effect of dynamic 3-D culture on proliferation, distribution, and osteogenic differentiation of human mesenchymal stem cells.* Journal of Biomedical Materials Research Part A, 2009. **89A**(1): p. 96-107.
24. Wang, T.W., et al., *Regulation of adult human mesenchymal stem cells into osteogenic and chondrogenic lineages by different bioreactor systems.* Journal of Biomedical Materials Research Part A, 2009. **88A**(4): p. 935-946.
25. Yu, X.J., et al., *Bioreactor-based bone tissue engineering: The influence of dynamic flow on osteoblast phenotypic expression and matrix mineralization.* Proceedings of the National Academy of Sciences of the United States of America, 2004. **101**(31): p. 11203-11208.
26. Zhang, Z.Y., et al., *A biaxial rotating bioreactor for the culture of fetal mesenchymal stem cells for bone tissue engineering.* Biomaterials, 2009. **30**(14): p. 2694-2704.
27. Bancroft, G.N., V.I. Sikavitsas, and A.G. Mikos, *Design of a flow perfusion bioreactor system for bone tissue-engineering applications.* Tissue Engineering, 2003. **9**(3): p. 549-554.
28. Gomes, M.E., et al., *Effect of flow perfusion on the osteogenic differentiation of bone marrow stromal cells cultured on starch-based three-dimensional scaffolds.* Journal of Biomedical Materials Research Part A, 2003. **67A**(1): p. 87-95.
29. Holtorf, H.L., J.A. Jansen, and A.G. Mikos, *Flow perfusion culture induces the osteoblastic differentiation of marrow stromal cell-scaffold constructs in the absence of dexamethasone.* Journal of Biomedical Materials Research Part A, 2005. **72A**(3): p. 326-334.
30. Janssen, F.W., et al., *A perfusion bioreactor system capable of producing clinically relevant volumes of tissue-engineered bone: In vivo bone formation showing proof of concept.* Biomaterials, 2006. **27**(3): p. 315-323.
31. Zhao, F., R. Chella, and T. Ma, *Effects of shear stress on 3-D human mesenchymal stem cell construct development in a perfusion bioreactor system:*

Experiments and hydrodynamic modeling. Biotechnology and Bioengineering, 2007. **96**(3): p. 584-595.
32. Bilodeau, K. and D. Mantovani, *Bioreactors for tissue engineering: Focus on mechanical constraints. A comparative review.* Tissue Engineering, 2006. **12**(8): p. 2367-2383.
33. Sikavitsas, V.I., J.S. Temenoff, and A.G. Mikos, *Biomaterials and bone mechanotransduction.* Biomaterials, 2001. **22**(19): p. 2581-2593.
34. Rubin, J., C. Rubin, and C.R. Jacobs, *Molecular pathways mediating mechanical signaling in bone.* Gene, 2006. **367**: p. 1-16.
35. Weinbaum, S., S.C. Cowin, and Y. Zeng, *A Model for the Excitation of Osteocytes by Mechanical Loading-Induced Bone Fluid Shear Stresses.* Journal of Biomechanics, 1994. **27**(3): p. 339-360.
36. Grellier, M., et al., *Responsiveness of human bone marrow stromal cells to shear stress.* Journal of Tissue Engineering and Regenerative Medicine, 2009. **3**(4): p. 302-309.
37. Jaasma, M.J., N.A. Plunkett, and F.J. O'Brien, *Mechanical stimulation of osteoblasts by steady and dynamic fluid flow.* Tissue Engineering, 2007. **13**(7): p. 1723-1723.
38. Kapur, S., D.J. Baylink, and K.H.W. Lau, *Fluid flow shear stress stimulates human osteoblast proliferation and differentiation through multiple interacting and competing signal transduction pathways.* Bone, 2003. **32**(3): p. 241-251.
39. Kreke, M.R., W.R. Huckle, and A.S. Goldstein, *Fluid flow stimulates expression of osteopontin and bone sialoprotein by bone marrow stromal cells in a temporally dependent manner.* Bone, 2005. **36**(6): p. 1047-1055.
40. Kreke, M.R., et al., *Effect of intermittent shear stress on mechanotransductive signaling and osteoblastic differentiation of bone marrow stromal cells.* Tissue Engineering Part A, 2008. **14**(4): p. 529-537.
41. Godara, P., C.D. McFarland, and R.E. Nordon, *Design of bioreactors for mesenchymal stem cell tissue engineering.* Journal of Chemical Technology and Biotechnology, 2008. **83**(4): p. 408-420.
42. Sikavitsas, V.I., G.N. Bancroft, and A.G. Mikos, *Formation of three-dimensional cell/polymer constructs for bone tissue engineering in a spinner flask and a rotating wall vessel bioreactor.* Journal of Biomedical Materials Research, 2002. **62**(1): p. 136-148.
43. Kim, H.J., et al., *Bone regeneration on macroporous aqueous-derived silk 3-D scaffolds.* Macromolecular Bioscience, 2007. **7**(5): p. 643-655.
44. Ichinohe, N., T. Takamoto, and Y. Tabata, *Proliferation, osteogenic differentiation, and distribution of rat bone marrow stromal cells in nonwoven fabrics by different culture methods.* Tissue Engineering Part A, 2008. **14**(1): p. 107-116.
45. Hosseinkhani, H., et al., *Perfusion culture enhances osteogenic differentiation of rat mesenchymal stem cells in collagen sponge reinforced with poly(glycolic acid) fiber.* Tissue Engineering, 2005. **11**(9-10): p. 1476-1488.
46. Goldstein, A.S., et al., *Effect of convection on osteoblastic cell growth and function in biodegradable polymer foam scaffolds.* Biomaterials, 2001. **22**(11): p. 1279-1288.

47. Botchwey, E.A., et al., *Bone tissue engineering in a rotating bioreactor using a microcarrier matrix system.* Journal of Biomedical Materials Research, 2001. **55**(2): p. 242-253.
48. Botchwey, E.A., et al., *Human osteoblast-like cells in three-dimensional culture with fluid flow.* Biorheology, 2003. **40**(1-3): p. 299-306.
49. Botchwey, E.A., et al., *Quantitative analysis of three-dimensional fluid flow in rotating bioreactors for tissue engineering.* Journal of Biomedical Materials Research Part A, 2004. **69A**(2): p. 205-215.
50. Terai, H., et al., *In vitro engineering of bone using a rotational oxygen-permeable bioreactor system.* Materials Science & Engineering C-Biomimetic and Supramolecular Systems, 2002. **20**(1-2): p. 3-8.
51. Yoshimoto, H., et al., *A biodegradable nanofiber scaffold by electrospinning and its potential for bone tissue engineering.* Biomaterials, 2003. **24**(12): p. 2077-2082.
52. Song, K.D., et al., *Three-dimensional fabrication of engineered bone with human bio-derived bone scaffolds in a rotating wall vessel bioreactor.* Journal of Biomedical Materials Research Part A, 2008. **86A**(2): p. 323-332.
53. Cartmell, S.H., et al., *Effects of medium perfusion rate on cell-seeded three-dimensional bone constructs in vitro.* Tissue Eng, 2003. **9**(6): p. 1197-203.
54. Hosseinkhani, H., et al., *Ectopic bone formation in collagen sponge self-assembled peptide-amphiphile nanofibers hybrid scaffold in a perfusion culture bioreactor.* Biomaterials, 2006. **27**(29): p. 5089-5098.
55. Hosseinkhani, H., et al., *Impregnation of plasmid DNA into three-dimensional scaffolds and medium perfusion enhance in vitro DNA expression of mesenchymal stem cells.* Tissue Eng, 2005. **11**(9-10): p. 1459-75.
56. Hosseinkhani, H., et al., *Enhanced ectopic bone formation using a combination of plasmid DNA impregnation into 3-D scaffold and bioreactor perfusion culture.* Biomaterials, 2006. **27**(8): p. 1387-1398.
57. Gomes, M.E., et al., *Influence of the porosity of starch-based fiber mesh scaffolds on the proliferation and osteogenic differentiation of bone marrow stromal cells cultured in a flow perfusion bioreactor.* Tissue Engineering, 2006. **12**(4): p. 801-809.
58. Holtorf, H.L., et al., *Flow perfusion culture of marrow stromal cells seeded on porous biphasic calcium phosphate ceramics.* Annals of Biomedical Engineering, 2005. **33**(9): p. 1238-1248.
59. Bjerre, L., et al., *Flow perfusion culture of human mesenchymal stem cells on silicate-substituted tricalcium phosphate scaffolds.* Biomaterials, 2008. **29**(17): p. 2616-2627.
60. Gomes, M.E., R.L. Reis, and A.G. Mikos, *Bone tissue engineering constructs based on starch scaffolds and bone marrow cells cultured in a flow perfusion bioreactor.* Advanced Materials Forum Iii, Pts 1 and 2, 2006. **514-516**: p. 980-984.
61. Karageorgiou, V. and D. Kaplan, *Porosity of 3D biornaterial scaffolds and osteogenesis.* Biomaterials, 2005. **26**(27): p. 5474-5491.

62. Kim, K., et al., *Stereolithographic bone scaffold design parameters: osteogenic differentiation and signal expression.* Tissue Eng Part B Rev, 2010. **16**(5): p. 523-39.
63. Gomes, M.E., et al., *In vitro localization of bone growth factors in constructs of biodegradable scaffolds seeded with marrow stromal cells and cultured in a flow perfusion bioreactor.* Tissue Engineering, 2006. **12**(1): p. 177-188.
64. Kannan, R.Y., et al., *The roles of tissue engineering and vascularisation in the development of micro-vascular networks: a review.* Biomaterials, 2005. **26**(14): p. 1857-1875.
65. Hoeben, A., et al., *Vascular endothelial growth factor and angiogenesis.* Pharmacological Reviews, 2004. **56**(4): p. 549-580.
66. Bessa, P.C., M. Casal, and R.L. Reis, *Bone morphogenetic proteins in tissue engineering: the road from laboratory to clinic, part II (BMP delivery).* J Tissue Eng Regen Med, 2008. **2**(2-3): p. 81-96.
67. Bessa, P.C., M. Casal, and R.L. Reis, *Bone morphogenetic proteins in tissue engineering: the road from the laboratory to the clinic, part I (basic concepts).* J Tissue Eng Regen Med, 2008. **2**(1): p. 1-13.
68. Betz, M.W., et al., *Tissue response and orbital floor regeneration using cyclic acetal hydrogels.* J Biomed Mater Res A, 2008. **90**(3): p. 819-29.
69. Betz, M.W., et al., *Macroporous hydrogels upregulate osteogenic signal expression and promote bone regeneration.* Biomacromolecules, 2010. **11**(5): p. 1160-8.
70. Frohlich, M., et al., *Bone Grafts Engineered from Human Adipose-Derived Stem Cells in Perfusion Bioreactor Culture.* Tissue Engineering Part A, 2010. **16**(1): p. 179-189.
71. Gimble, J.M., et al., *Adipose tissue: Derived stromal cells are multipotent.* Journal of Bone and Mineral Research, 2000. **15**: p. S508-S508.
72. Halvorsen, Y.D.C., et al., *Extracellular matrix mineralization and osteoblast gene expression by human adipose tissue-derived stromal cells.* Tissue Engineering, 2001. **7**(6): p. 729-741.
73. Zuk, P.A., et al., *Human adipose tissue is a source of multipotent stem cells.* Molecular Biology of the Cell, 2002. **13**(12): p. 4279-4295.
74. Zuk, P.A., et al., *Multilineage cells from human adipose tissue: Implications for cell-based therapies.* Tissue Engineering, 2001. **7**(2): p. 211-228.
75. Janssen, F.W., et al., *Online measurement of oxygen consumption by goat bone marrow stromal cells in a combined cell-seeding and proliferation perfusion bioreactor.* Journal of Biomedical Materials Research Part A, 2006. **79A**(2): p. 338-348.
76. Braccini, A., et al., *Three-dimensional perfusion culture of human bone marrow cells and generation of osteoinductive grafts.* Stem Cells, 2005. **23**(8): p. 1066-1072.
77. Timmins, N.E., et al., *Three-dimensional cell culture and tissue engineering in a T-CUP (Tissue Culture Under Perfusion).* Tissue Engineering, 2007. **13**(8): p. 2021-2028.
78. Sikavitsas, V.I., et al., *Influence of the in vitro culture period on the in vivo performance of cell/titanium bone tissue-engineered constructs using a rat*

cranial critical size defect model. Journal of Biomedical Materials Research Part A, 2003. **67A**(3): p. 944-951.
79. Xie, Y.Z., et al., *Three-dimensional flow perfusion culture system for stem cell proliferation inside the critical-size beta-tricalcium phosphate scaffold.* Tissue Engineering, 2006. **12**(12): p. 3535-3543.
80. Li, D., et al., *Effects of flow shear stress and mass transport on the construction of a large-scale tissue-engineered bone in a perfusion bioreactor.* Tissue Eng Part A, 2009. **15**(10): p. 2773-83.
81. Porter, B.D., et al., *Noninvasive image analysis of 3D construct mineralization in a perfusion bioreactor.* Biomaterials, 2007. **28**(15): p. 2525-2533.
82. Seitz, S., et al., *Influence of in vitro cultivation on the integration of cell-matrix constructs after subcutaneous implantation.* Tissue Engineering, 2007. **13**(5): p. 1059-1067.
83. Zhao, F. and T. Ma, *Perfusion bioreactor system for human mesenchymal stem cell tissue engineering: Dynamic cell seeding and construct development.* Biotechnology and Bioengineering, 2005. **91**(4): p. 482-493.
84. Zhao, F., et al., *Effects of oxygen transport on 3-d human mesenchymal stem cell metabolic activity in perfusion and static cultures: experiments and mathematical model.* Biotechnol Prog, 2005. **21**(4): p. 1269-80.
85. Zhao, F., et al., *Perfusion Affects the Tissue Developmental Patterns of Human Mesenchymal Stem Cells in 3D Scaffolds.* Journal of Cellular Physiology, 2009. **219**(2): p. 421-429.
86. Wang, Y.C., et al., *Application of perfusion culture system improves in vitro and in vivo osteogenesis of bone marrow-derived osteoblastic cells in porous ceramic materials.* Tissue Engineering, 2003. **9**(6): p. 1205-1214.
87. Uemura, T., et al., *Transplantation of cultured bone cells using combinations of scaffolds and culture techniques.* Biomaterials, 2003. **24**(13): p. 2277-2286.
88. Scaglione, S., et al., *Effects of fluid flow and calcium phosphate coating on human bone marrow stromal cells cultured in a defined 2D model system.* Journal of Biomedical Materials Research Part A, 2008. **86A**(2): p. 411-419.
89. Stolberg, S. and K.E. McCloskey, *Can Shear Stress Direct Stem Cell Fate?* Biotechnology Progress, 2009. **25**(1): p. 10-19.
90. Li, D., K. Dai, and T. Tang, *Effects of dextran on proliferation and osteogenic differentiation of human bone marrow-derived mesenchymal stromal cells.* Cytotherapy, 2008. **10**(6): p. 587-96.
91. Li, Y., et al., *Effects of filtration seeding on cell density, spatial distribution, and proliferation in nonwoven fibrous matrices.* Biotechnology Progress, 2001. **17**(5): p. 935-944.
92. Kitagawa, T., et al., *Three-dimensional cell seeding and growth in radial-flow perfusion bioreactor for in vitro tissue reconstruction.* Biotechnology and Bioengineering, 2006. **93**(5): p. 947-954.
93. Kim, S.S., et al., *Dynamic seeding and in vitro culture of hepatocytes in a flow perfusion system.* Tissue Engineering, 2000. **6**(1): p. 39-44.
94. Vunjak-Novakovic, G., et al., *Dynamic cell seeding of polymer scaffolds for cartilage tissue engineering.* Biotechnology Progress, 1998. **14**(2): p. 193-202.

95. Detsch, R., et al., *3D-Cultivation of bone marrow stromal cells on hydroxyapatite scaffolds fabricated by dispense-plotting and negative mould technique.* Journal of Materials Science-Materials in Medicine, 2008. **19**(4): p. 1491-1496.
96. Leukers, B., et al., *Hydroxyapatite scaffolds for bone tissue engineering made by 3D printing.* Journal of Materials Science-Materials in Medicine, 2005. **16**(12): p. 1121-1124.
97. Leukers, B., et al., *Biocompatibility of ceramic scaffolds for bone replacement made by 3D printing.* Materialwissenschaft Und Werkstofftechnik, 2005. **36**(12): p. 781-787.
98. Wang, Y., et al., *Perfusion culture system improves osteogenesis of rat bone marrow derived osteoblastic cells in porous ceramic materials.* Journal of Bone and Mineral Research, 2002. **17**: p. S338-S338.
99. Chen, X., et al., *Bioreactor expansion of human adult bone marrow-derived mesenchymal stem cells.* Stem Cells, 2006. **24**(9): p. 2052-2059.
100. Marolt, D., et al., *Bone and cartilage tissue constructs grown using human bone marrow stromal cells, silk scaffolds and rotating bioreactors.* Biomaterials, 2006. **27**(36): p. 6138-6149.
101. Kolf, C.M., E. Cho, and R.S. Tuan, *Mesenchymal stromal cells. Biology of adult mesenchymal stem cells: regulation of niche, self-renewal and differentiation.* Arthritis Res Ther, 2007. **9**(1): p. 204.
102. Porada, C.D., E.D. Zanjani, and G. Almeida-Porad, *Adult mesenchymal stem cells: a pluripotent population with multiple applications.* Curr Stem Cell Res Ther, 2006. **1**(3): p. 365-9.
103. Estes, B.T., J.M. Gimble, and F. Guilak, *Mechanical signals as regulators of stem cell fate.* Curr Top Dev Biol, 2004. **60**: p. 91-126.
104. Szpalski, C., et al., *Bone Tissue Engineering: Current Strategies and Techniques; Part I: Scaffolds.* Tissue Eng Part B Rev, 2012.
105. Szpalski, C., et al., *"Bone Tissue Engineering: Current Strategies and Techniques-Part II: Cell types".* Tissue Eng Part B Rev, 2012.
106. Thompson, A.D., et al., *Osteogenic Differentiation of Bone Marrow Stromal Cells Induced by Coculture with Chondrocytes Encapsulated in Three-Dimensional Matrices.* Tissue Engineering Part A, 2009. **15**(5): p. 1181-1190.
107. Kim, K., et al., *The influence of stereolithographic scaffold architecture and composition on osteogenic signal expression with rat bone marrow stromal cells.* Biomaterials, 2011. **32**(15): p. 3750-63.
108. Yoon, D.M. and J.P. Fisher, *Effects of exogenous IGF-1 delivery on the early expression of IGF-1 signaling molecules by alginate embedded chondrocytes.* Tissue Eng Part A, 2008. **14**(7): p. 1263-73.
109. Yoon, D.M., et al., *Effect of construct properties on encapsulated chondrocyte expression of insulin-like growth factor-1.* Biomaterials, 2007. **28**(2): p. 299-306.
110. McCoy, R.J. and F.J. O'Brien, *Influence of Shear Stress in Perfusion Bioreactor Cultures for the Development of Three-Dimensional Bone Tissue Constructs: A Review.* Tissue Eng Part B Rev, 2010. **16**(6): p. 587-601.
111. Yeatts, A.B. and J.P. Fisher, *Bone tissue engineering bioreactors: dynamic culture and the influence of shear stress.* Bone, 2011. **48**(2): p. 171-81.

112. Yeatts, A.B. and J.P. Fisher, *Tubular perfusion system for the long-term dynamic culture of human mesenchymal stem cells.* Tissue Eng Part C Methods, 2011. **17**(3): p. 337-48.
113. Yeatts, A.B., C.N. Gordon, and J.P. Fisher, *Formation of an aggregated alginate construct in a tubular perfusion system.* Tissue Eng Part C Methods, 2011. **17**(12): p. 1171-8.
114. Song, K.D., et al., *Three-dimensional fabrication of engineered bone in rotating wall vessel bioreactor: Investigation of culture time.* Tissue Engineering, 2006. **12**(4): p. 1081-1082.
115. Liu, C.X., et al., *Influence of perfusion and compression on the proliferation and differentiation of bone mesenchymal stromal cells seeded on polyurethane scaffolds.* Biomaterials, 2012. **33**(4): p. 1052-1064.
116. Rauh, J., et al., *Bioreactor systems for bone tissue engineering.* Tissue Eng Part B Rev, 2011. **17**(4): p. 263-80.
117. Salter, E., et al., *Bone tissue engineering bioreactors: a role in the clinic?* Tissue Eng Part B Rev, 2012. **18**(1): p. 62-75.
118. Rodrigues, C.A., et al., *Stem cell cultivation in bioreactors.* Biotechnol Adv, 2011. **29**(6): p. 815-29.
119. David, B., et al., *A perfusion bioreactor for engineering bone constructs: an in vitro and in vivo study.* Tissue Eng Part C Methods, 2011. **17**(5): p. 505-16.
120. Khan, O.F., M.D. Chamberlain, and M.V. Sefton, *Toward an In Vitro Vasculature: Differentiation of Mesenchymal Stromal Cells Within an Endothelial Cell-Seeded Modular Construct in a Microfluidic Flow Chamber.* Tissue Eng Part A, 2011.
121. Lovett, M., et al., *Simple modular bioreactors for tissue engineering: a system for characterization of oxygen gradients, human mesenchymal stem cell differentiation, and prevascularization.* Tissue Eng Part C Methods, 2010. **16**(6): p. 1565-73.
122. da Silva, M.L.A., et al., *Chondrogenic differentiation of human bone marrow mesenchymal stem cells in chitosan-based scaffolds using a flow-perfusion bioreactor.* J Tissue Eng Regen Med, 2011. **5**(9): p. 722-732.
123. Arikawa, T., K. Omura, and I. Morita, *Regulation of bone morphogenetic protein-2 expression by endogenous prostaglandin E2 in human mesenchymal stem cells.* Journal of Cellular Physiology, 2004. **200**(3): p. 400-406.
124. Schulz, R.M. and A. Bader, *Cartilage tissue engineering and bioreactor systems for the cultivation and stimulation of chondrocytes.* European Biophysics Journal with Biophysics Letters, 2007. **36**(4-5): p. 539-568.
125. Wescoe, K.E., et al., *The Role of the Biochemical and Biophysical Environment in Chondrogenic Stem Cell Differentiation Assays and Cartilage Tissue Engineering.* Cell Biochemistry and Biophysics, 2008. **52**(2): p. 85-102.
126. Zuscik, M.J., et al., *Regulation of chondrogenesis and chondrocyte differentiation by stress.* Journal of Clinical Investigation, 2008. **118**(2): p. 429-438.
127. Fitzgerald, J.B., et al., *Shear- and compression-induced chondrocyte transcription requires MAPK activation in cartilage explants.* Journal of Biological Chemistry, 2008. **283**(11): p. 6735-6743.

128. Hung, C.T., et al., *Mitogen-activated protein kinase signaling in bovine articular chondrocytes in response to fluid flow does not require calcium mobilization.* Journal of Biomechanics, 2000. **33**(1): p. 73-80.
129. Abulencia, J.P., et al., *Shear-induced cyclooxygenase-2 via a JNK2/c-Jun-dependent pathway regulates prostaglandin receptor expression in chondrocytic cells.* Journal of Biological Chemistry, 2003. **278**(31): p. 28388-28394.
130. Papachristou, D.J., et al., *JNK/ERK-AP-1/Runx2 induction "paves the way" to cartilage load-ignited chondroblastic differentiation.* Histochemistry and Cell Biology, 2005. **124**(3-4): p. 215-223.
131. Gemmiti, C.V. and R.E. Guldberg, *Fluid flow increases type II collagen deposition and tensile mechanical properties in bioreactor-grown tissue-engineered cartilage.* Tissue Engineering, 2006. **12**(3): p. 469-479.
132. Li, Z., et al., *Mechanical load modulates chondrogenesis of human mesenchymal stem cells through the TGF-beta pathway.* Journal of Cellular and Molecular Medicine, 2010. **14**(6): p. 1338-1346.
133. Meyer, E.G., et al., *Low oxygen tension is a more potent promoter of chondrogenic differentiation than dynamic compression.* J Biomech, 2010. **43**(13): p. 2516-23.
134. Spiteri, C.G., et al., *Substrate architecture and fluid-induced shear stress during chondrocyte seeding: Role of alpha 5 beta 1 integrin.* Biomaterials, 2008. **29**(16): p. 2477-2489.
135. Davis, R.J., *Signal transduction by the JNK group of MAP kinases.* Cell, 2000. **103**(2): p. 239-52.
136. Weston, C.R. and R.J. Davis, *The JNK signal transduction pathway.* Curr Opin Cell Biol, 2007. **19**(2): p. 142-9.
137. Weston, C.R. and R.J. Davis, *The JNK signal transduction pathway.* Curr Opin Genet Dev, 2002. **12**(1): p. 14-21.
138. Zarubin, T. and J. Han, *Activation and signaling of the p38 MAP kinase pathway.* Cell Res, 2005. **15**(1): p. 11-8.
139. Cuadrado, A. and A.R. Nebreda, *Mechanisms and functions of p38 MAPK signalling.* Biochem J, 2010. **429**(3): p. 403-17.
140. Robinson, M.J. and M.H. Cobb, *Mitogen-activated protein kinase pathways.* Curr Opin Cell Biol, 1997. **9**(2): p. 180-6.
141. Johnson, G.L. and R. Lapadat, *Mitogen-activated protein kinase pathways mediated by ERK, JNK, and p38 protein kinases.* Science, 2002. **298**(5600): p. 1911-2.
142. Lai, C.F. and S.L. Cheng, *Signal transductions induced by bone morphogenetic protein-2 and transforming growth factor-beta in normal human osteoblastic cells.* J Biol Chem, 2002. **277**(18): p. 15514-22.
143. Afzal, F., et al., *Smad function and intranuclear targeting share a Runx2 motif required for osteogenic lineage induction and BMP2 responsive transcription.* J Cell Physiol, 2005. **204**(1): p. 63-72.
144. Guicheux, J., et al., *Activation of p38 mitogen-activated protein kinase and c-Jun-NH2-terminal kinase by BMP-2 and their implication in the stimulation of osteoblastic cell differentiation.* J Bone Miner Res, 2003. **18**(11): p. 2060-8.

145. Lee, J.W., et al., *Chondrogenic differentiation of mesenchymal stem cells and its clinical applications.* Yonsei Med J, 2004. **45 Suppl**: p. 41-7.
146. Tuli, R., et al., *Transforming growth factor-beta-mediated chondrogenesis of human mesenchymal progenitor cells involves N-cadherin and mitogen-activated protein kinase and Wnt signaling cross-talk.* J Biol Chem, 2003. **278**(42): p. 41227-36.
147. Watanabe, H., M.P. de Caestecker, and Y. Yamada, *Transcriptional cross-talk between Smad, ERK1/2, and p38 mitogen-activated protein kinase pathways regulates transforming growth factor-beta-induced aggrecan gene expression in chondrogenic ATDC5 cells.* J Biol Chem, 2001. **276**(17): p. 14466-73.
148. Jaiswal, R.K., et al., *Adult human mesenchymal stem cell differentiation to the osteogenic or adipogenic lineage is regulated by mitogen-activated protein kinase.* J Biol Chem, 2000. **275**(13): p. 9645-52.
149. Huang, Y.F., et al., *c-Jun N-terminal kinase 1 negatively regulates osteoblastic differentiation induced by BMP-2 via phosphorylation of Runx2 at Ser104.* J Bone Miner Res, 2012.
150. Woods, A. and F. Beier, *RhoA/ROCK signaling regulates chondrogenesis in a context-dependent manner.* J Biol Chem, 2006. **281**(19): p. 13134-40.
151. Celil, A.B., J.O. Hollinger, and P.G. Campbell, *Osx transcriptional regulation is mediated by additional pathways to BMP2/Smad signaling.* J Cell Biochem, 2005. **95**(3): p. 518-28.
152. Simmons, C.A., et al., *Cyclic strain enhances matrix mineralization by adult human mesenchymal stem cells via the extracellular signal-regulated kinase (ERK1/2) signaling pathway.* J Biomech, 2003. **36**(8): p. 1087-96.
153. Huang, H.D., R.D. Kamm, and R.T. Lee, *Cell mechanics and mechanotransduction: pathways, probes, and physiology.* American Journal of Physiology-Cell Physiology, 2004. **287**(1): p. C1-C11.
154. Wang, N., J.D. Tytell, and D.E. Ingber, *Mechanotransduction at a distance: mechanically coupling the extracellular matrix with the nucleus.* Nature Reviews Molecular Cell Biology, 2009. **10**(1): p. 75-82.
155. Iqbal, J. and M. Zaidi, *Molecular regulation of mechanotransduction.* Biochemical and Biophysical Research Communications, 2005. **328**(3): p. 751-755.
156. Katsumi, A., et al., *Integrins in mechanotransduction.* Journal of Biological Chemistry, 2004. **279**(13): p. 12001-12004.
157. Butler, P.J., et al., *Rate sensitivity of shear-induced changes in the lateral diffusion of endothelial cell membrane lipids: a role for membrane perturbation in shear-induced MAPK activation.* Faseb Journal, 2001. **15**(14): p. 216-218.
158. Liu, L.Y., et al., *Extracellular signal-regulated kinase1/2 activated by fluid shear stress promotes osteogenic differentiation of human bone marrow-derived mesenchymal stem cells through novel signaling pathways.* International Journal of Biochemistry & Cell Biology, 2011. **43**(11): p. 1591-1601.
159. Glossop, J.R. and S.H. Cartmell, *Effect of fluid flow-induced shear stress on human mesenchymal stem cells: Differential gene expression of IL1B and MAP3K8 in MAPK signaling.* Gene Expression Patterns, 2009. **9**(5): p. 381-388.

160. Chen, N.X., et al., *Ca(2+) regulates fluid shear-induced cytoskeletal reorganization and gene expression in osteoblasts.* Am J Physiol Cell Physiol, 2000. **278**(5): p. C989-97.
161. Riddle, R.C., et al., *MAP kinase and calcium signaling mediate fluid flow-induced human mesenchymal stem cell proliferation.* American Journal of Physiology-Cell Physiology, 2006. **290**(3): p. C776-C784.
162. Sekiya, I., et al., *SOX9 enhances aggrecan gene promoter/enhancer activity and is up-regulated by retinoic acid in a cartilage-derived cell line, TC6.* Journal of Biological Chemistry, 2000. **275**(15): p. 10738-10744.
163. Salasznyk, R.M., et al., *Focal adhesion kinase signaling pathways regulate the osteogenic differentiation of human mesenchymal stem cells.* Experimental Cell Research, 2007. **313**(1): p. 22-37.
164. Coates, E. and J.P. Fisher, *Gene expression of alginate-embedded chondrocyte subpopulations and their response to exogenous IGF-1 delivery.* Journal of Tissue Engineering and Regenerative Medicine, 2012. **6**(3): p. 179–192.
165. De Boer, J., H.J. Wang, and C. Van Blitterswijk, *Effects of Wnt signaling on proliferation and differentiation of human mesenchymal stem cells.* Tissue Engineering, 2004. **10**(3-4): p. 393-401.
166. Boland, G.M., et al., *Wnt 3a promotes proliferation and suppresses osteogenic differentiation of adult human mesenchymal stem cells.* J Cell Biochem, 2004. **93**(6): p. 1210-30.
167. de Boer, J., et al., *Wnt signaling inhibits osteogenic differentiation of human mesenchymal stem cells.* Bone, 2004. **34**(5): p. 818-826.
168. Akiyama, H., et al., *Interactions between Sox9 and beta-catenin control chondrocyte differentiation.* Genes & Development, 2004. **18**(9): p. 1072-1087.
169. Liu, G.Z., et al., *Canonical Wnts function as potent regulators of osteogenesis by human mesenchymal stem cells.* Journal of Cell Biology, 2009. **185**(1): p. 67-75.
170. Chang, J., et al., *Noncanonical Wnt-4 signaling enhances bone regeneration of mesenchymal stem cells in craniofacial defects through activation of p38 MAPK.* Journal of Biological Chemistry, 2007. **282**(42): p. 30938-30948.
171. Arnsdorf, E.J., P. Tummala, and C.R. Jacobs, *Non-canonical Wnt signaling and N-cadherin related beta-catenin signaling play a role in mechanically induced osteogenic cell fate.* PLoS One, 2009. **4**(4): p. e5388.
172. Javed, A., et al., *Structural coupling of smad and Runx2 for execution of the BMP2 osteogenic signal.* Journal of Biological Chemistry, 2008. **283**(13): p. 8412-8422.
173. Zhang, Y., X.H. Feng, and R. Derynck, *Smad3 and Smad4 cooperate with c-Jun/c-Fos to mediate TGF-beta-induced transcription.* Nature, 1998. **394**(6696): p. 909-913.
174. D'Alonzo, R.C., et al., *Physical interaction of the activator protein-1 factors c-Fos and c-Jun with Cbfa1 for collagenase-3 promoter activation.* Journal of Biological Chemistry, 2002. **277**(1): p. 816-822.
175. Nakashima, K., et al., *The novel zinc finger-containing transcription factor Osterix is required for osteoblast differentiation and bone formation.* Cell, 2002. **108**(1): p. 17-29.

176. Wang, X., C.H. Goh, and B. Li, *p38 mitogen-activated protein kinase regulates osteoblast differentiation through osterix.* Endocrinology, 2007. **148**(4): p. 1629-37.
177. Meury, T., S. Verrier, and M. Alini, *Human endothelial cells inhibit BMSC differentiation into mature osteoblasts in vitro by interfering with osterix expression.* J Cell Biochem, 2006. **98**(4): p. 992-1006.
178. Bi, W.M., et al., *Sox9 is required for cartilage formation.* Nature Genetics, 1999. **22**(1): p. 85-89.
179. Lefebvre, V., et al., *SOX9 is a potent activator of the chondrocyte-specific enhancer of the pro alpha 1(II) collagen gene.* Molecular and Cellular Biology, 1997. **17**(4): p. 2336-2346.
180. Furumatsu, T., et al., *Smad3 induces chondrogenesis through the activation of SOX9 via CREB-binding protein/p300 recruitment.* Journal of Biological Chemistry, 2005. **280**(9): p. 8343-8350.
181. Abecassis, L., et al., *Evidence for a role of MSK1 in transforming growth factor-beta-mediated responses through p38 alpha and Smad signaling pathways.* Journal of Biological Chemistry, 2004. **279**(29): p. 30474-30479.
182. Malda, J., T.J. Klein, and Z. Upton, *The roles of hypoxia in the In vitro engineering of tissues.* Tissue Engineering, 2007. **13**(9): p. 2153-2162.
183. Mohyeldin, A., T. Garzon-Muvdi, and A. Quinones-Hinojosa, *Oxygen in Stem Cell Biology: A Critical Component of the Stem Cell Niche.* Cell Stem Cell, 2010. **7**(2): p. 150-161.
184. Das, R., et al., *The Role of Hypoxia in Bone Marrow-Derived Mesenchymal Stem Cells: Considerations for Regenerative Medicine Approaches.* Tissue Engineering Part B-Reviews, 2010. **16**(2): p. 159-168.
185. Fink, T., et al., *Induction of adipocyte-like phenotype in human mesenchymal stem cells by hypoxia.* Stem Cells, 2004. **22**(7): p. 1346-1355.
186. Sun, X.T. and Y.Y. Wei, *The role of hypoxia-inducible factor in osteogenesis and chondrogenesis.* Cytotherapy, 2009. **11**(3): p. 261-267.
187. Ma, T., et al., *Hypoxia and Stem Cell-Based Engineering of Mesenchymal Tissues.* Biotechnology Progress, 2009. **25**(1): p. 32-42.
188. Murphy, C.L., et al., *Hypoxia HIF-mediated articular chondrocyte function: prospects for cartilage repair.* Arthritis Research & Therapy, 2009. **11**(1).
189. Harrison, J.S., et al., *Oxygen saturation in the bone marrow of healthy volunteers.* Blood, 2002. **99**(1): p. 394-394.
190. Brighton, C.T. and Heppenst.Rb, *Oxygen Tension in Zones of Epiphyseal Plate, Metaphysis and Diaphysis - in-Vitro and in-Vivo Study in Rats and Rabbits.* Journal of Bone and Joint Surgery-American Volume, 1971. **A 53**(4): p. 719-728.
191. Potier, E., et al., *Hypoxia affects mesenchymal stromal cell osteogenic differentiation and angiogenic factor expression.* Bone, 2007. **40**(4): p. 1078-87.
192. Heppenstall, R.B., G. Grislis, and T.K. Hunt, *Tissue Gas Tensions and Oxygen-Consumption in Healing Bone Defects.* Clinical Orthopaedics and Related Research, 1975(106): p. 357-365.
193. Goh, F., et al., *Dual perfluorocarbon method to noninvasively monitor dissolved oxygen concentration in tissue engineered constructs in vitro and in vivo.* Biotechnol Prog, 2011.

194. Liu, J., et al., *In vitro and in vivo bioluminescent imaging of hypoxia in tissue-engineered grafts.* Tissue Eng Part C Methods, 2010. **16**(3): p. 479-85.
195. Lennon, D.P., J.M. Edmison, and A.I. Caplan, *Cultivation of rat marrow-derived mesenchymal stem cells in reduced oxygen tension: Effects on in vitro and in vivo osteochondrogenesis.* Journal of Cellular Physiology, 2001. **187**(3): p. 345-355.
196. Grayson, W.L., et al., *Hypoxia enhances proliferation and tissue formation of human mesenchymal stem cells.* Biochem Biophys Res Commun, 2007. **358**(3): p. 948-53.
197. Grayson, W.L., et al., *Effects of hypoxia on human mesenchymal stem cell expansion and plasticity in 3D constructs.* Journal of Cellular Physiology, 2006. **207**(2): p. 331-339.
198. Hung, S.P., et al., *Hypoxia promotes proliferation and osteogenic differentiation potentials of human mesenchymal stem cells.* Journal of Orthopaedic Research, 2012. **30**(2): p. 260-6.
199. Fehrer, C., et al., *Reduced oxygen tension attenuates differentiation capacity of human mesenchymal stem cells and prolongs their lifespan.* Aging Cell, 2007. **6**(6): p. 745-757.
200. Xu, Y., et al., *In vitro expansion of adipose-derived adult stromal cells in hypoxia enhances early chondrogenesis.* Tissue Engineering, 2007. **13**(12): p. 2981-2993.
201. Baumgartner, L., et al., *Human mesenchymal stem cells: Influence of oxygen pressure on proliferation and chondrogenic differentiation in fibrin glue in vitro.* Journal of Biomedical Materials Research Part A, 2010. **93A**(3): p. 930-940.
202. Kanichai, M., et al., *Hypoxia promotes chondrogenesis in rat mesenchymal stem cells: a role for AKT and hypoxia-inducible factor (HIF)-1alpha.* J Cell Physiol, 2008. **216**(3): p. 708-15.
203. Hirao, M., et al., *Oxygen tension regulates chondrocyte differentiation and function during endochondral ossification.* Journal of Biological Chemistry, 2006. **281**(41): p. 31079-31092.
204. Coates, E.E. and J.P. Fisher, *Phenotypic variations in chondrocyte subpopulations and their response to in vitro culture and external stimuli.* Ann Biomed Eng, 2010. **38**(11): p. 3371-88.
205. Nguyen, L.H., et al., *Unique biomaterial compositions direct bone marrow stem cells into specific chondrocytic phenotypes corresponding to the various zones of articular cartilage.* Biomaterials, 2011. **32**(5): p. 1327-38.
206. Schrobback, K., et al., *Effects of Oxygen on Zonal Marker Expression in Human Articular Chondrocytes.* Tissue Eng Part A, 2012.
207. Potier, E., et al., *Prolonged hypoxia concomitant with serum deprivation induces massive human mesenchymal stem cell death.* Tissue Eng, 2007. **13**(6): p. 1325-31.
208. Semenza, G.L., *Hypoxia-inducible factor 1 (HIF-1) pathway.* Sci STKE, 2007. **2007**(407): p. cm8.
209. Yang, D.C., et al., *Hypoxia Inhibits Osteogenesis in Human Mesenchymal Stem Cells through Direct Regulation of RUNX2 by TWIST.* PLoS One, 2011. **6**(9).
210. Tsai, C.C., et al., *Hypoxia inhibits senescence and maintains mesenchymal stem cell properties through down-regulation of E2A-p21 by HIF-TWIST.* Blood, 2011. **117**(2): p. 459-469.

211. Basciano, L., et al., *Long term culture of mesenchymal stem cells in hypoxia promotes a genetic program maintaining their undifferentiated and multipotent status.* Bmc Cell Biology, 2011. **12**.
212. Robins, J.C., et al., *Hypoxia induces chondrocyte-specific gene expression in mesenchymal cells in association with transcriptional activation of Sox9.* Bone, 2005. **37**(3): p. 313-22.
213. Comerford, K.M., E.P. Cummins, and C.T. Taylor, *c-Jun NH2-terminal kinase activation contributes to hypoxia-inducible factor 1alpha-dependent P-glycoprotein expression in hypoxia.* Cancer Res, 2004. **64**(24): p. 9057-61.
214. McGuigan, A.P. and M.V. Sefton, *Vascularized organoid engineered by modular assembly enables blood perfusion.* Proc Natl Acad Sci U S A, 2006. **103**(31): p. 11461-6.
215. Ishaug, S.L., et al., *Bone formation by three-dimensional stromal osteoblast culture in biodegradable polymer scaffolds.* Journal of Biomedical Materials Research, 1997. **36**(1): p. 17-28.
216. Martin, I., D. Wendt, and M. Heberer, *The role of bioreactors in tissue engineering.* Trends in Biotechnology, 2004. **22**(2): p. 80-86.
217. van den Dolder, J., et al., *Flow perfusion culture of marrow stromal osteoblasts in titanium fiber mesh.* Journal of Biomedical Materials Research Part A, 2003. **64A**(2): p. 235-241.
218. Yoon, D.M., et al., *Addition of Hyaluronic Acid to Alginate Embedded Chondrocytes Interferes with Insulin-like Growth Factor-1 Signaling In Vitro and In Vivo.* Tissue Engineering Part A, 2009. **15**(11): p. 3449-3459.
219. Augst, A.D., H.J. Kong, and D.J. Mooney, *Alginate hydrogels as biomaterials.* Macromolecular Bioscience, 2006. **6**(8): p. 623-633.
220. Abbah, S.A., et al., *Osteogenic behavior of alginate encapsulated bone marrow stromal cells: An in vitro study.* Journal of Materials Science-Materials in Medicine, 2008. **19**(5): p. 2113-2119.
221. Chang, S.C.N., et al., *Cranial repair using BMP-2 gene engineered bone marrow stromal cells.* Journal of Surgical Research, 2004. **119**(1): p. 85-91.
222. Wang, L., et al., *Evaluation of sodium alginate for bone marrow cell tissue engineering.* Biomaterials, 2003. **24**(20): p. 3475-3481.
223. Ueng, S.W.N., et al., *Development of a biodegradable alginate carrier system for antibiotics and bone cells.* Journal of Orthopaedic Research, 2007. **25**(1): p. 62-72.
224. Bidarra, S.J., et al., *Immobilization of Human Mesenchymal Stem Cells within RGD-Grafted Alginate Microspheres and Assessment of Their Angiogenic Potential.* Biomacromolecules, 2010. **11**(8): p. 1956-1964.
225. Mauney, J.R., V. Volloch, and D.L. Kaplan, *Role of adult mesenchymal stem cells in bone tissue-engineering applications: Current status and future prospects.* Tissue Engineering, 2005. **11**(5-6): p. 787-802.
226. Portner, R., et al., *Bioreactor design for tissue engineering.* Journal of Bioscience and Bioengineering, 2005. **100**(3): p. 235-245.
227. Meuwly, F., et al., *Packed-bed bioreactors for mammalian cell culture: Bioprocess and biomedical applications.* Biotechnology Advances, 2007. **25**(1): p. 45-56.

228. Williams, C. and T.M. Wick, *Perfusion Bioreactor for small diameter tissue-engineered arteries.* Tissue Engineering, 2004. **10**(5-6): p. 930-941.
229. Williams, C. and T.M. Wick, *Endothelial cell-smooth muscle cell co-culture in a perfusion bioreactor system.* Annals of Biomedical Engineering, 2005. **33**(7): p. 920-928.
230. Huang, H.Y., et al., *In Vitro Maturation of "Biotube" Vascular Grafts Induced by a 2-Day Pulsatile Flow Loading.* Journal of Biomedical Materials Research Part B-Applied Biomaterials, 2009. **91B**(1): p. 320-328.
231. Engbers-Buijtenhuijs, P., et al., *Biological characterisation of vascular grafts cultured in a bioreactor.* Biomaterials, 2006. **27**(11): p. 2390-2397.
232. Chen, C.W., et al., *Macroporous Hydrogel Scaffolds and Their Characterization By Optical Coherence Tomography.* Tissue Eng Part C Methods, 2011. **17**(1): p. 101-112.
233. Guo, L.K., et al., *Osteogenic differentiation of human mesenchymal stem cells on chargeable polymer-modified surfaces.* Journal of Biomedical Materials Research Part A, 2008. **87A**(4): p. 903-912.
234. Bacabac, R.G., et al., *Dynamic shear stress in parallel-plate flow chambers.* Journal of Biomechanics, 2005. **38**(1): p. 159-167.
235. Allen, J.W. and S.N. Bhatia, *Formation of steady-state oxygen gradients in vitro - Application to liver zonation.* Biotechnology and Bioengineering, 2003. **82**(3): p. 253-262.
236. Truskey, G.A., F. Yuan, and D.F. Katz, *Transport Phenomena in Biological Systems*. 2004, Upper Saddle River: Pearson Prentice Hall. 793.
237. Kurosawa, H., M. Matsumura, and H. Tanaka, *Oxygen Diffusivity in Gel Beads Containing Viable Cells.* Biotechnology and Bioengineering, 1989. **34**(7): p. 926-932.
238. Peng, C.A. and B.O. Palsson, *Determination of specific oxygen uptake rates in human hematopoietic cultures and implications for bioreactor design.* Annals of Biomedical Engineering, 1996. **24**(3): p. 373-381.
239. Betz, M.W., et al., *Cyclic acetal hydrogel system for bone marrow stromal cell encapsulation and osteodifferentiation.* Journal of Biomedical Materials Research Part A, 2008. **86A**(3): p. 662-670.
240. Kim, K., et al., *Effect of Initial Cell Seeding Density on Early Osteogenic Signal Expression of Rat Bone Marrow Stromal Cells Cultured on Cross-Linked Poly(propylene fumarate) Disks.* Biomacromolecules, 2009. **10**(7): p. 1810-17.
241. Martin, I., T. Smith, and D. Wendt, *Bioreactor-based roadmap for the translation of tissue engineering strategies into clinical products.* Trends in Biotechnology, 2009. **27**(9): p. 495-502.
242. Utting, J.C., et al., *Hypoxia inhibits the growth, differentiation and bone-forming capacity of rat osteoblasts.* Experimental Cell Research, 2006. **312**(10): p. 1693-1702.
243. Patel, M., et al., *Cyclic Acetal Hydroxyapatite Nanocomposites for Orbital Bone Regeneration.* Tissue Engineering Part A, 2010. **16**(1): p. 55-65.
244. Folkestad, L. and T. Westin, *Long-term sequelae after surgery for orbital floor fractures.* Otolaryngology-Head and Neck Surgery, 1999. **120**(6): p. 914-921.

245. Rinna, C., et al., *Orbital floor restoration.* Journal of Craniofacial Surgery, 2005. **16**(6): p. 968-972.
246. Betz, M.W., et al., *Challenges associated with regeneration of orbital floor bone.* Tissue Eng Part B Rev, 2010. **16**(5): p. 541-50.
247. Iida, K., et al., *Hypoxia enhances colony formation and proliferation but inhibits differentiation of human dental pulp cells.* Arch Oral Biol, 2010. **55**(9): p. 648-54.
248. Hwang, C.M., et al., *Fabrication of three-dimensional porous cell-laden hydrogel for tissue engineering.* Biofabrication, 2010. **2**(3): p. 035003.
249. Bianco, P., et al., *Bone sialoprotein (BSP) secretion and osteoblast differentiation: relationship to bromodeoxyuridine incorporation, alkaline phosphatase, and matrix deposition.* J Histochem Cytochem, 1993. **41**(2): p. 183-91.
250. Augello, A. and C. De Bari, *The regulation of differentiation in mesenchymal stem cells.* Hum Gene Ther, 2010. **21**(10): p. 1226-38.
251. Nichol, J.W. and A. Khademhosseini, *Modular Tissue Engineering: Engineering Biological Tissues from the Bottom Up.* Soft Matter, 2009. **5**(7): p. 1312-1319.
252. McGuigan, A.P. and M.V. Sefton, *Design criteria for a modular tissue-engineered construct.* Tissue Eng, 2007. **13**(5): p. 1079-89.
253. McGuigan, A.P., B. Leung, and M.V. Sefton, *Fabrication of cell-containing gel modules to assemble modular tissue-engineered constructs [corrected].* Nat Protoc, 2006. **1**(6): p. 2963-9.
254. Rowley, J.A., G. Madlambayan, and D.J. Mooney, *Alginate hydrogels as synthetic extracellular matrix materials.* Biomaterials, 1999. **20**(1): p. 45-53.
255. Callister, W.D., *Materials science and engineering : an introduction*. 6th ed. 2003, New York, NY: John Wiley & Sons. xxi, 820 p.
256. Leung, B.M. and M.V. Sefton, *A modular approach to cardiac tissue engineering.* Tissue Eng Part A, 2010. **16**(10): p. 3207-18.
257. Palmiero, C., et al., *Engineered dermal equivalent tissue in vitro by assembly of microtissue precursors.* Acta Biomater, 2010. **6**(7): p. 2548-53.
258. Lee, K.Y., et al., *Controlling mechanical and swelling properties of alginate hydrogels independently by cross-linker type and cross-linking density.* Macromolecules, 2000. **33**(11): p. 4291-4294.
259. Bajpai, S.K. and S. Sharma, *Investigation of swelling/degradation behaviour of alginate beads crosslinked with Ca2+ and Ba2+ ions.* Reactive & Functional Polymers, 2004. **59**(2): p. 129-140.
260. Moe, S.T., et al., *Swelling of Covalently Cross-Linked Alginate Gels - Influence of Ionic Solutes and Nonpolar-Solvents.* Macromolecules, 1993. **26**(14): p. 3589-3597.
261. Kuo, C.K. and P.X. Ma, *Ionically crosslinked alginate hydrogels as scaffolds for tissue engineering: Part 1. Structure, gelation rate and mechanical properties.* Biomaterials, 2001. **22**(6): p. 511-521.
262. Mancini, M., M. Moresi, and R. Rancini, *Mechanical properties of alginate gels: empirical characterisation.* Journal of Food Engineering, 1999. **39**(4): p. 369-378.
263. Drury, J.L., R.G. Dennis, and D.J. Mooney, *The tensile properties of alginate hydrogels.* Biomaterials, 2004. **25**(16): p. 3187-99.

264. Yoon, D.M. and J.P. Fisher, *Chondrocyte signaling and artificial matrices for articular cartilage engineering.* Adv Exp Med Biol, 2006. **585**: p. 67-86.
265. Rowley, J.A. and D.J. Mooney, *Alginate type and RGD density control myoblast phenotype.* J Biomed Mater Res, 2002. **60**(2): p. 217-23.
266. Murphy, C.M., M.G. Haugh, and F.J. O'Brien, *The effect of pore size on osteoblast activity in collagen-glycosaminoglycan scaffolds.* Tissue Engineering Part A, 2008. **14**(5): p. 914-914.
267. Stamatialis, D.F., et al., *Membranes for bioartificial organs and tissue engineering.* Tissue Engineering Part A, 2008. **14**(5): p. 755-755.
268. Zhang, J.C., et al., *Fabrication of three dimensional polymeric scaffolds with spherical pores.* Journal of Materials Science, 2006. **41**(6): p. 1725-1731.
269. He, L.M., et al., *Microstructure and Properties of Nano-Fibrous Pcl-B-Plla Scaffolds for Cartilage Tissue Engineering.* European Cells & Materials, 2009. **18**: p. 63-74.
270. Liu, X.H., Y.J. Won, and P.X. Ma, *Porogen-induced surface modification of nano-fibrous poly(L-lactic acid) scaffolds for tissue engineering.* Biomaterials, 2006. **27**(21): p. 3980-3987.
271. Kim, T.K., et al., *Gas foamed open porous biodegradable polymeric microspheres.* Biomaterials, 2006. **27**(2): p. 152-159.
272. Mooney, D.J., et al., *Novel approach to fabricate porous sponges of poly(D,L-lactic-co-glycolic acid) without the use of organic solvents.* Biomaterials, 1996. **17**(14): p. 1417-1422.
273. Tsivintzelis, I., E. Pavlidou, and C. Panayiotou, *Porous scaffolds prepared by phase inversion using supercritical CO2 as antisolvent - I. Poly(L-lactic acid).* Journal of Supercritical Fluids, 2007. **40**(2): p. 317-322.
274. Duarte, A.R.C., J.F. Mano, and R.L. Reis, *Preparation of starch-based scaffolds for tissue engineering by supercritical immersion precipitation.* Journal of Supercritical Fluids, 2009. **49**(2): p. 279-285.
275. Reverchon, E., S. Cardea, and C. Rapuano, *A new supercritical fluid based process to produce scaffolds for tissue replacement.* J Supercrit Fluids, 2008. **45**: p. 365-373.
276. Cardea, S., P. Pisanti, and E. Reverchon, *Generation of chitosan nanoporous structures for tissue engineering applications using a supercritical fluid assisted process.* Journal of Supercritical Fluids, 2010. **54**(3): p. 290-295.
277. Reverchon, E., P. Pisanti, and S. Cardea, *Nanostructured PLLA-Hydroxyapatite Scaffolds Produced by a Supercritical Assisted Technique.* Industrial & Engineering Chemistry Research, 2009. **48**(11): p. 5310-5316.
278. Kim, K., et al., *Early Osteogenic Signal Expression of Rat Bone Marrow Stromal Cells is Influenced by Both Hydroxyapatite Nanoparticle Content and Initial Cell Seeding Density in Biodegradable Nanocomposite Scaffolds.* Acta Biomater, 2011. **7**(3): p. 1249-64.
279. Ma, P.X., *Scaffolds for Tissue Engineering.* Materials Today, 2004. **7**(5): p. 30-40.
280. Dulgar-Tulloch, A.J., R. Bizios, and R.W. Siegel, *Human mesenchymal stem cell adhesion and proliferation in response to ceramic chemistry and nanoscale topography.* J Biomed Mater Res A, 2009. **90**(2): p. 586-94.

281. Mendonca, D.B., et al., *Titanium surface topography affects collagen biosynthesis of adherent cells.* Bone, 2011. **49**(3): p. 463-72.
282. Shanmugasundaram, S., H. Chaudhry, and T.L. Arinzeh, *Microscale versus nanoscale scaffold architecture for mesenchymal stem cell chondrogenesis.* Tissue Eng Part A, 2011. **17**(5-6): p. 831-40.
283. Bitar, M., et al., *Effect of cell density on osteoblastic differentiation and matrix degradation of biomimetic dense collagen scaffolds.* Biomacromolecules, 2008. **9**(1): p. 129-135.
284. Oh, S.H., et al., *In vitro and in vivo characteristics of PCL scaffolds with pore size gradient fabricated by a centrifugation method.* Biomaterials, 2007. **28**(9): p. 1664-1671.
285. Bjerre, L., et al., *Flow perfusion culture of human mesenchymal stem cells on coralline hydroxyapatite scaffolds with various pore sizes.* Journal of Biomedical Materials Research Part A, 2011. **97A**(3): p. 251-263.
286. Yeatts, A.B., et al., *Human mesenchymal stem cell position within scaffolds influences cell fate during dynamic culture.* Biotechnol Bioeng, 2012.
287. Both, S.K., et al., *Differential bone-forming capacity of osteogenic cells from either embryonic stem cells or bone marrow-derived mesenchymal stem cells.* J Tissue Eng Regen Med, 2011. **5**(3): p. 180-90.
288. Rai, B., et al., *Differences between in vitro viability and differentiation and in vivo bone-forming efficacy of human mesenchymal stem cells cultured on PCL-TCP scaffolds.* Biomaterials, 2010. **31**(31): p. 7960-7970.